

Supramolecular behaviour of substituted pyridinium salts and merocyanine dyes

Dissertation

Zur Erlangung des akademischen Grades

doctor rerum naturalium (Dr. rer. nat.)

vorgelegt der

Naturwissenschaftlichen Fakultät II – Chemie und Physik
der Martin-Luther-Universität Halle-Wittenberg

von Frau Dipl.-Ing. Diana Ster

geb. am 01.02.1979 in Baia Mare

Gutachter:

1. Prof. Dr. G. Israel
2. Prof. Dr. R. Zentel

Halle (Saale), den 17.10.2007

urn:nbn:de:gbv:3-000012638

[<http://nbn-resolving.de/urn/resolver.pl?urn=nbn%3Ade%3Agbv%3A3-000012638>]

Contents

1. Introduction and problems	1
1.1. Theoretical part and literature	1
1.1.1. Ionic liquid crystals	1
1.1.1.1. General aspects	1
1.1.1.2. Pyridinium salts	3
1.1.1.3. Stilbazolium salts	6
1.1.2. Merocyanine dyes	7
1.1.2.1. Supramolecular behaviour	7
1.1.2.2. Spectral properties	10
1.2. Introduction of the synthesized and investigated compounds	12
2. Results and discussions	14
2.1. Synthesis	14
2.1.1. Synthesis of merocyanine dyes	14
2.1.2. Synthesis of <i>N</i> -alkyl-4'-substituted-stilbazolium compounds	18
2.1.3. Synthesis of <i>N</i> -alkyl-4- and -3-phenyl-pyridinium salts	20
2.2. Properties of <i>N</i>-alkyl-4- and -3-substituted-pyridinium salts	21
2.2.1. Liquid crystalline properties	21
2.2.1.1. <i>N</i> -alkyl-4-phenyl-pyridinium salts	21
2.2.1.2. <i>N</i> -alkyl-3-phenyl-pyridinium salts	29
2.2.1.3. <i>N</i> -alkyl-4-methyl-pyridinium salts	33
2.2.2. UV/Vis investigations of <i>N</i> -alkyl-3- and -4-substituted pyridinium salts	35
2.2.3. Lyotropic properties of <i>N</i> -octadecyl-4-methyl-pyridinium iodide	39
2.3. Properties of <i>N</i>-alkyl-4'-substituted-stilbazolium salts	44
2.3.1. Liquid crystalline properties	44
2.3.1.1. <i>N</i> -alkyl-4'-hydroxy-stilbazolium halides	44
2.3.1.2. <i>N</i> -alkyl-4'-methoxy-stilbazolium halides	46
2.3.1.3. <i>N</i> -alkyl-stilbazolium halides	47
2.3.2. Spectral properties	49
2.3.2.1. Photoisomerization of <i>N</i> -alkyl-4'-substituted-stilbazolium salts	49

2.3.2.2. Concentration dependence measurements of <i>N</i> -alkyl-4'-substituted-stilbazolium salts	54
2.4. Properties of merocyanine dyes	56
2.4.1. Spectral investigations	56
2.4.1.1. Protonation-deprotonation equilibrium	56
2.4.1.2. <i>Cis-trans</i> isomerization of merocyanine dyes	59
2.4.1.3. Aggregation behaviour of merocyanine dyes in solution	61
2.4.1.4. Aggregation behaviour of merocyanine dyes in solid state	66
2.4.1.5. Solvatochromic effect	67
2.4.1.6. Substituent effect	70
2.4.1.7. Fluorescence investigations of merocyanine dyes	71
2.5. Photo-E.M.F. measurements of <i>N</i>-alkyl-3- and -4-substituted pyridinium salts and stilbazolium compounds	72
3. Summary	74
4. Experimental part	79
General procedures and analytical data of the synthesized compounds	80
4.1. Synthesis of stilbazolium dyes 6 – 9	83
4.1.1. Dialkylated diesters 1a – d	83
4.1.2. Monoesters 2a – d	84
4.1.3. Alcohols 3a – e	85
4.1.4. Alkyl halides 4a – e	86
4.1.5. Picolinium salts with <i>N</i> -(2,2-dialkyl ethyl) substituents 5a – e	88
4.1.6. <i>N</i> -(2,2-dialkyl ethyl)-4'-oxy-stilbazolium dyes 6a – e	89
4.1.7. <i>N</i> -(2,2-dialkyl ethyl)-4'-oxy-3'-alcoxy-stilbazolium dyes 7 – 9	94
4.2. Synthesis of stilbazolium dyes with secondary <i>N</i>-alkyl chain	97
4.2.1. Alcohols with secondary alkyl chain 10a – e	97
4.2.2. Halides with secondary alkyl chain 11a – e	98
4.2.3. Picolinium salts with secondary <i>N</i> -alkyl chain 12a – g	99
4.2.4. 4'-Hydroxy-stilbazolium dyes with secondary <i>N</i> -alkyl chain 13a – g	101
4.3. Synthesis of <i>N</i>-alkyl-4'-substituted-stilbazolium salts	107
4.3.1. <i>N</i> -alkyl-4-methyl-pyridinium salts 14a – n	107
4.3.2. <i>N</i> -alkyl-4'-oxy- and -hydroxy-stilbazolium compounds 15a – n	111

4.3.3. <i>N</i> -alkyl-4'-methoxy-stilbazolium salts 16a – f	120
4.3.4. <i>N</i> -alkyl-stilbazolium salts 17a – f	124
4.3.5. <i>N</i> -docosyl-4'-nitro-stilbazolium bromide 19	128
4.3.6. <i>N</i> -docosyl-4'-dimethylamino-stilbazolium bromide 20	129
4.4. Synthesis of <i>N</i>-alkyl-4- and -3-phenyl-pyridinium salts	131
4.4.1. <i>N</i> -alkyl-4-phenyl-pyridinium salts 21a – j	131
4.4.2. <i>N</i> -alkyl-3-phenyl-pyridinium salts 22a – f	136
5. References	140
6. Appendix	144

Abbreviations and symbols

AFM	Atomic Force Microscopy
A	Absorbance
bs	Broad singlet
c	Concentration
cmc	critical micelle concentration
Col _h	Columnar hexagonal
Col _r	Columnar rectangular
Cr	Crystalline state
cwmc	Critical wormlike micellar concentration
<i>d</i>	Layer periodicity distance
d	Doublet
D	Distance between the alkyl chains or aromatic cores
dec.	Decomposition
D-band	Dimer band
DBr	Deuterium bromide
DMF	Dimethyl formamide
DMSO	Dimethyl sulfoxide
<i>DN</i>	Donor number
D ₂ O	Deuterium oxide
DSC	Differential Scanning Calorimetry
E	Transition energy
E(t)	Dimroth parameter
h	Planck's constant
H _I	Hexagonal phase
H _{II}	Inverted hexagonal phase
HCl	Hydrochloric acid
HI	Hydrogen iodide
HOMO	Highest occupied molecular orbital
I _I	Cubic phase of spherical micelles
Iso	Isotropic state
ITC	Isothermal titration calorimetry
I _{II}	Inverted cubic phase of spherical micelles

J	Coupling constant
KOD	Kalium deuterioxide
l	Path length of the cell
L_{α}	Lamellar phase
L	Diameter of the fibre
LC	Liquid crystals
LiAlH_4	Lithium aluminium hydride
LiCl	Lithium chloride
m	Complex multiplet
M	Mesophase M
MC	Merocyanine dye
M-band	Monomer band
MeOH	Methanol
m. p.	Melting point
n	Number of carbon-atoms in the alkyl chain
N	Nematic phase
N_A	Avogadro's number
N_{col}	Columnar nematic phase
N_d	Discotic nematic phase
NMR	Nuclear magnetic resonance
P	Phosphorous
r.t.	Room temperature
R	Correlation coefficient
r_X^-	Ionic radius
SmA	Smectic A phase
SmC	Smectic C phase
SmG	Smectic G phase
t	Triplet
T	Temperature
T_c	Clearing temperature
T_m	Melting temperature
V_I	Bicontinuous cubic phase
V_{II}	Inverted bicontinuous phase
$U(t)$	Voltage

Z	Kosower parameter
ΔT	Mesophase temperature range
λ	Wavelength
ε	Absorption coefficient
ε_r	Dielectric constant (at 25°C)
μ	Dipole moment
ΔH	Transition enthalpy
δ	Chemical shift
κ	Specific conductivity
$\chi_{R, B}$	Brooker's parameters
2D	Two dimensional
3D	Three dimensional

1. Introduction and Problems

1.1. Theoretical part and literature

1.1.1 Ionic liquid crystals

1.1.1.1. General aspects

Ionic liquid crystals (Ionic LCs) can be considered as materials combining the properties of liquid crystals and ionic liquids. The ionic character means that some of the properties of ionic LCs may differ significantly from that of conventional liquid crystals.¹

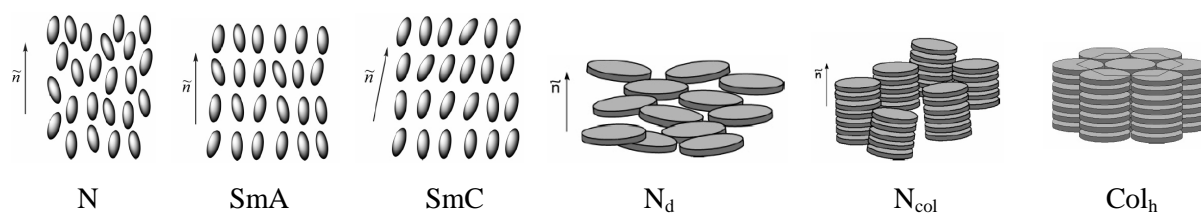
Ionic liquids is now a commonly accepted term for low-temperature molten salts. The low vapour pressure of the ionic liquids as well as miscibility with water and other solvents makes ionic liquids good candidates as solvents in organic reactions.¹ Properties of ionic liquids can be controlled to a large degree by variation of cation and the anion. The effect of the altering the anion has been quite widely investigated. Increasing the size of the anion gives rise to a reduction in the melting points of salts through reduction of Coulombic attraction contributions to the lattice energy of the crystal and increasing charge-transfer of the ions. The size and shape of the cation also play an important role in determining the melting points of the salts. A large range of ionic liquids form liquid-crystalline phases by increasing the amphiphilic character of the aromatic unit and by substitution with longer alkyl chain.²

Liquid crystals are partially ordered, anisotropic fluids, thermodynamically located between the three dimensionally ordered crystal state and the isotropic liquid.³ There are two classes of liquid crystals: thermotropic phases which occur by heating, and lyotropic phases which are induced in the presence of a solvent. Some compounds exhibit both thermotropic and lyotropic phases, as in the case of amphotropic molecules. Thermotropic liquid crystals can be enantiotropic, in which the liquid crystalline phase occurs in heating and cooling, and monotropic, in which the mesophase is observed only on cooling. Typical candidates for the formation of liquid crystals may be ionic liquids.

Ionic liquid crystals still represent a relatively small class of molecular and macromolecular species, although alkali metal salts and long-chain alkananoates were among the first thermotropic liquid crystals studied by Vorländer⁴.

Ionic liquid crystals are suitable to design anisotropic ion-conductive materials because they have ions as charge-carriers and anisotropic structural organization. Potential new applications may arise by combination of their anisotropic structural organization with optical and (photo) electrical properties of light absorbing molecular units.

Thermotropic liquid crystals are classified according to their chemical structure in calamitic for rod-like molecules, discotic for disc-like molecules and sanidic for brick- or lath-like molecules. The thermotropic phases are formed from a rigid aromatic core which can be rod-like (or calamitic) and disc-like (or discotic) and to which flexible chains are attached.³ In the nematic phase, the molecules tend to align themselves parallel to each other with their long axis parallel to a preferential direction (N , N_d). Rod-like molecules also form smectic phases (SmA , SmC ,...) in which the molecules are arranged in layers while the discotic molecules form columns which aggregate to columnar nematic (N_{col}) and columnar hexagonal or rectangular phase (Col_h , Col_r).⁵ A representation of some possible mesophases is given in Scheme 1.



Scheme 1. Schematic representation of some phases which are formed by rod-like and disc-like molecules: nematic phase (N), smectic A phase (SmA), smectic C phase (SmC) and by disc-like molecules respectively: discotic nematic phase (N_d), columnar nematic phase (N_{col}) and columnar hexagonal phase (Col_h), \vec{n} : preferential direction, called “director” of the phase.¹

Lyotropic phases are formed by molecules with a polar head group, which can be ionic or non-ionic, and a flexible lipophilic chain. Such structure is also typical for tensides. The formation of lyotropic phases is caused by the separation of hydrophilic polar and hydrophobic non-polar parts of the individual molecules and depends on the molecular structure of the molecules, solvent, concentration and temperature.⁵

The self-organization of the amphiphilic molecules in water, with formation of micelles or lyotropic LC phases, is driven by entropy changes in the aqueous phase, the so-called “hydrophobic effect”.⁶

Ionic liquid crystals can have also surfactant (**surface active agents**) or tenside properties. By aggregation of the surfactant monomers in water different aggregate morphologies including micelles, vesicles double layers (L_α) and inverted structures can be

formed. At low concentration, below the critical micelle concentration cmc, ionic surfactants behave as simple electrolytes. Above the critical micelle concentration (cmc for spherical micelles and cmc for worm-like micelles, simple fibres) the monomers assemble to form aggregates.⁷ An illustration of the most important lyotropic phases is given in Figure 1.

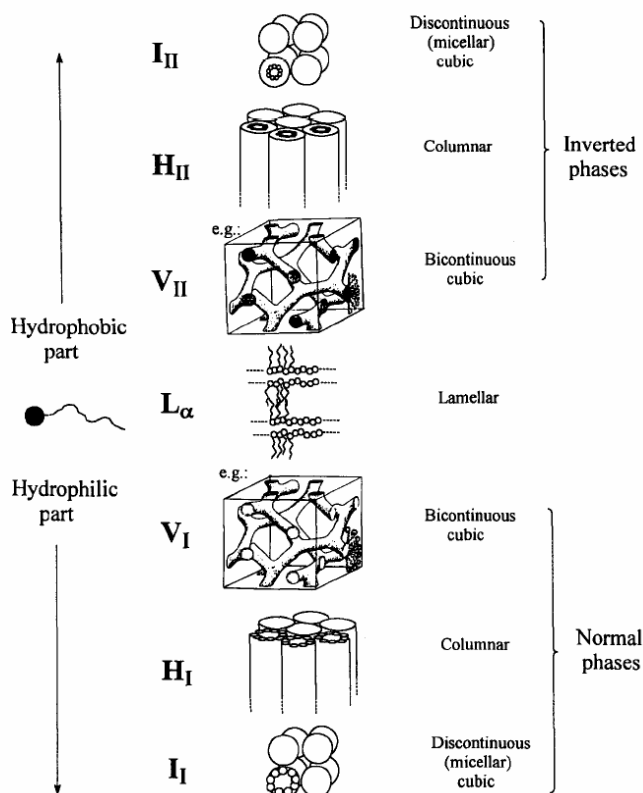


Figure 1. Illustration of the major lyotropic liquid crystalline phases (I_I and I_{II} – cubic and inverted cubic mesophases of spherical micelles; H_I and H_{II} – hexagonal and inverted hexagonal phases; V_I and V_{II} – bicontinuous cubic and inverted bicontinuous cubic phases; L_α – lamellar mesophase with alkyl chains in the molten state.⁵

The driving forces for the formation of ionic LCs are hydrophobic interactions of the alkyl groups and ionic, dipole-dipole, cation- π interactions as well as π - π stacking of the core groups.⁸ Therefore, the properties and stabilities of LC phases should depend on the relative contributions of these interaction forces, depending on the structure of the individual molecule from each series.

1.1.1.2. Pyridinium salts

In 1938 Knight and Shaw⁹ reported the first liquid crystalline pyridinium halides with alkyl chains n between 12 and 18 carbons and chloride and iodide as counter ions as well as a C_{12} pyridinium salt with a bromide anion. The clearing point temperatures decrease on

increasing the size of the anion in order chloride > bromide > iodide, whereas the melting points were less affected by changing the counter ion. The mesophase type of the salts was not identified. Later on, investigations on *N*-hexadecyl-pyridinium chloride indicate the formation of the SmA phase.¹⁰

Changing the anion with hexafluorophosphate results in the formation of SmA phases for the *N*-alkyl-pyridinium salts with alkyl chains $n = 16, 18$ (Figure 2a). Substitution of the methyl group on the 4-position of the pyridinium ring, compounds $[C_n\text{-4-Mepy}][PF_6]$, lowers the melting points and reduces the stability of the mesophase relative to pyridinium salts $[C_n\text{-py}][PF_6]$. The salts with $n = 16$ and 18 carbon atoms in the alkyl chain display only monotropic SmA phases, while salts with $n < 16$ do not show any liquid crystalline phases. Substitution of the methyl group at the 3-position of the pyridinium ring, compounds $[C_n\text{-3-Mepy}][PF_6]$, indicates the formation of the enantiotropic SmA phase when the alkyl chain is $n = 18$. The salt with $n = 16$ shows a monotropic behaviour over a temperature range of 3 °C.¹¹ Substitution of the methyl group at the 3-position of the pyridinium ring increases the tendency of formation of SmA phases related to the corresponding *N*-alkyl-4-methyl-pyridinium hexafluorophosphate salts $[C_n\text{-4-Mepy}][PF_6]$.

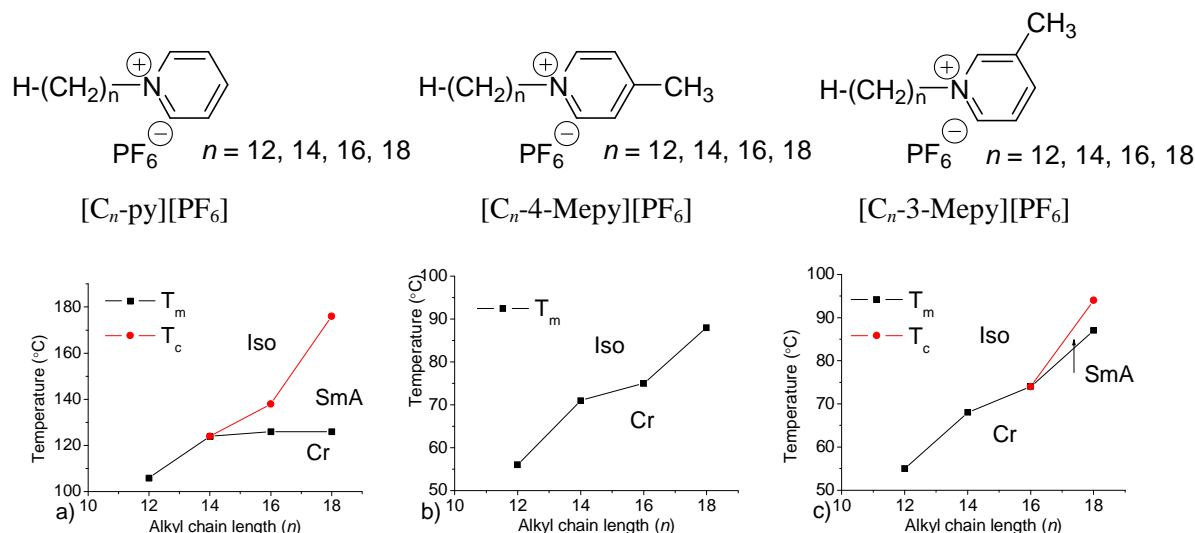


Figure 2. Transition temperatures T (°C) as a function of the alkyl chain length (n), on heating, for a) $[C_n\text{-py}][PF_6]$ b) $[C_n\text{-4-Mepy}][PF_6]$ c) $[C_n\text{-3-Mepy}][PF_6]$, n = number of C-atoms in the alkyl chain, Cr – Crystalline state; SmA – Smectic A phase; Iso – Isotropic liquid state; T_m – melting temperature; T_c – clearing temperature.¹¹

Changing the counter ion from hexafluorophosphate to bromide, compounds $[C_n\text{-4-Mepy}][Br]$, enantiotropic SmA phases for the salts with $n = 16, 18$ (Figure 3a) are induced,

indicating the significant influence of the counter ions on the LC behaviour¹². The stability of the mesophase increases with increasing alkyl chain length n .

Increasing the polarity of the salts by replacing the methyl group with a cyano group reduces the mesophase temperature range due to an increase of the melting points (Figure 3b).¹² In the case of non-ionic thermotropic liquid crystals, usually the presence of cyano group enhances the liquid crystalline properties and increases the mesophase temperature range.¹³ A partially bilayered SmB phase was found for *N*-hexadecyl-4-cyano-pyridinium iodide.¹⁴

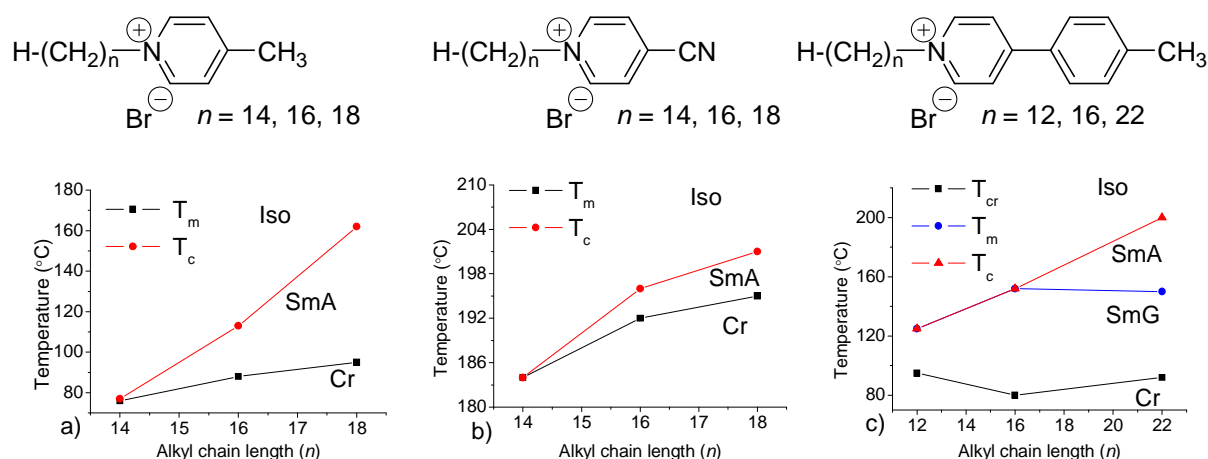


Figure 3. Transition temperatures T ($^{\circ}\text{C}$) as a function of the alkyl chain length (n), measured by DSC on heating, for a) *N*-alkyl-4-methyl-pyridinium bromide salts b) *N*-alkyl-4-cyano-pyridinium bromide salts c) *N*-alkyl-4-(*p*-tolyl)-pyridinium bromide salts.^{12, 15}

Tabrizian *et al.*¹⁵ compared the thermotropic behaviour of *N*-alkyl-(4-methyl or 4-(*p*-tolyl)-pyridinium bromides with alkyl chain lengths n from 12 to 22 (Figure 3c). The clearing temperatures are similar for both series, for the same alkyl chain ($n = 22$), indicating that ionic forces are primarily responsible for maintaining the layered structure of the compounds up to high temperature. Elongation of the ionic head group to a 4-phenyl-pyridinium unit induces the formation of a more ordered mesophase, identified as SmG.

Smectic phases were also found for *N*-alkyl-pyridinium and *N*-alkyl-3-methyl-imidazolium salts having chloride, tetrachlorocobaltate (II) and tetrachloronickelate (II) counter ions.¹⁶

The effect of the branching on the 4-position of the pyridinium unit was investigated for 1-methyl-4(C_{12} -alkyl)-pyridinium iodides¹⁷ and showed that the alkyl chain branching near the head group lowers the clearing points and, to a small extent, the melting points.

The suggested arrangement for the SmA phase of the *N*-alkyl-pyridinium salts is presented in Figure 4, in which the anions are positioned between the aromatic rings in an interdigitated structure.^{11, 15, 16, 17, 18}

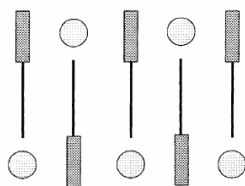


Figure 4. The propose interdigitated structure of the SmA phase of *N*-alkyl-pyridinium derivatives.^{11, 14, 15, 16, 17, 18} (organic moieties are represented by rectangles, alkyl chains by black lines and counter ions by circles).

Most of the salts can also form lyotropic liquid crystals.¹⁹ *N*-alkyl-pyridinium chlorides with alkyl chains n between 10 and 14 carbons form cubic phases (I₁) in water, while the bromides with alkyl chains n containing 18 and 20 carbons have a similar behaviour in formamide.²⁰

Formation of lyotropic liquid crystalline phases was also observed for different branched 1-alkyl-4-(C₁₂-alkyl)-pyridinium halides.²¹⁻²⁶ The branching of the 4-(C₁₂-alkyl) group and the hydrophobicity of the alkyl chains attached to the nitrogen lead to the formation of spherical micelles, rod-like micelles or vesicles.

The effect of the counter ion on the micelle formation was investigated for 1-methyl-4-*n*-dodecyl-pyridinium surfactants.⁷ It has been suggested that the degree of counter ion adsorption is inversely proportional to the effective radius of the hydrated ion.²⁷

Most of the investigations were carried out on pyridinium derivatives with a single aromatic core. Therefore, investigations on pyridinium derivatives with an elongated aromatic unit are of interest because the introduction of new additional forces may have an influence on the liquid crystalline behaviour.

1.1.1.3. Stilbazolium salts

In the case of stilbazolium type compounds, Figures 5a and b, besides ionic interactions, the formation of liquid crystalline phases should also be influenced by much stronger dipole-dipole interactions, for instance by introduction of hydroxy and methoxy groups at the 4'-position of the stilbazolium unit. Reports in the literature are spare and controversial. Therefore, more investigations of stilbazolium type compounds would contribute greatly to a better understanding of their behaviour.

Kosaka et al.²⁸ investigated *N*-alkyl-stilbazolium salts having an electron accepting NO₂ group at the 4'-position of the stilbazolium head group. These compounds, with a bromide counter ion, have a relatively narrow mesophase temperature range. The melting temperature shows an odd-even effect on variation of the alkyl chain length *n* from 5 to 10 carbon atoms (Figure 5a).

Replacing the bromides with chlorides the salts show a large temperature range of the SmA phase (Figure 5b). The iodide salts with *n* < 10 do not display any liquid crystalline behaviour. Thus, the counter ions play an important role in formation of liquid crystalline phases.

The introduction of cyano and methoxy groups in the 4'-position of the stilbazolium unit indicates that the salts with alkyl chains *n* between 6 and 10 carbons do not form liquid crystalline phases.²⁸

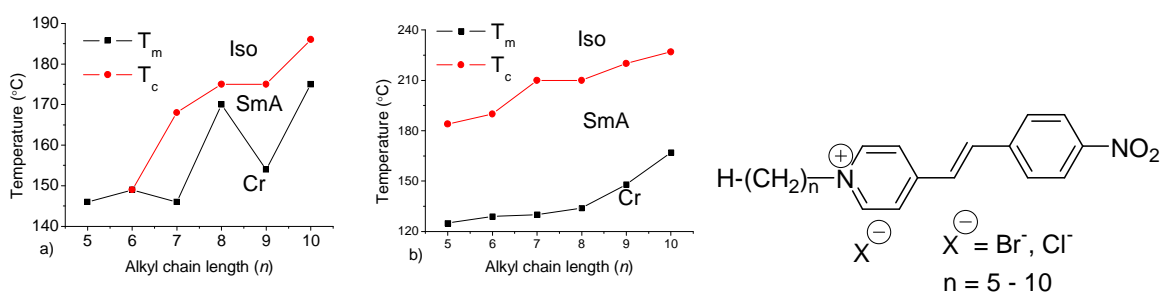


Figure 5. Transition temperatures *T* (°C) as a function of the alkyl chain length (*n*) a) for *N*-alkyl-4'-nitro-stilbazolium bromides b) for *N*-alkyl-4'-nitro-stilbazolium chlorides.

A dialkylamino group attached at the 4'-position of the stilbazolium core and alkyl chains between 14 and 18 carbon atoms attached to the pyridinium ring result in salts that show a reduced tendency for formation of SmA phases in the case of bromides.²⁹ Replacing the bromides by the bulky tetrakis(β-dikenoato)lanthanide (III) anions, the compounds do not display liquid crystalline properties, in contrast to results obtained by other authors.³⁰

These examples indicate the influence of the 4'-substituents at the stilbazolium core on the liquid crystalline behaviour.

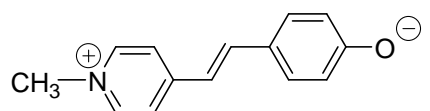
1.1.2. Merocyanine dyes

1.1.2.1. Supramolecular behaviour

Highly organized dye assemblies are crucial for the energy- and electron-transfer reactions in photochemistry and are also important for advanced functional organic materials

for electronics and photonics.³¹ Dye assemblies can be formed through various non-covalent weak forces, including hydrophobic, electrostatic, hydrogen-bonding, π - π stacking as well as coordinative interactions.³² Most of the dye assemblies give columnar liquid crystalline phases³³⁻³⁷ or organogels³⁸⁻⁴⁰ in the presence of solvents. Nevertheless, rational control of dye-dye interactions in supramolecular architectures is still a difficult task.

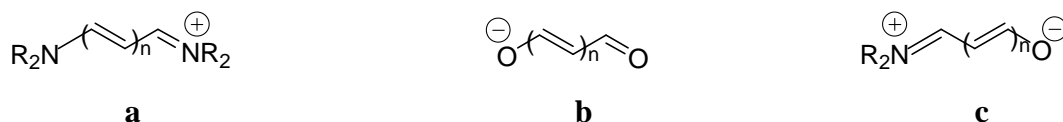
Merocyanine dyes of *N*-methyl-4'-oxy-stilbazolium type have a very similar molecular structure compared with stilbazolium salts forming LC phases, see Figure 5.



N-methyl-4'-oxy-stilbazolium dye

So, one can assume also the existence of LC-phases for merocyanines with structures derived from the stilbazolium compounds. This structural similarity may bear the chance for the synthesis of self-organized merocyanines or other polymethines shown in Scheme 2.

Polymethine dyes have attracted attention because of their use as sensitizers in colour photography⁴¹ and because of their extreme hyperpolarizability which makes them good candidates for nonlinear optics⁴²⁻⁴⁹. The term “polymethine dyes” was introduced by König⁴⁹ in 1922, and includes the cationic cyanine dyes **a**, the anionic oxonols **b** and the dipolar merocyanines **c** (Scheme 2).^{50, 51}



Scheme 2. General electronic structure of cyanine dyes **a**, oxonols dyes **b** and merocyanine dyes **c**.⁵⁰

Dyes used in any technical application mostly contain aromatic groups to increase attractive π - π forces. In the case of these organic dyes the driving forces for self-organization are attractive interactions between π -systems, leading to the formation of stacks of molecules.⁵² Therefore, the non dipolar merocyanine dyes of stilbazolium type are good candidates for aggregate formation. They have large dipole moments giving an antiparallel orientation of the stilbazolium unit which may lead to the formation of aggregates. The spectral properties of these dyes are known to be strongly affected by their aggregation behaviour, and extensive efforts are being made to control the mode of dye aggregation and especially the structure-aggregation relation.

The aggregation of the polymethine dyes was discovered by Scheibe⁵³ and Jelley⁵⁴ and it is a reversible process which depends on the dye concentration, the solvent and temperature, being influenced also by the salt effect.

Würthner *et al.*⁴⁰ investigated the spectral properties of a merocyanine dye attached to a tris (n-dodecyloxy)xylylene unit. Due to the high dipolarity of the **MC** dye, the electrostatic interactions are the dominant driving force for aggregation and leads to the formation of dimers with antiparallel dipole moments in solution.

A well-defined isosbestic point at 523 nm indicates the presence of two-state equilibrium between the monomer and the D-band (Figure 6).

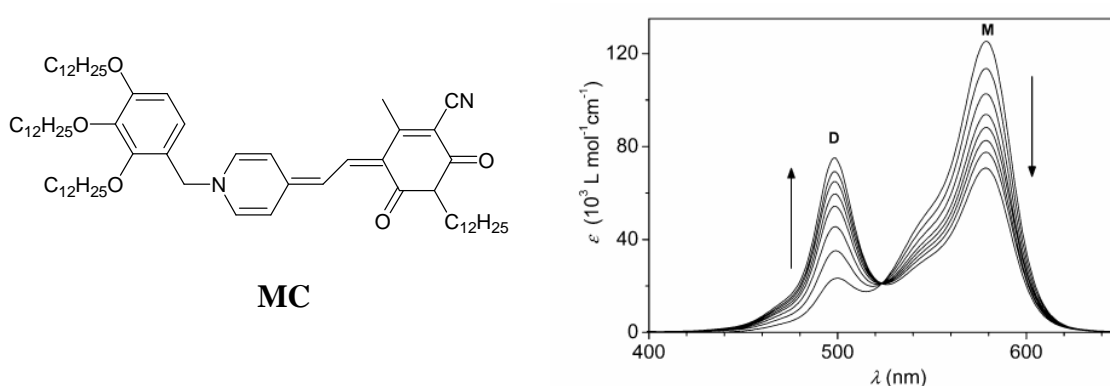
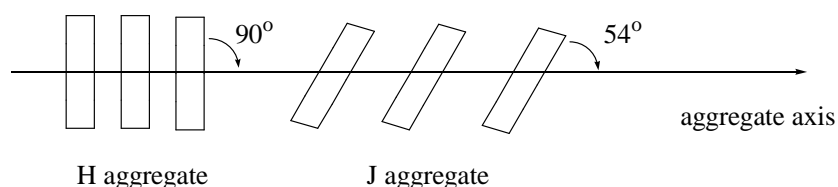


Figure 6. Concentration dependence in UV/Vis absorption spectra of the merocyanine **MC** dye in trichloroethene. The arrows indicate changes upon increasing concentration from $3 \times 10^{-6} \text{ mol l}^{-1}$ to $4.3 \times 10^{-5} \text{ mol l}^{-1}$.⁴⁰

Besides the formation of the dimers which absorb at shorter wavelength than the monomer, there are other two types of aggregates characterized by typical absorption bands: H-aggregates with a hypsochromic shift to shorter wavelength, and J-aggregates with a bathochromically shifted absorption band (to longer wavelength) relative to the monomer band depending on the angle of slippage, α , between successive molecular planes, (where α is the angle between the line-of-centres of a column, stacking axis, of dye molecules and the long axes of any one of the parallel molecules). When $\alpha > 54^\circ$ gives a hypsochromic shift, so called H-agregates, while $\alpha < 54^\circ$ results in a bathochromic shift characteristic of J-aggregates (Scheme 3).⁵⁵



Scheme 3. Schematic representation of different type of polymethine dye aggregate structures in solution.

Experimental investigations of ionic cyanine dyes revealed that the formation of J-aggregates is concomitant with the formation of supramolecular lyotropic liquid-crystalline phases with nematic or smectic order.⁵⁵

Merocyanine dyes of stilbazolium type with long alkyl chains may be also good candidates for thermotropic liquid crystalline behaviour. The simple *N*-alkyl-4-methylpyridinium salts with long alkyl chains *n*, which are intermediates for preparation of stilbazolium type compounds, display liquid crystalline phases on heating.^{15,18} For pyridinium derivatives the driving forces for the formation of liquid crystalline phases are hydrophobic forces between long alkyl chains and ionic interactions in ion pairs. Elongating the aromatic unit to stilbazolium type compounds introduces stronger dipole-dipole interactions which can influence the formation of liquid crystalline phases. Until now thermotropic behaviour of merocyanine dyes is not known.

1.1.2.2. Spectral properties

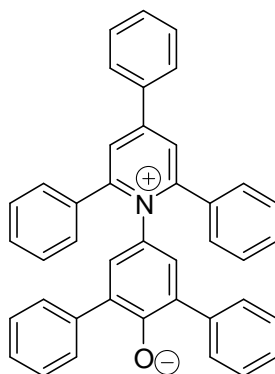
Merocyanines do show very interesting spectral and photochemical behaviour. Besides the possibility of aggregation, merocyanine dyes are sensitive to solvents showing large solvatochromic effect.⁵⁶⁻⁵⁹ In acidic or basic medium the dyes can undergo protonation-deprotonation reactions.⁴⁷ The presence of the C = C double bond between the aromatic rings creates the possibility of *cis-trans* isomerization, as is known for stilbene compounds.^{60, 61}

The extraordinary sensitivity of the electronic spectra of these compounds to solvent effects permits their use as sensitive probes of solvent polarity.⁶² The first solvatochromism of merocyanine dyes was reported by Brooker in 1951.⁶³ The term *solvatochromism* is used to describe the pronounced change in position (and sometimes intensity) of the UV/Vis absorption band that accompanies a change in the polarity of the medium. A hypsochromic (or blue) shift with increasing solvent polarity is usually named *negative solvatochromism*, while the *positive solvatochromism* corresponds to a bathochromic (or red) shift.⁶⁴ *N*-methyl-4'-oxy-stilbazolium dye exhibits one of the largest known *negative solvatochromic* effect, λ_{\max}

= 620 nm in chloroform at 442 nm in water, connected with a concomitant reduction of the extinction coefficient ϵ_{\max} as the solvent polarity increases. This strong *negative solvatochromism* was shown to be linearly correlated with the Dimroth parameter E_t for solvents with $E_t \geq 36$.⁶⁰ The electronic transition of stilbazolium betaine is associated with an intramolecular charge-transfer between donor and acceptor group, producing an excited state with a dipole moment appreciably different from that of the ground state.⁶⁴

N-methyl-4'-oxy-stilbazolium dye have a similar structure as 2,6-diphenyl-4-(2,4,6-triphenylpyridinium-1-yl)phenolate, which is a standard compound for investigation of solvatochromic behaviour.

The largest solvatochromic effect was observed for pyridinium *N*-phenolate betaine⁶⁵. A solution of this betaine changes the colour from red in methanol to yellow in anisole, thus comprising the whole visible region. The large solvent shift of this dye has been used to introduce an empirical parameter of solvent polarity, named $E_T(30)$ value, which is defined as the transition energy of the dissolved betaine dye measured in kcal mol^{-1} .⁶⁵



2,6-Diphenyl-4-(2,4,6-triphenylpyridinium-1-yl)phenolate

The similarity is only formal. Pyridinium betaines having an even number of methines are assigned as charge-transfer systems in contrast to polymethines with an odd number of methines.

Another parameter, Z was introduced by Kosower⁶⁶ for 1-ethyl-4-(methoxycarbonyl)pyridinium iodide which exhibits a negative solvatochromism. In this case the long wavelength band of the ground state ion pair complex corresponds to an intermolecular transfer of an electron from the iodide to the pyridinium ion with annihilation of charge during the transition. The Z parameter was defined as the molar transition energy, E_T , in kcal/mol according with the relation:⁶⁵⁻⁶⁷

$$E_T/(\text{kcal/mol}) = h c \nu N_A = 2.859 \cdot 10^{-3} \nu' / \text{cm}^{-1} = Z$$

where h is Planck's constant, c is the velocity of light, ν' is the wavenumber of the photon which produces the electronic excitation, and N_A is the Avogadro's number.

Therefore, it is of interest to investigate the spectral properties of the pyridinium salts due to the presence of the intermolecular charge-transfer, as well as of stilbazolium compounds with different alkyl chains which have an additional intramolecular charge-transfer.

1.2. Introduction of the synthesized and investigated compounds

Merocyanine dyes are known as thermotropic liquid crystals only when they have attached to aromatic core large substituents which alone do form thermotropic LC phases. Such compounds act like a covalently bound host-guest pair.⁶⁸

A new concept to overcome the strong dipole-dipole forces in merocyanines is the introduction of branched alkyl-substituents of two different types: *N*-(2,2-dialkyl-ethyl) substituents and secondary *N*-alkyl chains, compounds **6a** – **e** and **13a** – **g** respectively. The introduction of the methoxy and hexyloxy groups on the 3'-position of the stilbazolium core, compounds **7** and **9**, should also reduce the strong dipole moments.

In the same context is the reduction of the donor strength from the oxygen in the merocyanines **15**, by protonation or alkylation, salts **15h** – **n**, **16a** – **f** and **17a** – **f**. Both reactions will reduce the dipole moments μ to lower values, creating the possibility of obtaining thermotropic LC phases, as is known for a few stilbazolium compounds^{28,29}.

Some of the intermediate compounds as *N*-alkyl-4-methyl-pyridinium salts **14** with long alkyl chains n will form LC phases. Therefore, their properties will be also investigated.

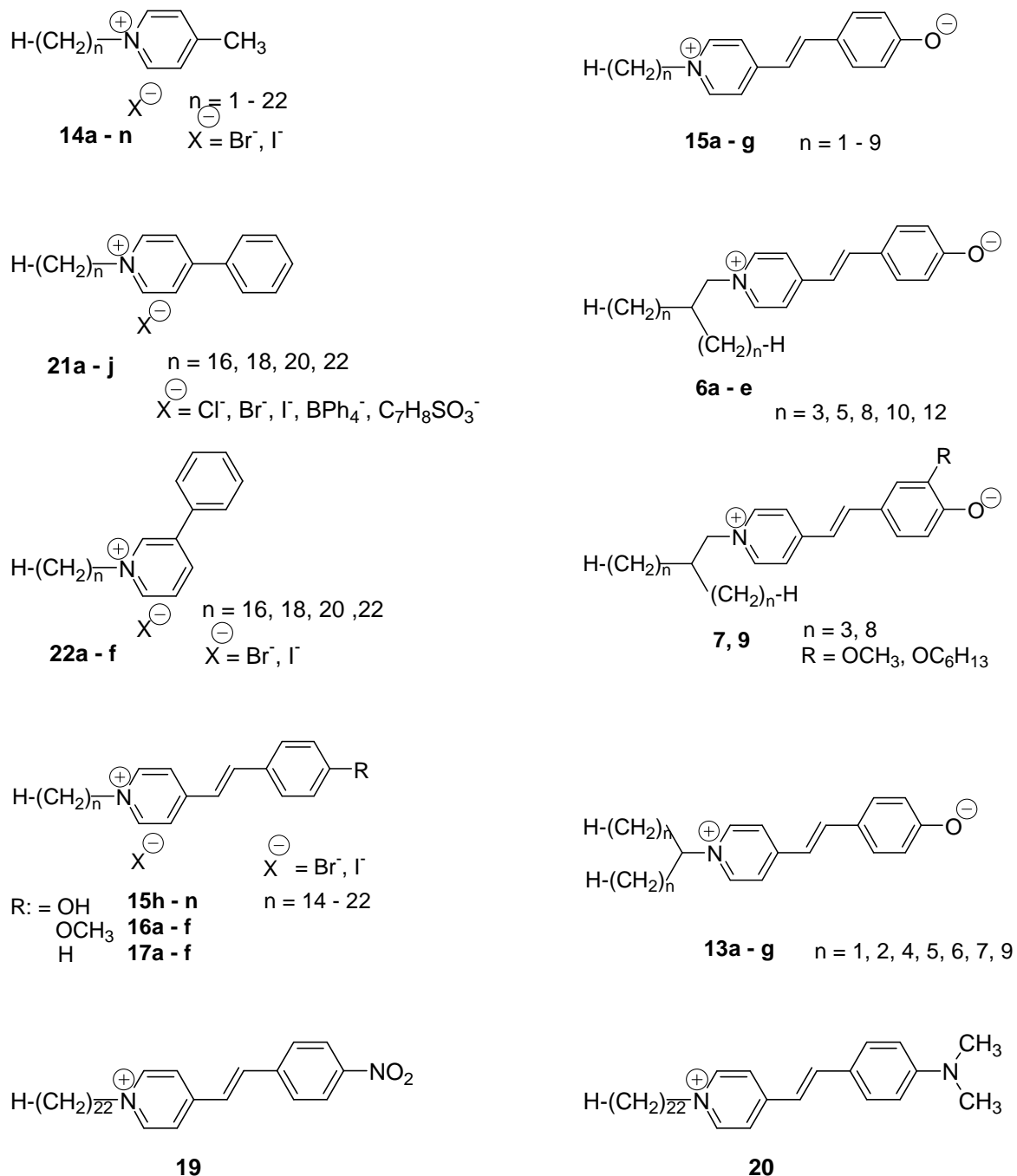
In the course of structure-property relations were synthesized and characterized two series of 4-phenyl and 3-phenyl-substituted *N*-alkyl-pyridinium salts **21a** – **j** and **22a** – **f** to get informations about the dimensional influence of the aromatic core on the LC-properties of these compounds. The influence of the counter ions and of the alkyl chains on the LC behaviour as well as on the spectral properties will be deeply discussed.

Compared with pyridinium derivatives, stilbazolium compounds exhibit much stronger dipole-dipole interactions in addition to the ionic forces. Therefore, it is of interest to investigate the structure-property relationship between pyridinium derivatives and stilbazolium halides with long alkyl chains.

N-alkyl-pyridinium ions will show mainly Coulombic forces. 4-Phenyl and 4-styryl substituted pyridinium ions should have additional charge-transfer forces. Introduction of hydroxy, methoxy and oxy substituents on the 4'-position of stilbazolium unit may increase the dipole moments, dominating the intermolecular forces.

UV/Vis spectroscopy has been utilized to investigate the aggregation behaviour of the pyridinium and stilbazolium compounds in solution, as well as the influence of the different substituents attached to the pyridinium ring on the spectral properties.

The general structure of the synthesized and investigated compounds is presented in the following scheme:



Scheme 4. General structure of the synthesized and investigated compounds, n – number of C-atoms in the alkyl chain.

2. Results and discussions

2.1. Synthesis

In this chapter will be presented the synthesis of the *N*-alkyl-4-methyl-pyridinium salts **14a – n**, *N*-alkyl-4-phenyl and 3-phenyl-pyridinium salts **21a – j** and **22a – f** respectively, *N*-alkyl-4'-substituted-stilbazolium salts **15h – n**, **16a – f**, **17a – f** and merocyanine dyes of stilbazolium type with different alkyl chains **6a – e**, **7**, **9**, **13a – g** and **15a – g**. The full procedures including the analytical data are presented in Experimental Part (chapter 4). The structure of compounds was identified by ^1H and ^{13}C NMR-spectroscopy, mass spectroscopy and elemental analysis. The new compounds are signed by an asterix.

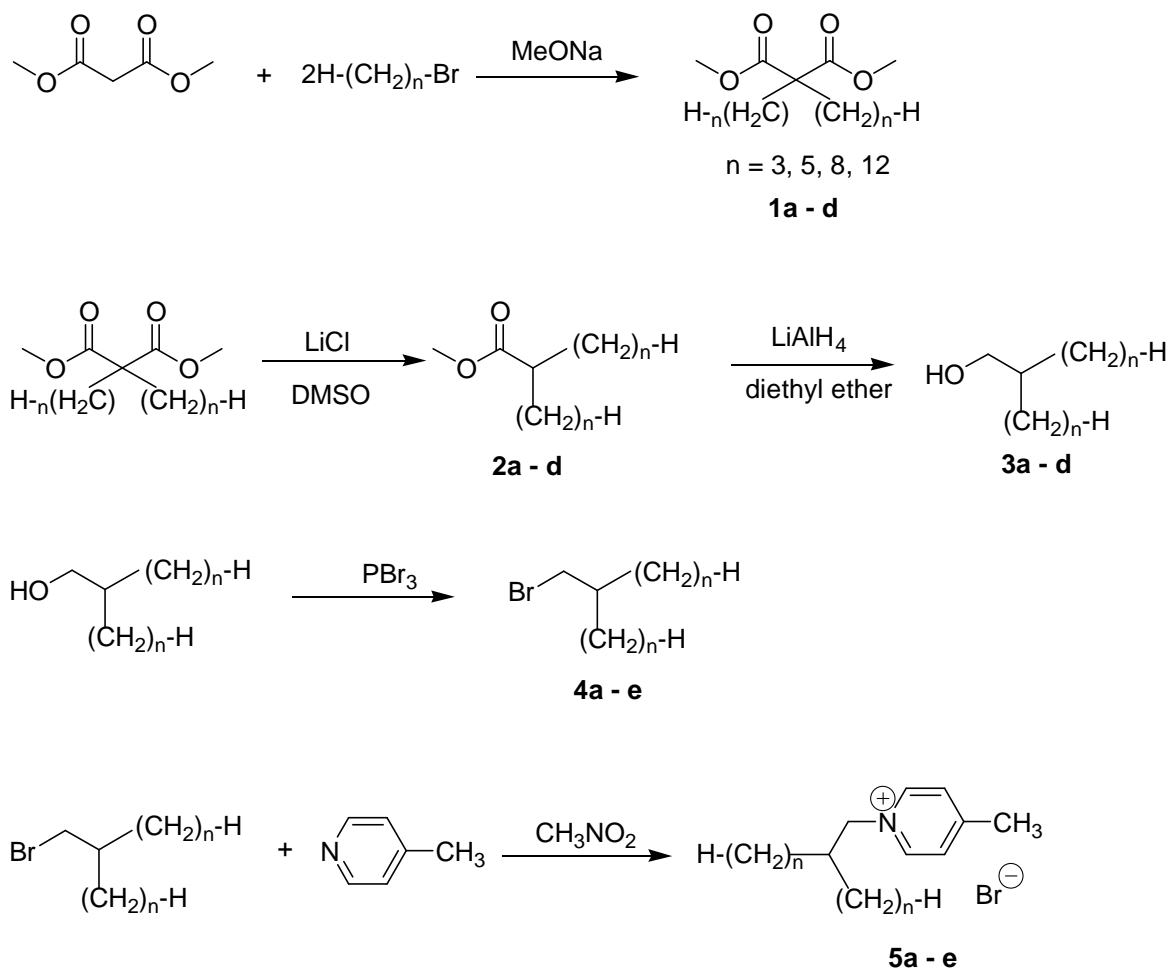
2.1.1. Synthesis of merocyanine dyes

Stilbazolium dyes with *N*-(2,2-dialkyl ethyl) chains, secondary alkyl and for comparison normal alkyl chains attached to the *N*-position of the stilbazolium unit were synthesized in the following procedures, in which the most important step is the condensation of pyridinium salts with 4-hydroxy-benzaldehyde.

For preparation of stilbazolium dyes **6a – e** with *N*-(2,2-dialkyl ethyl) substituents, the corresponding picolinium bromide salts were utilized for condensation with 4-hydroxy-benzaldehyde.

Compounds **4a – e** were prepared according to Scheme 5 by the following procedure: the first step was the double alkylation of dimethylmalonate in the presence of sodium methanolat using a modified procedure⁶⁹ to get the dialkylated diesters **1a – d**. The key step for the formation of **1a – d** is to obtain the monoalkylated diesters which are alkylated again with *n*-alkyl bromides by using a longer reaction time. The next step was the formation of dialkylated monoesters **2a – d** in the presence of lithium chloride and dimethyl sulfoxide⁷⁰ which were converted to the corresponding alcohols **3a – d** using lithium aluminium hydride as catalyst and dried diethyl ether as solvent. The alcohols were converted in the bromo compounds **4a – e** in the presence of phosphorous tribromide. Bromides **4a – b** with short alkyl chains were purified by water steam distillation while the compounds with long alkyl chains were purified by column chromatography.

4-Picolinium salts with *N*-(2,2-dialkyl ethyl) substituents were obtained by alkylation of 4-picoline with bromides **4a – e** in nitromethane (Scheme 5).

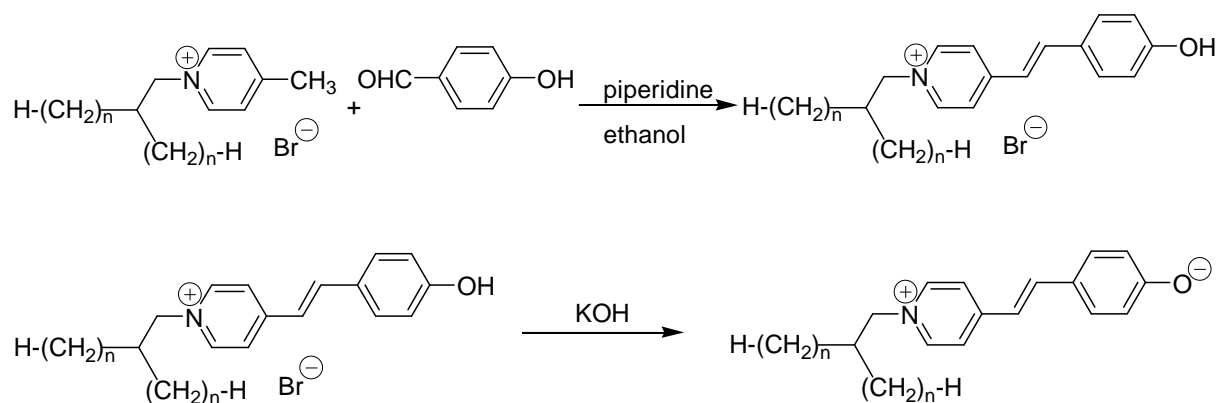


Comp.	5a*	5b*	5c*	5d*	5e*
<i>n</i>	3	5	8	10	12

Scheme 5. Synthesis of *N*-(2,2-dialkyl ethyl)-4-methyl-pyridinium bromides **5a – e**.

N-(2,2-dialkyl ethyl)-4-methyl-pyridinium bromide salts **5a – e** were converted to the corresponding dyes **6a – e** by Knoevenagel condensation with 4-hydroxy-benzaldehyde in the presence of piperidine and dry ethanol to give the corresponding stilbazolium salts, which were deprotonated using an aqueous solution of KOH.⁷¹

The dyes with long alkyl chains are not soluble in water therefore the deprotonation procedure was made using a mixture of KOH solution in water and methylen chloride and stirring over night at room temperature, followed by extractions with methylen chloride. A serie of stilbazolium dyes **6a – e** with 8, 12, 18, 22, 26 carbons in the lateral chains were synthesized (Scheme 6).

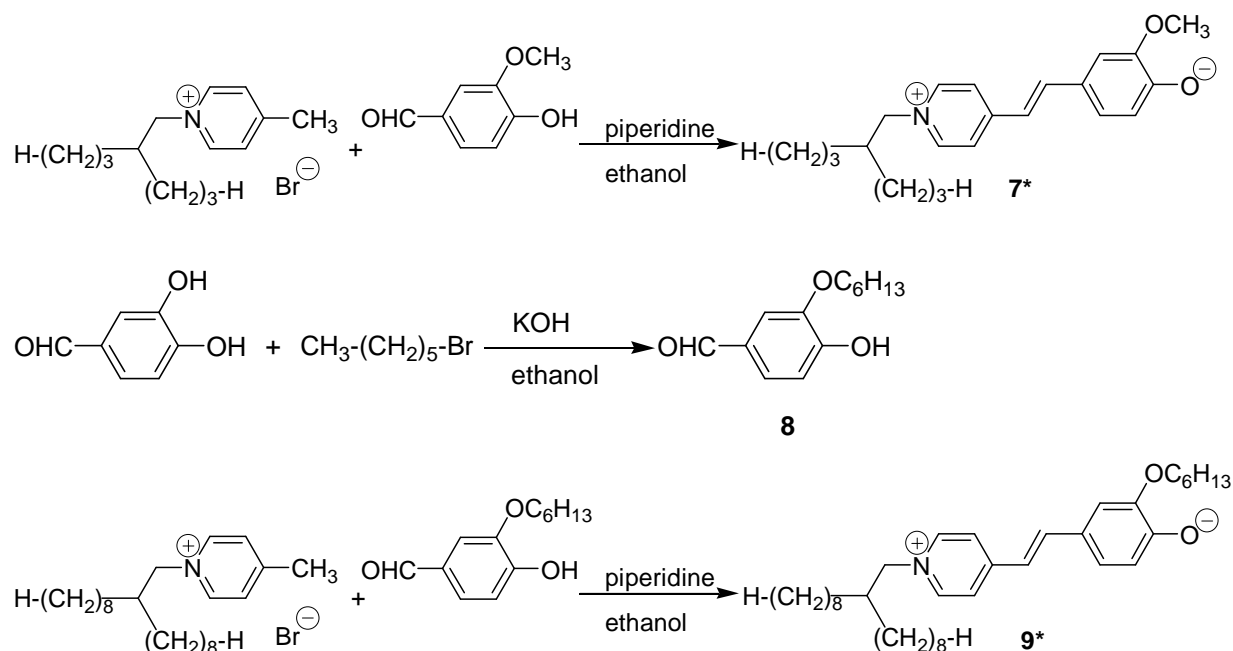


Comp.	6a*	6b*	6c*	6d*	6e*
<i>n</i>	3	5	8	10	12

Scheme 6. Synthesis of *N*-(2,2-dialkyl ethyl)-4'-oxy-stilbazolium dyes **6a** – **e**.

Dyes **7** and **9** were obtained by the same route using for condensation 1-(2-propyl)-pentyl-4-methyl-pyridinium bromide **5a** and 4-hydroxy-3-methoxy-benzaldehyde to give *N*-(2-propyl)-pentyl-4'-oxy-3'-methoxy-stilbazolium dye **7**. The substitution of 1-bromohexane to 3,4-dihydroxy-benzaldehyde in the presence of potassium hydroxide will lead to the formation of 4-hydroxy-3-hexyloxy-benzaldehyde **8**.⁷²

N-(2-octyl)-decyl-4'-oxy-3'-hexyloxy-stilbazolium dye **9** was obtained by condensation of **5c** with 4-hydroxy-3-hexyloxy-benzaldehyde **8** in the presence of piperidine and ethanol (Scheme 7).

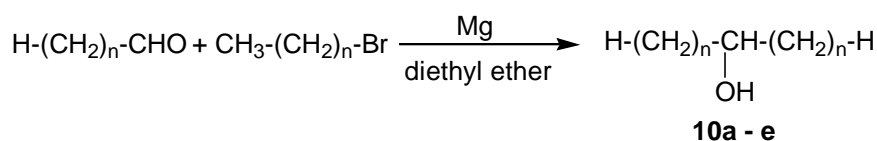


Scheme 7. Synthesis of *N*-(2,2 dialkyl ethyl)-4'-oxy-3'-alkoxy-stilbazolium dyes **7** and **9**.

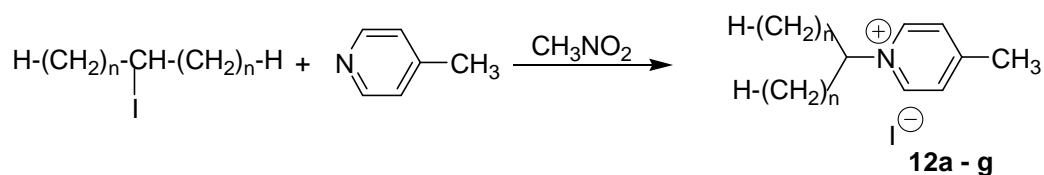
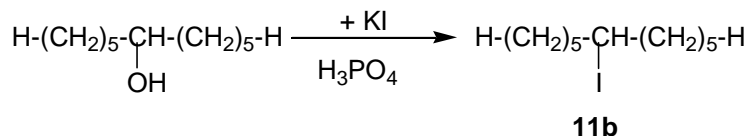
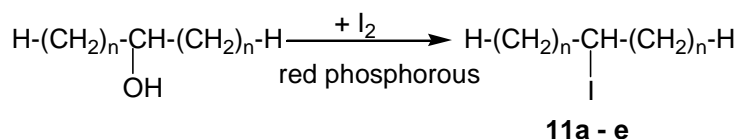
A next serie of dyes **13a – g**, not known in the literature, were synthesized from the corresponding salts **12a – g** and 4-hydroxy-benzaldehyde (Scheme 8). The first step was the preparation of the alcohols **10a – e** by Grignard reaction.⁶⁹ Secondary iodo-compounds **11a – e** were synthesized from the corresponding alcohols using red phosphorous and iodine. A good control of the temperature at 80-85 °C is required due to elimination of the HI and the formation of olefins at higher temperatures.

Compound **11b** was obtained by another procedure⁷³ using orthophosphoric acid and potassium iodide. Before mixing the potassium iodide and the alcohol, the orthophosphoric acid solution was cooled to room temperature, otherwise evolution of hydrogen iodide and formation of iodine take place. The reaction was heated up to 100 °C for 30 h. In order to increase the yields and to avoid elimination the procedure with iodine and red phosphorous was preferred.

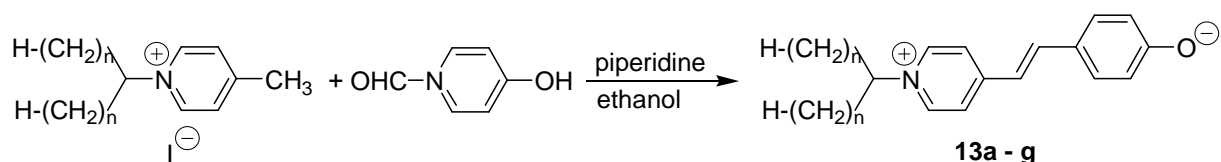
Salts **12a – g** with *N*-secondary alkyl chains were synthesized by alkylation of the corresponding iodide compounds **11** with 4-picoline in nitromethane.



Comp.	10a	10b	10c	10d	10e
<i>n</i>	4	5	6	7	9



Comp.	12a	12b*	12c*	12d*	12e*	12f*	12g*
<i>n</i>	1	2	4	5	6	7	9

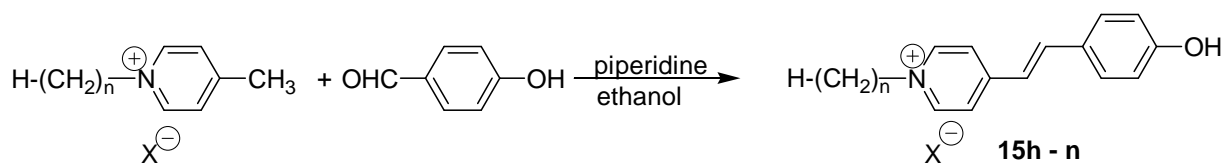
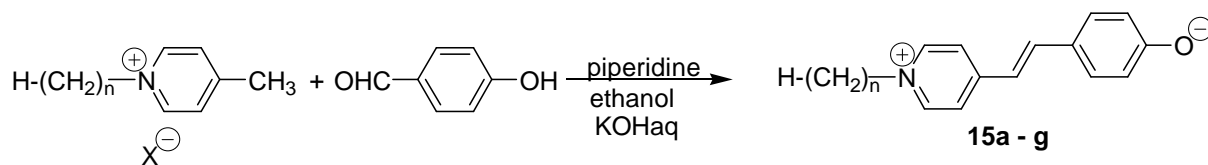
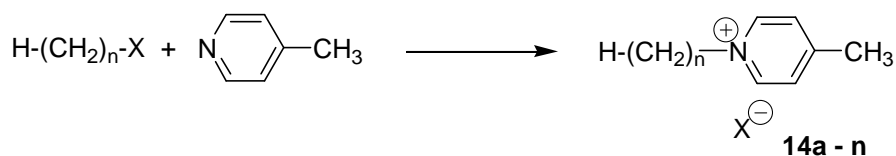


Comp.	13a*	13b*	13c*	13d*	13e*	13f*	13g*
<i>n</i>	1	2	4	5	6	7	9

Scheme 8. Synthesis of secondary *N*-alkyl substituted-4'-oxy-stilbazolium dyes **13a – g**.

2.1.2. Synthesis of *N*-alkyl-4'-substituted-stilbazolium compounds

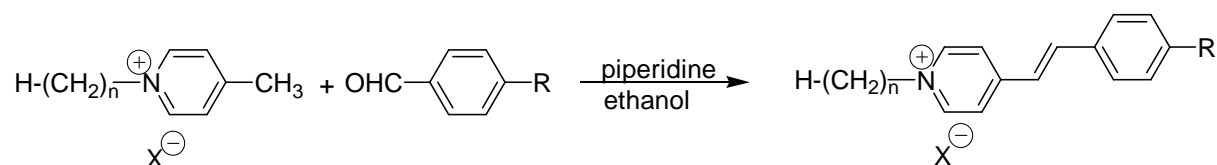
For comparison, stilbazolium compounds **15a – n** with *n*-alkyl chains at the nitrogen atom were synthesized starting with the quaternisation using *n*-alkyl bromides and iodides respectively of 4-picoline, followed by condensation of the salts (**14a – n**) with the commercial available 4-hydroxy-benzaldehyde (Scheme 9).⁷¹



Comp.	15a	15b	15c	15d	15e	15f	15g*	15h	15i	15j	15k	15l*	15m*	15n
<i>n</i>	1	3	4	5	6	8	9	14	16	16	18	18	20	22
<i>X</i>	-	-	-	-	-	-	-	Br ⁻	Br ⁻	I ⁻	Br ⁻	I ⁻	Br ⁻	Br ⁻

Scheme 9. Synthesis of *N*-alkyl-4'-oxy-stilbazolium dyes **15a – g** and *N*-alkyl-4'-hydroxy-stilbazolium salts **15h – n**.

Stilbazolium salts **16a – f** and **17a – f** were obtained by the same route as **15a – n**, by condensation of *N*-alkyl-4-methyl-pyridinium salts with 4-methoxy-benzaldehyde and benzaldehyde respectively (Scheme 10).



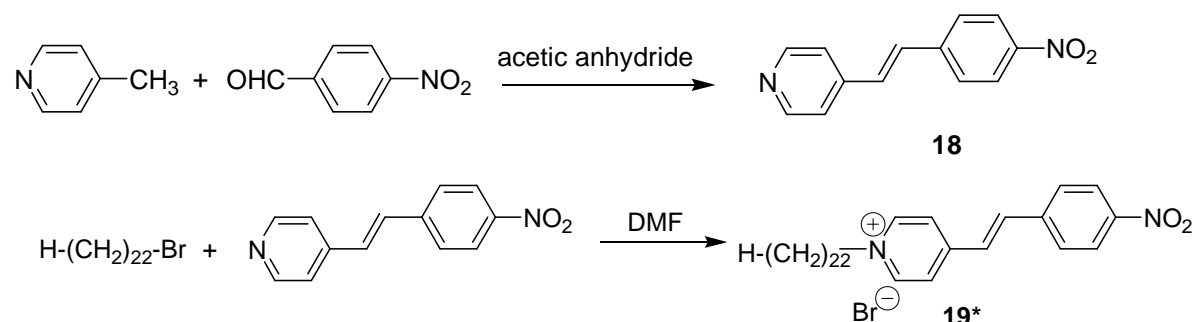
R: OCH₃ **16a - f**

H **17a - f**

Comp.	16a*	16b	16c	16d	16e*	16f*
Comp.	17a*	17b*	17c	17d	17e*	17f*
<i>n</i>	14	16	18	18	20	22
X ⁻	Br ⁻	Br ⁻	Br ⁻	I ⁻	Br ⁻	Br ⁻

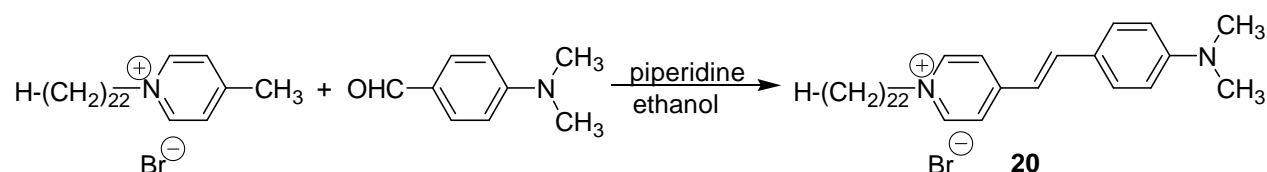
Scheme 10. Synthesis of *N*-alkyl-4'-methoxy-stilbazolium salts **16a – f** and *N*-alkyl-stilbazolium salts **17a – f** respectively.

N-docosyl-4'-nitro-stilbazolium bromide **19** was synthesized by alkylation of 4-(4-nitro-styryl)-pyridine **18** with 1-bromodocosane and using as solvent dimethyl formamide (Scheme 11).²⁸



Scheme 11. Synthesis of *N*-docosyl-4'-nitro-stilbazolium bromide **19**.

Compound **20** was prepared by condensation of 1-docosyl-4-methyl-pyridinium bromide with 4-dimethylamino-benzaldehyde in the presence of piperidine and ethanol to give *N*-docosyl-4'-dimethylamino-stilbazolium bromide **20** (Scheme 12).

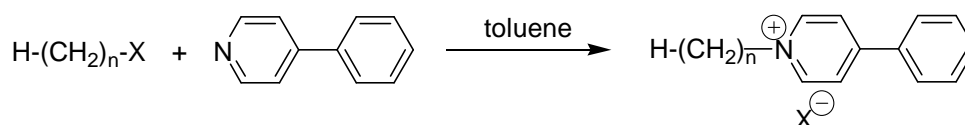


Scheme 12. Synthesis of *N*-docosyl-4'-dimethylamino-stilbazolium bromide **20**.

2.1.3. Synthesis of *N*-alkyl-4- and -3-phenyl-pyridinium salts

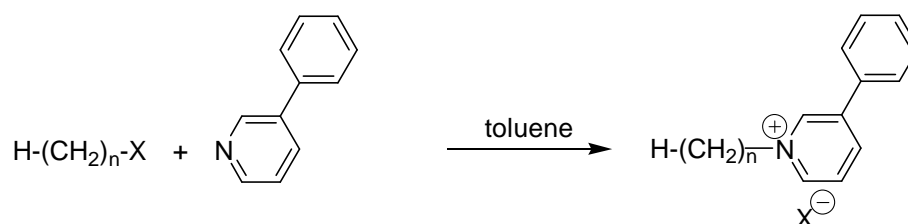
New series of *N*-alkyl-4- and -3-phenyl-pyridinium compounds **21** and **22** were synthesized by alkylation of 4-phenyl-pyridine or 3-phenyl-pyridine in toluene with the commercial available *n*-alkyl halides to give *N*-alkyl-4-phenyl-pyridinium salts **21a – j** and *N*-alkyl-3-phenyl-pyridinium halides **22a – f** (Schemes 13 and 14).

Salts **21f**, **h**, **i** and **j** were obtained by a modified ion exchange procedure⁷⁴ from **21g**, Dowex ion exchange resin, NaCl or NaI, NaBPh₄, C₇H₈SO₃H and methanol as a solvent.



Comp.	21a*	21b*	21c*	21d*	21e*	21f*	21g*	21h*	21i*	21j*
<i>n</i>	16	16	18	18	20	22	22	22	22	22
X ⁻	Br ⁻	I ⁻	Br ⁻	I ⁻	Br ⁻	Cl ⁻	Br ⁻	I ⁻	BPh ₄ ⁻	C ₇ H ₈ SO ₃ ⁻

Scheme 13. Synthesis of *N*-alkyl-4-phenyl-pyridinium salts **21a – j**.



Comp.	22a*	22b*	22c*	22d*	22e*	22f*
<i>n</i>	16	16	18	18	20	22
X ⁻	Br ⁻	I ⁻	Br ⁻	I ⁻	Br ⁻	Br ⁻

Scheme 14. Synthesis of *N*-alkyl-3-phenyl-pyridinium salts **22a – f**.

2.2. Properties of *N*-alkyl-4- and -3-substituted-pyridinium salts

N-Alkyl-4-methyl-pyridinium salts **14h – n**, *N*-alkyl-4-phenyl-pyridinium salts **21a – j** and *N*-alkyl-3-phenyl-pyridinium salts **22a – f** with alkyl chains $n > 14$ have been investigated by polarizing microscopy, differential scanning calorimetry, X-ray measurements as well as atomic force microscopy and UV/Vis spectroscopy. The influence of the alkyl chain length n , counter ions and of the different substituents attached to the pyridinium ring on the liquid crystalline properties of the compounds has been investigated. Because some of the salts have also surfactant behaviour, their properties in aqueous solution have been studied by differential scanning calorimetry, isothermal titration calorimetry and atomic force microscopy. UV/Vis spectroscopy has been utilized to investigate the spectral properties of the pyridinium derivatives in solvents with different polarities.

2.2.1. Liquid crystalline properties

2.2.1.1. *N*-alkyl-4-phenyl-pyridinium salts

N-alkyl-4-phenyl-pyridinium salts **21d – i** show under polarizing microscopy focal-conic fan textures with homeotropic regions characteristic for smectic A phase, SmA (Figure 7a).

The transition temperatures and the corresponding enthalpies obtained by differential scanning calorimetry and polarizing microscopy for compounds **21a – j** are summarized in Table 1. The salts **21a** and **21b** with $n = 16$ do not form any LC phases.

Differential scanning calorimetry of compounds **21e** and **21g** show on heating first a large-enthalpy transition (melting point) followed by two transitions with a smaller enthalpy change indicating the presence of two mesophases. On cooling from the isotropic liquid, first the formation of a fan-like texture with homeotropic regions is observed under the polarising microscope, an indication of a smectic A phase. During the second phase transition the viscosity of the sample increases and a grainy texture is formed (see Figure 7b). A small transition enthalpy of this phase, in the case of compounds **21e** and **21g**, was detected by DSC on cooling at 122 °C. This mesophase M, appearing also for compound **21c**, could not be identified by X-ray methods, therefore the exact phase type cannot be assigned and the phase will be named M.

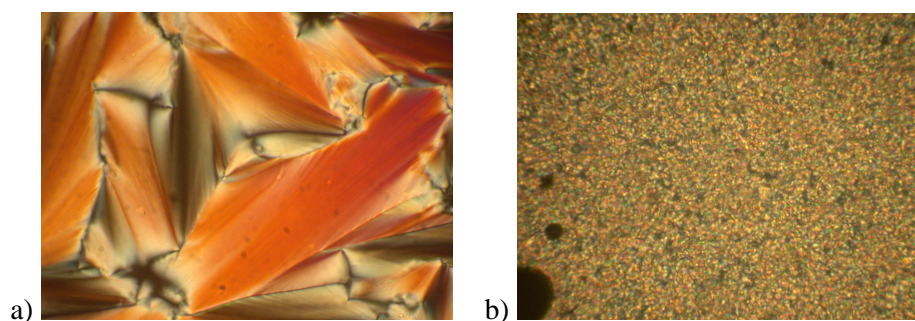


Figure 7. a) Fan-shaped texture in the smectic A phase of *N*-eicosyl-4-phenyl-pyridinium bromide **21e** at 152 °C on cooling b) Grainy texture in mesophase M of *N*-octadecyl-4-phenyl-pyridinium bromide **21c** at 100 °C on cooling.

The stability of the liquid-crystalline phase of compounds **21d** – **i** increases markedly with increasing alkyl chain length n (see Table 1). The phase diagram of the salts with a bromide anion is presented in Figure 8. Elongating the chain has no large influence on the melting temperature of the compounds, while the clearing temperature increases drastically. This may be explained by increasing hydrophobic stabilization of the aromatic unit by alkyl groups. The SmA temperature range ΔT increases from 22 °C up to 70 °C for the bromides **21e** ($n = 20$) and **21g** ($n = 22$).

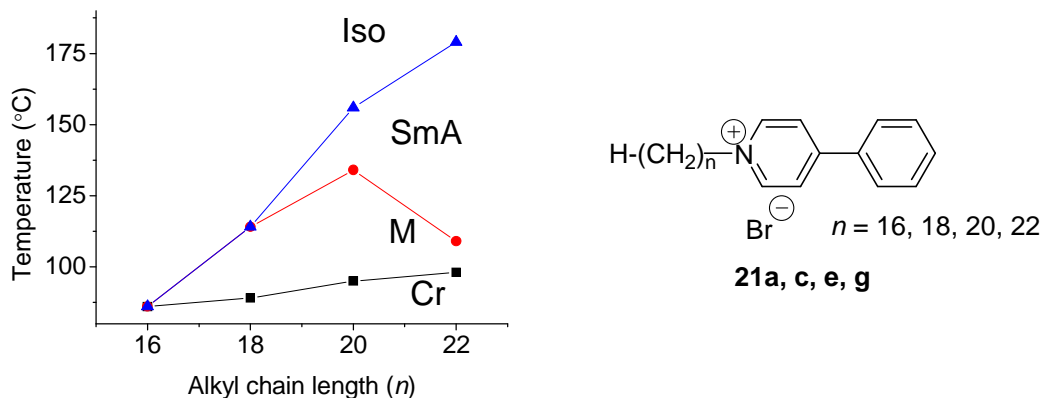


Figure 8. Transition temperatures T (°C) as a function of the alkyl chain length (n) for *N*-alkyl-4-phenyl-pyridinium bromides **21a**, **21c**, **21e**, **21g**.

Table 1 also contains thermal data for *N*-alkyl-4-phenyl-pyridinium iodides **21b**, **d**, **h**. Compared with the bromides, iodides have similar melting temperatures and generally lower clearing points with increasing alkyl chain length n .

Comp.	<i>n</i>	X ⁻	Phase transitions T (°C) ΔH (kJ/mol)	ΔT (°C)
21a	16	Br ⁻	Cr 86 Iso 49	-
21b	16	I ⁻	Cr 83 Iso 41	-
21c	18	Br ⁻	Cr 89 M 114 Iso 50.5 0.2	-
21d	18	I ⁻	Cr 90 SmA 98 Iso 51.9 0.05	8
21e	20	Br ⁻	Cr 95 M 134 SmA 156 Iso 46.8 1.1 0.12	22
21f	22	Cl ⁻	Cr 72 SmA 213 Iso 53.6 1.9	141
21g	22	Br ⁻	Cr 98 M 109 SmA 179 Iso 56.9 0.3 0.7	70
21h	22	I ⁻	Cr 95 SmA 161 Iso 66.3 0.7	66
21i	22	B(C ₆ H ₅) ₄ ⁻	Cr 78 SmA 151 Iso 67.2 1.2	73
21j	22	C ₇ H ₈ SO ₃ ⁻	Cr 94 Iso 52.6	-

Table 1. Transition temperatures T (°C) and enthalpies ΔH (kJ/mol) from Differential Scanning Calorimetry for *N*-alkyl-4-phenyl-pyridinium salts **21a – j**, ΔT (°C) – temperature range of the smectic A phase.

The anion effect was investigated in more detail for salts **21f – j** having 22 carbon atoms in the lateral chain. A large influence on the temperature range of the SmA phase was observed when replacing the bromide by iodide, chloride and tetraphenylborate. Compound **21j** with the flat *p*-toluenesulfonate exhibits no liquid crystalline phase. The melting temperatures of the salts with bromide and iodide anions are similar but the clearing temperatures decrease in the direction Cl⁻ > Br⁻ > I⁻ > BPh₄⁻, with increasing ion radius *r*_{X⁻} (Table 2). Reducing the size of the anion leads to a better stabilization of the layers, also supported by observations on CPK models, because an anion with a smaller size is readily accommodated near the pyridinium cation. When the halides are replaced with tetraphenylborate which is composed of four phenyl units arranged tetrahedrally and has a larger size than the halides the clearing temperature decreases. For instance, upon increasing

the size of the counter ion from iodide ($r_{\Gamma^-} = 0.22$ nm, r_{Γ^-} – ionic radius of iodide) to tetraphenylborate ($r_{\text{BPh}_4^-} = 0.42$ nm, $r_{\text{BPh}_4^-}$ – ionic radius of tetraphenylborate) the clearing temperature decreases by 10 °C. Replacing the bromide with chloride leads to a decrease of the melting point and a strong increase in the clearing point of the salt **21f**. For this compound at temperatures higher than 200 °C a partial decomposition is observed.

Compound **21g** shows the additional mesophase M from 98 °C to 109 °C, which is observed only for the two Br^- -compounds **21c** and **21e** bearing different chain lengths (Figure 7c).

Comp.	21f	21g	21h	21i
X^-	Cl^-	Br^-	Γ^-	BPh_4^-
r_{x^-}	0.181	0.196	0.222	0.421
T	Cr 72 SmA 213 Iso*	Cr 98 M 109 SmA 179 Iso	Cr 95 SmA 161 Iso	Cr 78 SmA 151 Iso
ΔH	53.6 1.9	56.9 0.3 0.7	66.3 0.7	67.2 1.2
d	-	3.76 (130) 3.71 (150)	3.95 (130) 3.86 (150)	- 3.7 (150)

* Partial decomposition observed

Table 2. Influence of the size of the counter ions on the mesophase stability. r_{x^-} (nm) – ionic radius of Cl^- , Br^- , Γ^- , BPh_4^- ; ⁷⁵ **T** (°C) – Transition temperature; ΔH (kJ/mol) – Transition enthalpy; Cr – Crystalline state; SmA – Smectic A phase; Iso – Isotropic liquid state, **d** (nm) – layer distance at different temperatures (**T** (°C), given in parentheses).

The formation of a smectic A phase was confirmed by X-ray investigations on aligned samples of compounds **21e** and **21i**. The diffraction patterns show first and second order layer reflections on the meridian in the small angle region along with a diffuse outer scattering with a maximum of the intensity on the equator. This indicates a layer structure with liquid-like distributed lateral distances of the molecules, the long axes of the molecules being parallel to the layer normal (Figures 9 and 10). The maximum of the outer diffuse scattering of **21e** at $D = 0.45$ nm, corresponds to the average lateral distance of molecules of about 0.5 nm and is typically found for alkyl chains.⁷⁶ The formation of layered structures in the case of pyridinium salts is attributed to the attachment of the aliphatic chains to an ionic head group.

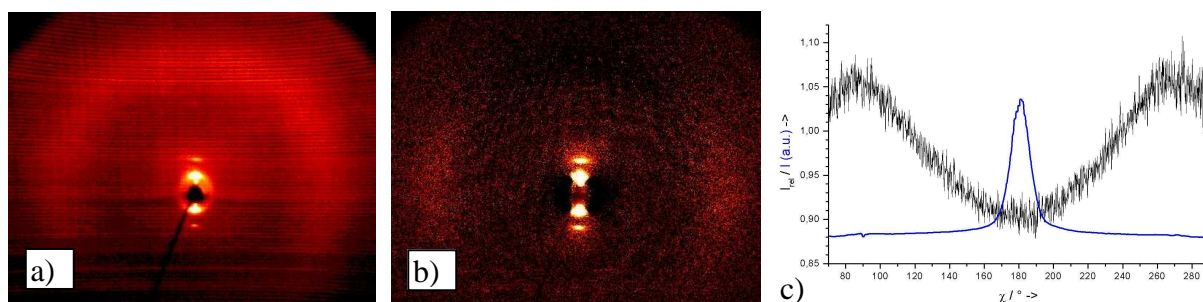


Figure 9. 2D X-ray diffraction patterns of the SmA phase for surface-aligned samples of *N*-eicosyl-4-phenyl-pyridinium bromide **21e** at 149 °C on cooling a) original b) the scattering of the isotropic liquid has been subtracted to enhance the visibility of the anisotropic distribution of the outer diffuse scattering, c) χ -scans for the 2D X-ray patterns in the SmA phase, black lines ... outer diffuse scattering, maxima on the equator of the patterns at $\chi \approx 90$ and 270° , $I_{\text{rel}} = I(\text{T}) / I(\text{isotropic liquid})$, blue lines ... layer reflections, maxima on the meridian of the patterns at $\chi \approx 180$, $I / \text{a.u.}$

In case of **21i** this value is slightly enhanced to 0.48 nm corresponding to an average lateral distance of the chains of about 0.54 nm, which may be explained by packing requirements described below.

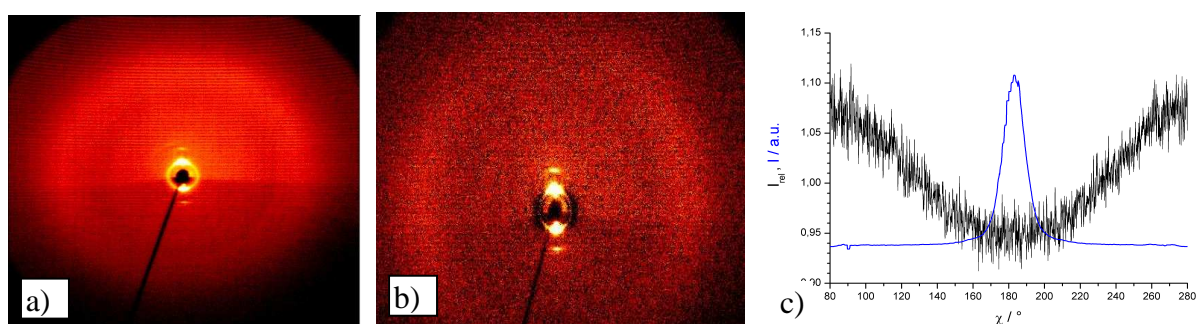


Figure 10. 2D X-ray diffraction patterns of the SmA phase for surface-aligned samples of **21i** at 149 °C in cooling a) original b) the scattering of the isotropic liquid has been subtracted to enhance the visibility of the anisotropic distribution of the outer diffuse scattering, c) χ -scans for the 2D X-ray patterns in the SmA phase of **21i** at 149 °C.

The layer spacing for **21e** is calculated as $d = 3.55$ nm at 130 °C (Table 3). Since the long axes of the molecules are, on average, parallel to the layer normal, this distance is the length of the building unit of the layers. A CPK model for the molecular packing in the smectic A phase of compound **21e** shows a head-to-tail arrangement of the molecules within the layer, and the bromide anion is localized between the aromatic rings (Figure 11). The location of the anion near the positive charged pyridinium ring indicates that the electrostatic interactions will stabilize the layers in the SmA phase by ionic pairing. The thickness of the

layer d calculated from CPK model is 3.55 nm, in agreement with the value obtained by X-ray measurements.

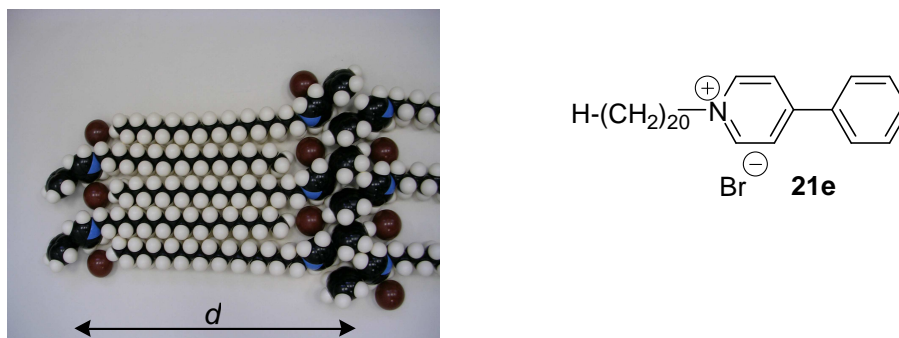


Figure 11. CPK model of compound **21e** assuming the all-*trans* conformation of the alkyl chains.

Upon increasing the number of carbon atoms n in the alkyl chain from 20 to 22, the layer distance determined by the X-ray measurements increases to $d = 3.76$ nm for compound **21g** at 130 °C, an expected enhancement for an elongation of the chains by two methylene groups. When the bromide ion is replaced by iodide, compound **21h**, the thickness of the layer is 3.95 nm at the same temperature. Obviously, the packing of the chains, most likely the degree of intercalation, is modified to accommodate the slightly bigger iodide ions. In the case of compound **21i** the layer distance d is 3.7 nm at 150 °C, with its much larger tetraphenylborate⁷⁷ counter ion which has a tetrahedral arrangement of the phenyl units. The comparatively small layer distance may be explained assuming a shortening of the effective chain length by a stronger disorder of the alkyl chains to fit the large space occupied by the anions. One hint of such stronger disorder may be the above mentioned slightly enhanced $D = 0.54$ nm of the outer diffuse X-ray scattering for **21i**.

The X-Ray data obtained from Guinier method are presented in Table 3. The results do not show large variation of the layer spacing d in the SmA phase by decreasing the temperature.

Comp.	T (°C)	θ_{obs} (°)	d_{obs} (nm)	n
21e	136	1.247	3.54	1
	130	1.243	3.55	1
	122	1.239	3.56	1
	115	230	3.59	1
21g	150	1.191	3.71	1
	140	1.182	3.73	1
	130	1.174	3.76	1
	120	1.162	3.80	1
	110	1.135	3.46	1
	100	2.549	1.73	1
21h	150	1.145	3.86	1
	140	1.135	3.89	1
	130	1.119	3.95	1
	120	1.105	4.00	1
	110	1.090	4.05	1
	100	1.075	4.11	1
21i	150	1.184	3.73	1
		2.351	1.88	2

Table 3. X-ray data for the SmA phases from Guinier powder patterns at different temperatures: θ_{obs} – experimental scattering angle; d_{obs} – experimental d spacing; n – order of reflection.

Mesophase M, observed by polarizing microscopy in the case of bromides **21c**, **e**, and **g** was investigated by 2D X-ray measurements. X-ray diffraction patterns of the phase M are presented in Figure 12 for compound **21c**. The type of the phase does not correspond to any classical thermotropic liquid crystals. The assumption that M is a liquid crystalline phase was made from the results obtained by DSC, which indicates a low energy transition between phase M and SmA mesophase typically for liquid crystals. Moreover, polarizing microscopy

investigation of this phase shows a grainy texture with a high viscosity with clearly changes by shearing.

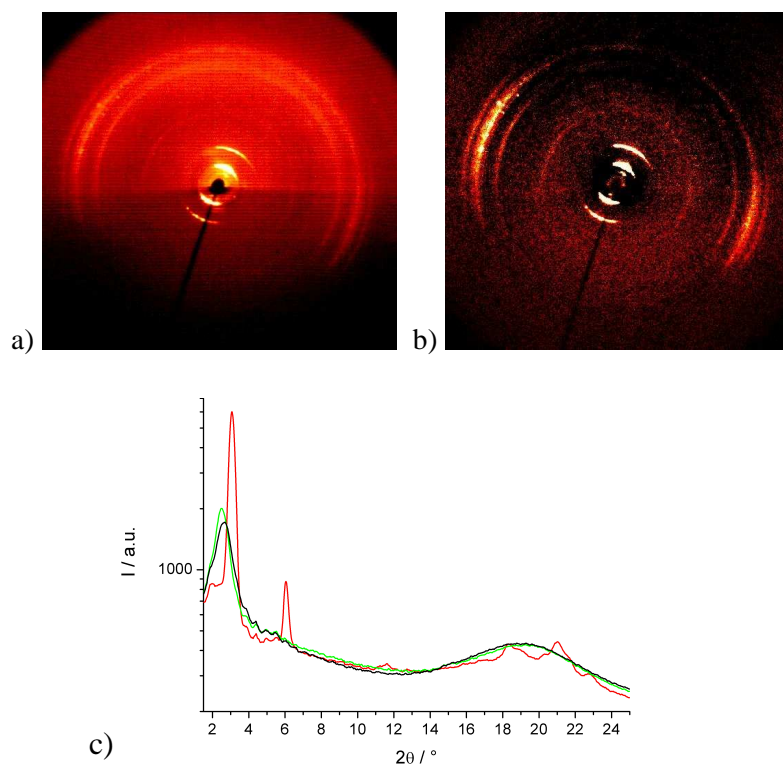


Figure 12. 2D X-ray diffraction patterns of the M phase of *N*-octadecyl-4-phenyl-pyridinium bromide **21c** a) original, at 113 °C, on cooling b) at 113 °C, the scattering of the isotropic liquid has been subtracted to enhance the visibility of the anisotropic distribution of the outer diffuse scattering c) θ -scans, χ integrated over $-15 - 335^\circ$, black ... 166 °C, green ... 125 °C, red ... 116 °C.

Similar results in 2D X-ray diffraction patterns of the M phase were obtained for compound **21e**. The layer reflections at different temperatures are presented in Figure 13.

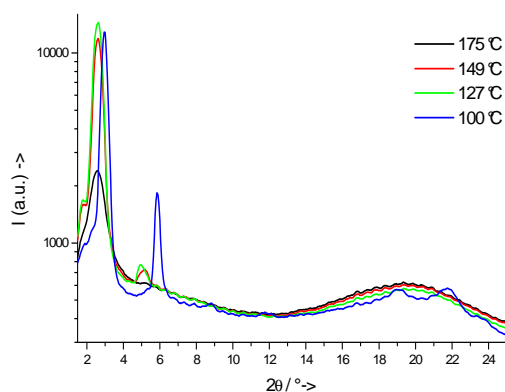


Figure 13. Layer reflection at different temperatures of compound *N*-eicosyl-4-phenyl-pyridinium bromide **21e** in cooling at different temperatures, θ -scans, χ integrated over $-15 - 330^\circ$.

Compared to salt **21g** no significant changes in the layer spacing were observed in the SmA phase of **21e**. The small decrease of the d value by increasing the temperature may be attributed to a disorder of the alkyl chains concomitant with lowering the viscosity of the sample (Table 3).

Dielectric measurements were made for compound **21d**. Due to the high conductivity no data about the dielectric permittivity can be given. The specific conductivity was calculated from the dielectric loss measured between 10^5 - 10^6 Hz with a voltage of 1V. Figure 14 shows the temperature dependence of the specific conductivity for the non-oriented liquid crystalline salt **21d**. The conductivity decreases linearly with the reciprocal absolute temperature in the isotropic and SmA phases. With beginning of the crystallization at about 80 °C, deviations from the linearity are observed. At the transition from the isotropic into the smectic A phase only a very small decrease of the slope and no step in the conductivity is seen.

A disadvantage of the measurements was that the sample could not be oriented and so the conductivity could not be investigated parallel and perpendicular to the layer normal. Nevertheless, the experimental data show that the formation of the smectic layers, which should increase stepwise the mean viscosity and therefore also to reduce the conductivity, has practically no influence on the conductivity. The small decrease of the slope of the conductivity in the SmA phase may be related to the better transport of charge carriers parallel to the layers in the smectic A phase than in the isotropic liquid.

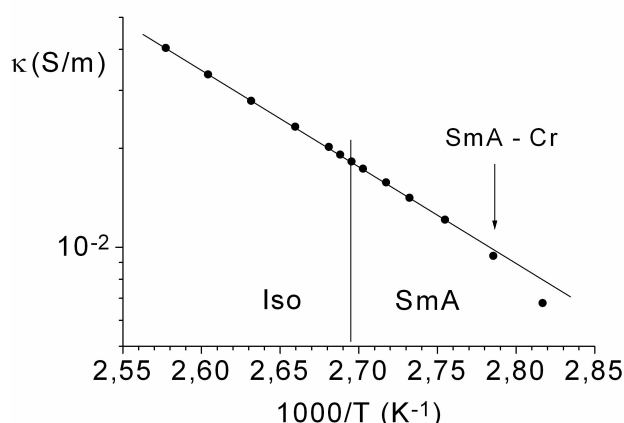


Figure 14. Specific conductivity κ (S/m) of *N*-octadecyl-4-phenyl-pyridinium iodide **21d** versus reciprocal temperature $1000/T$ (K^{-1}).

2.2.1.2. *N*-alkyl-3-phenyl-pyridinium salts

Changing the phenyl group from the *para* to the *meta* position, as shown for compounds **22a** – **f**, may influence the stability of the mesophase. Therefore, *N*-alkyl-3-

phenyl-pyridinium salts were synthesized in order to study the influence of the *meta*-substituted phenyl group on the mesophase behaviour.

Polarizing microscopy investigations indicate the formation of fan-like textures characteristic for the SmA phase (Figure 15a).

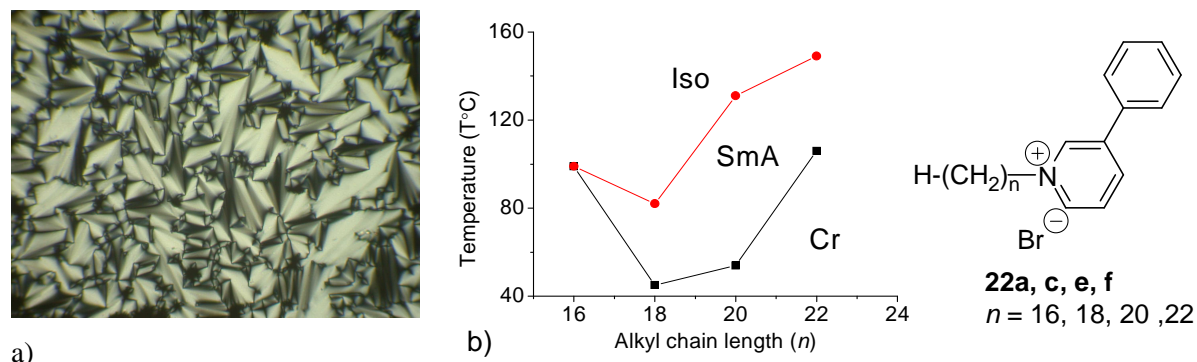


Figure 15. a) Fan-like texture of *N*-eicosyl-3-phenyl-pyridinium bromide **22e** in cooling at 129 °C b) Transition temperatures T (°C) as a function of the alkyl chain length (n) for *N*-alkyl-3-phenyl-pyridinium bromides **22a**, **c**, **e**, **f**.

The transition temperatures T measured by DSC and confirmed by polarizing microscope for compounds of type **22** are summarized in Table 4. Comparable to the *para*-substituted compounds **21**, the salts **22** containing alkyl chains with $n \geq 18$ do form SmA phases. No M-phases were detected.

Comp.	n	X^-	Phase transitions (T/°C) ΔH (kJ/mol)	ΔT (°C)
22a	16	Br^-	Cr 99 Iso 28.7	-
22b	16	I^-	Cr 77 Iso 30.6	-
22c	18	Br^-	Cr 45 SmA 82 Iso 31.4 0.34	37
22d	18	I^-	Cr 44 SmA 65 Iso 27.1 1.0	21
22e	20	Br^-	Cr 54 SmA 131 Iso 33.4 0.8	77
22f	22	Br^-	Cr_1 67 Cr_2 106 SmA 149 Iso 40.9 41.8 1.1	43

Table 4. Transition temperatures T (°C) and enthalpies ΔH (kJ/mol) from Differential Scanning Calorimetry for *N*-alkyl-3-phenyl-pyridinium halides **22a** – **f**, ΔT (°C) – temperature range of the smectic A phase.

The influence of the alkyl chains n on the transition temperatures T of the bromides **22a**, **c**, **e** and **f** is summarized in Figure 15b. An increase in the melting and clearing temperatures for **22c**, **e** and **f** was observed with increasing the alkyl chain length. The SmA temperature range increases from 37 °C for **22c** to 77 °C for compound **22e**. A decrease in the stability of the SmA phase was observed for compound **22f** with $n = 22$ carbons in the lateral chain.

The salt **22d**, with iodide as counter ion, shows a small temperature range of the SmA phase than the corresponding bromide, indicating that the size of the anion has an influence on the stability of the mesophase.

The SmA phase of **22e** was confirmed by X-ray measurements. The sample which is fibre-like aligned at the sample-air interface shows two-dimensional X-ray patterns measured at 129 °C and 109 °C on cooling which are characteristic for layer structures with liquid-like distributed lateral distances of the molecules and with a preference for the orientation of their long axes parallel to the layer normal (Figures 16a and b). The layer distance d amounts to 3.9 nm at 129 °C and the outer diffuse scattering shows its maximum at $D = 0.46$ nm. At 109 °C the maxima are much weaker, but the patterns show no other distinct differences.

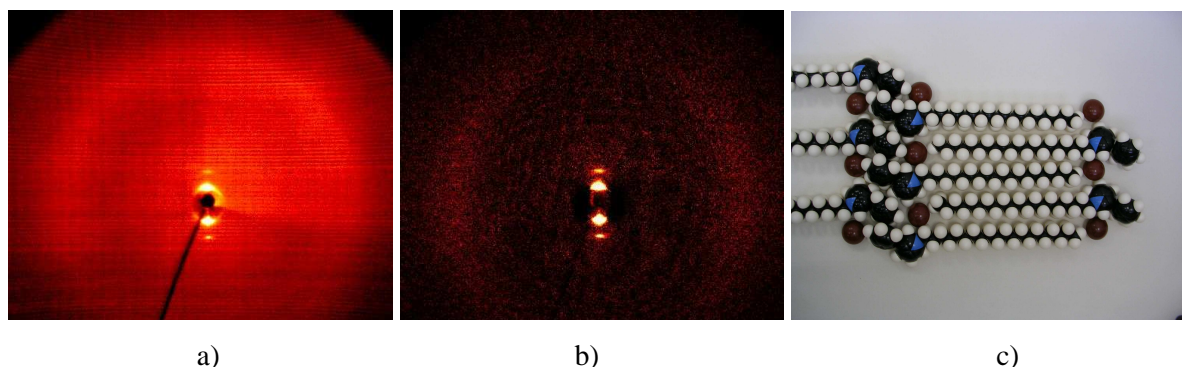


Figure 16. a) 2D X-ray diffraction pattern of the smectic A phase for the surface-aligned *N*-eicosyl-3-phenyl-pyridinium bromide **22e** at 129 °C on cooling b) 2D X-ray diffraction pattern at 129 °C on cooling - the scattering of the isotropic liquid has been subtracted to enhance the visibility of the anisotropic distribution of the outer diffuse scattering. c) CPK model of compound **22e** assuming the all-*trans* conformation of the alkyl chains.

The results obtained by Guinier method for *N*-eicosyl-3-phenyl-pyridinium bromide **22e** at different temperatures are presented in Table 5 and indicates an increase of the layer distance by lowering the temperature. This is attributed to a strong order of the alkyl chains which are more stretched by decreasing the temperature.

T (°C)	θ_{obs} (°C)	d_{obs} (nm)	n
125	1.125	3.93	1
	2.268	1.95	2
110	1.112	3.97	1
	2.241	1.97	2
95	1.100	4.02	1
	2.206	2.00	2
80	1.088	4.06	1
	2.169	2.04	2
65	1.062	4.16	1
	2.122	2.08	2
50	1.038	4.26	1
	2.088	2.12	2

Table 5. X-ray data for the SmA phase of *N*-eicosyl-3-phenyl-pyridinium bromide **22e** from Guinier powder patterns (T – temperature, θ_{obs} – experimental scattering angle; d_{obs} – experimental d spacing; n – order of reflection).

Upon increasing the length of the alkyl chains to 22 carbon atoms, compound **22f**, the thickness of the layer decreases to 3.8 nm. Therefore, one can assume that different other arrangements of the layers in the SmA phase are possible depending on the bent angle between the aromatic unit and the alkyl chain, stretching of the alkyl chains and position of the bromide near the pyridinium ring. The X-ray data obtained by Guinier method at different temperatures indicates a small increase of the layer distance by decreasing the temperature (Table 6).

T (°C)	θ_{obs} (°C)	d_{obs} (nm)	n
140	1.175	3.76	1
130	1.162	3.80	1
120	1.138	3.88	1
110	1.138	3.88	1

Table 6. X-ray data for the SmA phase of *N*-docosyl-3-phenyl-pyridinium bromide **22f** from Guinier powder patterns (T – temperature; θ_{obs} – experimental scattering angle; d_{obs} – experimental d spacing; n – order of reflection).

The CPK model of salt **22e** shows a head to tail arrangement of the molecules with the anion localized between the aromatic rings (Figure 16c), a similar arrangement as for salts **21**.

By increasing the alkyl chain length n the melting temperatures become lower than in the case of the *para*-substituted phenyl bromides **21**, but the SmA temperature range becomes larger.

2.2.1.3. *N*-alkyl-4-methyl-pyridinium salts

In order to compare the influence of the substituents at the pyridinium ring on the stability of the SmA phase, *N*-alkyl-4-methyl-pyridinium halides **14h** – **n** with different alkyl chains n were synthesized. Compounds of type **14** with $n > 14$ show focal conic textures characteristic of a SmA phase under polarizing microscopy (Figure 17a).

The transition temperatures and enthalpies are presented in Table 7 indicating that compounds **14** exhibit more stable mesophases. Salts **14** with $n \geq 16$ have larger ΔT values than **21** and the related compounds **22**.

Comp.	n	X^-	Phase transitions (T/°C) ΔH (kJ/mol)	ΔT (°C)
14h	14	Br ⁻	Cr 77 Iso 25.4	-
14i	16	Br ⁻	Cr 85 (84) SmA 119 (109) Iso 39.1 (44) 0.3 (0.3)	34
14j	16	I ⁻	Cr 67 SmA 104 Iso 11.1 0.3	37
14k	18	Br ⁻	Cr 82 (92) SmA 168 (158) Iso 38.8 (59) 0.8 (0.7)	86
14l	18	I ⁻	Cr 84 SmA 142 Iso 44.6 0.6	58
14m	20	Br ⁻	Cr 84 SmA 197 Iso 51.6 0.9	113
14n	22	Br ⁻	Cr 91 (94) SmA 207 (206) Iso 75.4 (69) 1.1 (2)	116

Table 7. Transition temperatures T (°C) and enthalpies ΔH (kJ/mol) from Differential Scanning Calorimetry for *N*-alkyl-4-methyl-pyridinium halides **14h** – **n**, ΔT (°C) – temperature range of the smectic A phase. The values in parentheses correspond to those reported in reference 15.

Transition temperatures and corresponding enthalpies summarized in Table 7 agree to a great extent with those from known compounds **14i**, **k** and **n**.¹⁵ The packing of the molecules is considered to be interdigitated, with the anions sandwiched between the pyridinium rings (Figure 17b).

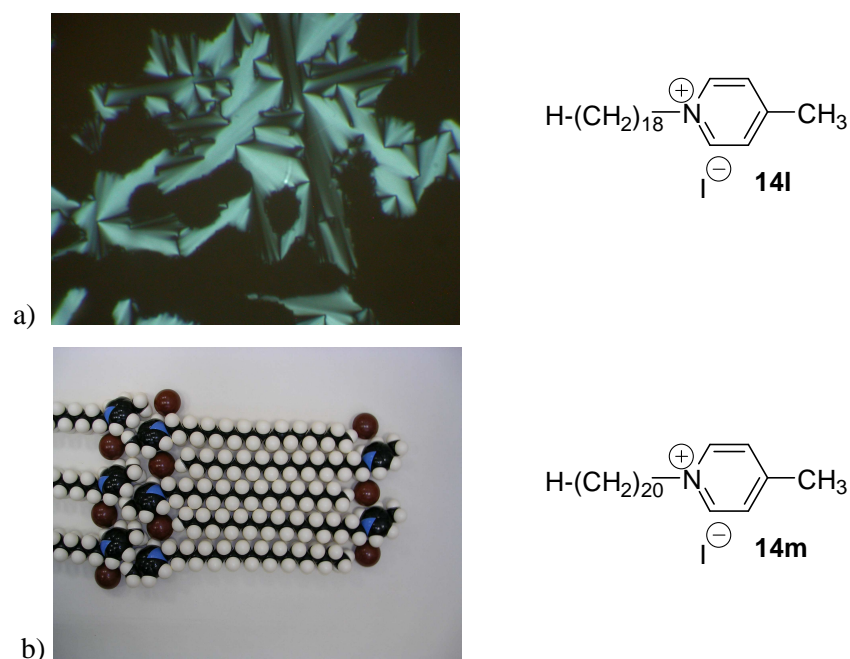


Figure 17. a) Fan-shaped texture of compound **14i** in cooling at 135 °C b) CPK model of compound **14m** assuming the all-*trans* conformation of the alkyl chains.

The presence of the methyl instead of phenyl group in the *para*-position of the pyridinium ring induces a larger temperature range for the SmA phase than *N*-alkyl-3-phenyl and 4-phenyl-substituted pyridinium salts with comparable long alkyl chains. This indicates that elongation of the aromatic unit plays an important role in the stability of the SmA phase. When the aromatic core is extended by replacing the methyl group with a phenyl substituent, compounds **21**, the clearing temperatures decrease indicating that an aromatic core destabilizes the mesophases. Additionally, it leads to the formation of an ordered intermediate phase M. The M phase was observed only in the case of *N*-alkyl-4-phenyl-pyridinium salts having bromide as counter ion. The more bulky 3-phenyl-pyridinium head group in **22** lowers the melting points drastically and reduces the temperature range of LC phases. The temperature range of the SmA phase increases upon attaching substituents to the pyridinium unit in the order 4-methyl (**14**) > 3-phenyl (**22**) > 4-phenyl (**21**).

2.2.2. UV/Vis investigations of *N*-alkyl-3- and -4-substituted pyridinium salts

Compounds **14**, **21** and **22** were investigated by UV/Vis spectroscopy and show deviations from the Lambert-Beer law indicating the presence of new species in solution in the case of iodides.

To gain a better understanding of this effect the spectral properties of *N*-octadecyl-4-phenyl-pyridinium iodide **21d** in 1,2-dichloroethane were investigated (Figure 18a). The UV/Vis spectrum shows two absorption bands at 219 nm and 305 nm and with increasing concentration a new one at 370 nm. A plot of the maximum absorbance at 305 and 370 nm *versus* concentration shows deviations from the Lambert-Beer law which indicates that additional ion pairs are formed in solution. The long wavelength absorption corresponds to a charge-transfer band which arises from an ion pair between the iodide anion as electron donor and the pyridinium ring as acceptor. This ion pairing in solution will support the suggested structure in the CPK models in Figures 11 and 16c with the localization of X^- near the pyridinium ring.

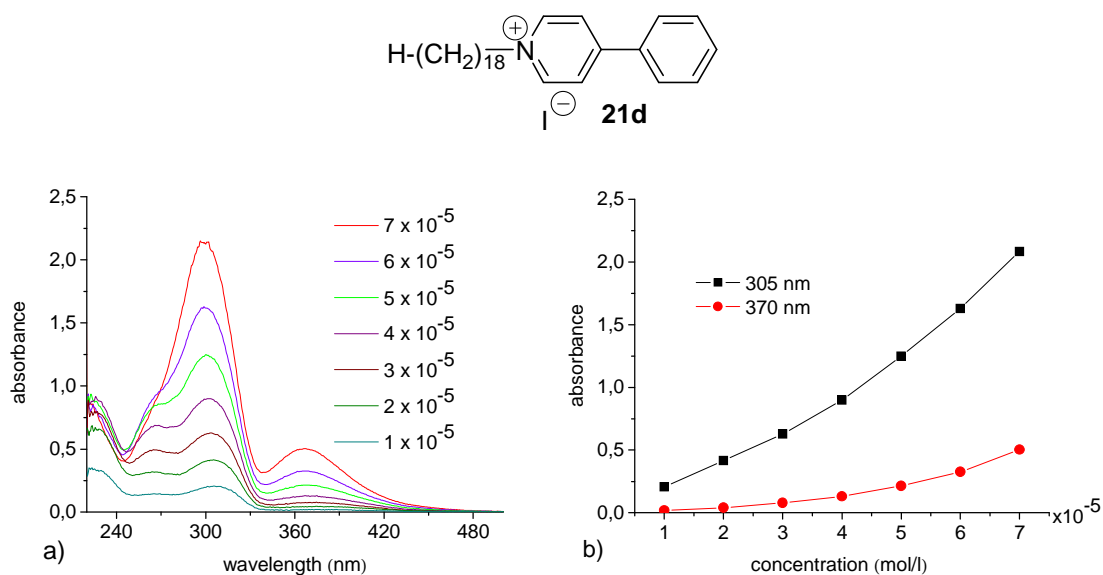


Figure 18. a) Concentration dependence of *N*-octadecyl-4-phenyl-pyridinium iodide **21d** in 1, 2-dichloroethane, $l = 1$ cm, l – path length of the quartz cell, b) Lambert-Beer plot $A = f(\text{conc.})$ at $\lambda = 305$ nm and 370 nm respectively.

The concentration dependence experiment of *N*-octadecyl-4-phenyl-pyridinium iodide **21d** presented in Figure 18a shows a shift of the maximum of the absorbance from 305 nm at concentration 1×10^{-5} mol l^{-1} to 297 nm at 7×10^{-5} mol l^{-1} . The shift of 8 nm of the maximum

absorbance may be caused from the absorption overlap of the band centered at 305 nm and the broad charge-transfer band at 370 nm or may confirm the existence of a second charge-transfer band which may be assigned to a electronic transition from the highest occupied molecular orbital (HOMO) of the iodide ion to two closely located vacant molecular orbitals in the pyridinium ion.⁷⁸

When the iodide ion was replaced by the more electrophilic bromide, the charge-transfer band was no longer present, and a linear correlation of Lambert-Beer plot indicates that no other light absorbing species are formed in 1,2-dichloroethane (Figure 19b). Concentration dependence of *N*-docosyl-4-phenyl-pyridinium bromide **21g** measured between $1 \times 10^{-4} \text{ mol l}^{-1}$ and $1 \times 10^{-5} \text{ mol l}^{-1}$ shows the presence of two absorption bands at 278 nm and 297 nm attributed to π - π^* transitions of the aromatic unit.

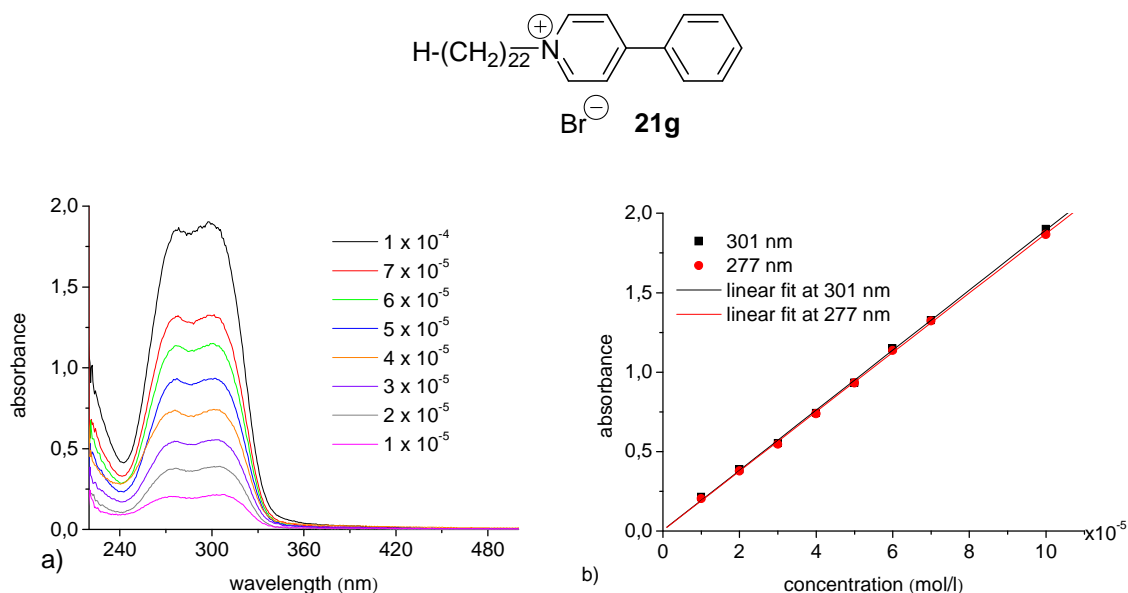


Figure 19. a) Concentration dependence of *N*-docosyl-4-phenyl-pyridinium bromide **21g** in 1, 2-dichloroethane, $l = 1 \text{ cm}$, l – path length of the cell b) Lambert-Beer plot $A = f(\text{conc.})$, $R_1 = 0.999$ (at $\lambda = 301 \text{ nm}$), $R_2 = 0.999$ (at $\lambda = 277 \text{ nm}$).

In order to investigate the influence of the counter ions and of the substituents attached to the pyridinium ring on the absorption spectra of the compounds, similar investigations were made in polar solvent acetonitrile.

Figure 20a shows the concentration dependence of *N*-octadecyl-4-phenyl-pyridinium iodide **21d** in acetonitrile, in the concentration range between $1 \times 10^{-5} \text{ mol l}^{-1}$ and $1 \times 10^{-4} \text{ mol l}^{-1}$. Two absorptions were identified in the spectra with the maximum of the absorbance at 295 nm and 247 nm corresponding to π - π^* and n - π^* transitions respectively. A small absorption at

350 nm approximately indicates a weak charge-transfer transition between the pyridinium cation and iodide anion.

A plot of the absorbance as a function of concentration at 295 nm and 247 nm does obey the Lambert-Beer law indicating that the ion pairing is very low in polar aprotic solvents (Figure 20b).

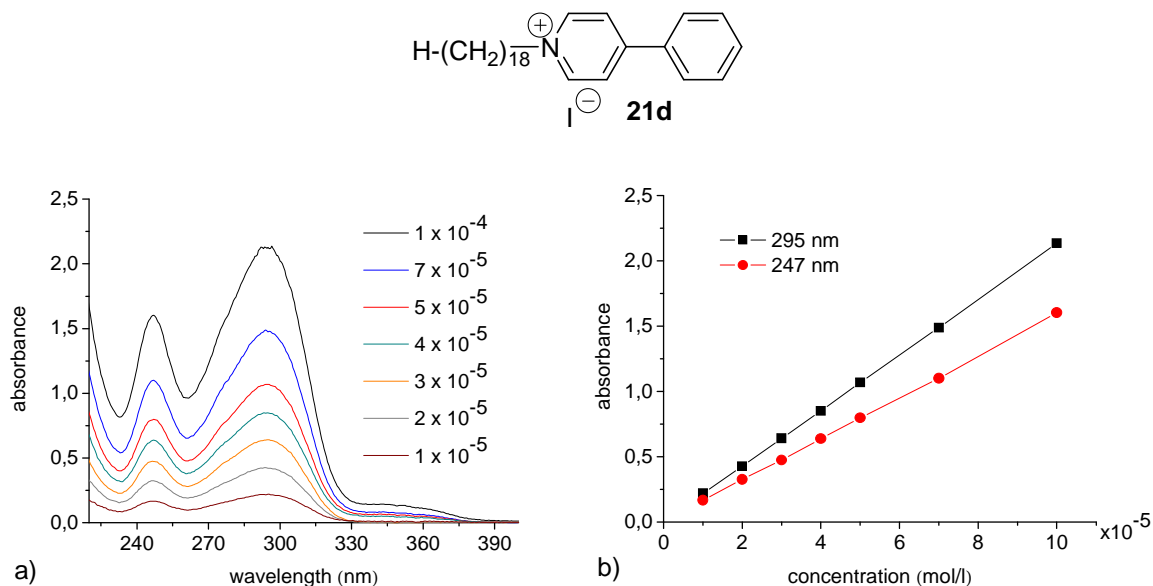


Figure 20. a) Concentration dependence of *N*-octadecyl-4-phenyl-pyridinium iodide **21d** in acetonitrile, $l = 1$ cm, l – path length of the cell b) Lambert-Beer plot $A = f(\text{conc.})$, $R_1 = 0.999$ (at $\lambda = 295$ nm) $R_2 = 0.999$ (at $\lambda = 247$ nm).

Replacing the iodide with bromide the spectra of *N*-docosyl-4-phenyl-pyridinium bromide **21g** in acetonitrile show a π - π^* band at 295 nm as in the case of the corresponding iodide salt. The small absorption found for **21d** at $\lambda \geq 330$ nm is not seen when using bromide as counter ion, compound **21g**, indicating the presence of the charge-transfer band only in the case of iodide (Figures 21a and b). Concentration dependent measurements show a linear Lambert-Beer plot between 5×10^{-6} mol l^{-1} and 1×10^{-4} mol l^{-1} at $\lambda = 295$ nm. Compared with iodide salt, in the case of bromide salt **21g** the n - π^* band becomes blurred in polar aprotic solvent acetonitrile.

Similar investigations were made for salts **21h** – **j** with chloride, tetraphenylborate and *p*-toluenesulfonate as counter ions. The measurements were made in acetonitrile in the concentration range between 1×10^{-4} mol l^{-1} and 1×10^{-5} mol l^{-1} using quartz cells with path length l of 1 cm. Salts **21h**, **i** and **j** show a linear plot of Lambert-Beer law at 295 nm indicating that no other species are formed in acetonitrile (Figures A1-A3, Appendix).

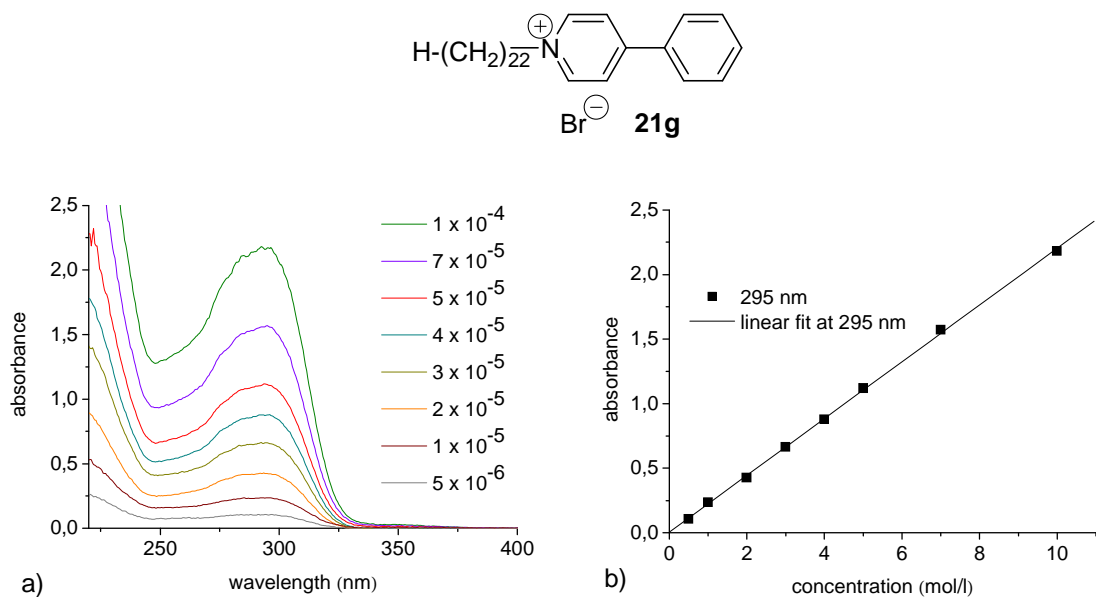


Figure 21. a) Concentration dependence of *N*-docosyl-4-phenyl-pyridinium bromide **21g** in acetonitrile, $l = 1$ cm, b) Lambert-Beer plot $A = f(\text{conc.})$ at $\lambda = 295$ nm, $R = 0.999$.

When the phenyl group is introduced in the *meta*-position of the pyridinium ring, compound **22f**, the position of the π - π^* band at 294 nm is not greatly affected related to the corresponding salt **21g**. Variation of the concentration between 1×10^{-4} mol l^{-1} and 5×10^{-6} mol l^{-1} in the case of **22f** does obey the Lambert-Beer law in acetonitrile (Figures 22a and b). As a result, salt **22f** does not show a charge-transfer band.

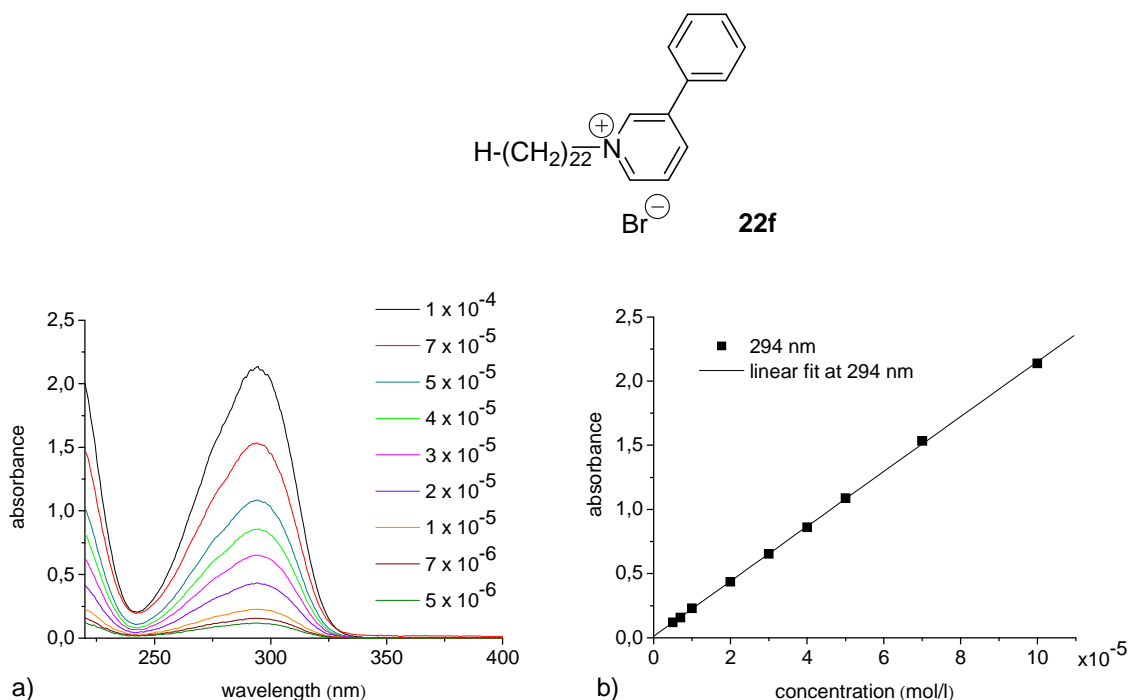


Figure 22. a) Concentration dependence of *N*-docosyl-3-phenyl-pyridinium bromide **22f** in acetonitrile, $l = 1$ cm, b) Lambert-Beer plot $A = f(\text{conc.})$ at $\lambda = 294$ nm, $R = 0.999$.

For comparison, the spectra of *N*-dodecyl-4-methyl-pyridinium bromide **14n** have been investigated in acetonitrile (Figure 23). Concentration dependence measurements were made between $1 \times 10^{-5} \text{ mol l}^{-1}$ and $1 \times 10^{-4} \text{ mol l}^{-1}$, indicating a linear correlation of Lambert-Beer plot. The spectra show shifts of the maximum of the absorbance related to the corresponding *N*-alkyl-4- and -3-phenyl-pyridinium bromides, caused by the replacement of the phenyl group with a methyl substituent. The spectra show a large intensity absorption band with its maximum at $\lambda = 220 \text{ nm}$ attributed to the $\pi\text{-}\pi^*$ transition of the pyridinium ring and weak $n\text{-}\pi^*$ vibrational bands with the maximum of the absorbance at $\lambda = 255 \text{ nm}$ and 289 nm respectively.

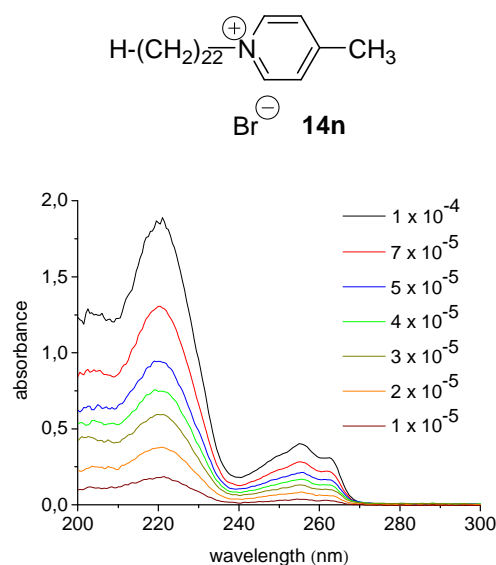


Figure 23. Concentration dependence of *N*-dodecyl-4-methyl-pyridinium bromide **14n** in acetonitrile, $l = 1 \text{ cm}$, l – path length of the cell.

2.2.3. Lyotropic properties of *N*-octadecyl-4-methyl-pyridinium iodide

N-alkyl-4-methyl-pyridinium iodide **14l** behaves like a tenside or a soap. Therefore, lyotropic investigations were made on *N*-octadecyl-4-methyl-pyridinium iodide **14l** using differential scanning calorimetry, isothermal titration calorimetry and atomic force microscopy.

These experiments were made in collaboration with Prof. Dr. A. Blume group in Physical Chemistry Department (Martin-Luther-University Halle).

Differential scanning calorimetry:

The salt **14I** is soluble in polar solvents as alcohols and in water. At room temperature the solubility in water is relatively small. Within a narrow temperature range the solubility increases rapidly around a certain temperature which is known as Krafft point⁷⁹. At low temperatures the low monomer solubility determines the total solubility, while at higher temperature when the monomer solubility has reached the critical micelle concentration [cmc] it is determined by micelle solubility which is much higher.⁸⁰

In order to determine the Krafft point, differential scanning calorimetry measurements of salt **14I** were made in water with a heating cooling rate of 60 °C min⁻¹ in the temperature range between 5 and 80 °C (Figure 24). The Krafft point was obtained at 50 °C.

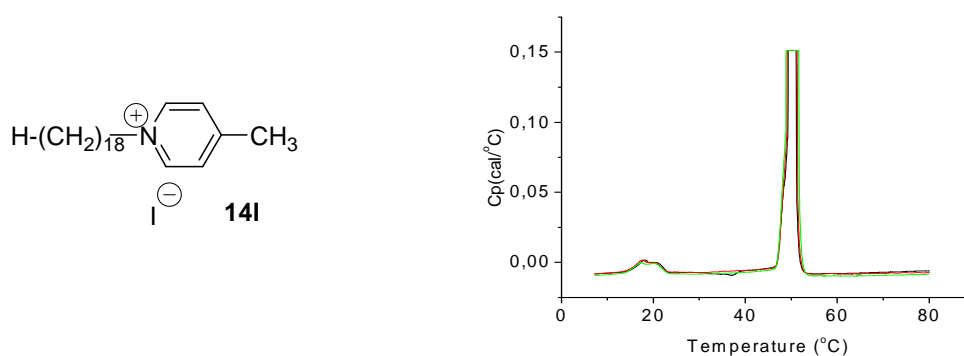


Figure 24. Differential scanning calorimetry (DSC) measurements of salt *N*-octadecyl-4-methylpyridinium iodide **14I** in water, $c = 30$ mM.

Isothermal titration calorimetry

N-octadecyl-4-methylpyridinium iodide **14I** was investigated by isothermal titration calorimetry ITC in order to measure critical micelle concentration cmc and the heat of demicellization ΔH_{demic} . ITC has the advantage that the cmc and ΔH_{demic} can be determined from the same experiment whereas with other methods ΔH_{demic} has to be calculated from the temperature dependence of the cmc using van't Hoff reaction isobar.⁸¹

The concentration of the surfactant was chosen after several attempts in the way that the cmc was achieved during the experiment. The measurements were performed in the temperature interval range between r.t. up to 70 °C. Figure 25 shows the experimental titration of the surfactant solution **14I** at concentration 2 mM in water. The solution was titrated by 75 injections, each injection having a content of 3.75 μl solution. The equilibrium time between two consecutive injections was 4 min.

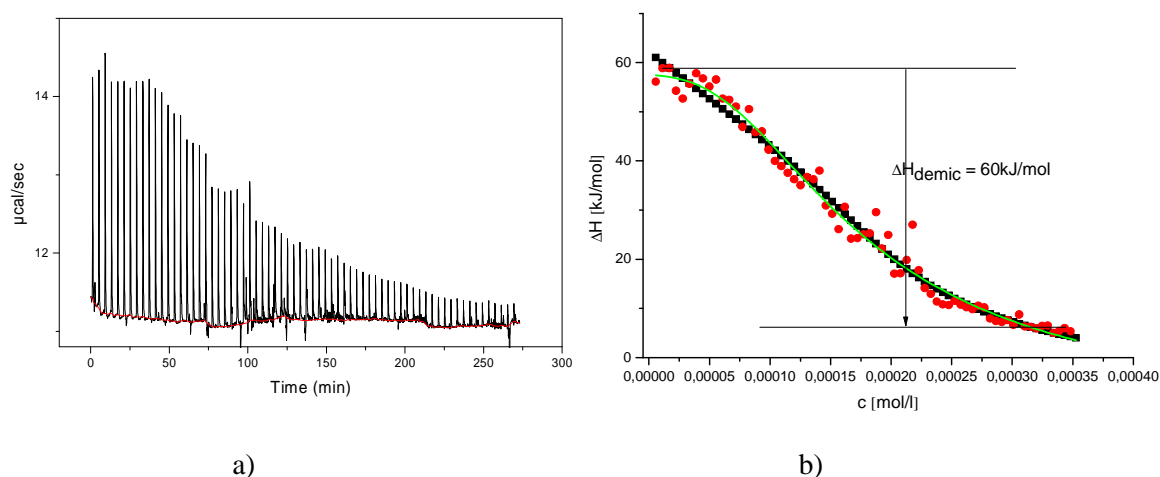


Figure 25. a) Titration of 75 x 3.75 μl of *N*-octadecyl-4-methyl-pyridinium iodide **14I** of concentration 2 mM in water at $T = 50\text{ }^{\circ}\text{C}$ b) Reaction enthalpy versus concentration • experimental data ■ calculated curve using the mass action model [80] – correlation fit of the experimental data

The titration experiment of **14I** in water indicates that each injection produces an exothermic heat. A large enthalpy energy is observed at the beginning of measurements due to demicellization process caused by the dilution of the micelles and the formation of the monomers, below cmc, followed by a large decrease of the enthalpy which indicates that the critical micelle concentration was achieved. If the titration is continued, only the heat of the dilution of the micelles is measured. The critical micelle concentration corresponds to the concentration where the first derivative of the curve shows a minimum and was calculated to $\text{cmc} = 1.4854 \times 10^{-4} \text{ mol l}^{-1}$. The aggregation number was calculated to ~ 5 .

By integration of the peaks the reaction enthalpy as a function of the concentration was obtained. ΔH_{demic} was calculated as 60 kJ/mol from the difference between two extrapolated lines (Figure 25b). The simulation of the calorimetric titration curve was made by converting the equations of the mass action model⁸⁰ to appropriate equation files by the computer software SCIENTIST, Version 2.02 (MicroMath, Inc., Salt Lake City, Utah).

Atomic force microscopy

N-octadecyl-4-methyl-pyridinium iodide **14I** has been investigated by atomic force microscopy. The measurements have been performed at $55\text{ }^{\circ}\text{C}$ using as support mica and graphite. AFM investigations indicate the organization of the salts in fibres.

The experiments made on mica are presented in Figure 26. The fibres, having different diameters, are composed of double layers of salt molecules (Figure 27). The number of double layers can be calculated from the distance and the height of the fibres, in different

places. The length d of the salt molecule **14I** is 27 Å. A number of 95 double layers, (95 x 54 Å) corresponding to a distance of 1.03 µm (blue) were calculated for the fibre shown in Figure 26. A possible arrangement of the molecules in double layers is presented in Figure 27. In similar way was calculated a number of 110 double layers (110 x 54 Å) corresponding to a distance of 1.19 µm (yellow).

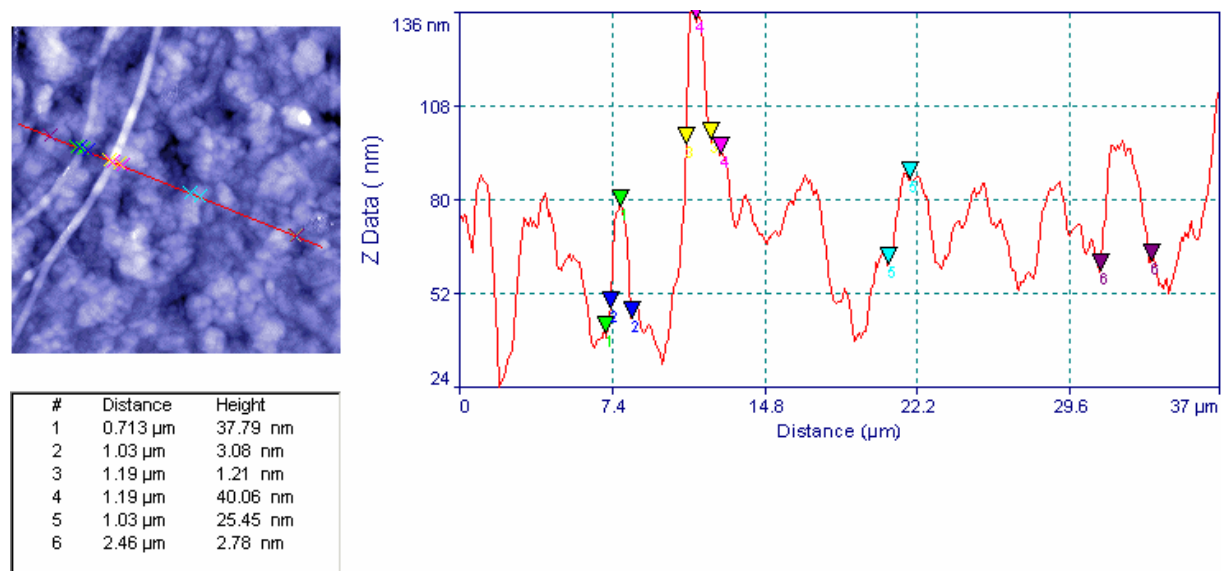


Figure 26. AFM image of *N*-octadecyl-4-methyl-pyridinium iodide **14I** on mica support.

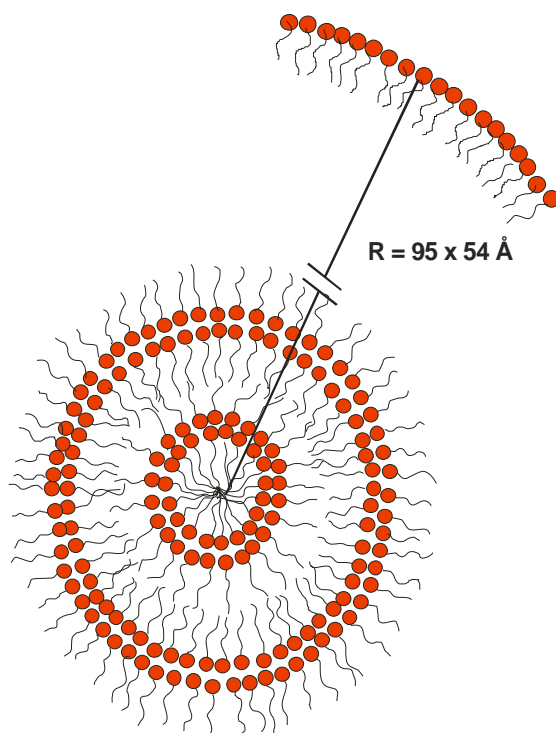


Figure 27. The arrangement of the molecules of *N*-octadecyl-4-methyl-pyridinium iodide **14I** in double layers, R – radius of the fibre.

Formation of fibres with a larger diameter than on mica was observed on graphite support. A number of 207 double layers ($207 \times 54 \text{ \AA}$) were calculated from a diameter of the fibre of $2.24 \text{ }\mu\text{m}$ (green). Measuring the diameter of the fibre in other places was found a number of 345 double layers ($345 \times 54 \text{ \AA}$) corresponding to a diameter of $3.73 \text{ }\mu\text{m}$ (yellow), see Figure 28.

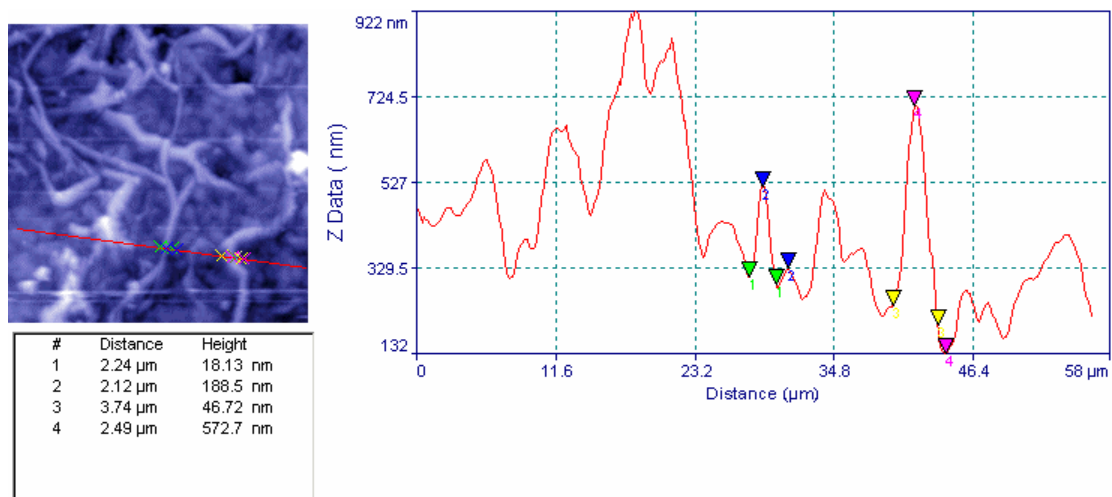


Figure 28. AFM image of the fibres of *N*-octadecyl-4-methyl-pyridinium iodide **14I** on graphite support.

2.3. Properties of *N*-alkyl-4'-substituted stilbazolium salts

In this chapter will be presented investigations on *N*-alkyl-4'-substituted stilbazolium salts in solid state and in solution. The salts exhibit both ionic and much stronger dipolar interactions compared with *N*-alkyl-3- and -4-substituted-pyridinium salts. Therefore, it is of interest to investigate the LC properties of the stilbazolium halides with electron donors like hydroxy, methoxy and, for comparison, hydrogen substituents at the 4'-position and long alkyl chains attached at the quaternary ammonium group, compounds **15** – **17**.

The influence of these structural changes, including the counter ions, on the mesophase behaviour of the compounds was investigated by polarizing microscopy, differential scanning calorimetry and X-ray diffraction. The presence of the C = C double bond between the aromatic rings gives the possibility of *cis-trans* isomerization. Besides thermotropic behaviour, stilbazolium salts are good candidates for aggregate formation in solution, due to the presence of dipolar interactions between the stilbazolium units which can lead to formation of dimeric aggregates. Therefore, spectral properties of stilbazolium salts were investigated by UV/Vis spectroscopy in solvents with different polarities.

2.3.1. Liquid crystalline properties

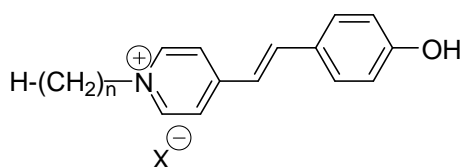
2.3.1.1. *N*-alkyl-4'-hydroxy-stilbazolium halides

Investigations by polarizing microscopy on compounds **15h** – **n** with $n \geq 14$ show the formation of focal-conic fan and homeotropic textures characteristic for smectic A phases, SmA, Figure 29a.

The influence of the length of the hydrocarbon chains n attached to the quaternary ammonium group on the transition temperatures of the mesophases for **15h** – **n** is shown in Table 8. The melting points are nearly constant in the case of bromides, but the clearing points increase with increasing the alkyl chain length. At temperatures higher than 200 °C the compounds may partially decompose as can be derived from decreasing clearing points after heating the substances several times into the isotropic liquid.

When the counter ion is changed from bromide to iodide both the melting point and the clearing point decrease drastically meaning that the stability of the smectic A phase is influenced by the size of the anion. The stability range of the mesophase is shifted to lower temperatures, at which less decomposition effects can be expected and X-ray investigations

are possible. Powder patterns of *N*-octadecyl-4'-hydroxy-stilbazolium iodide **15i** have been recorded, from which a layer distance d of 3.85 nm is obtained for the SmA phase at 160 °C. A similar supramolecular arrangement can be expected from the molecular packing model presented in Figure 29b showing a head-to-tail orientation of the stilbazolium unit with the anion sandwiched between the aromatic rings. Thus, this model is assumed as representative for compounds of type **15**.



Comp.	n	X^-	Phase transitions (T/°C)	ΔT (°C)
			ΔH (kJ/mol)	
15h	14	Br ⁻	Cr 173 SmA 186 Iso 7.5 0.3	13
15i	16	Br ⁻	Cr 177 SmA 221 Iso* 12.0 2.0	≥ 44
15j	16	I ⁻	Cr 143 SmA 181 Iso 2.3 9.5	38
15k	18	Br ⁻	Cr 172 SmA 230 Iso* 22.6 0.9	≥ 58
15l	18	I ⁻	Cr 130 SmA 184 Iso 17.6 6.81	54
15m	20	Br ⁻	Cr 172 SmA 260 Iso* 14.7 2.6	≥ 88
15n	22	Br ⁻	Cr 176 SmA 245 Iso* 17.3 3.5	≥ 68

* Partial decomposition observed

Table 8. Transition temperatures T (°C) and enthalpies ΔH (kJ/mol) from Differential Scanning Calorimetry of *N*-alkyl-4'-hydroxy-stilbazolium halides **15h** – **n**, ΔT (°C) – temperature range of the smectic A phase.

A growing of bâtonnets, Figure 29a, followed by the formation of a fan-shaped texture is observed on cooling by polarizing microscopy. Partial decomposition is not only evident from the microscopic observations of gas bubbles in the melt, but also by the lowering of the clearing point in the second and third cooling. Due to decomposition of the samples, the transition temperatures are given for the first heating, but the SmA texture was observed by

polarizing microscopy even at higher temperatures. In all cases the stilbazolium compounds exhibit a tendency to supercool before crystallization or to form glasses.

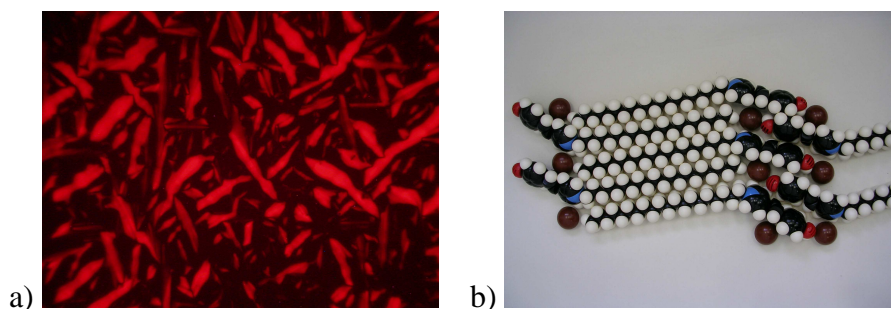


Figure 29. a) Growing of bâtonnets in SmA phase of *N*-octadecyl-4'-hydroxy-stilbazolium iodide **15l** at 164.3 °C b) CPK model of *N*-eicosyl-4'-hydroxy-stilbazolium bromide **15m**, assuming the all-*trans* conformation of the alkyl chains.

2.3.1.2. *N*-alkyl-4'-methoxy-stilbazolium halides

N-alkyl-4'-methoxy-stilbazolium salts **16a** – **f** were investigated by polarizing microscopy and differential scanning calorimetry. Upon cooling from isotropic liquid, the formation of the fan-like textures, characteristic for SmA, was observed by polarizing microscopy (Figure 30).

The transition temperatures and the corresponding enthalpies are summarized in Table 9. The salts with $n \geq 16$ have relatively low melting points without large changes by increasing the alkyl chain length. The clearing points are higher than 200 °C inducing a partial thermal decomposition. In the case of the salt with $n = 14$ the tendency to form liquid crystalline phases is reduced by a large increase of the melting point.

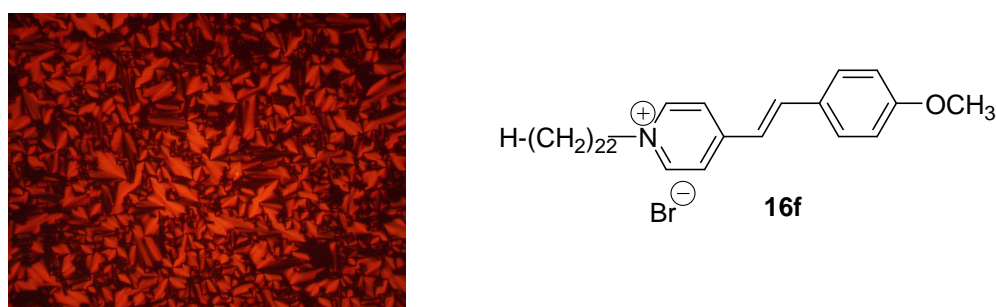


Figure 30. SmA phase of *N*-docosyl-4'-methoxy-stilbazolium bromide **16f** in cooling at 200 °C.

Elongation of the aromatic core and the introduction of hydroxy and methoxy groups to the stilbazolium head group have a large influence on the formation of LC phases by introduction of stronger dipole-dipole interactions between the stilbazolium units. The clearing points increase drastically inducing partial decomposition of the compounds. The

mesophase temperature range of the methoxy substituted salts is larger than the corresponding hydroxy substituted compounds in which the hydrogen bonding between the OH groups will influence the mesophase by increasing the melting points. Generally, introduction of dipolar interactions increases the stability of LC-phases in contrast to aromatic rings.

Comp.	<i>n</i>	X ⁻	Phase transitions (T/°C)	ΔT (°C)
			ΔH (kJ/mol)	
16a	14	Br ⁻	Cr 231 SmA 247 Iso*	≥ 16
			4.2 6.97	
16b	16	Br ⁻	Cr 54 SmA 227 Iso*	≥ 173
			9.4 2.83	
16c	18	Br ⁻	Cr 63 SmA 255 Iso*	≥ 192
			15.7 5.9	
16d	18	I ⁻	Cr ₁ 67 Cr ₂ 245 Iso°	-
			10.4 15.7	
16e	20	Br ⁻	Cr 68 SmA 227 Iso*	≥ 159
			16.8 2	
16f	22	Br ⁻	Cr 75 SmA 214 Iso*	≥ 139
			18.5 2.1	

* Partial decomposition observed

Table 9. Transition temperatures T (°C) and enthalpies ΔH (kJ/mol) from Differential Scanning Calorimetry of *N*-alkyl-4'-methoxy-stilbazolium halides **16a – f**, ΔT (°C) – temperature range of the smectic A phase.

2.3.1.3. *N*-alkyl-stilbazolium halides

Compounds **17a – f** with $n \geq 18$ show, under polarizing microscopy, focal conic textures characteristic for SmA phase (Figure 31). Substitution of methoxy group by hydrogen increases the melting points resulting in a decreasing of the mesophase temperature range.

Compound **17d** with iodide anion does not form any LC phases.

The phase transition and the corresponding enthalpies ΔH are presented in Table 10. The salts **17a** and **17b** with alkyl chain length $n = 14$ and 16 and bromide as anion do not display LC phases. Increasing the alkyl chain length to $n \geq 18$ the stilbazolium salts form LC phases. The melting points are relatively constant, but the clearing points are higher than 200 °C, temperature at which a partial decomposition is observed.

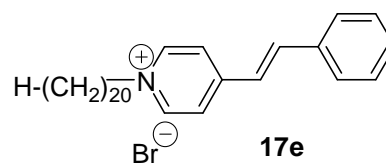
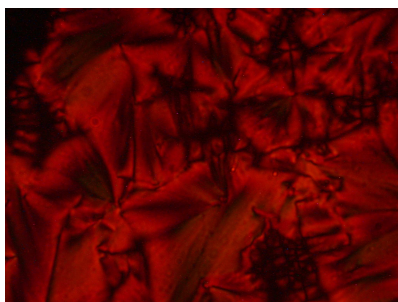


Figure 31. Fan-shaped texture of SmA phase of *N*-eicosyl-stilbazolium bromide **17e** in cooling at 195 °C.

Comp.	<i>n</i>	X ⁻	Phase transitions (T/°C) ΔH (kJ/mol)	ΔT (°C)
17a	14	Br ⁻	Cr 209 Iso* 2.9	-
17b	16	Br ⁻	Cr 200 Iso 2.2	-
17c	18	Br ⁻	Cr 153 SmA 217 Iso* 4.8 2.5	≥ 64
17d	18	I ⁻	Cr 189 Iso 10.6	-
17e	20	Br ⁻	Cr 141 SmA 216 Iso* 2.6 0.3	≥ 75
17f	22	Br ⁻	Cr 149 SmA 247 Iso* 4.4 1.3	≥ 98

* Partial decomposition observed

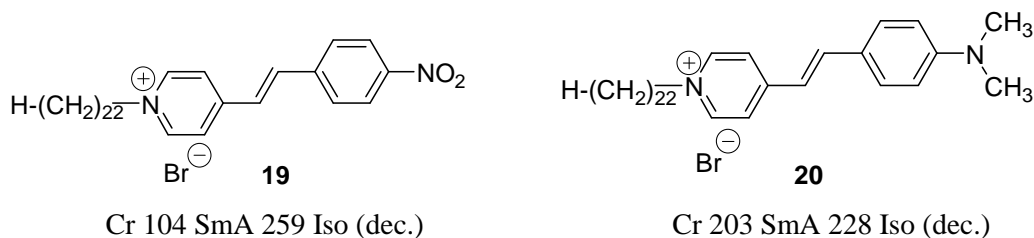
Table 10. Transition temperatures *T* (°C) and enthalpies Δ*H* (kJ/mol) from Differential Scanning Calorimetry of *N*-alkyl-stilbazolium halides **17a** – **f**, Δ*T* (°C) – temperature range of the smectic A phase.

The DSC measurements of compounds **15** – **17** show peaks corresponding to crystalline – crystalline, crystalline – melting and melting – isotropic liquid transitions (Tables 8 – 10) with significant changes in enthalpies. For instance, in the case of **17f**, the enthalpy energy decreases from 4.4 kJ/mol for the crystal – melting transition to 1.3 kJ/mol for the SmA – isotropic transition.

Compared with serie **21**, salts **17** have only the additional C = C double bond between the aromatic rings, which may indicate that series **17** and **21** should have similar liquid crystalline behaviour. Both of the series display SmA phases on heating. Compounds **21** with bromide anion show an additional phase M, which is not present in the case of salts **17**.

Compared with bromides **21**, the SmA temperature range is larger in the case of salts **17**. Also, a relatively large increase of the melting and clearing points is observed for salts **17**, leading to a partial decomposition at temperatures higher than 200 °C. The increase of the transition temperatures may be attributed to the elongation of the aromatic core by a C = C double bond which will induce additional π - π interactions and weak dipolar interactions in the case of **17**.

In order to compare the mesophase behaviour of stilbazolium salts having a donor group in the 4'-position, *N*-docosyl-4'-nitro-stilbazolium bromide and *N*-docosyl-4'-dimethylamino-stilbazolium bromide were prepared. Salts **19** and **20** were investigated by differential scanning calorimetry and polarizing microscopy. Both of the salts show liquid crystalline behaviour up to high temperatures leading to a partially decomposition above 200 °C.



2.3.2. Spectral properties

2.3.2.1. Photoisomerization of *N*-alkyl-4'-substituted-stilbazolium salts

The presence of C = C double bond between two aromatic rings offer the possibility of *cis-trans* isomerization. However, the stilbazolium compounds were obtained in the stable *trans* form, as confirmed by ¹H NMR and 3D X-ray investigations. The *trans* form is more stable than the *cis* form, but each isomer should be converted into the other by irradiation with the appropriate wavelength.

Therefore, irradiation experiments were made on *N*-docosyl-4'-methoxy-stilbazolium bromide **16f** in solvents with different polarities: in ethanol as polar protic solvent, acetonitrile as polar aprotic solvent and chloroform as non-polar aprotic solvent. The irradiation experiments were made under stirring using quartz cells with the path length *l* of 1 cm. The cells were closed, handled in the dark and assured that the evaporation of the solvent does not take place. The solutions were irradiated with light at $\lambda = 254$ nm, 405 nm and 546 nm.

The UV/Vis absorption spectrum of *N*-docosyl-4'-methoxy-stilbazolium bromide **16f** in ethanol shows two absorption bands at 254 nm and 392 nm corresponding to π - π^* transitions. Irradiation with light at $\lambda = 405$ nm indicates a decrease of the maximum of the

absorbance at 383 nm concomitant with an increase of the maximum of the absorbance at 253 nm (Figure 32a). After 60 s no changes were observed in the spectrum indicating that the photostationary state was achieved. The presence of the isosbestic point indicates that the changes are due to a single photochemical reaction, which can be *cis-trans* isomerization of the C = C double bond which is present between the aromatic rings.

Figure 32b shows the UV/Vis spectra of **16f** after irradiation with light at $\lambda = 254$ nm. The spectra indicate a decrease of the maximum of the absorbance at 405 nm concomitant with an increase of the maximum of the absorbance at 254 nm. The photostationary state was achieved after 10 min. of irradiation, indicating a much slowly photochemical reaction compared with the results obtained by irradiation with light at $\lambda = 405$ nm.

The thermal back reaction *cis* \rightarrow *trans* was measured in the dark in ethanol and the spectra do not show changes after 23 h.

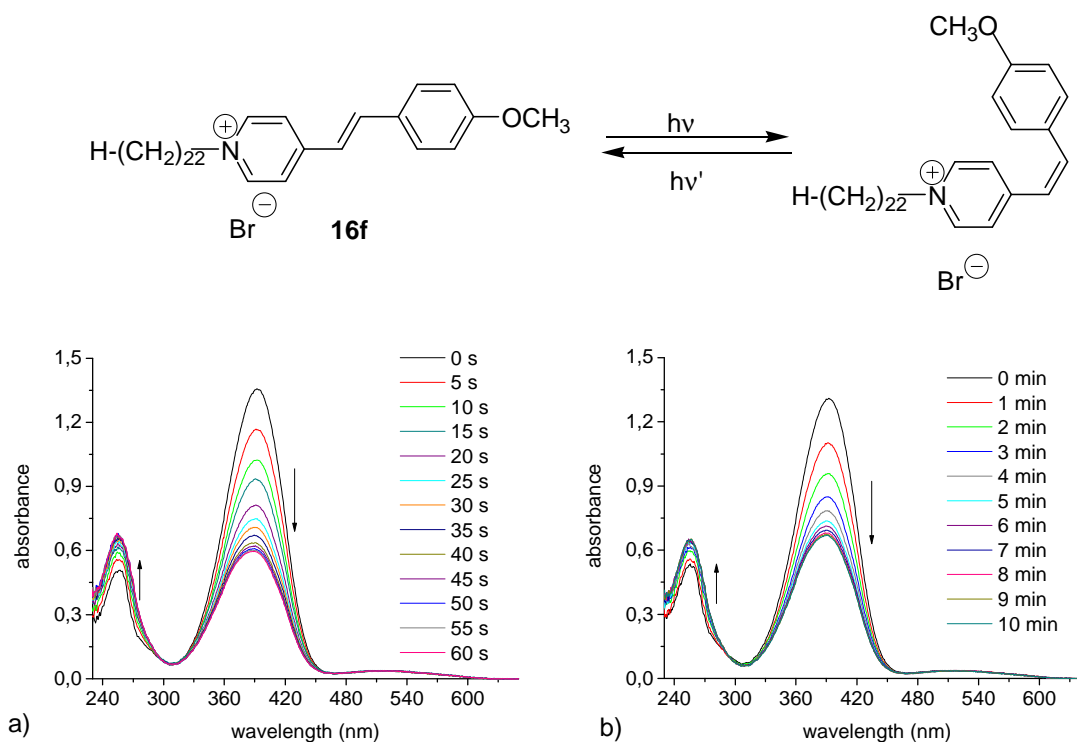


Figure 32. UV/Vis absorption spectra of *N*-docosyl-4'-methoxy-stilbazolium bromide **16f** in ethanol, $c = 5 \times 10^{-5} \text{ mol l}^{-1}$, c = concentration of solution in mol l^{-1} , $l = 1 \text{ cm}$, l – path length of the quartz cell a) before and after irradiation with light at $\lambda = 405$ nm b) before and after irradiation with light at $\lambda = 254$ nm.

UV/Vis absorption spectra of **16f** were recorded in a solvent with a lower polarity than ethanol. Thus, irradiation measurements were made in the polar aprotic solvent acetonitrile with $\lambda = 405$ nm and 254 nm respectively, Figures 33a and b.

The photostationary state was achieved in 60 s by irradiation with light at $\lambda = 405$ nm and in 9 min. by irradiation with light at $\lambda = 254$ nm indicating similarities with results obtained in ethanol. The thermal back reaction was measured for 19 h in the dark indicating a very slowly back reaction to the *trans* form. By irradiation with light at $\lambda = 546$ nm the UV/Vis absorption spectra show no changes indicating that the longer absorption band is a charge-transfer band.

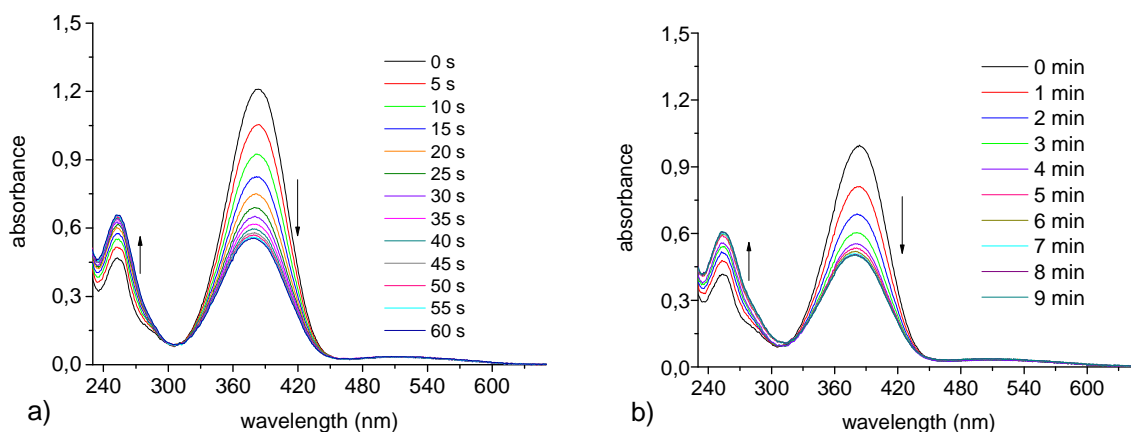


Figure 33. UV/Vis absorption spectra of *N*-docosyl-4'-methoxy-stilbazolium bromide **16f** in acetonitrile, $c = 5 \times 10^{-5} \text{ mol l}^{-1}$, c – concentration of solution, $l = 1 \text{ cm}$, l – path length of the cell a) before and after irradiation with light at $\lambda = 405$ nm b) before and after irradiation at $\lambda = 254$ nm.

Figures 34a and b show UV/Vis absorption spectra of **16f** in chloroform, a non-polar aprotic solvent, before and after irradiation with light at $\lambda = 405$ nm and at 254 nm respectively.

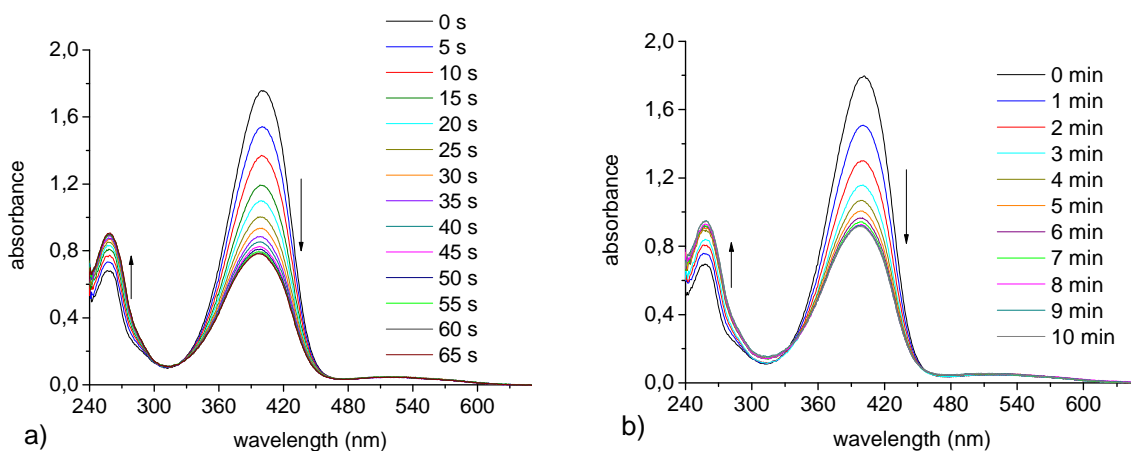


Figure 34. UV/Vis absorption spectra of *N*-docosyl-4'-methoxy-stilbazolium bromide **16f** in chloroform, $c = 5 \times 10^{-5} \text{ mol l}^{-1}$, c – concentration of solution, $l = 1 \text{ cm}$, l – path length of the cell a) before and after irradiation with light at $\lambda = 405$ nm b) before and after irradiation at $\lambda = 254$ nm.

Similar results, as in the case of investigations made in ethanol and acetonitrile, indicates that the solvent has no large influence on the *cis-trans* reaction of *N*-alkyl-4'-substituted-stilbazolium salts. The photostationary state was achieved after 60 s by irradiation with light at $\lambda = 405$ nm and in 10 min. by irradiation with light at $\lambda = 254$ nm.

In order to prove that a *cis-trans* isomerization takes place an irradiated solution of *N*-docosyl-4'-hydroxy-stilbazolium bromide **16f** in chloroform was investigated by $^1\text{H-NMR}$ spectroscopy.

The UV/Vis spectrum of **16f** in chloroform shows two absorption bands at $\lambda = 260$ nm ($\epsilon = 1.2 \times 10^4 \text{ l mol}^{-1} \text{ cm}^{-1}$) and at $\lambda = 400$ nm ($\epsilon = 3.1 \times 10^4 \text{ l mol}^{-1} \text{ cm}^{-1}$). By irradiation with light for 1 h at $\lambda = 405$ nm the maximum absorbance at $\lambda = 400$ nm decreases to almost half ($\epsilon = 1.59 \times 10^4 \text{ l mol}^{-1} \text{ cm}^{-1}$) concomitant with an increase of the maximum absorbance at $\lambda = 260$ nm (Figure 35). After evaporation of the solvent by distillation the $^1\text{H NMR}$ spectrum was measured immediately in CDCl_3 and care was taken that the sample is kept in the dark.

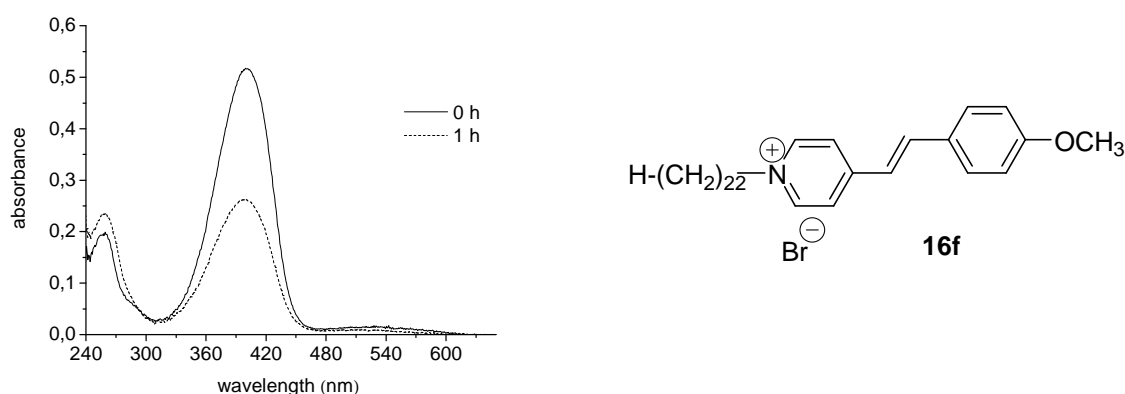


Figure 35. UV/Vis absorption spectra of *N*-docosyl-4'-methoxy-stilbazolium bromide **16f** in chloroform before and after irradiation with light at $\lambda = 405$ nm for 1 h, $c = 1.65 \times 10^{-3} \text{ mol/l}$, c – concentration of solution, $l = 0.1$ mm, l – path length of the cell.

$^1\text{H NMR}$ spectra of the irradiated sample prove the formation of the *cis* isomer (Figure 36). Before irradiation the spectrum shows two doublets with a coupling constant $J_{H,H} = 16.2$ Hz attributed to the olefinic protons in the *trans* form. By irradiation with light at $\lambda = 405$ nm, additional new signals are present in the spectrum. After subtraction of the signals which corresponds to *trans* form, the new signals were attributed to *cis* form of the dye. The coupling constant of the olefinic protons was $J_{H,H} = 12.03$ Hz, in agreement with the coupling constant of the olefinic protons in the *cis* form.⁸² The *cis/trans* ratio of **16f** was calculated from the $^1\text{H NMR}$ spectrum as 0.64.

The thermal back reaction of the sample kept in the dark was measured after 6 days by ^1H NMR spectroscopy indicating a decrease in the *cis/trans* ratio to 0.2.

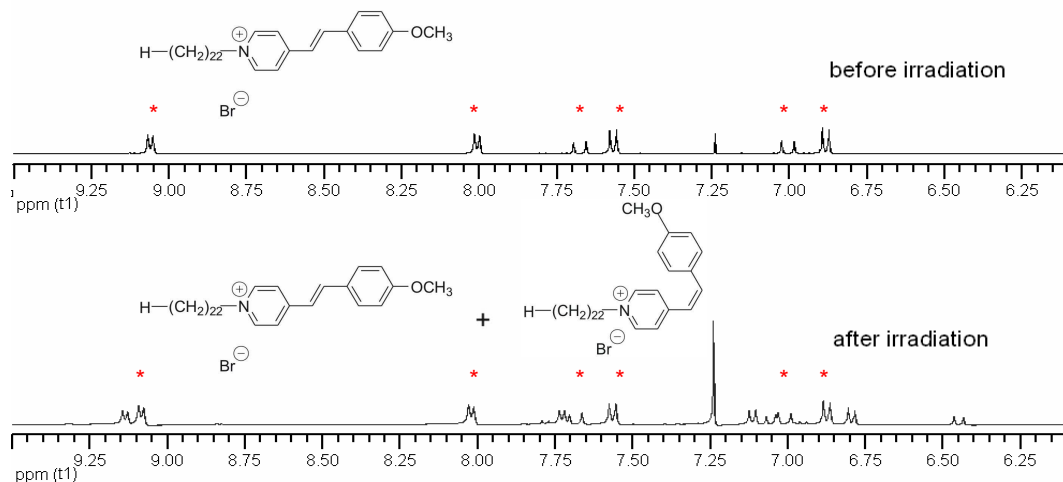


Figure 36. ^1H -NMR spectra of *N*-docosyl-4'-methoxy-stilbazolium bromide **16f** in CDCl_3 after and before irradiation with light at $\lambda = 405$ nm, * – signals corresponding to the *trans* form of the dye.

The *cis-trans* isomerization of stilbazolium compounds can be explained through a „phantom” state X which involves a 90° twisted configuration about the ethylenic bond in the first exciting singlet state for an avoided crossing with ground state.^{60,61} A possible mechanism, of the isomerization of *trans* into the *cis* form is presented in the Figure 37.

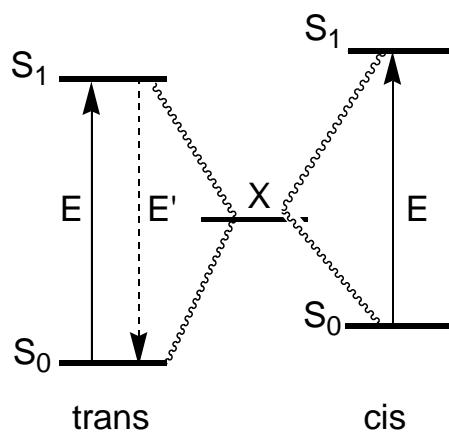


Figure 37. Possible mechanism for excited *cis* and *trans* forms of *N*-docosyl-4'-methoxy-stilbazolium bromide **16f**.⁶¹

2.3.2.2. Concentration dependence measurements of *N*-alkyl-4'-substituted-stilbazolium salts

UV/Vis spectroscopy has been utilized to investigate aggregate formation in solution of *N*-alkyl-4'-substituted-stilbazolium salts. The salts having hydroxy and methoxy substituents on the 4'-position of the stilbazolium core may form aggregates in solution due to the presence of dipole-dipole interactions between the stilbazolium head groups. Therefore, concentration dependence investigations were made in solvents with different polarities.

Concentration dependence measurements were made for salt *N*-docosyl-4'-methoxy-stilbazolium bromide **16f** in acetonitrile in the concentration range between $1 \times 10^{-4} \text{ mol l}^{-1}$ and $1 \times 10^{-5} \text{ mol l}^{-1}$ (Figure 38a). The spectra show two absorption bands with maximum of the absorbance at $\lambda = 283$ and 384 nm . A linear correlation of the absorbance as a function of concentration of these two absorptions indicates that no other species are formed in acetonitrile (Figure 38b).

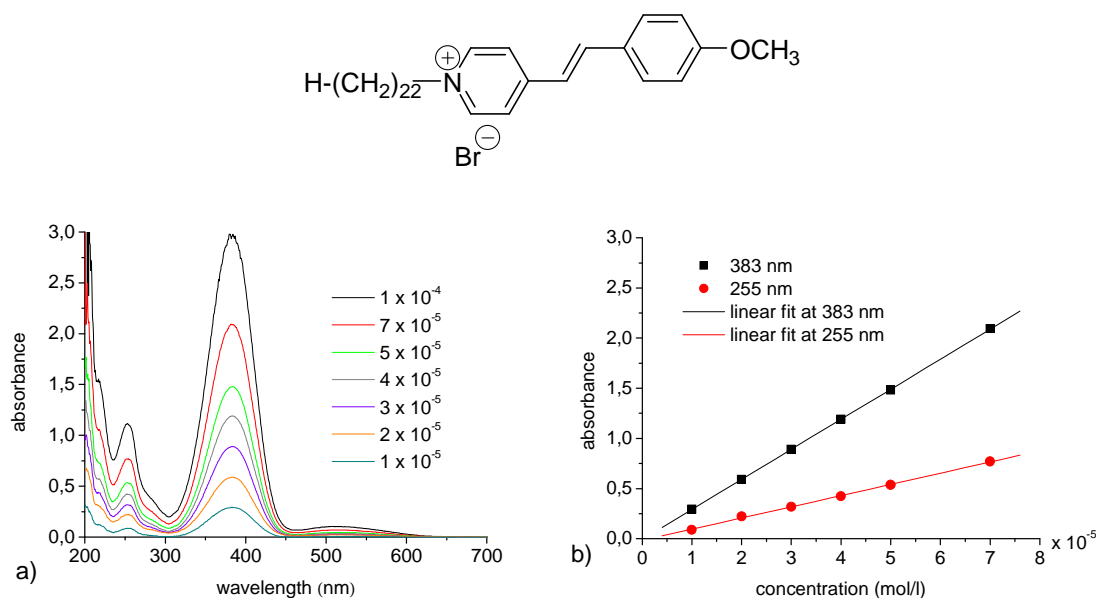


Figure 38. a) Concentration dependence measurements of *N*-docosyl-4'-methoxy-stilbazolium bromide **16f** in acetonitrile, $l = 1 \text{ cm}$, b) Lambert-Beer plot $A = f(\text{conc.})$, $R_1 = 0.999$ (at $\lambda = 383 \text{ nm}$) and $R_2 = 0.999$ (at $\lambda = 255 \text{ nm}$).

Similar behaviour of salt **16f** was found in the non-polar solvent chloroform in the concentration range between $5 \times 10^{-5} \text{ mol l}^{-1}$ and $7 \times 10^{-6} \text{ mol l}^{-1}$. The concentration dependence spectra show a linear decrease of the maximum of the absorbance at 400 nm by decreasing the concentration indicating that no aggregation takes place at these concentrations (Figures 39a and b).

A small absorption band is observed for **16f** at $\lambda > 500$ nm in acetonitrile and chloroform corresponding to a charge-transfer band.

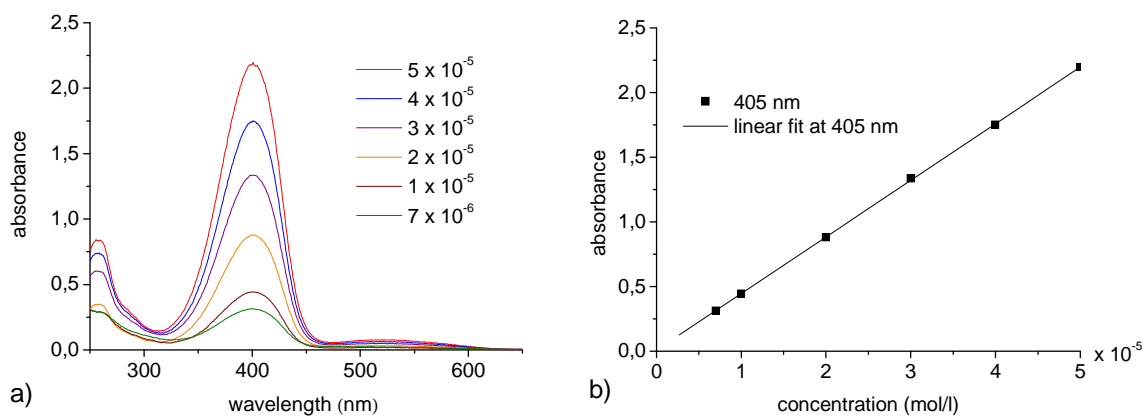


Figure 39. a) Concentration dependence measurements of *N*-docosyl-4'-methoxy-stilbazolium bromide **16f** in chloroform, $l = 1$ cm, b) Lambert-Beer plot $A = f(\text{conc.})$ at 405 nm, $R = 0.999$.

Concentration dependence measurements of the stilbazolium salts with hydroxy, hydrogen, nitro and dimethylamino substituents attached to the 4'-position of the stilbazolium core were made in acetonitrile and chloroform. A linear plot of Lambert-Beer law indicates that no aggregation takes place in solution (Figures A4-A11, Appendix).

2.4. Properties of merocyanine dyes

Merocyanine dyes have dipole moments with antiparallel orientation which can favour, depending on the substituents, the formation of J-type aggregates with a head-to-head arrangement of the molecules. Therefore, spectral properties of the *N*-alkylated dyes **6**, **13** and **15** were investigated in solvents with different polarities.

The dyes are sensitive to solvent medium, showing protonation-deprotonation equilibrium as well as to the solvent polarity, having a large solvatochromic effect. Investigations of the dyes in the solid state by 3D X-ray measurements will be also presented.

Dyes **6a** – **e** and **13a** – **g** as well as **15a** – **g** do not show any liquid crystalline properties.

2.4.1. Spectral investigations

2.4.1.1. Protonation-deprotonation equilibrium

UV/Vis spectra recorded in aqueous solution at different pH are shown in Figure 40. A well defined isosbestic point, as reported for **15a**⁵⁵, shows the presence of two-state equilibrium between protonated and non-protonated form of the *N*-(2-propyl)-pentyl-4'-oxy-stilbazolium dye **6a**, using buffer solutions with pH between 4 and 10.

UV/Vis absorption spectra of **6a** show two absorptions with maximum of the absorbance at $\lambda = 378$ nm attributed to protonated form of the dye and the second with the maximum of the absorbance at $\lambda = 450$ nm corresponding to non-protonated dye. At pH > 10 a deviation from the isosbestic point may be attributed to side reactions, for example ring cleavage.

The pK_a value was calculated from the UV/Vis spectra by using the relation:

$$\text{pK}_a = \text{pH} - \log [M]/[MH^+], \text{ where}$$

[M] and [MH⁺] are the concentration of non-protonated and protonated form of the merocyanine dye.

The extinction coefficient was calculated using the Lambert-Beer law⁸³: $A = \epsilon \times l \times c$, where A – extinction, ϵ – extinction coefficient [$\text{l mol}^{-1} \text{cm}^{-1}$], l – path length of the cell [cm] and c – concentration of the solution [mol l^{-1}]. The extinction coefficient $\epsilon = 2.2 \times 10^4 \text{ l mol}^{-1}$

cm^{-1} was obtained from the spectrum of the protonated form at $\text{pH} = 4$ and used to calculate the concentration of the protonated form of **6a** in buffer solutions. In the similar way, from the spectrum at $\text{pH} = 10$ was calculated the extinction coefficient of the non-protonated dye $\epsilon = 2.4 \times 10^4 \text{ l mol}^{-1} \text{ cm}^{-1}$ which was utilized to calculate the concentration of non-protonated form of **6a** in buffer solutions. From the averaged values obtained at different pH the pK_a value was calculated to $\text{pK}_a \approx 8.5$ for the dye **6a**.

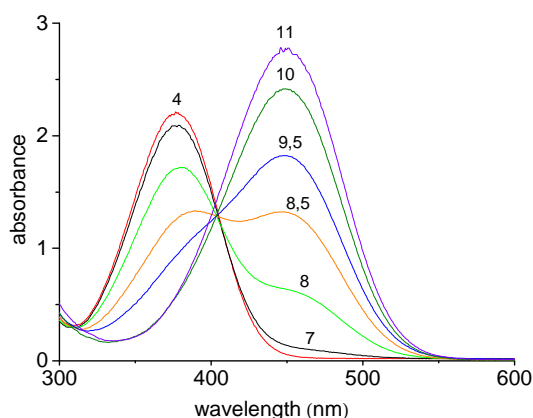


Figure 40. a) pH-dependence of *N*-(2-propyl)-pentyl-4'-oxy-stilbazolium dye **6a** in buffer solutions at $\text{pH} = 4, 7, 8, 8.5, 9.5, 10$ and 11 , $c = 1 \times 10^{-4} \text{ mol l}^{-1}$, $T = 22 \text{ }^\circ\text{C}$, $l = 1 \text{ cm}$.

The pH dependence of dye **6a** was confirmed by ^1H NMR and ^{13}C NMR spectroscopy using DMSO-d_6 as a solvent and DBr for acidification and KOD to obtain a basic medium.

The presence of the protonated and non-protonated form was probed in the case of compound **15n** in DMF by adding small amounts of KOH in the sample which shifts the equilibrium to the non-protonated dye. An isosbestic point between the protonated and non-protonated dye was obtained also by adding small amounts of HCl in the solution which indicates that the dye is protonated, Figures 41a and b.

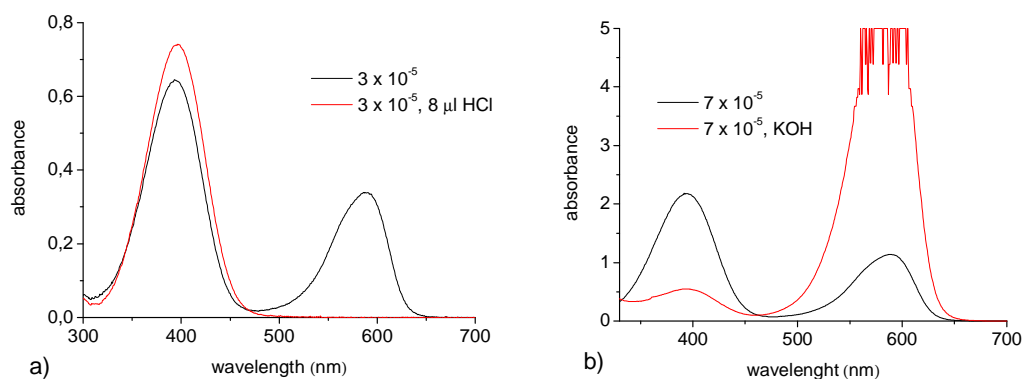


Figure 41. Protonation-deprotonation experiment of compound **15n** in DMF, $T = 22 \text{ }^\circ\text{C}$, $l = 1 \text{ cm}$, a) using HCl , b) using KOH .

NMR-experiment

^1H NMR spectra show changes of chemical shifts in basic and acidic medium. The NMR experiments were made in DMSO using solutions with a concentration between $6.8 \times 10^{-2} \text{ mol l}^{-1}$ and $7.2 \times 10^{-2} \text{ mol l}^{-1}$. For acidification were used 5 μl of DBr (40 % in D_2O , Chemotrade) and to obtain a basic medium 0.5 μl KOD (30 % in D_2O , Chemotrade). The spectrum in DMSO- d_6 is similar with the one obtained in a basic medium indicating that the dye is deprotonated. The experiment made in acidic medium indicates a shift of the spectrum with 0.5 ppm and a change in position of H^6 and H^3 which are inverted (Figure 42a).

The chemical shifts of protonated and non-protonated form of dye **6a** were investigated by ^{13}C NMR spectroscopy in DMSO- d_6 . The results provide the alternating shifts of the carbons corresponding to protonated and non-protonated dye **6a** which are common for polymethine dyes. A large difference was observed for the carbon C^{10} nearby oxygen, which is most shifted in the case of the non-protonated form and for the $\text{C}=\text{C}$ double bond caused by a high electronic density in the case of carbon number 5 of the protonated dye (Figure 42b).

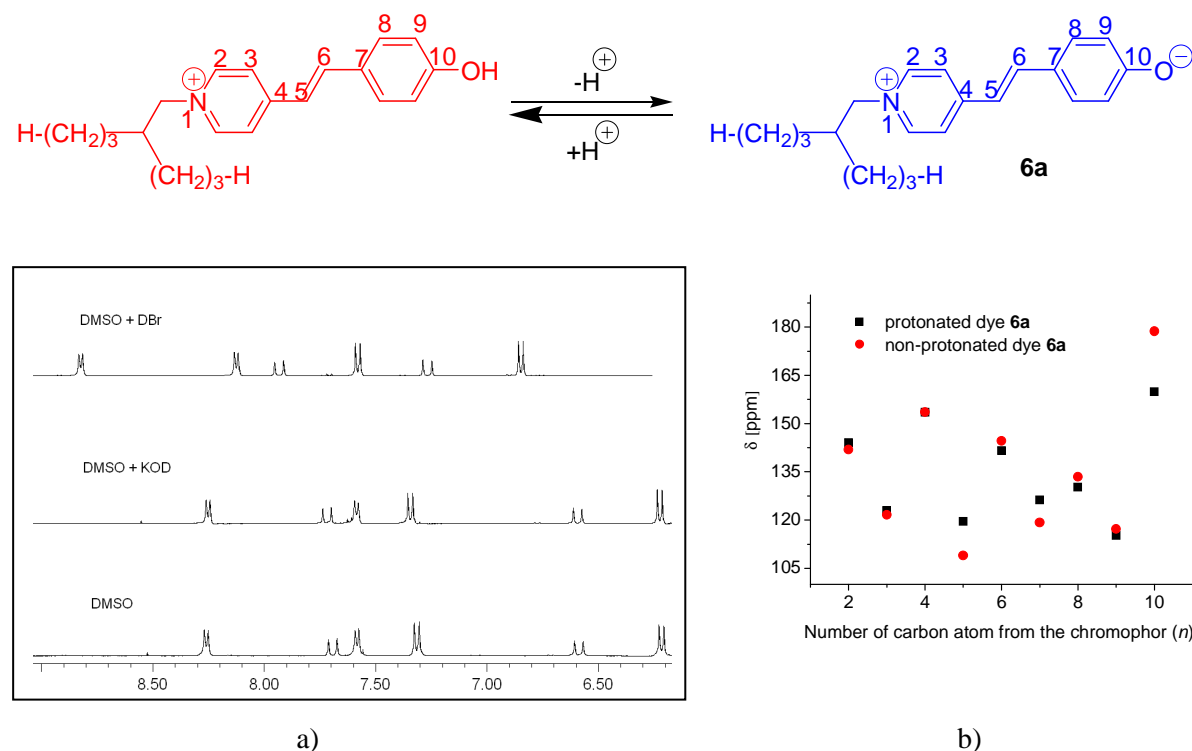


Figure 42. a) pH-dependence of dye **6a** in ^1H NMR using as solvent DMSO- d_6 in acidic and in basic medium respectively b) Chemical shifts of the carbon atoms n of dye **6a** in ^{13}C NMR using as solvent DMSO- d_6 in acidic and basic medium, $c = 1 \times 10^{-4} \text{ mol l}^{-1}$, $l = 1 \text{ cm}$.

UV/Vis spectra of 1-(1-octyl-nonyl)-4'-oxy-stilbazolium dye **13g** were measured in the hygroscopic solvent DMSO and indicates a slowly increase of the absorption at $\lambda = 397 \text{ nm}$ by time. Addition of 8 μl water to 3 ml of dye solution **13g** at concentration $5 \times 10^{-5} \text{ mol l}^{-1}$

drops down the absorption band of the non-protonated dye to nearly zero which means that small amounts of water protonated the dye (Figure 43). Therefore, most of the ^1H NMR and ^{13}C NMR spectra presented in experimental part and using the hygroscopic solvent DMSO- d_6 show the chemical shifts of the protonated form.

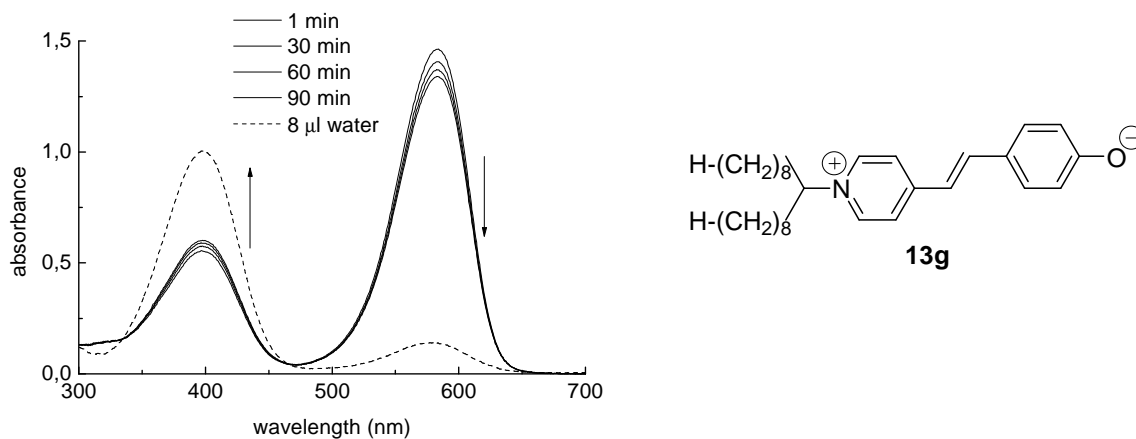


Figure 43. Time-dependent measurements and influence of water on the UV/Vis spectra of dye **13g** in DMSO, ... water influence on the UV/Vis spectrum of dye **13g** in DMSO.

2.4.1.2. *Cis-trans* isomerization of merocyanine dyes

Cis-trans isomerization of *N*-docosyl-4'-hydroxy-stilbazolium bromide **15n** was investigated by UV/Vis spectroscopy in dried chloroform. The spectrum of non-irradiated solution shows a mixture of protonated and non-protonated dye. The vibrational long wavelength absorption at ~ 580 nm is attributed to the $\pi\text{-}\pi^*$ transition of non-protonated dye while the absorption band with the maximum at $\lambda = 400$ nm is attributed to the $\pi\text{-}\pi^*$ transition of the protonated dye. By irradiating the solution with light at $\lambda = 405$ nm for 301 min. the vibrational absorbance of the non-protonated dye decreases to zero while the absorbance of the protonated compound at 390 nm decreases to a photostationary state. An increase of short wavelength absorption band at 250 nm was observed also. The experiment shows that the non-protonated form is converted to protonated form by irradiation with light at $\lambda = 405$ nm (Figure 44).

The irradiated solution at 405 nm was kept for 750 minutes in the dark and the thermal back reaction *cis-trans* was measured by UV/Vis spectroscopy. The spectrum show that the vibrational long absorption band of the non-protonated dye **15n** is not longer active. A slowly thermal back reaction was observed for protonated dye.

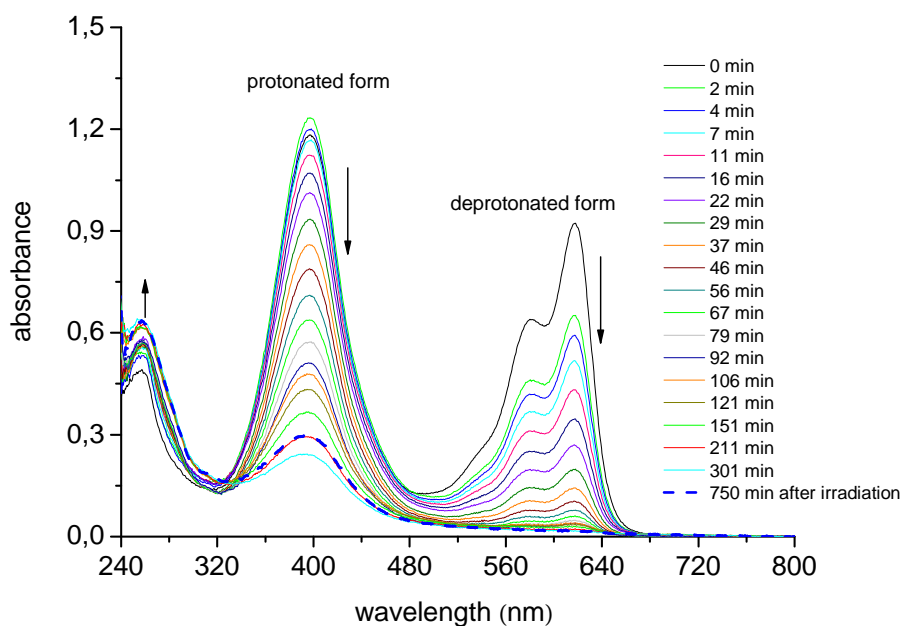


Figure 44. UV/Vis absorption spectra of *N*-docosyl-4'-hydroxy-stilbazolium bromide **15n** in chloroform before and after irradiation with light at $\lambda = 405$ nm, - - thermal back reaction, $T = 22$ °C, $c = 5 \times 10^{-5}$ mol l⁻¹, $l = 1$ cm, l – path length of the cell.

Irradiation measurements with light at $\lambda = 577$ nm were made in the case of **15n**. The results indicate a slowly decrease of the vibrational absorption of the non-protonated dye, concomitant with an increase of the absorbance of protonated form. After irradiation for 68 min. at 577 nm the photostationary state was achieved, Figure 45.

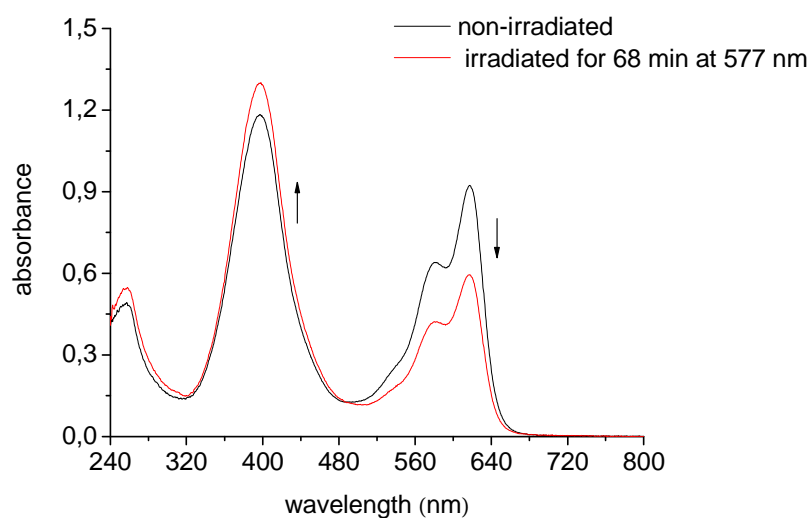


Figure 45. UV/Vis absorption spectra of *N*-docosyl-4'-hydroxy-stilbazolium bromide **15n** in chloroform before and after irradiation with light at $\lambda = 577$ nm, - - thermal back reaction, $T = 22$ °C, $c = 5 \times 10^{-5}$ mol l⁻¹, $l = 1$ cm, l – path length of the cell.

2.4.1.3. Aggregation behaviour of merocyanine dyes in solution

UV/Vis spectroscopy has been utilized to study dye behaviour in solution using solvents with different polarities. Merocyanine dyes may form aggregates in solution, depending on the temperature and dye concentration as well as on the solvent polarity and on the salt effect.⁵⁰ The aggregation behaviour of the new synthesized *N*-alkylated stilbazolium compounds was investigated in solvents with different polarities.

The aggregation behaviour of the dye **15a** was studied in a saturated solution of the dye in water. The measurements were made in cells with the distance of 1 mm, 0.3 mm, 0.1 mm and 10 μm . UV/Vis spectra show two absorption bands with maximum at 263 nm and 430 nm respectively. By increasing the thickness of the path cell the maximum of the absorbance of the both bands increases linearly, indicating that no other species are formed in solution (Figure 46a).

Using a solvent with a higher dipole moment than water ($\epsilon_r = 78$, $\mu = 6.2 \times 10^{-30} \text{ C m}$), as propylene carbonate ($\epsilon_r = 65$, $\mu = 16.5 \times 10^{-30} \text{ C m}$)⁶⁴ three absorption bands are identified in the spectrum with a maximum absorbance at $\lambda = 270 \text{ nm}$, 390 nm and at 540 nm respectively. UV/Vis absorption spectra of a saturated solution of **15a** were investigated in cells with path length of 2 mm, 1 mm, 0.3 mm and 0.1 mm (Figure 46b).

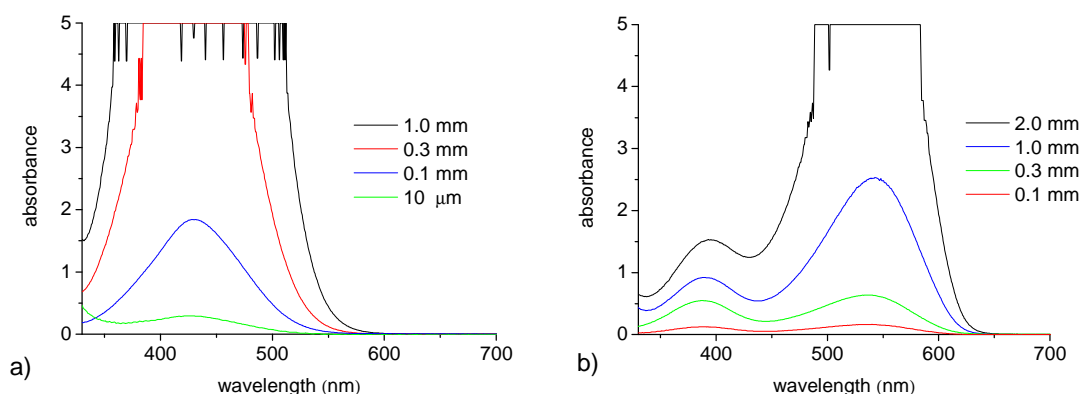


Figure 46. UV/Vis absorption spectra of *N*-methyl-4'-oxy-stilbazolium dye **15a** measured in quartz cells at $T = 22^\circ\text{C}$ and using as solvents a) water, $l = 1 \text{ mm}$, 0.3 mm, 0.1 mm and 10 μm b) propylene carbonate $l = 2 \text{ mm}$, 1 mm, 0.3 mm and 0.1 mm respectively.

The long wavelength absorption band measured in propylene carbonate at $\lambda_{\text{max}} = 540 \text{ nm}$ corresponds to an intramolecular charge-transfer between the oxy group as electron donor and pyridinium ring as electron acceptor and is attributed to non-protonated form of the merocyanine dye **15a**, as is shown in Figure 43 for a similar compound **13g**. The absorption band with maximum at $\lambda = 390 \text{ nm}$ corresponds to a $\pi\text{-}\pi^*$ transition of the protonated form of

15a. The maximum of the absorbance of the dye decreases with the thickness indicating that no aggregation takes place in propylene carbonate.

Two absorption bands with maximum at $\lambda = 400$ nm and near 600 nm respectively were detected in protic and in some polar aprotic solvents. In order to investigate the nature of these absorptions, concentration dependence measurements of compound **13g** were made in the polar protic solvent methanol ($\epsilon_r = 32.6$, $\mu = 9.6 \times 10^{-30}$ C m), in cells with a path length l of 1 cm. The absorption band in methanol is shifted to lower wavelength, compared with spectra in water, due to changes in the electronic system of the dye. The spectrum shows a maximum of the absorbance at 398 nm which corresponds for π - π^* transition of the protonated form of the dye, and a small absorption at 500 nm attributed to the π - π^* band of the non-protonated dye (Figure 47a).

A Lambert-Beer plot of the extinction as a function of the concentration shows a linear correlation indicating that no other species are formed in solution (Figure 47b).

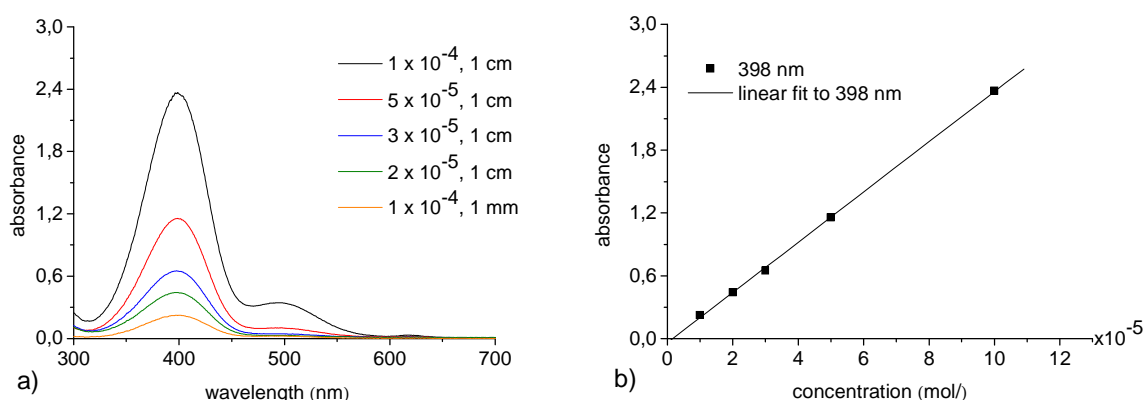


Figure 47. a) Concentration dependence measurements of 1-(1-octyl-nonyl)-4'-hydroxy-stilbazolium dye **13g** in methanol, $T = 22$ °C, c – concentration [mol l^{-1}], b) Lambert-Beer plot $A = f(\text{conc.})$, $R = 0.999$.

Concentration dependence measurements of *N*-(2-propyl)-pentyl-4'-oxy-stilbazolium dye **6c** were made in dipolar aprotic solvents DMSO ($\epsilon_r = 46.5$, $\mu = 13.5 \times 10^{-30}$ C m), in the concentration range between 1×10^{-5} mol l^{-1} and 1×10^{-4} mol l^{-1} (Figures 48a and b). The dye shows in DMSO a strong absorption band at 583 nm of the non-protonated form and a weak one at 397 nm of the protonated form of the dye. A plot of absorbance as a function of concentration gives a linear behaviour which indicates that no aggregation takes place. At concentrations below 1×10^{-5} mol l^{-1} the absorption band at 397 nm increases meaning that available protons from traces of water or other sources may result in the formation of the

protonated dye. Using the Lambert-Beer law, the extinction coefficient was calculated for compound **6c** as $\epsilon = 3.5 \times 10^4 \text{ l mol}^{-1} \text{ cm}^{-1}$.

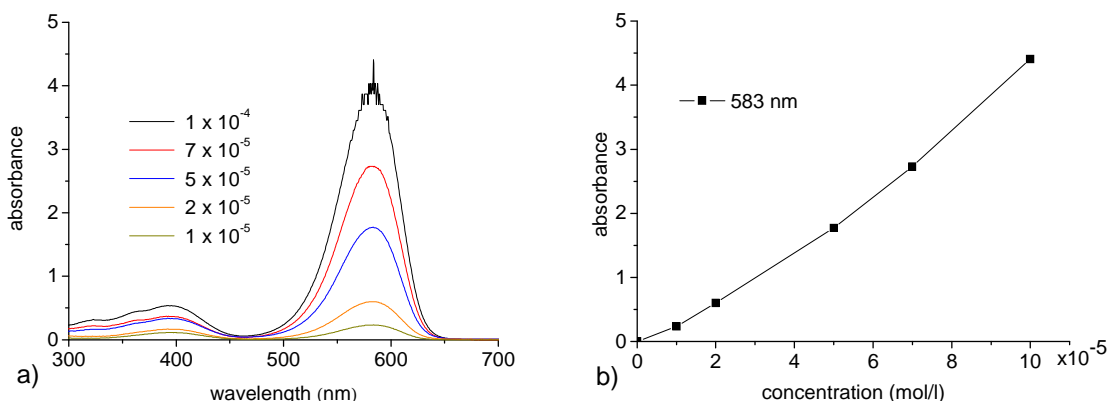


Figure 48. a) Concentration dependence in mol l^{-1} of *N*-(2-propyl)-pentyl-4'-oxy-stilbazolium dye **6c** in DMSO at $T = 22 \text{ }^\circ\text{C}$, $l = 1 \text{ cm}$, l – path length of the cell, b) Lambert-Beer plot $A = f(\text{conc.})$, $R = 0.999$.

Similar behaviour was found for dye **13g** in DMSO. A plot of extinction as a function of concentration, in the concentration range between $6 \times 10^{-5} \text{ mol l}^{-1}$ and $1 \times 10^{-5} \text{ mol l}^{-1}$, indicates a linear correlation. At low concentration the absorption band with maximum at $\lambda = 397 \text{ nm}$ increases and the absorption band at 583 nm decreases meaning that by dilution the water containing solvent will protonate the dye and changes the equilibrium between these two states (Figures 49a and b). Some deviations may be caused due to baseline problems.

Similar results were obtained for **13g** in DMF ($\epsilon_r = 36.7$, $\mu = 12.7 \times 10^{-30} \text{ C m}$), (Figure A12, Appendix).

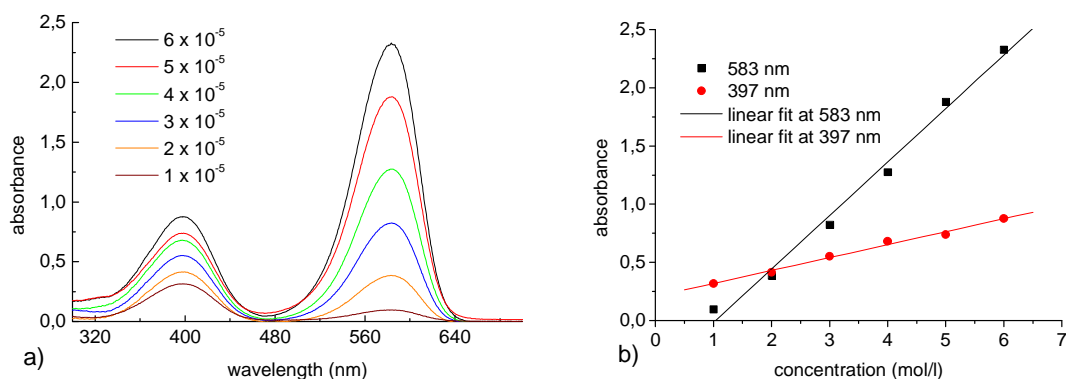


Figure 49. a) Concentration dependence in mol l^{-1} of 1-(1-octyl-nonyl)-4'-oxy-stilbazolium dye **13g** in DMSO, $T = 22 \text{ }^\circ\text{C}$, $l = 1 \text{ cm}$, l – path length of the cell b) Lambert-Beer plot $A = f(\text{conc.})$, $R_1 = 0.995$ (at $\lambda = 583 \text{ nm}$), $R_2 = 0.996$ (at $\lambda = 397 \text{ nm}$).

In a solvent with a lower polarity than DMSO and DMF, such as acetone ($\epsilon_r = 20.5$, $\mu = 9 \times 10^{-30}$ C m),) the maximum of the absorbance of non-protonated dye **13g** is shifted to longer wavelength λ . Lambert-Beer law shows a linear correlation between absorbance and concentration at 595 nm and 394 nm, indicating that no other species are formed in acetone in concentration range between 5×10^{-4} mol l⁻¹ and 1×10^{-5} mol l⁻¹ (Figures 50a and b).

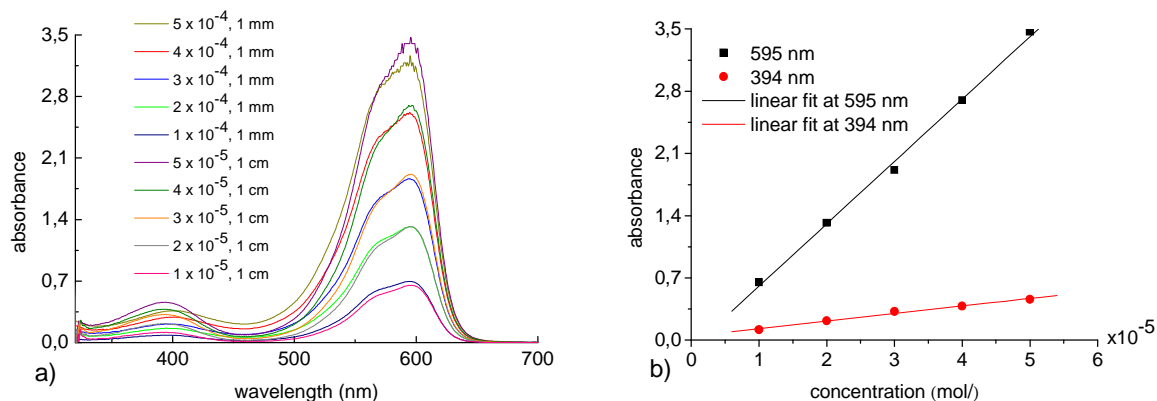


Figure 50. a) Concentration dependence in mol l⁻¹ of 1-(1-octyl-nonyl)-4'-oxy-stilbazolium dye **13g** in acetone at T = 22 °C, l = 1 mm and 1cm b) Lambert-Beer plot A = f (conc.), R₁ = 0.998 (at $\lambda = 595$ nm), R₂ = 0.995 (at $\lambda = 394$ nm).

Similar behaviour of dye **13g** was found in the low polar solvent methylene chloride ($\epsilon_r = 9$, $\mu = 3.8 \times 10^{-30}$ C m) in the concentration between 5×10^{-5} mol l⁻¹ and 1×10^{-5} mol l⁻¹ (Figure 51a). A linear plot of Lambert-Beer low at $\lambda = 602$ nm show that no other species are formed in solution (Figure 51b).

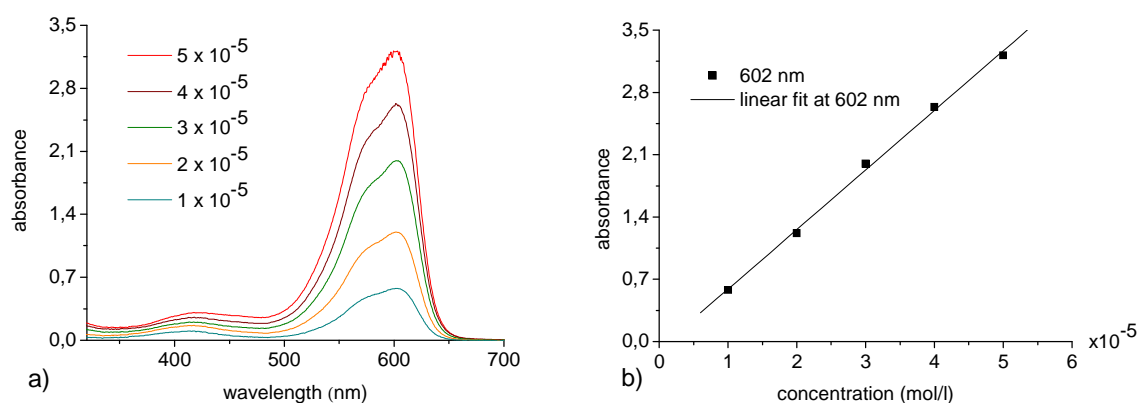


Figure 51. a) Concentration dependence in mol l⁻¹ of 1-(1-octyl-nonyl)-4'-oxy-stilbazolium dye **13g** in methylene chloride at T = 22 °C, l = 1 cm, b) Lambert-Beer plot A = f (conc.) at $\lambda = 602$ nm, R = 0.999.

Figure 52a shows the concentration dependence measurements of **13g** in butyl acetate ($\epsilon_r = 5.1$), in the range between 1×10^{-4} and 5×10^{-5} mol l $^{-1}$. The UV/Vis absorption spectra show vibrational bands at longer wavelength with maximum of the absorbance at $\lambda = 572$ nm and 614 nm respectively corresponding to non-protonated dye and a small one at with the maximum absorbance of $\lambda = 397$ nm which is attributed to the protonated form. The maximum absorbance increases with increasing the concentration indicating that no aggregation takes place. The presence of the water in samples by dilution or other sources causes small deviations from Lambert-Beer law (Figure 52b).

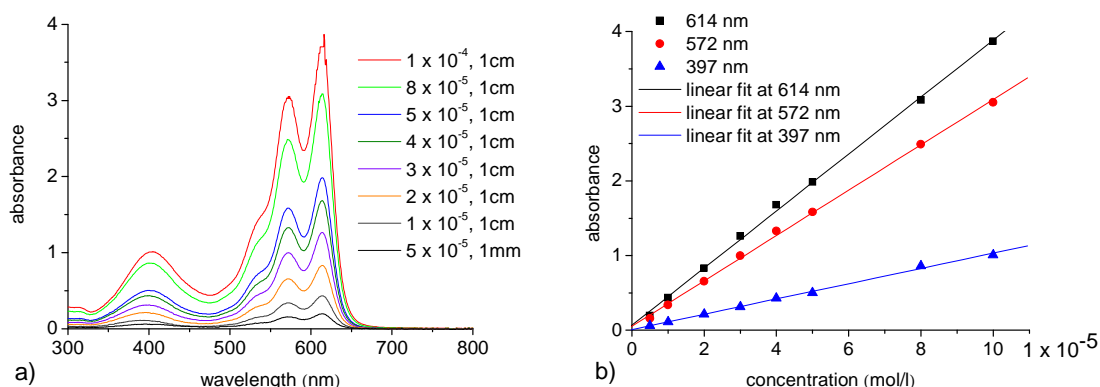


Figure 52. a) Concentration dependence in mol l $^{-1}$ of 1-(1-octyl-nonyl)-4'-oxy-stilbazolium dye **13g** in butyl acetate, T = 22 °C b) Lambert-Beer plot $A = f(\text{conc.})$, $R_1 = 0.999$ (at $\lambda = 614$ nm), $R_2 = 0.999$ (at $\lambda = 572$ nm), $R_3 = 0.998$ (at $\lambda = 397$ nm).

In the low polar solvent trichloroethene ($\epsilon_r = 3.42$ (16 °), $\mu = 2.7 \times 10^{-30}$ C m), UV/Vis spectra of the non-protonated dye **13g** are shifted to longer wavelengths at 580 nm and 625 nm in the concentration range between 2×10^{-4} mol l $^{-1}$ and 1×10^{-5} mol l $^{-1}$ (Figure 53a).

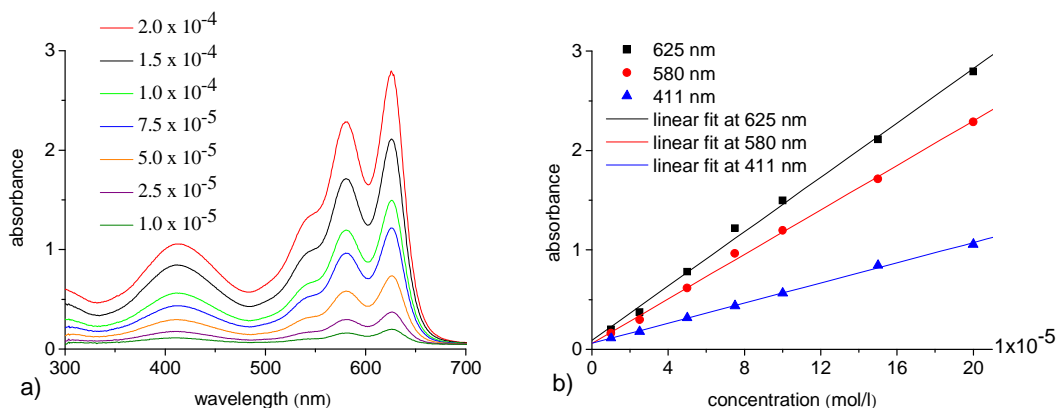


Figure 53. a) Concentration dependence of 1-(1-octyl-nonyl)-4'-oxy-stilbazolium dye **13g** in trichloroethene, T = 22 °C b) Lambert-Beer plot $A = f(\text{conc.})$, $R_1 = 0.998$ (at $\lambda = 625$ nm), $R_2 = 0.998$ (at $\lambda = 580$ nm), $R_3 = 0.999$ (at $\lambda = 411$ nm).

Concentration dependence measurements in trichlorethene show similarities with spectra obtained in butyl acetate. Dilution of the dye solution causes deviations from the linear behaviour of Lambert-Beer law due to the presence of more protons in solution (Figure 53b).

N-(2-octyl)-decyl-4'-oxy-3'-hexyloxy-stilbazolium dye **9** was investigated by UV/Vis spectroscopy in butyl acetate using quartz cells with path length of 1 mm, 2 mm, 5 mm and 1 cm (Figure 54a). Compared with the spectrum of dye **13g** the intensity of the long wavelength absorption spectra is inverted. A linear correlation of the Lambert-Beer plot indicates that no aggregation takes place in butyl acetate (Figure 54b).

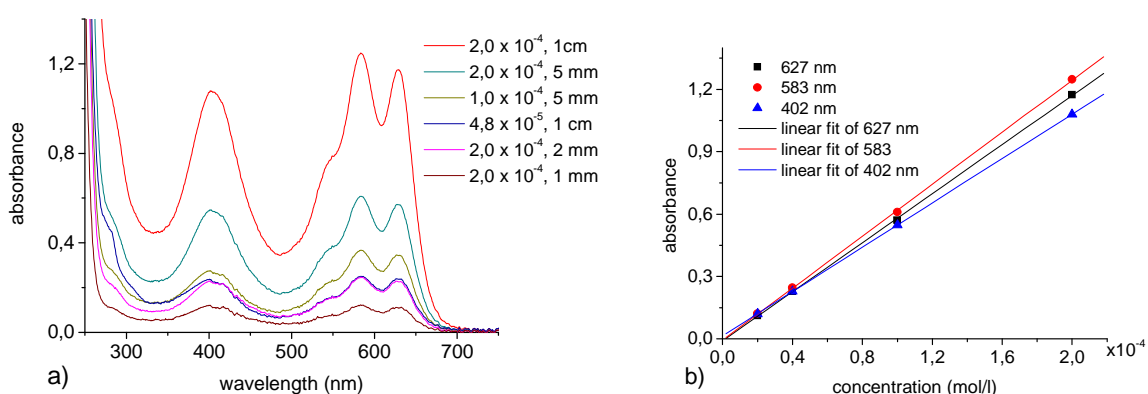


Figure 54. a) Concentration dependence of *N*-(2-octyl)-decyl-4'-oxy-3'-hexyloxy-stilbazolium dye **9** in butyl acetate, $T = 22^\circ\text{C}$ b) Lambert-Beer plot $A = f(\text{conc.})$.

2.4.1.4. Aggregation behaviour of merocyanine dyes in solid state

Single crystal X-ray diffraction investigations were made to prove the molecular model of *N*-methyl-4'-oxy-stilbazolium dye **15a**⁸⁴ in the solid state.

The dye was obtained in *trans* conformation. The packing of the molecules is presented in Figure 55 and show the formation of the dimers having an antiparallel orientation. The dyes pack in a tetragonal arrangement which form channels occupied by three molecules of water per dye molecule. Two molecules of dimers having an antiparallel fashion are oriented in the horizontal plane with the distance between the molecules of 3.5 Å. The next dimer is oriented vertically. The distance between the dimers in horizontal plane is 11 Å. The molecules are connected by hydrogen-bonds.

The presence of the water can be confirmed also by elemental analysis which indicates deviations between the calculated and experimental results even after drying of the sample for longer time at 78 °C under vacuum.

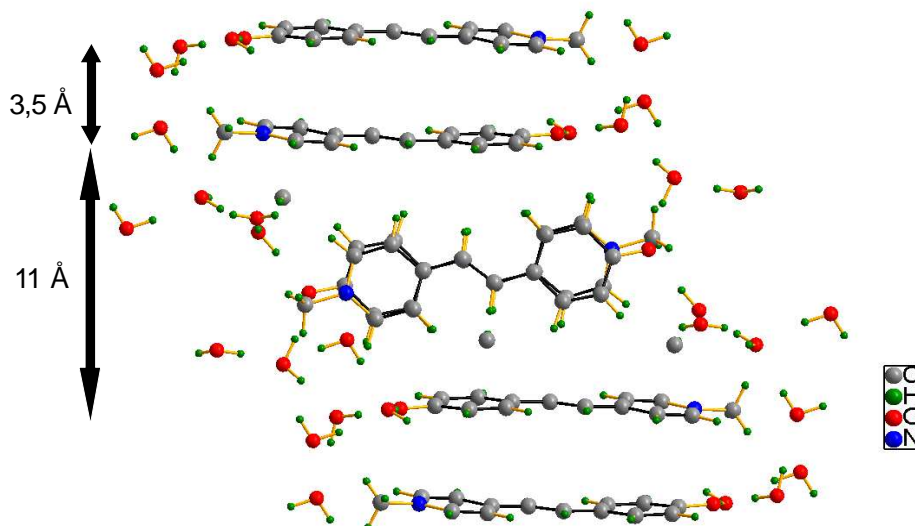


Figure 55. Formation of dimeric aggregates of *N*-methyl-4'-oxy-stilbazolium dye **15a** as obtained by single-crystal X-ray diffraction analysis.

Additional data obtained by 3D X-ray measurements for **15a** are given in Appendix.

2.4.1.5. Solvatochromic effect

Solvatochromic effect of 1-(1-octyl-nonyl)-4'-oxy-stilbazolium dye **13g** was investigated by UV/Vis spectroscopy in 13 solvents with different polarities. The spectra show a large change of the maximum of the absorbance from $\lambda = 495$ nm in methanol to $\lambda = 625$ nm in trichloroethene due to a change in the electronic structure of the dye. The investigations indicate the largest shift of **13g** in trichloroethene. Increasing the alkyl chain length, the dye is no longer soluble in water therefore most of the measurements were made in non-polar solvents.

Extensive studies were made on **15a** to prove the large solvatochromic effect found between 442 nm in water and 620 nm in chloroform.⁵⁹ UV/Vis investigations indicate changes in the electronic ground-state structure with increasing solvent polarity. The π - π^* absorption band is attributed to the non-protonated form in non-polar solvents, while the π - π^* absorption band in polar solvents corresponds to the protonated form of the dye.

The dyes can be used as indicator of solvent polarity and several empirical parameters are used to characterize the solvent properties.

In order to establish the solvent dependence of π - π^* transition energy, Brooker et al.⁴¹ proposed two solvent polarity parameters: χ_R for bathochromic shifts and χ_B for hypsochromic shifts.

Figure 56a shows a plot of χ_R parameter characteristic for red shifts as a function of the energy of π - π^* transition of **13g**. A relatively good correlation coefficient $R = 0.951$ was obtained in low polar and polar aprotic solvents. A plot of χ_B parameter, characteristic for blue shifts against the energy of π - π^* transition of dye **13g** shows a good correlation in polar protic and aprotic solvents (Figure 56b).

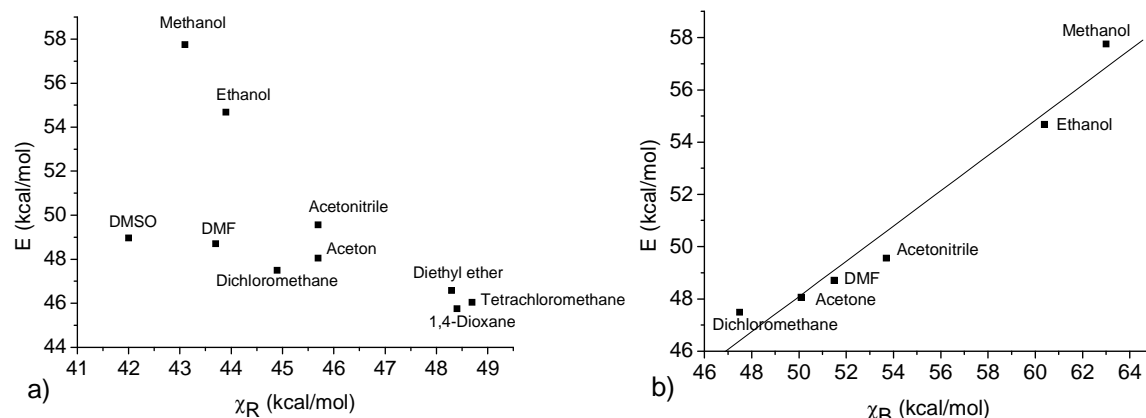


Figure 56. a) χ_R (kcal mol⁻¹) parameter of Brooker as a function of E (kcal mol⁻¹) of 1-(1-octyl-nonyl)-4'-oxy-stilbazolium dye **13g** b) χ_B (kcal mol⁻¹) parameter of Brooker as a function of E (kcal mol⁻¹), $E = 0.674 \cdot \chi_B + 14.389$ ($R = 0.980$).

The wavelength (nm) and the wavenumber (cm⁻¹) of the π - π^* transition of dye **13g** in different solvents as well as empirical parameters of the solvent polarity determined by Kosower (Z) and by Dimroth-Reichardt $E_T(30)$ in kcal mol⁻¹ are summarized in Table 11:

The solvent polarity parameter $E_T(30)$, proposed by Dimroth and Reichardt, indicates the transition energy of the N -phenolate betaine dye $E_T(30)$ due to the presence of the intramolecular charge-transfer. A plot of the $E_T(30)$ parameter as a function of the wavenumber ν' of dye **13g** shows a relatively linear correlation, with only a small deviation in the case of tetrachloromethane (Figure 57a).

Another parameter Z , proposed by Kosower, was utilized to measure the ionizing property of the solvents. The molar transition energy of the intermolecular charge-transfer of 1-ethyl-4-(methoxycarbonyl)-pyridinium iodide in different solvent has been used as an empirical parameter of the solvent polarity as a function of the energy of dye **13g**. Figure 57b shows a linear correlation between Z (kcal mol⁻¹) and E (kcal mol⁻¹).

No.	Solvent	λ (nm)	ν_{\max} (cm^{-1})	ν'_{\max} (cm^{-1})	E (Kcal/mol)	Z (kcal/mol)	$E_T(30)$ (kcal/mol)
1	Methanol	495	20202	20704	57.75	83.6	55.4
2	Ethanol	523	19120		54.67	79.6	51.9
3	Propylene carbonate	552	18116		51.79	72.4	46.0
4	Acetonitrile	577	17331	17513	49.55	71.3	45.6
5	DMSO	584	17123	17483	48.96	70.2	45.1
6	DMF	587	17036	17182	48.70	68.4	43.2
7	Acetone	595	16807	17094	48.05	65.5	42.2
8	Methylene chloride	602	16611	16556	47.49	64.7	40.7
9	Butyl acetate	614-42	16287		46.57	-	38.5
10	1,4-Dioxane	618-35	16181	16287	46.26	-	36.0
11	Trichloroethene	625-45	16000		45.74	-	35.9
12	Diethyl ether	614-42	16287	16367	46.57	-	34.5
13	Tetrachloromethane	621-45	16103	16181	46.04	-	32.7

Table 11. λ – wavelength of **13g** in nm, ν'_{\max} – wavenumber of **13g** in cm^{-1} , ν_{\max} – wavenumber of **15a** in cm^{-1} , $E_T(30)$ (kcal mol^{-1}) – empirical parameter of solvent polarity proposed by Dimroth-Reichardt, Z (kcal mol^{-1}) – Kosower empirical parameter.

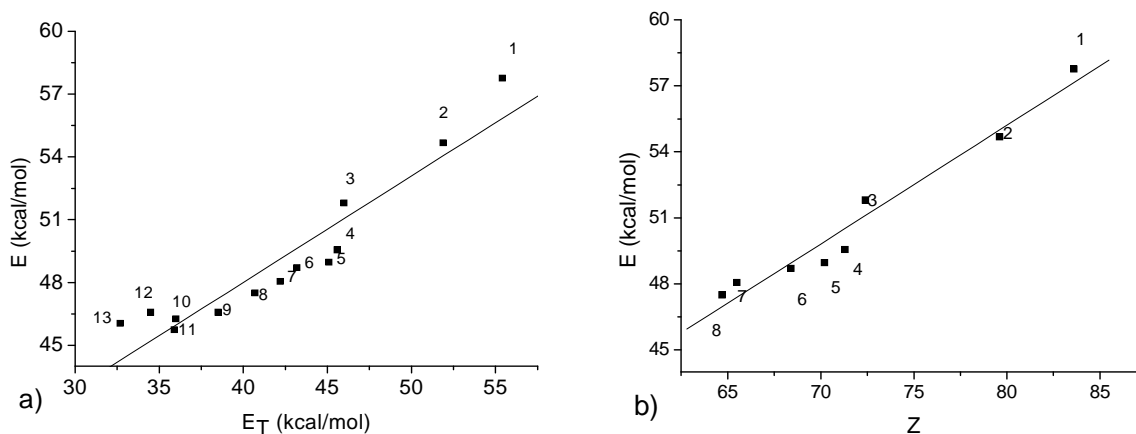


Figure 57. a) $E_T(30)$ (kcal mol^{-1}) parameter of *N*-phenolate betaine as a function of E (kcal mol^{-1}) of **13g**; $E = 0.508 E_T + 27.668$ ($R = 0.944$) b) Linear correlation of Z (kcal mol^{-1}) parameter of Kosower as a function of energy E of **13g** in (kcal mol^{-1}), $E = 0.539 \cdot Z + 12.082$ ($R = 0.980$).

All the parameters presented before characterizes the acceptor properties of the solvents. Gutmann introduced a donor numbers which characterizes the donor ability of the solvents. The donor number was defined as a negative molar enthalpy value of the donor with antimony pentachloride which was chosen as reference acceptor.⁵⁴ Dye **13g** does not show a good correlation with donor number *DN* in polar aprotic and non-polar solvents.

Generally, a good correlation of dye **13g** was measured with Kosower parameter Z , Dimroth-Reichardt $E_T(30)$ parameter as well as with χ_B parameter of Brooker.

2.4.1.6. Substituent effect

In the case of stilbazolium salts **15**, **16**, **17** besides dipolar interactions, the ionic interactions are the driving forces due to a presence of an intermolecular charge-transfer between the pyridinium cation and the anion. The influence of the substituents attached to the 4'-position of stilbazolium unit on the UV/Vis absorption spectra measured in acetonitrile at concentration $3 \times 10^{-5} \text{ mol l}^{-1}$ is presented in Table 12. Merocyanine dye **13g** with long alkyl chain shows the most shifted absorption band at 577 nm (Figure A13, Appendix). The stilbazolium salts possessing electron accepting dimethylamino and nitro groups in the 4'-position of the stilbazolium core have the π - π^* transition band at 474 nm and 343 nm respectively. Compounds **15** and **16** with hydroxy and methoxy groups in the 4'-position of the stilbazolium head group show a shift of the maximum of the absorbance to longer wavelengths compared with hydrogen substituted salts (Figures A4-A7, Appendix).

The substituents at the 4'-position of the stilbazolium unit will shift the maximum absorbance to longer wavelength in order $O^- > N(CH_3)_2 > OH > OCH_3 > H > NO_2$.

Compounds	19	17f	16f	15n	20	13g
Substituents	NO ₂	H	OCH ₃	OH	N(CH ₃) ₂	O ⁻
λ (nm)	344	347	383.0	386	473	577

Table 12. Influence of the substituents attached to the 4'-position of the stilbazolium unit on the UV/Vis absorption spectra in acetonitrile.

Compared with spectra of dye **13g** in butyl acetate, compound **9** shows a shift of the vibrational band of non-protonated form. The first vibrational band is shifted with 11 nm to longer wavelength while the second vibrational band is shifted with 13 nm.

Related with *N*-methyl-stilbazolium dye **15a** spectra, dye **13g** with secondary and long alkyl chain shows a shift of 10 nm to longer wavelength of the π - π^* band.

The effect of different branched alkyl chains attached to *N*-position of the stilbazolium core on the liquid crystalline behaviour was investigated for dyes **6a – e** and **13a – g** as well as **15a – g**. The dyes do not form liquid crystalline phases. The melting points of dyes **13** are between 85 and 130 °C and do not show large variation by increasing the alkyl chain length. Similar melting points, between 93 and 123 °C, were found for dyes **6a – c**. Increasing the

number of C-atoms, dyes **6d** and **6e**, results in a large increase of the melting points to 170 – 180 °C. As a results, the attachment of long *N*-(2,2-dialkyl ethyl) and secondary *N*-alkyl chains will not reduce in large extent the strong dipole-dipole interactions. The presence of water, as probed by 3D X-ray measurements (see chapter 2.4.1.4), and the instability of the dyes at temperatures > 100 °C, may cause deviations of the melting points. Generally the dyes of type **6** and **13** show a tendency to form glasses on cooling.

2.4.1.7. Fluorescence investigations of merocyanine dyes

The fluorescence spectrum gives information about the molecular structure of the dyes as derived from the absorption spectrum. Fluorescence investigations were made for 1-(1-octyl-nonyl)-4'-oxy-stilbazolium dye **13g** in ethanol and propylene carbonate. The experiments were made in a 1 cm path cell at concentration $1 \times 10^{-4} \text{ mol l}^{-1}$.

The red emission band represents the fluorescence spectrum of **13g** in ethanol, the blue band corresponds for the fluorescence of the solvent (propylene carbonate) and the green emission band represents the fluorescence of the dye in propylene carbonate. The excitation spectrum (black) indicates that only the protonated form of the dye shows fluorescence (Figure 58).

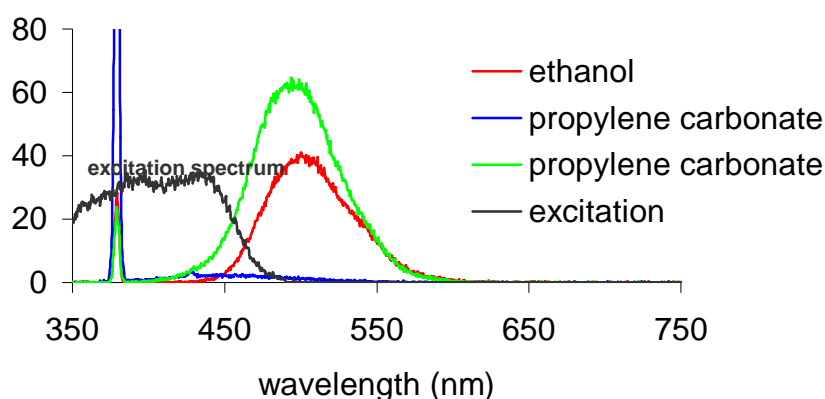


Figure 58. Fluorescence measurements of 1-(1-octyl-nonyl)-4'-hydroxy-stilbazolium dye **13g** in ethanol...red, propylene carbonate...green, fluorescence of propylene carbonate...blue, excitation spectrum...black.

2.5. Photo-E.M.F measurements of *N*-alkyl-3- and -4-substituted pyridinium salts and stilbazolium compounds

The photoconducting properties of *N*-alkyl-3- and -4-substituted-pyridinium salts, *N*-alkyl-4'-substituted stilbazolium salts as well as of the stilbazolium dyes were investigated by Photo-ElectroMotive-Force (Dember-effect). Laser flash irradiation generates in photoconductors electron/holes pairs which cause a diffusion of the charge carriers h^+ and e^- into the inner part of the crystal giving a charge separation due to different mobilities of electrons and holes.⁸⁵ The transient electrical potential between the illuminated and the dark sides of the crystal was measured by this method.⁸⁶ The voltage $U(t)$ is directly proportionally with the number of separated charges. When no voltage is measured the samples do not show any semiconductor properties. When the electrons move faster than the holes we have an n-type photoconductor because the illuminated side of the sample is positively charged (Figure 59).

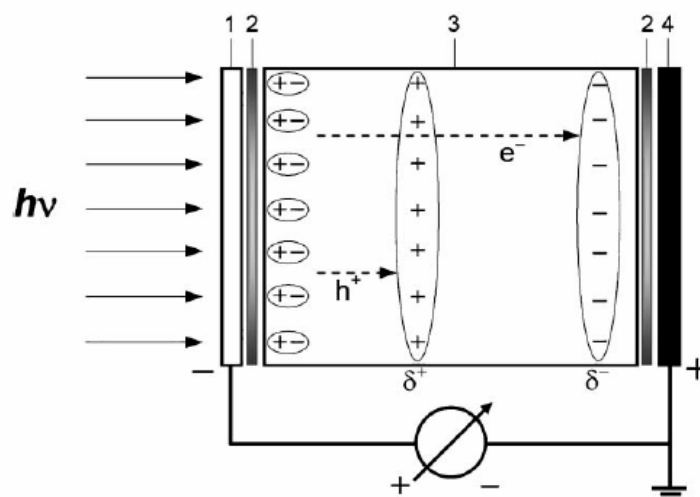


Figure 59. Measurement principle of the photo-emf for an n-type photoconductor⁷²: 1. Transparent NESAs-glass electrode 2. Isolating polyethylene foil 3. Sample 4. Metal rear electrode.

Sample preparation:

General procedure: A solution of polyvinyl butyral (PVB) in 1, 2-dichloroethane (10 % mass PVB) and 100 mg of investigated compound were mixed for 3 min. at room temperature in a ball-mill apparatus (Ardenne vibrator, the ball-mill diameter was 1 cm) in order to obtain the wanted optical density. After mixing, the suspension was poured on the flat glass plate which was treated before with chlortrimethylsilan. The plates were dried for two days at room

temperature under solvent atmosphere. The solvent residue was removed by drying the plates for one week in a desiccator, under vacuum and using molecular sieves (3 Å). A layer thickness with a size between 60 and 90 μm was obtained.

Semiconducting properties of the following substances: *N*-(2-propyl)-pentyl-4'-oxy-stilbazolium dye **6c**, *N*-eicosyl-4-methyl-pyridinium bromide **14m**, *N*-methyl-4'-oxy-stilbazolium dye **15a**, *N*-eicosyl-4'-methoxy-stilbazolium bromide **16e**, *N*-eicosyl-stilbazolium bromide **17e**, *N*-eicosyl-4-phenyl-pyridinium bromide **21e** and *N*-eicosyl-3-phenyl-pyridinium bromide **22e** were investigated.

Pieces with an area of 1 cm² were placed between the electrodes, see Figure 56, thermalized to 25 °C and flash illuminated using a 100 kV N₂-laser, τ_{flash} = 0.4 ns. The photoinduced time dependent electrical potential is recorded by a digital storage oscilloscope with an over all time resolution of n ≥ 30 ns.

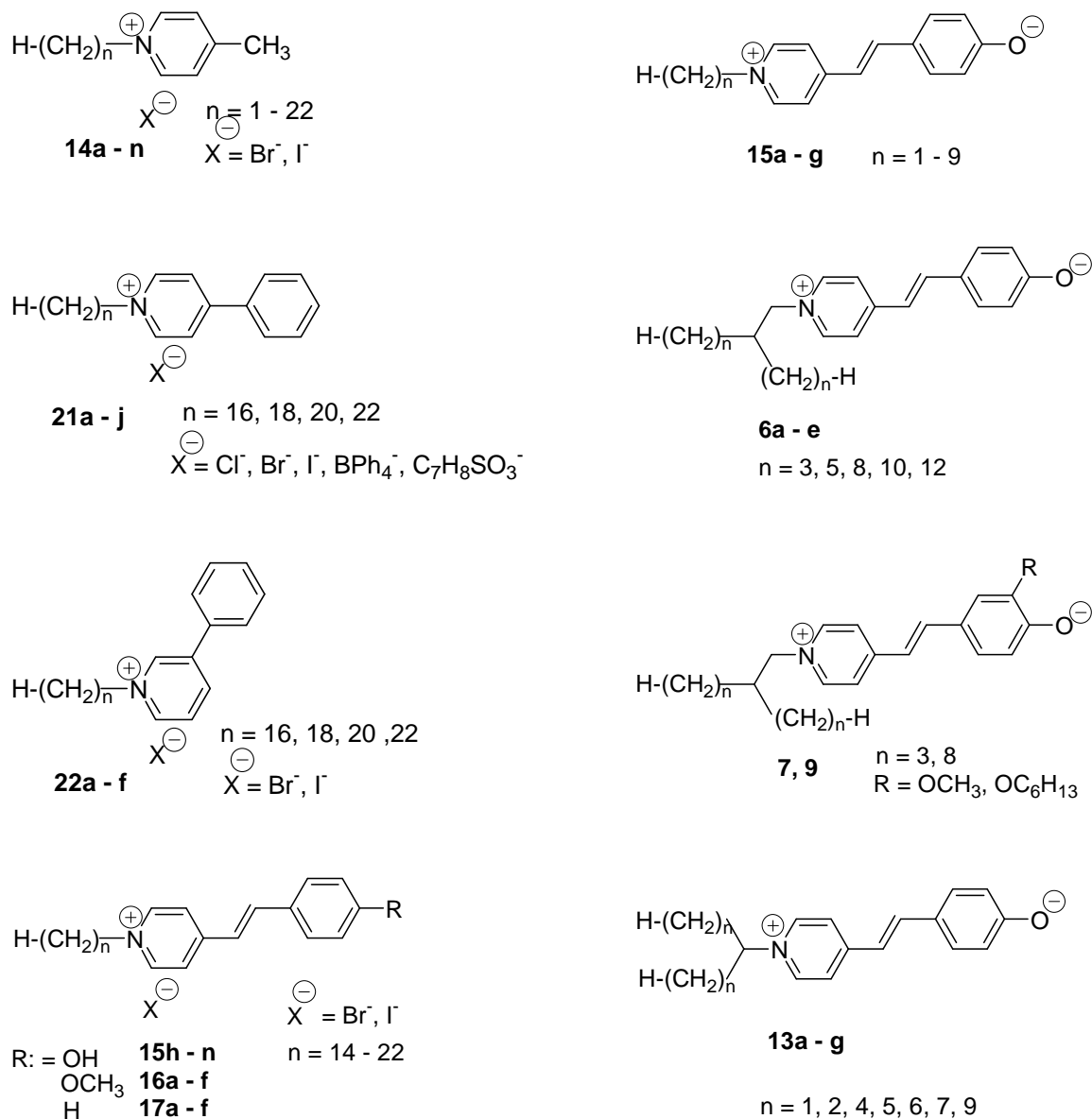
The investigated compounds were measured with a time resolution between 20 ms and 250 ns at 25 °C.

The investigated compounds have no photoconducting properties. The absence of a photo change can be explained using the picture from 3D X-ray structure of *N*-methyl-4'-oxy-stilbazolium dye **15a**. Dimers with distance of 3.5 Å would be able to transport localized h⁺/e⁻ pairs, but a distance of 11 Å to the next dimer is too large for an effective charge separation and transport.

3. Summary

N-alkyl-3-substituted and 4-substituted pyridinium salts **14**, **21**, **22**, *N*-alkyl-4'-substituted-stilbazolium salts **15** – **17** as well as merocyanine dyes of the stilbazolium type with *N*-alkyl **15a** – **g**, secondary *N*-alkyl **13a** – **g** and *N*-(2,2-dialkyl ethyl)-substituents **6a** – **e**, **7** and **9** were synthesized and characterized by polarizing microscopy, differential scanning calorimetry, X-ray and UV/Vis spectroscopy. The compounds were synthesized in order to study the effect of the elongation of aromatic core group, the influence of the alkyl chains, the counter ions and of the different substituents attached to the stilbazolium unit on their liquid crystalline behaviour.

The general structure of the synthesized and investigated compounds is shown in Scheme 15:





Scheme 15. General structure of the synthesized and investigated compounds, n – number of C-atoms in the alkyl chain.

N -alkyl-3- and -4-substituted-pyridinium salts with long alkyl chains $n \geq 18$ display SmA phases upon heating above their melting point. The formation of SmA phase was confirmed by polarizing microscopy and X-ray diffraction measurements. A CPK model of the investigated compounds shows a head to tail arrangement of the molecules within the layer with the anion localized between the aromatic rings.

The simple 4-methyl substituted compounds **14**, induces a large stability of the SmA phase compared with corresponding salts **21** and **22**, indicating that elongation of the aromatic core destabilizes the mesophase. Additionally, it leads to the formation of an ordered intermediate mesophase M in the case of bromides **21**. The more bulky 3-phenyl-pyridinium head group in **22** lowers the melting points drastically and reduces the temperature range of LC phases. The SmA temperature range increases upon attaching substituents to the pyridinium unit in the order 4-methyl (**14**) > 3-phenyl (**22**) > 4-phenyl (**21**).

The alkyl chains and the counter ions have a large influence on the stability of the SmA phase. Increasing the length of the alkyl chain n of salts **14**, **21** and **22** causes the melting points to remain nearly constant while the clearing temperatures increase.

By changing the anion from iodide to bromide and then to chloride, as in the case of compounds **21** with alkyl chain $n = 22$, the tendency to form LC phases increases depending on the size of the anion. Reducing the size of the anion leads to a better stabilization of the layers, as supported by observations on CPK models, because an anion with a smaller size is readily accommodated near the pyridinium ring. Replacement of the halides by a counter ion with a larger size, as tetraphenylborate, results in a decrease of the stability of the SmA phase. Therefore, it can be conclude that the increase in the clearing points is caused by a decrease in the size of the anion in the order chloride > bromide > iodide > tetraphenylborate. The presence of the flat anion p-toluenesulfonate, in N -docosyl-4-phenyl-pyridinium salt **21j**, indicates that the tendency to form a SmA phase is suppressed.

UV/Vis investigations on N -alkyl-3- and -4-substituted-pyridinium iodides, measured in low polar 1, 2-dichloroethane, show deviations from Lambert-Beer law which indicates that additional ion pairs are formed in solution due to the presence of a charge-transfer

complex between the pyridinium cation and the iodide ion. When the iodide ion was replaced by bromide, the charge-transfer band is no longer present and a linear Lambert-Beer plot indicates that no other species are formed in solution.

AFM investigations on *N*-octadecyl-4-methyl-pyridinium iodide at 55 °C indicated the formation of fibres on mica and graphite supports. A model using the dimension of molecules in the long axis showed the formation of 95 double layers on mica and 207 double layers on graphite. Isothermal titration calorimetry of the same compound gives a critical micelle concentration of $1.5 \times 10^{-4} \text{ mol l}^{-1}$ in water.

N-Alkyl-4'-substituted-stilbazolium salts **15** – **17** with alkyl chain $n > 14$ show fan-shaped textures characteristic of SmA phase under polarizing microscopy. Stilbazolium compounds **15** – **17** show higher temperatures of the transition SmA-isotropic liquid in comparison to the pyridinium salts of type **14**, **20**, **21**. Thus, thermal decomposition of the salts upon heating above 200 °C has a major influence on the stability of their mesophases. Therefore, besides the ionic interactions, the liquid crystalline behaviour is influenced, in the case of salts **15** and **16**, also by stronger dipolar interactions by introducing hydroxy and methoxy groups in the 4'-position of the stilbazolium unit. This can be easily explained by the chemical structure allowing strong mesomeric interactions between the methoxy and hydroxy group as electron donors and the quaternary ammonium group as an acceptor (intramolecular charge-transfer).

Generally, the salts with bromide anion show an increase of the mesophase temperature range ΔT with increasing alkyl chain length n .

The stability of the SmA phase decreases by increasing anion size.

By replacing the hydroxy group from the 4'-position of the stilbazolium core with an oxy substituent, by deprotonation, the dipole-dipole interactions will be the governing forces for association. This interaction leads to a head-tail dimerization of the dye molecules and affords high activation barriers for reorganization to liquid crystalline (supramolecular) arrangements. In order to reduce the activation carriers for reorganization at the stilbazolium units, long *N*-alkyl chains, secondary and *N*-(2,2-dialkyl ethyl) substituents were attached to the aromatic core.

Deprotonation of the hydroxy group from the 4'-position of the stilbazolium unit, resulted in the formation of merocyanine compounds, in which the dipole-dipole interactions are the governing forces. Elongation of the alkyl chain length up to $n = 22$ carbons as well as the attachment of secondary *N*-alkyl substituents, in the case of merocyanines **13a** – **g**, or *N*-(2,2-dialkyl ethyl) substituents, in the case of merocyanines **6a** – **e**, **7** and **9**, do not overcome

the strong dipolar interactions. This explains why the compounds regularly have no liquid crystalline properties.

UV/VIS spectroscopy has been utilized to study merocyanine dye aggregation in solution using a significant number of solvents with different polarities. Lambert-Beer plots indicate that the dyes do not show aggregation in non aqueous/organic solvents over a wide range of concentrations ($< 10^{-3} \text{ mol l}^{-1}$).

Aggregation of the merocyanine dyes takes place in the solid state. 3D X-ray investigations of a dye molecule with a short alkyl chain show the formation of dimers with antiparallel oriented dipole moments. The dimers pack in a flat tetragonal arrangement which form channels occupied by three molecules of water per dye molecule.

The dyes are sensitive to the acidity of the solvent, showing protonation-deprotonation equilibrium. Generally, these dyes may be used as very sensitive indicator molecules for protons.

Fluorescence investigations made for the 1-(1-octyl-nonyl)-4'-oxy-stilbazolium dye **13g** in ethanol and propylene carbonate show that only the protonated form of the dye fluoresces.

The influence of the substituents attached to the 4'-position of stilbazolium unit on the UV/Vis absorption spectra measured in acetonitrile at a concentration $3 \times 10^{-5} \text{ mol l}^{-1}$ is presented in Table 13. The substituents on the 4'-position of the stilbazolium unit shift the maximum absorbance to longer wavelength in order $\text{O}^- > \text{N}(\text{CH}_3)_2 > \text{OH} > \text{OCH}_3 > \text{H} > \text{NO}_2$.

Compounds	19	17f	16f	15n	20	13g
Substituents	NO ₂	H	OCH ₃	OH	N(CH ₃) ₂	O ⁻
<i>n</i>	22	22	22	22	22	9
λ (nm)	344	347	383.0	386	473	577

Table 13. Influence of the substituents on the 4'-position of the stilbazolium unit on the UV/Vis absorption spectra.

Cis-trans isomerization of the stilbazolium salts and dyes was investigated by ¹H NMR and UV/Vis spectroscopy and indicate a slow thermal back reaction to the *trans* form. Merocyanines do not form a stable *cis* isomer at room temperature.

The investigated solid compounds, merocyanines with *N*-alkyl chain, *N*-(2,2-dialkyl ethyl) substituents as well as *N*-eicosyl-3- and -4-substituted pyridinium bromides of type **14**, **21** and **22** and *N*-eicosyl-4-substituted-stilbazolium bromides of type **16** and **17**, do not show

any photo-polarisation in PEMF-measurements. This is in agreement with the solid state structure of merocyanines. Absorption of light results in a local excited state but the large distances between the merocyanine dimers (11 Å) do not allow any dissociation of the e^-/h^+ pairs to free charge carriers.

4. Experimental part

The following substances were commercial available:

Acetic anhydride (Acros)
p- Anisaldehyde (Acros)
Benzaldehyde (Acros)
1-Bromodocosane (Aldrich)
1-Bromoeicosane (Aldrich)
1-Bromohexadecane (Acros)
1-Bromooctadecane (Acros)
1-Bromooctane (Acros)
1-Bromopentane (Lancaster)
1-Bromopropane (Acros)
1-Bromotetradecane (Acros)
Decyl aldehyde (Acros)
3, 4-Dihydroxybenzaldehyde (Acros)
Dimethyl malonate (Acros)
Heptaldehyde (Acros)
Hexanal (Acros)
4-Hydroxybenzaldehyde (Acros)
1-Iodohexadecane (Aldrich)
1-Iodohexane (Acros)
Iodomethane (Acros)
1-Iodononane (Aldrich)
1-Iodooctane (Acros)
1-Iodopropane (Acros)
Lithium aluminium hydride (Acros)
Lithium chloride (Lancaster)
Magnesium (Acros)
4-Methoxybenzaldehyde (Acros)
4-Nitrobenzaldehyde (Acros)
3-Pentanol (Acros)
4-Phenylpyridine (Fluka)

3-Phenylpyridine (Fluka)

4-Picoline (Acros)

Piperidine (Reachim)

Sodium sulfate anhydrous (Acros)

Vanillin (Acros)

General procedures and analytical data of the synthesized compounds

All the solvents were dried using general standard procedures.⁶⁹

The investigated compounds were dried for at least two days under vacuum (2 Torr) at temperatures below the melting points or maximum 100 °C for high melting salts and using P₂O₅ as drying agent.

The structure of the intermediates and final compounds was confirmed by ¹H and ¹³C NMR using a Varian Gemini 200 and Varian Unity 400 and 500 spectrometers. Due to the bad solubility of dyes in low polar solvents the spectra of merocyanines of type **6**, **7**, **9** and **15** were made in DMSO-d₆. Therefore, most of the NMR spectra of the dyes measured in the hygroscopic DMSO-d₆ show the protonated form of the dye.

Elemental analysis was performed by a Leco CHNS-932 instrument.

The MS spectra were taken on the instrument AMD 402 from Intectra GmbH (70 eV). ESI-MS spectra were obtained using a Finnigan LQC spectrometer from Thermo Electron Corp. (4.1 kV) and using as a solvent methanol.

The calorimetric measurements were made using a Perkin-Elmer DSC-7 differential scanning calorimeter with a heating-cooling rate of 10 °C·min⁻¹. In the case of pyridinium salts **14**, **21** and **22** the transition temperatures, which are summarized in Tables 1 – 4, correspond to the second heating. Due to a partial decomposition of the stilbazolium salts, the transition temperatures presented in Tables 5 – 7 correspond to the first heating. The samples were heated to ca. 120 °C before DSC measurements to remove traces of water. Thermogravimetric measurements were made using a STA 409 instrument (Netzsch) and show that the compounds start to decompose at temperatures above 200 °C. Salts **21e** and **16e** show by thermogravimetric analysis a loss of weight at 100 °C which corresponds to 0.8 mol water (2.78 %) for salt **21e** and 0.16 mol water (0.52 %) for salt **16e**.

Microscopic investigations were performed by a Nikon Optiphot 2 polarizing microscope which was connected with a Mettler FP 82 HT heating stage.

X-ray investigations on powder-like samples were carried out with a Guinier equipment (film camera and goniometer, both by Huber) with samples in a temperature-

controlled heating stage using quartz-monochromatized CuK α radiation (calibration of the film patterns with the powder pattern of Pb(NO₃)₂). Two-dimensional patterns for aligned samples on a temperature controlled heating stage were recorded with a 2D detector (HI-STAR, Siemens). The substances had to be heated, for orientation, into the isotropic liquid during the sample preparation for the X-ray investigations. Furthermore, the samples for the Guinier measurements were sealed in glass capillaries (1 mm), those for the 2D measurements were drops on a glass plate aligned at the sample – glass or at the sample – air interface. Taking into account the influences of water and partial decomposition, the transition temperatures and even the phases observed under the conditions of the different X-ray measurements may differ from each other and from that found by the other methods.

3D X-ray investigations were made for single crystals of **15a**. Intensity data were collected on a STOE IPDS diffractometer with Mo K α radiation ($\lambda = 0.71073$ Å, graphite monochromator). The structure was solved by direct methods with SHELX-86⁸⁷ and refined using full-matrix least-square routines against F^2 with SHELX-97⁸⁸. Hydrogen atoms were added to the model according to the “riding model” and refined with isotropic displacement parameters while the non-hydrogen atoms were refined with anisotropic displacement parameters.

The conductivity of *N*-octadecyl-4-phenyl-pyridinium iodide **21d** was measured with a Solartron Schlumberger Impedance Analyzer SI1260 in combination with a Chelsea interface. The measurements were made over the frequency range of 10³ -10⁷ Hz using a capacitor made from brass and coated with gold. The distance between the electrodes was 0.1 mm. The capacitor was calibrated with cyclohexane.

The UV/Vis measurements were made on UV 3101 PC spectrometer from Shimadzu Company and the fluorescence measurements were recorded on a Perkin Elmer LS 50B instrument. Steady state photolysis was carried out on a optical bench equipped with a High Pressure silver lamp HBO200 (OSRAM), a cell filled with water and containing filters (Monochromat filters HgMon 365, HgMon 405, HgMon 436 or HgMon 577 or Zeiss MIF 254 with $\Delta\lambda$ 4 nm and filters Schitt code 805, 601 and 781) as well as a cell holder with a magnet stirrer. For UV/Vis measurements as well as for photoisomerization experiments were utilized quartz cells Suprasil (Hellma) with crew caps.

Lyotropic investigations were made on VP-DSC scanning calorimeter (MicroCal, Inc., Northampton, MA) with a heating rate of 1 °C·min⁻¹.

Isothermal titration calorimetry was performed with a MicroCal OMEGA titration calorimeter and an MCS ITC unit (MicroCal, Inc., Northampton, MA). The reaction cell ($V =$

1.34 ml) was filled with water. The removable integrated injection stirrer syringe was loaded with surfactant **14k**, and the two solutions were mixed by injecting 75 x 3.75 μ l of micellar surfactant solution (2 mM) in the reaction cell. During the experiment the syringe was rotated with ~ 400 rpm. The experimental data were analyzed using the Origin software (MicroCal).

AFM investigations were made using a TMX 2010 Explorer of TopoMetrix atomic force microscope. The samples were heated to isotropic before measurements. The measurements were performed at 55 °C on mica and graphite supports.

Melting points of *N*-(2,2-diethyl ethyl) stilbazolium dyes **6a** – **e**, **7** and **9** and of secondary *N*-alkyl-stilbazolium dyes **13a** – **g** were taken by polarizing microscope and differential scanning calorimetry measurements. Due to the partial decomposition of the dyes at temperatures ≥ 100 °C and also the presence of the water may shift the melting points.

pH-dependence measurements of dye **6a** were made by UV/Vis spectroscopy using buffer solutions (Fluka) with pH = 4 (containing citric acid/sodium hydroxyde/sodium chloride), pH = 7 (containing sodium hydroxide/potassium dihydrogen phosphate), pH = 8, 8.5 and 9 respectively (containing sodium tetraborate/hydrochloric acid), pH = 10 (containing sodium tetraborate/sodium hydroxide) and pH = 11 (containing boric acid/sodium hydroxide).

For column chromatography was utilized Silica gel 60 (0.063 - 0.200 mm or 0.040 - 0.063 mm) and for reverse phase chromatography Silica gel 60 RP - 18 (0.040 - 0.063 mm) from Merck.

Purification of the merocyanine dyes by column chromatography:

General procedure:

Merocyanine dyes were purified by column chromatography with Silica gel 60 using diethyl ether and ethanol as eluents. The dimensions of the column were 45 x 4.5 cm. The bottom of the column was filled with glass wadding. The silica gel was mixed with diethyl ether in a glass beaker and then poured into the column. Care was taken to avoid air bubbles. To the top of the stationary state was added a layer of sand in order to protect the shape of the organic layer. The dye (2 g) was dissolved in a small amount of ethanol and pipetted onto the top of the stationary state. The ratio dye/silica gel was 1/75. After adding the dye solution, 4-hydroxy-benzaldehyde was eluted first with diethyl ether (500 ml). After collecting the aldehyde, ethanol (500 ml) was then used to elute the pure dye. For a good separation, the eluent was collected in small fractions (2 ml). In the case of purification by reverse phase chromatography, the preparation of the column was similar but Silica gel 60 RP-18 was used and methanol was employed as solvent instead of ethanol.

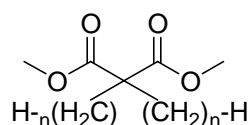
4.1. Synthesis of stilbazolium dyes 6 – 9

4.1.1. Dialkylated diesters 1a – d

General procedure:

Sodium methanolat was prepared using methanol (500 ml) and sodium (1 mol, 2.3 g) in a three-necked flask equipped with a dropping funnel, thermometer and reflux condenser with calcium chloride. 1 mol of dimethylmalonate and 1.05 mol 1-bromoalkanes were added with a dropping funnel to the hot solution of sodium methanolat during 2 h. After heating at reflux for 16 h and stirring over night at room temperature, the methanol was removed under reduced pressure and the mixture was poured into ice. The organic phase was separated, and the water phase was extracted for three times with diethyl ether (3 x 100 ml). The organic phases were combined and dried over anhydrous sodium sulfate. After evaporation of the diethyl ether by distillation, the monoalkylated ester was obtained. The crude product was utilized for the next step without further purification. The procedure was repeated using the monoalkylated diester and the halogen derivative in the ratio 1/1.05, by the same procedure, in order to get the double alkylated diester. Compounds **1a** and **1b** were purified by distillation under reduced pressure and compounds **1c** and **1d** were utilized for the next step without further purification due to the high boiling points.

Comp.	1a	1b	1c	1d
<i>n</i>	3	5	8	12
Yield (%)	61.0	36.75	51.4	63.0



Di-n-propyl-malonic acid dimethyl ester 1a:

b.p. = 75 °C at 7 Torr

¹H NMR (CDCl₃, *J*/Hz, 400 MHz) δ = 3.52 (s, 6 H, OCH₃), 1.70-1.65 (m, 4 H, CH₂), 1.29-1.14 (m, 8 H, (CH₂)₂), 0.74 (t, ³*J*(H,H) = 7.26, 6 H, CH₃).

Di-n-pentyl-malonic acid dimethyl ester 1b:

b.p. = 110 – 115 °C at 7 Torr

^1H NMR (CDCl_3 , J/Hz , 400 MHz) δ = 3.66 (s, 6 H, OCH_3), 1.84-1.80 (m, 4 H, CH_2), 1.29-1.18-1.05 (m, 12 H, $(\text{CH}_2)_3$), 0.83 (t, $^3J(\text{H,H}) = 6.9$, 6 H, CH_3).

Di-n-octyl-malonic acid dimethyl ester 1c:

^1H NMR (CDCl_3 , J/Hz , 400 MHz) δ = 3.60 (s, 6 H, OCH_3), 1.81-1.75 (m, 4 H, CH_2), 1.20-1.17-1.02 (m, 24 H, $(\text{CH}_2)_6$), 0.78 (t, $^3J(\text{H,H}) = 6.8$, 6 H, CH_3).

Di-n-dodecyl-malonic acid dimethyl ester 1d:

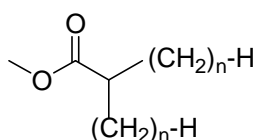
^1H NMR (CDCl_3 , J/Hz , 200 MHz) δ = 3.71 (s, 6 H, OCH_3), 1.87-1.80 (m, 4 H, CH_2), 1.24-1.15 (m, 40 H, $(\text{CH}_2)_{10}$), 0.86 (t, $^3J(\text{H,H}) = 6.6$, 6 H, CH_3).

4.1.2. Monoesters 2a – d

General procedure:

A solution of **2b** (0.097 mol, 26.4 g) in dimethyl sulfoxide (338 ml) containing water (0.097 mol, 1.75 g) and lithium chloride (0.19 mol, 8.05 g) was heated for 8 h at reflux temperature. The reaction mixture was diluted with water and the organic phase was separated. The water phase was extracted with (3 x 200 ml) diethyl ether and the extracts were combined, washed with water (3 x 100 ml) and brine (100 ml) and dried over sodium sulfate. The products **2a** and **2b** were purified by distillation under reduced pressure, and the products **2c** and **2d** were purified by column chromatography using silica gel and chloroform as eluent to give a colourless liquid.

Comp.	<i>n</i>	Diester 1a - d	LiCl	H_2O	DMSO
2a	3	0.097 mol	0.190 mol	0.097 mol	338 ml
2b	5	0.126 mol	0.246 mol	0.126 mol	440 ml
2c	8	0.514 mol	0.990 mol	0.514 mol	900 ml
2d	12	0.461 mol	0.900 mol	0.461 mol	600 ml



2a - d

Comp.	2a	2b	2c	2d
<i>n</i>	3	5	8	12
Yield (%)	48.5	72.0	92.8	85.3

2-n-Propyl-pentanoic acid methyl ester 2a:

b.p. = 45 – 50 °C at 7 Torr

^1H NMR (CDCl_3 , J/Hz , 400 MHz) δ = 3.65 (s, 3 H, OCH_3), 2.38-2.33 (m, 1 H, **CH**), 1.62-1.22 (m, 8 H, $(\text{CH}_2)_2$), 0.88 (t, $^3J(\text{H,H}) = 7.26$, 6 H, CH_3).

2-n-Pentyl-heptanoic acid methyl ester 2b:

b.p. = 85 – 90 °C at 7 Torr

^1H NMR (CDCl_3 , J/Hz , 400 MHz) δ = 3.63 (s, 3 H, OCH_3), 2.33-2.26 (m, 1 H, **CH**), 1.57-1.20 (m, 16 H, $(\text{CH}_2)_4$), 0.85 (t, $^3J(\text{H,H}) = 6.64$, 6 H, CH_3).

2-n-Octyl-decanoic acid methyl ester 2c:

^1H NMR (CDCl_3 , J/Hz , 400 MHz) δ = 3.62 (s, 3 H, OCH_3), 2.32-2.19 (m, 1 H, **CH**), 1.59-1.21 (m, 28 H, $(\text{CH}_2)_7$), 0.83 (t, $^3J(\text{H,H}) = 6.8$, 6 H, CH_3).

2-n-Dodecyl-tetradecanoic acid methyl ester 2d:

^1H NMR (CDCl_3 , J/Hz , 400 MHz) δ = 3.65 (s, 3 H, OCH_3), 2.27-2.25 (m, 1 H, **CH**), 1.55-1.22 (m, 44 H, $(\text{CH}_2)_{11}$), 0.83 (t, $^3J(\text{H,H}) = 6.9$, 6 H, CH_3).

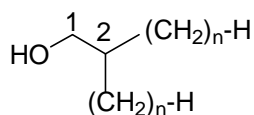
4.1.3. Alcohols **3a** – **e**

General procedure:

In a three-necked flask equipped with dropping funnel, thermometer and reflux condenser with calcium chloride was added by dropping 0.069 mol **2a** (11 g) in diethyl ether (82 ml) to 0.069 mol lithium aluminium hydride (2.62 g) suspension in diethyl ether. After heating for 10 h at reflux, the reaction mixture was cooled to room temperature, hydrolyzed with ice and acidified with hydrochloric acid. The organic phase was separated and the water phase was extracted with diethyl ether (3 x 100 ml). The organic phases were combined, washed with brine and dried over sodium sulphate. After evaporation of diethyl ether by distillation, the residue was fractionally distilled under reduced pressure. The alcohol **3e** was utilized for the next step without purification.

Comp.	<i>n</i>	monoester	LiAlH_4	diethyl ether	Yield (%)
3a	3	0.069 mol	0.069 mol	82 ml	80.2
3b	5	0.090 mol	0.090 mol	100 ml	75.7
3c	8	0.477 mol	0.477 mol	275 ml	50.3
3e	12	0.393 mol	0.393 mol	250 ml	48.6

3d [89]



2-Propyl-pentan-1-ol 3a:

colourless liquid, b.p. = 80 – 82 °C at 12 Torr

$^1\text{H NMR}$ (CDCl_3 , J/Hz , 400 MHz) δ = 3.38 (d, $^3J(\text{H,H}) = 5.60$, 2 H, CH_2^1), 1.39-1.35 (m, 1 H, CH^2), 1.27-1.20 (m, 8 H, $(\text{CH}_2)_2$), 0.80 (t, $^3J(\text{H,H}) = 7.0$, 6 H, CH_3).

2-Pentyl-heptan-1-ol 3b:

colourless liquid, b.p. = 96 – 97 °C at 7 Torr

$^1\text{H NMR}$ (CDCl_3 , J/Hz , 400 MHz) δ = 3.49 (d, $^3J(\text{H,H}) = 5.39$, 2 H, CH_2^1), 1.44-1.41 (m, 1 H, CH^2), 1.31-1.20 (m, 16 H, $(\text{CH}_2)_4$), 0.85 (t, $^3J(\text{H,H}) = 6.9$, 6 H, CH_3).

2-Octyl-decan-1-ol 3c:

colourless oil, b.p. = 150 °C at 20 Torr

$^1\text{H NMR}$ (CDCl_3 , J/Hz , 400 MHz) δ = 3.49 (d, $^3J(\text{H,H}) = 5.60$, 2 H, CH_2^1), 1.42 (bs, 1 H, CH^2), 1.24-1.15 (m, 28 H, $(\text{CH}_2)_7$), 0.85 (t, $^3J(\text{H,H}) = 6.8$, 6 H, CH_3).

2-Decyl-dodecan-1-ol 3d:

colourless oil

$^1\text{H NMR}$ (CDCl_3 , J/Hz , 400 MHz) δ = 3.50 (d, $^3J(\text{H,H}) = 5.39$, 2 H, CH_2^1), 1.43-1.42 (m, 1 H, CH^2), 1.24-1.03 (m, 36 H, $(\text{CH}_2)_9$), 0.86 (t, $^3J(\text{H,H}) = 6.8$, 6 H, CH_3).

2-Dodecyl-tetradecan-1-ol 3e:

yellowish solid, m.p. = 36 °C

$^1\text{H NMR}$ (CDCl_3 , J/Hz , 400 MHz) δ = 3.51 (d, $^3J(\text{H,H}) = 5.60$, 2 H, CH_2^1), 1.43-1.42 (m, 1 H, CH^2), 1.24-1.03 (m, 44 H, $(\text{CH}_2)_{11}$), 0.86 (t, $^3J(\text{H,H}) = 6.8$, 6 H, CH_3).

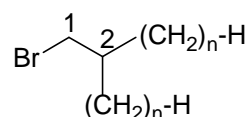
4.1.4. Alkyl halides 4a – e

General procedure:

0.069 mmol (6.21 g) of phosphorous tribromide was added with a dropping funnel to 0.023 mmol (9 g) of **3a** during two hours by keeping the temperature at -10 – 0 °C. The reaction was stirred over night at room temperature and heated the next day at 80 °C for 2 h. In the case of the compounds with long alkyl chains the mixture was heated at 80 °C for 2 days. After

cooling to room temperature the reaction mixture was poured into water and the organic phase was separated. The water phase was extracted with diethyl ether (3 x 100 ml) and the unified extracts were dried over sodium sulfate. The compounds were purified by water steam distillation and by column chromatography using silica gel 60 and petrolether as eluent to give a colourless liquid.

Comp.	<i>n</i>	3a - e	PBr₃	Yield
4a	3	0.069 mol	0.023 mol	68.1 %
4b	5	0.038 mol	0.013 mol	67.1 %
4c	8	0.120 mol	0.039 mol	93.0 %
4d	10	0.030 mol	0.010 mol	22.7 %
4e	12	0.189 mol	0.062 mol	46.3 %



4-(1-Bromomethyl)-heptane 4a:

¹H NMR (CDCl₃, *J*/Hz, 400 MHz) δ = 3.41 (d, ³*J*(H,H) = 4.77, 2 H, CH₂¹), 1.63-1.56 (m, 1 H, CH²), 1.42-1.17 (m, 8 H, (CH₂)₂), 0.89 (t, ³*J*(H,H) = 6.6, 6 H, CH₃).

6-(1-Bromomethyl)-undecane 4b:

¹H NMR (CDCl₃, *J*/Hz, 400 MHz) δ = 3.43 (d, ³*J*(H,H) = 4.77, 2 H, CH₂¹), 1.59-1.55 (m, 1 H, CH²), 1.41-1.22 (m, 16 H, (CH₂)₄), 0.88 (t, ³*J*(H,H) = 6.9, 6 H, CH₃).

9-(1-Bromomethyl)-heptadecane 4c:

¹H NMR (CDCl₃, *J*/Hz, 500 MHz) δ = 3.43 (d, ³*J*(H,H) = 4.76, 2 H, CH₂¹), 1.65 (bs, 1 H, CH²), 1.35-1.18 (m, 28 H, (CH₂)₇), 0.87 (t, ³*J*(H,H) = 6.9, 6 H, CH₃).

11-(1-Bromomethyl)-heneicosane 4d:

¹H NMR (CDCl₃, *J*/Hz, 400 MHz) δ = 3.42 (d, ³*J*(H,H) = 4.77, 2 H, CH₂¹), 1.58-1.56 (m, 1 H, CH²), 1.37-1.23 (m, 36 H, (CH₂)₉), 0.87 (t, ³*J*(H,H) = 6.9, 6 H, CH₃).

13-(1-Bromomethyl)-hexacosane 4e:

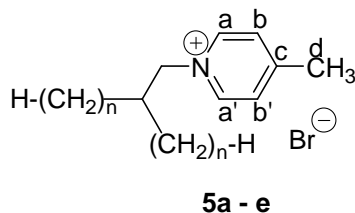
¹H NMR (CDCl₃, *J*/Hz, 400 MHz) δ = 3.42 (d, ³*J*(H,H) = 4.77, 2 H, CH₂¹), 1.58-1.52 (m, 1 H, CH²), 1.37-1.25 (m, 44 H, (CH₂)₁₁), 0.86 (t, ³*J*(H,H) = 6.8, 6 H, CH₃).

4.1.5. Picolinium salts with *N*-(2,2-dialkyl ethyl) substituents **5a - e**

General procedure:

4-Picoline and 1-bromoalkanes (1/1 molar ratio) were dissolved separately in a double volume of CH₃NO₂. The solutions were unified and heated for 18 h at 90 °C. After cooling to room temperature, the solvent was evaporated by reduced pressure. The unreacted 4-picoline was removed by washing several times with diethyl ether. Some of the salts were purified by column chromatography with silica gel and diethyl ether as eluent to collect the 4-picoline and then the solvent was changed with ethanol and small fractions were collected to get the pure product (see procedure, page 82.)

Comp.	<i>n</i>	4a - e	4-picoline	yield
5a	3	0.028 mol	0.028 mol	78.4 %
5b	5	0.025 mol	0.025 mol	52.5 %
5c	8	0.110 mol	0.110 mol	16.4 %
5d	10	0.049 mol	0.049 mol	25.4%
5e	12	0.006 mol	0.006 mol	15.5%



N-(2-propyl)-pentyl-4-methyl-pyridinium bromide **5a**:

¹H NMR (DMSO, *J*/Hz, 400 MHz) δ = 9.0 (d, ³*J*(H,H) = 6.64, 2 H, Ar-**H^{a,a'}**), 8.01 (d, ³*J*(H,H) = 6.22, 2 H, Ar-**H^{b,b'}**), 4.50 (d, ³*J*(H,H) = 7.67, 2 H, **CH₂¹**), 2.61 (s, 3 H, **CH₃^d**), 2.03-2.00 (m, 1 H, **CH²**), 1.33-1.07 (m, 8 H, **CH₂^{3,3',4,4'}**), 0.80 (t, ³*J*(H,H) = 6.9, 6 H, **CH₃^{5,5'}**). ¹³C NMR (DMSO, 100 MHz) δ = 158.85 (**C^c**), 143.86 (**C^{a,a'}**), 128.18 (**C^{b,b'}**), 63.24 (**C¹**), 38.34 (**C²**), 32.10, 21.34, 18.52 (**C^{3,3',4,4',d}**), 14.03 (**C^{5,5'}**).

MS (EI, 70 eV) *m/z*: 93, 106, 205 (**M⁺-HBr**).

m. p. = 153 °C

N-(2-pentyl)-heptyl-4-methyl-pyridinium bromide **5b**:

¹H NMR (DMSO, *J*/Hz, 400 MHz) δ = 9.0 (d, ³*J*(H,H) = 6.64, 2 H, Ar-**H^{a,a'}**), 7.97 (d, ³*J*(H,H) = 6.22, 2 H, Ar-**H^{b,b'}**), 4.43 (d, ³*J*(H,H) = 7.47, 2 H, **CH₂¹**), 2.58 (s, 3 H, **CH₃^d**), 1.97-1.94 (m, 1 H, **CH²**), 1.25-1.05 (m, 16 H, **CH₂^{3,3'-6,6'}**), 0.80 (t, ³*J*(H,H) = 7.0, 6 H, **CH₃^{7,7'}**). ¹³C NMR

(DMSO, 100 MHz) $\delta = 159.49$ (C^c), 144.43 ($C^{a,a'}$), 128.78 ($C^{b,b'}$), 64.00 (C^1), 39.34 (C^2), 31.88 , 30.38 , 25.47 , 22.39 , 21.90 ($C^{3,3'-6,6',d}$), 14.33 ($C^{7,7'}$).

N-(2-octyl)-decyl-4-methyl-pyridinium bromide **5c**:

1H NMR (DMSO, J /Hz, 400 MHz) $\delta = 8.97$ (d, $^3J(H,H) = 6.43$, 2 H, Ar- $H^{a,a'}$), 8.00 (d, $^3J(H,H) = 6.43$, 2 H, Ar- $H^{b,b'}$), 4.47 (d, $^3J(H,H) = 7.67$, 2 H, CH_2^1), 2.60 (s, 3 H, CH_3^d), 1.97 (m, 1 H, CH^2), 1.26 - 1.10 (m, 28 H, $CH_2^{3,3'-9,9'}$), 0.83 (t, $^3J(H,H) = 6.8$, 6 H, $CH_3^{10,10'}$). ^{13}C NMR (DMSO, 100 MHz) $\delta = 158.71$ (C^c), 143.77 ($C^{a,a'}$), 128.08 ($C^{b,b'}$), 63.33 (C^1), 38.71 (C^2), 31.18 , 29.74 , 29.05 , 28.70 , 28.49 , 25.17 , 22.00 , 21.33 ($C^{3,3'-9,9',d}$), 13.87 ($C^{10,10'}$).

MS (EI, 70 eV) m/z : 107, 232, 253, 345 (M^+ -HBr).

m. p. = 93 °C

N-(2-decyl)-dodecyl-4-methyl-pyridinium bromide **5d**:

1H NMR (DMSO, J /Hz, 400 MHz) $\delta = 8.89$ (d, $^3J(H,H) = 6.84$, 2 H, Ar- $H^{a,a'}$), 7.98 (d, $^3J(H,H) = 6.43$, 2 H, Ar- $H^{b,b'}$), 4.42 (d, $^3J(H,H) = 7.47$, 2 H, CH_2^1), 2.60 (s, 3 H, CH_3^d), 1.86 (m, 1 H, CH^2), 1.26 - 1.22 (m, 36 H, $CH_2^{3,3'-11,11'}$), 0.84 (t, $^3J(H,H) = 6.8$, 6 H, $CH_3^{12,12'}$). ^{13}C NMR (DMSO, 100 MHz) $\delta = 159.21$ (C^c), 144.15 ($C^{a,a'}$), 128.81 ($C^{b,b'}$), 64.08 (C^1), 39.31 (C^2), 31.79 , 30.34 , 29.61 , 29.49 , 29.31 , 28.87 , 25.89 , 22.60 , 21.92 ($C^{3,3'-11,11',d}$), 13.87 ($C^{12,12'}$).

N-(2-dodecyl)-tetradecyl-4-methyl-pyridinium bromide **5e**:

1H NMR (DMSO, J /Hz, 400 MHz) $\delta = 8.90$ (d, $^3J(H,H) = 6.44$, 2 H, Ar- $H^{a,a'}$), 7.98 (d, $^3J(H,H) = 6.43$, 2 H, Ar- $H^{b,b'}$), 4.43 (d, $^3J(H,H) = 7.47$, 2 H, CH_2^1), 2.60 (s, 3 H, CH_3^d), 1.97 (m, 1 H, CH^2), 1.28 - 1.06 (m, 44 H, $CH_2^{3,3'-13,13'}$), 0.84 (t, $^3J(H,H) = 6.8$, 6 H, $CH_3^{14,14'}$). ^{13}C NMR (DMSO, 400 MHz) $\delta = 158.88$ (C^c), 143.87 ($C^{a,a'}$), 128.20 ($C^{b,b'}$), 63.47 (C^1), 38.66 (C^2), 31.19 , 29.67 , 28.96 , 28.93 , 28.90 , 28.78 , 28.68 , 28.60 , 25.08 , 21.99 , 21.30 ($C^{3,3'-13,13',d}$), 13.84 ($C^{14,14'}$).

MS (EI, 70 eV) m/z : 94, 365, 457 (M^+ -HBr). EA: $C_{32}H_{60}BrN$ (Calc.) C: 71.34 %, H: 11.23 %, N: 2.60 %, (Found) C: 71.11 %, H: 11.36 %, N: 2.60 %.

m. p. = 80 °C

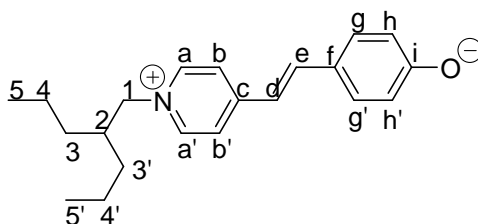
4.1.6. *N*-(2,2-dialkyl ethyl)-4'-oxy-stilbazolium dyes **6a – e**

General procedure:

In a two-necked flask equipped with thermometer and reflux condenser with calcium chloride tube were introduced 0.01 mmol (3 g) **5a**, 0.01 mmol (1.22 g) 4-hydroxy-benzaldehyde, 1.33

ml piperidine and dry ethanol (15 ml). The mixture was stirred under reflux for 8 h. After cooling the reaction to room temperature, the solvent was removed under reduced pressure and the dye was deprotonated with 0.35 M KOH solution in water up to pH > 10 followed by heating for 30 min. at 50 °C. The dyes with long alkyl chains *n* were deprotonated using a mixture of KOH solution in water and ethanol. Due to the ring opening of pyridinium ions by heating in ethanol for longer time, a two phase mixture of methylene chloride and aqueous KOH solution was stirred at room temperature for 1 day. After the phases were separated, the aqueous phase was extracted several times with methylene chloride. After evaporation of the solvent, the residue was purified by column chromatography using silica gel 60 and diethyl ether and ethanol as eluents or by reverse phase chromatography with methanol as solvent. The dyes having secondary *N*-alkyl chains **13a** – **g** were prepared by the same procedure.

N-(2-propyl)-pentyl-4'-oxy-stilbazolium dye **6a**:



Reagents: 4-Hydroxy-benzaldehyde (0.01 mol, 1.22 g),
 1-(2-propyl)-pentyl-4-methyl-pyridinium bromide (0.01 mol, 3 g),
 piperidine (1.33 ml),
 dry ethanol (15 ml),
 the dye was deprotonated using a mixture of 0.35 M KOH and ethanol and heating for 30 min.

Purification: Column chromatography using diethyl ether and ethanol as solvents (see experimental part, page 82).

Yield: 67.3 % (6.73 mmol), red powder, m. p. = 123 °C

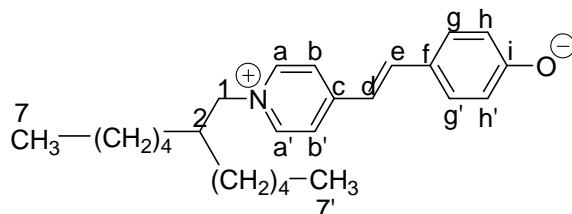
Analytical data: C₂₁H₂₇NO M_w = 309.45

¹H NMR (DMSO, *J*/Hz, 400 MHz) δ = 8.87 (d, ³*J*(H,H) = 6.64, 2 H, Ar-**H**^{a,a'}), 8.16 (d, ³*J*(H,H) = 6.84, 2 H, Ar-**H**^{b,b'}), 7.97 (d, ³*J*(H,H) = 16.18, 1 H, **CH**^c), 7.61 (d, ³*J*(H,H) = 8.71, 2 H, Ar-**H**^{g,g'}), 7.30 (d, ³*J*(H,H) = 16.39, 1 H, **CH**^d), 6.87 (d, ³*J*(H,H) = 8.51, 2 H, Ar-**H**^{h,h'}), 4.38 (d, ³*J*(H,H) = 7.47, 2 H, **CH**₂¹), 2.03-1.89 (m, 1 H, **CH**₂²), 1.33-0.93 (m, 16 H, **CH**₂^{3,3',4,4'}), 0.82 (t, ³*J*(H,H) = 6.8, 6 H, **CH**₃^{5,5'}). ¹³C NMR (DMSO, 100 MHz) δ = 159.86 (**C**ⁱ), 153.50 (**C**^c),

144.05 ($C^{a,a'}$), 141.53 (C^e), 130.19 ($C^{g,g'}$), 126.23 (C^f), 123.00 ($C^{b,b'}$), 119.55 (C^d), 115.90 ($C^{h,h'}$), 62.98 (C^1), 38.80, 32.26, 18.61 ($C^{2,3,3',4,4'}$), 14.08 ($C^{5,5'}$).

MS (EI, 70 eV) m/z : 168, 197, 309 (M^+).

N-(2-pentyl)-heptyl-4'-oxy-stilbazolium dye **6b**:



Reagents: 4-Hydroxy-benzaldehyde (13 mmol, 1.58 g),
1-(2-pentyl)-heptyl-4-methyl-pyridinium bromide (13 mmol, 4.31 g),
piperidine (1.73 ml),
dry ethanol (21.6 ml),
the dye was deprotonated using a mixture of 0.35 M KOH and CH_2Cl_2 and stirring over night; the dye was collected by extractions with CH_2Cl_2 .

Purification: Column chromatography using diethyl ether and ethanol (see experimental part, page 82).

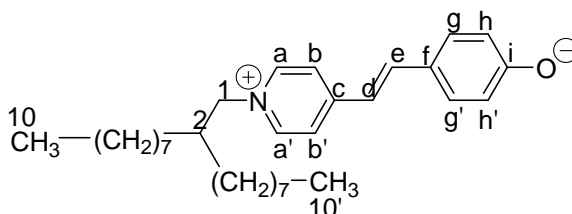
Yield: 32 % (4.16 mmol), red powder, m. p. = 124 °C

Analytical data: $C_{25}H_{36}NO$ $M_w = 366.55$

1H NMR (DMSO, J/Hz , 400 MHz) $\delta = 8.98$ (d, $^3J(H,H) = 6.85$, 2 H, Ar- $H^{a,a'}$), 8.23 (d, $^3J(H,H) = 6.84$, 2 H, Ar- $H^{b,b'}$), 8.05 (d, $^3J(H,H) = 16.39$, 1 H, CH^e), 7.62 (d, $^3J(H,H) = 8.71$, 2 H, Ar- $H^{g,g'}$), 7.35 (d, $^3J(H,H) = 16.18$, 1 H, CH^d), 6.87 (d, $^3J(H,H) = 8.51$, 2 H, Ar- $H^{h,h'}$), 4.43 (d, $^3J(H,H) = 7.26$, 2 H, CH_2^1), 1.96 (m, 1 H, CH^2), 1.22-1.10 (m, 16 H, $CH_2^{3,3'-6,6'}$), 0.76 (t, $^3J(H,H) = 6.8$, 6 H, $CH_3^{7,7'}$). ^{13}C NMR (DMSO, 100 MHz) $\delta = 160.17$ (C^i), 153.78 (C^c), 144.08 ($C^{a,a'}$), 141.78 (C^e), 130.42 ($C^{g,g'}$), 126.40 (C^f), 123.11 ($C^{b,b'}$), 119.46 (C^d), 116.06 ($C^{h,h'}$), 63.13 (C^1), 31.53, 30.04, 28.95, 25.12, 24.95, 21.96 ($C^{2-6,6'}$), 13.79 ($C^{7,7'}$).

MS (EI, 70 eV) m/z : 168, 197, 367 (MH^+).

N-(2-octyl)-decyl-4'-oxy-stilbazolium dye **6c**:



Reagents: 4-Hydroxy-benzaldehyde (5.9 mmol, 0.71 g),
 1-(2-octyl)-decyl-4-methyl-pyridinium bromide (5.9 mmol, 2.5 g),
 piperidine (0.78 ml),
 dry ethanol (9.9 ml),
 the dye was deprotonated using a mixture of 0.35 M KOH and CH₂Cl₂ and
 stirring over night; the dye was collected by extractions with CH₂Cl₂.

Purification: Column chromatography using diethyl ether and ethanol (see experimental part,
 page 82).

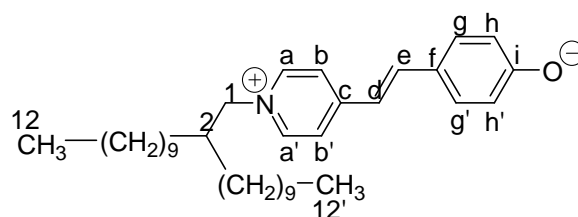
Yield: 28.3 % (1.67 mmol), red powder, m. p. = 93 °C

Analytical data: C₃₁H₄₈NO M_w = 450.71

¹H NMR (DMSO, J/Hz, 400 MHz) δ = 8.27 (d, ³J(H,H) = 7.05, 2 H, Ar-H^{a,a'}), 7.71 (d, ³J(H,H) = 15.35, 1 H, Ar-H^{e'}), 7.59 (d, ³J(H,H) = 6.22, 2 H, CH^{b,b'}), 7.34 (d, ³J(H,H) = 7.05, 2 H, Ar-H^{g,g'}), 6.61 (d, ³J(H,H) = 14.73, 1 H, CH^d), 6.23 (d, ³J(H,H) = 8.3, 2 H, Ar-H^{h,h'}), 4.00 (d, ³J(H,H) = 7.67, 2 H, CH₂¹), 1.85 (m, 1 H, CH₂²), 1.26-1.20 (m, 28 H, CH₂^{3,3'-9,9'}), 0.83 (t, ³J(H,H) = 6.2, 6 H, CH₃^{10,10'}). ¹³C NMR (DMSO, 100 MHz) δ = 171.21 (Cⁱ), 153.34 (C^c), 143.14 (C^e), 142.48 (C^{a,a'}), 131.65 (C^{g,g'}), 120.40 (C^{h,h'}), 118.94 (C^{b,b'}), 112.86 (C^f), 104.67 (C^d), 62.07 (C¹), 31.15, 29.97, 29.02, 28.65, 28.45, 25.26, 21.95, (C^{2,3,3'-11,11'}), 13.91 (C^{12,12'}).

MS (EI, 70 eV) m/z: 198, 252, 451 (MH⁺).

N-(2-decyl)-dodecyl-4'-oxy-stilbazolium dye **6d**:



Reagents: 4-Hydroxy-benzaldehyde (2 mmol, 0.24 g),
 1-(2-decyl)-dodecyl-4-methyl-pyridinium bromide (2 mmol, 0.96 g),
 piperidine (0.26 ml),
 dry ethanol (4 ml),
 deprotonation with a mixture of 0.35 M KOH and CH₂Cl₂ by stirring over
 night and then extractions with CH₂Cl₂.

Purification: Column chromatography using diethyl ether and ethanol (see experimental part,
 page 82).

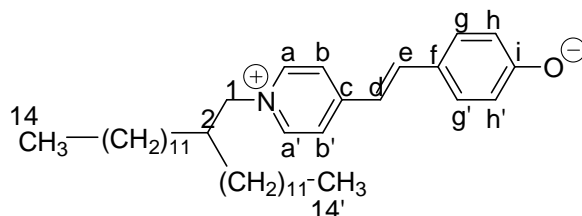
Yield: 36.5 % (0.73 mmol), red powder, m. p. = 170 °C

Analytical data: C₃₅H₅₆NO M_w = 506.85

^1H NMR (DMSO, J/Hz , 400 MHz) δ = 8.85 (d, $^3J(\text{H,H})$ = 6.84, 2 H, Ar- $\text{H}^{\text{a,a}'}$), 8.15 (d, $^3J(\text{H,H})$ = 6.64, 2 H, Ar- $\text{H}^{\text{b,b}'}$), 7.95 (d, $^3J(\text{H,H})$ = 16.18, 1 H, CH^{e}), 7.60 (d, $^3J(\text{H,H})$ = 8.71, 2 H, Ar- $\text{H}^{\text{g,g}'}$), 7.27 (d, $^3J(\text{H,H})$ = 16.18, 1 H, CH^{d}), 6.86 (d, $^3J(\text{H,H})$ = 8.71, 2 H, Ar- $\text{H}^{\text{h,h}'}$), 4.36 (d, $^3J(\text{H,H})$ = 7.47, 2 H, CH_2^{1}), 1.97 (m, 1 H, CH^{2}), 1.21-1.04 (m, 36 H, $\text{CH}_2^{3,3'-11,11'}$), 0.83 (t, $^3J(\text{H,H})$ = 6.7, 6H, $\text{CH}_3^{12,12'}$). ^{13}C NMR (DMSO, 100 MHz) δ = 160.08 (C^{i}), 153.59 (C^{c}), 144.11 ($\text{C}^{\text{a,a}'}$), 141.60 (C^{e}), 130.25 ($\text{C}^{\text{g,g}'}$), 126.22 (C^{f}), 123.00 ($\text{C}^{\text{b,b}'}$), 119.51 (C^{d}), 116.02 ($\text{C}^{\text{h,h}'}$), 63.20 (C^{1}), 31.26, 29.89, 28.97, 28.85, 28.71, 28.67, 25.22, 22.06 ($\text{C}^{3,3'-11,11'}$), 13.91 ($\text{C}^{12,12'}$).

MS (ESI) m/z : 198.3, 366.5, 506.5 (MH^+).

N-(2-dodecyl)-tetradecyl-4'-oxy-stilbazolium dye **6e**:



Reagents: 4-Hydroxy-benzaldehyde (1.95 mmol, 0.24 g),
1-(2-dodecyl)-tetradecyl-4-methyl-pyridinium bromide (1.95 mmol, 1.05 g),
piperidine (0.26 ml),
dry ethanol (3.5 ml),
the dye was deprotonated using a mixture of 0.35 M KOH and CH_2Cl_2 and stirring over night; the dye was collected by extractions with CH_2Cl_2 .

Purification: Column chromatography using diethyl ether and ethanol (see experimental part, page 82).

Yield: 58.98 % (1.15 mmol), red powder, m. p. = 180 °C

Analytical data: $\text{C}_{39}\text{H}_{63}\text{NO}$ M_w = 561.92

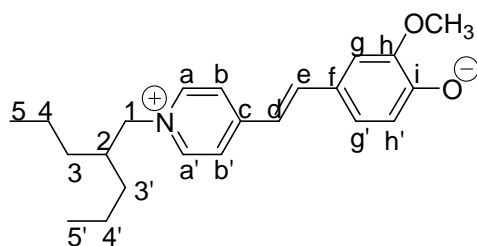
^1H NMR (DMSO, J/Hz , 400 MHz) δ = 8.84 (d, $^3J(\text{H,H})$ = 6.84, 2 H, Ar- $\text{H}^{\text{a,a}'}$), 8.14 (d, $^3J(\text{H,H})$ = 6.64, 2 H, Ar- $\text{H}^{\text{b,b}'}$), 7.94 (d, $^3J(\text{H,H})$ = 16.18, 1 H, CH^{e}), 7.60 (d, $^3J(\text{H,H})$ = 8.71, 2 H, Ar- $\text{H}^{\text{g,g}'}$), 7.27 (d, $^3J(\text{H,H})$ = 16.18, 1 H, CH^{d}), 6.86 (d, $^3J(\text{H,H})$ = 8.71, 2 H, Ar- $\text{H}^{\text{h,h}'}$), 4.36 (d, $^3J(\text{H,H})$ = 7.47, 2 H, CH_2^{1}), 1.97 (m, 1 H, CH^{2}), 1.22-1.14 (m, 44 H, $\text{CH}_2^{3,3'-13,13'}$), 0.83 (t, $^3J(\text{H,H})$ = 6.7, 6 H, $\text{CH}_3^{14,14'}$). ^{13}C NMR (DMSO, 50 MHz) δ = 160.05 (C^{i}), 153.54 (C^{c}), 144.09 ($\text{C}^{\text{a,a}'}$), 141.56 (C^{e}), 130.21 ($\text{C}^{\text{g,g}'}$), 126.18 (C^{f}), 122.96 ($\text{C}^{\text{b,b}'}$), 119.47 (C^{d}), 115.99 ($\text{C}^{\text{h,h}'}$), 63.23 (C^{1}), 31.25, 29.85, 28.97, 28.84, 28.97, 28.84, 28.70, 28.66, 25.19, 22.04 ($\text{C}^{3,3'-13,13'}$), 13.90 ($\text{C}^{14,14'}$).

MS (EI, 70 eV) m/z : 197, 365, 561 (M^+).

4.1.7. *N*-(2,2-dialkyl ethyl)-4'-oxy-3'-alcoxy-stilbazolium dyes 7 – 9

Merocyanine dyes with *N*-(2,2-dialkyl ethyl) substituents and alcoxy group in the meta position of the stilbazolium unit were synthesized using the corresponding *N*-(2,2-dialkyl ethyl) substituted salts and 4-hydroxy-3-alcoxy-benzaldehyde. Compound **7** was synthesized using for condensation the commercially available 4-hydroxy-3-methoxy-benzaldehyde, salt **5a**, piperidine and dry ethanol. The reaction mixture was heated under reflux for 8 h and purified by column chromatography as described in experimental part (page 82). Compound **9** was synthesized by the same route using for condensation 3-hexyloxy-4-hydroxy-benzaldehyde which was prepared by the following procedure: to a solution of 0.144 mol of 3,4-dihydroxybenzaldehyde in 200 ml ethanol was added 0.144 mol 1-bromohexane and 16.2 g potassium hydroxide in 200 ml ethanol. After stirring under reflux for 7.5 h the solvent was evaporated under reduced pressure and the brown residuu was poured into water and extracted with diethyl ether (pH basic). A yellow oil was obtained containing a mixture of 3-hexyloxy-4-hydroxy-benzaldehyde and 4-hexyloxy-3-hydroxy-benzaldehyde. The aqueous solution was acidified with diluted sulfuric acid and extracted again with diethyl ether. The organic extracts were combined and dried over anhydrous sodium sulfate. The oil was boiled with petrolether and filtered to give 3-hexyloxy-4-hydroxy-benzaldehyde.

N-(2-propyl)-pentyl-4'-oxy-3'-methoxy-stilbazolium dye **7**:



Reagents: 4-Hydroxy-3-methoxy-benzaldehyde (7 mmol, 1.06 g),
1-(2-propyl)-pentyl-4-methyl-pyridinium bromide (7 mmol, 2 g),
piperidine (0.93 ml),
dry ethanol (11.6 ml),
deprotonation by heating for 30 min. using a mixture of 0.35 M KOH and ethanol.

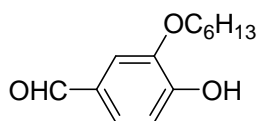
Purification: Column chromatography with diethyl ether and ethanol (see experimental part, page 82).

Yield: 53.4 % (3.74 mmol), red powder, m. p. = 141 °C

Analytical data: C₂₂H₃₀NO₂ M_w = 340.47

^1H NMR (DMSO, J/Hz , 400 MHz) δ = 8.86 (d, $^3J(\text{H,H})$ = 6.84, 2 H, Ar- $\text{H}^{\text{a,a'}}$), 8.15 (d, $^3J(\text{H,H})$ = 6.84, 2 H, Ar- $\text{H}^{\text{b,b'}}$), 7.95 (d, $^3J(\text{H,H})$ = 16.18, 1 H, CH^{e}), 7.38-7.34 (m, 2 H, CH^{d} , Ar- H^{g}), 7.18 (m, 1 H, Ar- $\text{H}^{\text{g'}}$), 6.86 (d, $^3J(\text{H,H})$ = 8.3, 1 H, Ar- H^{h}), 4.38 (d, $^3J(\text{H,H})$ = 7.67, 2 H, CH_2^{l}), 3.85 (s, 2 H, OCH_3), 2.02 (m, 1 H, CH^{2}), 1.25-1.14 (m, 8 H, $\text{CH}_2^{3,3',4,4'}$), 0.83 (t, $^3J(\text{H,H})$ = 6.8, 6 H, $\text{CH}_3^{5,5'}$). ^{13}C NMR (DMSO, 125 MHz) δ = 153.50 (C^{c}), 149.81 (C^{i}), 148.05 (C^{h}), 144.14 ($\text{C}^{\text{a,a'}}$), 141.91 (C^{e}), 126.76 (C^{f}), 123.51 ($\text{C}^{\text{g'}}$), 122.93 ($\text{C}^{\text{b,b'}}$), 119.79 (C^{d}), 115.73 ($\text{C}^{\text{h'}}$), 110.99 (C^{g}), 62.87 (C^{l}), 55.77 (OCH_3), 38.38, 29.4, 22.06, ($\text{C}^{2,3,3',4,4'}$), 14.11 ($\text{C}^{5,5'}$).
MS (EI, 70 eV) m/z : 93, 112, 227, 341 (MH^+).

3-hexyloxy-4-hydroxy-benzaldehyde **8**:



8

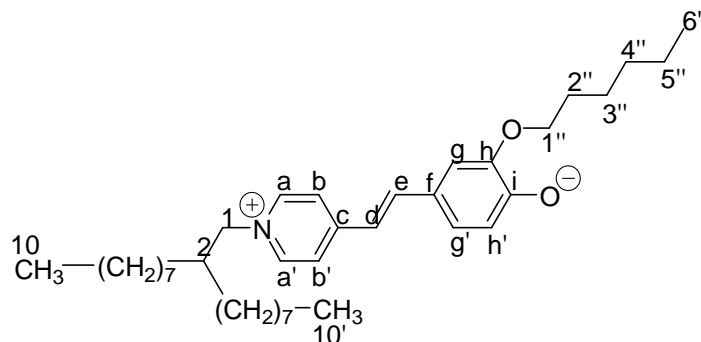
Reagents: 1-Bromohexane (0.144 mol, 11.94 g),
3,4-dihydroxy-benzaldehyde (0.144 mol, 10 g),
KOH (16.2 g),
ethanol (400 ml).

Yield: 6.94 % (2.23 g)

Analytical data: $\text{C}_{13}\text{H}_{18}\text{O}_3$ M_w = 222.28

^1H NMR (DMSO, J/Hz , 400 MHz) δ = 9.79 (s, 1 H, CHO), 7.39 (d, $J(\text{H,H})$ = 4.98, 1 H, Ar- H), 7.38 (s, 1 H, Ar- H), 7.02 (d, $J(\text{H,H})$ = 8.68, 1 H, Ar- H), 6.18 (s, 1 H, OH), 4.1 (t, $J(\text{H,H})$ = 6.64, 2 H, CH_2), 1.8 (m, 2 H, CH_2), 1.32 (m, 6 H, (CH_2)₃), 0.89 (t, $J(\text{H,H})$ = 7.3, 3 H, CH_3).

N-(2-octyl)-decyl-4'-oxy-3'-hexyloxy-stilbazolium dye **9**:



Reagents: 4-Hydroxy-3-hexyloxy-benzaldehyde (2.25 mmol, 0.5 g),
1-(2-octyl)-decyl-4-methyl-pyridinium bromide (2.25 mmol, 0.95 g),

piperidine (0.3 ml),

dry ethanol (3.75 ml),

the dye was deprotonated using a mixture of 0.35 M KOH and CH₂Cl₂ and stirring over night; the dye was collected by extractions with CH₂Cl₂.

Purification: Column chromatography using diethyl ether and ethanol (see experimental part, page 82).

Yield: 23.55 % (0.53 mmol), red solid, m. p. = 114 °C

Analytical data: C₃₇H₆₀NO₂ M_w = 550.87

¹H NMR (DMSO, *J*/Hz, 400 MHz) δ = 8.83 (d, ³*J*(H,H) = 7.05, 2 H, Ar-**H**^{a,a'}), 8.12 (d, ³*J*(H,H) = 6.64, 2 H, Ar-**H**^{b,b'}), 7.91 (d, ³*J*(H,H) = 16.18, 1 H, **CH**^e), 7.32-7.28 (m, 2 H, **CH**^d, Ar-**H**^g), 7.19 (m, 2 H, Ar-**H**^{g'}), 6.88 (d, ³*J*(H,H) = 8.09, 2 H, Ar-**H**^h), 4.35 (d, ³*J*(H,H) = 7.47, 2 H, **CH**₂¹), 4.02 (t, *J*(H,H) = 6.64, 2 H, **CH**₂^{1''}), 1.95 (m, 1 H, **CH**²), 1.73 (m, 2 H, **CH**₂^{2''}), 1.60-1.03 (m, 32 H, **CH**₂^{3,3'-9,9',3'',4''}), 0.90-0.81 (m, 9 H, **CH**₃^{10,10',6''}). ¹³C NMR (DMSO, 100 MHz) δ = 153.53 (**C**^c), 147.31 (**C**ⁱ), 143.99 (**C**^h), 141.95 (**C**^{a,a'}), 140.99 (**C**^e), 126.31 (**C**^f), 123.26 (**C**^{g'}), 122.76 (**C**^{b,b'}), 119.34 (**C**^d), 116.98 (**C**^{h'}), 115.88 (**C**^g), 68.39 (OCH₃), 63.00 (**C**¹), 38.87, 31.15, 30.92, 29.93, 28.85, 28.63, 28.55, 28.52, 28.44, 26.12, 24.76, 24.11, 21.94 (**C**^{2-9,9',2''-6''}), 13.76 (**C**^{10,10'}).

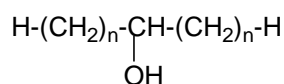
MS (EI, 70 eV) *m/z*: 252, 345, 552 (MH⁺).

4.2. Synthesis of stilbazolium dyes with secondary *N*-alkyl chain 13a – g

4.2.1. Alcohols with secondary alkyl chain 10a – e

General procedure:

In a 1 l three-necked flask equipped with a thermometer, dropping funnel and reflux condenser with calcium chloride was introduced under stirring 0.5 mol magnesium turnings (12.15 g), 50 ml dry diethyl ether and about 1/20 from 0.5 mol alkyl iodide. After the reaction starts the rest of alkyl halide dissolved in 125 ml diethyl ether was dropped slowly to keep the reflux constant. At the end of the dropping, the reaction was heated until the magnesium is dissolved. In the Grignard solution was added by dropping and under stirring 0.4 mol of aldehyde in the same volume of dry diethyl ether. After dropping, the reaction was heated for 2 h under reflux, cooled to room temperature, hydrolyzed with a mixture of ice and water and acidified with hydrochloric acid until the precipitate is dissolved. The organic phase is separated and the water phase extracted with diethyl ether (3 x 100 ml). The combined organic phases were washed with sodium hydrogen sulfite solution and water. After drying over anhydrous sodium sulfate the crude product was fractionally distilled to give the pure alcohol.



Comp.	<i>n</i>	R-CHO	R-I	Mg	Yield	b.p. (P)
10a	4	0.40 mol	0.50 mol	0.50 mol	42.4 %	97-98 °C (20 torr)
10b	5	0.40 mol	0.50 mol	0.50 mol	70.0 %	112.5 °C (10 torr)
10c	6	0.40 mol	0.50 mol	0.50 mol	60.0 %	137.5 °C (10 torr)
10d	7	0.40 mol	0.50 mol	0.50 mol	65.7 %	164.5 °C (10 torr)
10e	9	0.15 mol	0.19 mol	0.19 mol	61.8 %	169.0 °C (1 torr)

¹H NMR (CDCl₃, *J*/Hz, 400 MHz, **10b** at 200 MHz)

Comp.	<i>n</i>	H ¹ δ (ppm)	(CH ₂) _n δ (ppm)	(CH ₃) ₂ δ (ppm)
10a	4	3.52-3.49 (m, 1 H)	1.42-1.22 (m, 12 H)	0.85 (t, ³ <i>J</i> (H,H) = 7.0, 6 H)
10b	5	3.55-3.50 (m, 1H)	1.38-1.24 (m, 16 H)	0.84 (t, ³ <i>J</i> (H,H) = 6.4, 6 H)
10c	6	3.56-3.52 (m, 1 H)	1.46-1.23 (m, 20 H)	0.85 (t, ³ <i>J</i> (H,H) = 6.7, 6 H)
10d	7	3.57-3.54 (m, 1 H)	1.44-1.26 (m, 24 H)	0.86 (t, ³ <i>J</i> (H,H) = 6.7, 6 H)
10e	9	3.55-3.53 (m, 1 H)	1.46-1.24 (m, 32 H)	0.85 (t, ³ <i>J</i> (H,H) = 7.0, 6 H)

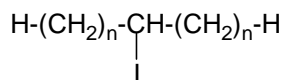
4.2.2. Halides with secondary alkyl chain 11a – e

General procedure:

In a three-necked flask equipped with thermometer, magnetic stirring, reflux condenser with calcium chloride and dropping funnel were introduced 0.084 mol (21.32 g) iodine and 0.055 mol (1.7 g) red phosphorous. To this mixture was added by dropping 0.169 mol (24.44 g) of **10a** at 60 – 70 °C. After heating at 85 °C for 2 h, the phosphorous red was filtered and the reaction mixture was poured into water. The organic phase was separated and the water phase was extracted with diethyl ether (3 x 100 ml). The extracts were combined, decolorized with sodium thiosulfate, washed with sodium chloride saturated solution and dried over anhydrous sodium sulfate.

Synthesis of **11b**:

95% orthophosphoric acid was prepared by mixing of 22.75 ml H₃PO₄ 85 % (0.39 mol, 38.2 g) with 9.94 g (0.07 mol) of phosphoric anhydride. The solution was cooled to room temperature before adding potassium iodide, otherwise evolution of hydrogen iodide and formation of iodine will take place. After addition of 0.35 mol (60.4 g) 6-undecanol and 0.33 mol (54.8 g) of potassium iodide the reaction mixture was heated for 5 h at 110 °C. After cooling to room temperature the reaction mixture was poured into water, the organic phase was separated and the water phase was extracted with diethyl ether (3 x 150 ml). The extracts were combined and decolorized with 10 % sodium thiosulfate solution, washed with sodium chloride saturated solution and dried over anhydrous sodium sulfate. The drying agent was filtered and the diethyl ether evaporated to give a brown oil which was purified by column chromatography using aluminium oxide neutral and petrolether as eluent. 71.2 g of mixture was fractionally distilled to give 6-iodoundecane, yield 12.77 %. In order to increase the yields and to avoid elimination, the procedure with iodine and red phosphorous was preferred.



11a - e

Comp.	<i>n</i>	Alcohol	I ₂	P red	Yield
11a	4	0.169 mol	0.084 mol	0.055 mol	92.50 %
11c	6	0.128 mol	0.064 mol	0.042 mol	78.10 %
11d	7	0.260 mol	0.130 mol	0.086 mol	88.46 %
11e	9	0.094 mol	0.047 mol	0.031 mol	87.74 %

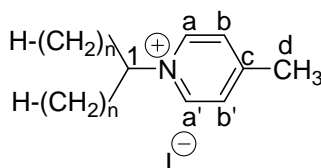
^1H NMR (CDCl_3 , J/Hz , 400 MHz, **11b** and **11c** at 500 MHz)

Comp.	n	^1H δ (ppm)	$(\text{CH}_2)_n$ δ (ppm)	$(\text{CH}_3)_2$ δ (ppm)
11a	4	4.13-4.06 (m, 1 H)	1.89-1.24 (m, 12 H)	0.86 (t, $^3J(\text{H,H}) = 6.8$, 6 H)
11b	5	4.13-4.07 (m, 1 H)	1.87-1.19 (m, 16 H)	0.88 (t, $^3J(\text{H,H}) = 7.0$, 6 H)
11c	6	4.13-4.07 (m, 1 H)	1.90-1.21 (m, 20 H)	0.87 (t, $^3J(\text{H,H}) = 6.9$, 6 H)
11d	7	4.10-4.08 (m, 1 H)	1.84-1.19 (m, 24 H)	0.86 (t, $^3J(\text{H,H}) = 6.7$, 6 H)
11e	9	4.12-4.07 (m, 1 H)	1.88-1.23 (m, 32 H)	0.85 (t, $^3J(\text{H,H}) = 7.0$, 6 H)

4.2.3. Picolinium salts with secondary *N*-alkyl chain **12a – g**

General procedure:

4-Picoline and the appropriate alkyl halide (1/1 molar ratio) were dissolved separately in double amount (volume) of nitromethane. The solutions were unified and heated for 5 h at 90 °C. After cooling to room temperature the solvent was evaporated and the salt was washed several times with diethyl ether to remove the unreacted 4-picoline and further purified by column chromatography using silica gel and diethyl ether and ethanol.



Salts	n	R-I (mol)	4-picoline (mol)	Yield (%)
12a	1	0.100	0.100	68.44
12b	2	0.040	0.040	53.27
12c	4	0.156	0.156	30.76
12d	5	0.046	0.046	31.13
12e	6	0.032	0.032	17.70
12f	7	0.044	0.044	13.63
12g	9	0.083	0.083	10.80

N-Isopropyl-4-methyl-pyridinium iodide **12a**:

^1H NMR (DMSO, J/Hz , 400 MHz) $\delta = 9.0$ (d, $^3J(\text{H,H}) = 6.84$, 2 H, Ar- $\text{H}^{\text{a,a'}}$), 7.98 (d, $^3J(\text{H,H}) = 6.43$, 2 H, Ar- $\text{H}^{\text{b,b'}}$), 4.93 (m, 1 H, CH^1), 2.6 (s, 3 H, CH_3^{d}), 1.57 (d, 6 H, $\text{CH}_3^{2,2'}$). ^{13}C NMR (DMSO, 100 MHz) $\delta = 158.87$ (C^{c}), 141.88 ($\text{C}^{\text{a,a'}}$), 128.41 ($\text{C}^{\text{b,b'}}$), 63.1 (C^1), 22.31 (C^{d}), 21.23 ($\text{C}^{2,2'}$).

MS (EI, 70 eV) m/z : 93, 128, 135 (M^+ -HI). EA: $C_9H_{14}IN$ (Calc.) C: 41.08 %, H: 5.36 %, N: 5.32 %, (Found) C: 40.87 %, H: 5.75 %, N: 5.32 %.

N-Isopentyl-4-methyl-pyridinium bromide **12b**:

1H NMR (DMSO, J /Hz, 400 MHz) δ = 9.00 (d, $^3J(H,H)$ = 6.64, 2 H, Ar- $H^{a,a'}$), 8.04 (d, $^3J(H,H)$ = 6.43, 2 H, Ar- $H^{b,b'}$), 4.63-4.48 (m, 1 H, CH^1), 2.62 (s, 3 H, CH_3^d), 2.05-1.85 (m, 4 H, $CH_2^{2,2'}$), 0.70 (t, $^3J(H,H)$ = 7.0, 6 H, $CH_3^{3,3'}$). ^{13}C NMR (DMSO, 100 MHz) δ = 159.37 (C^c), 142.21 ($C^{a,a'}$), 128.66 ($C^{b,b'}$), 74.52 (C^1), 27.27 ($C^{2,2'}$), 21.33 (C^d), 9.81 ($C^{3,3'}$).

EA: $C_{11}H_{18}BrN$ (Calc.) C: 54.11 %, H: 7.43 %, Br: 32.72 %, N: 5.74 %, (Found) C: 53.81 %, H: 7.84 %, Br: 32.77 %, N: 5.69 %.

N-(*l*'-Butyl)-pentyl-4-methyl-pyridinium iodide **12c**:

1H NMR (DMSO, J /Hz, 400 MHz) δ = 9.10 (d, $^3J(H,H)$ = 6.64, 2 H, Ar- $H^{a,a'}$), 8.04 (d, $^3J(H,H)$ = 6.22, 2 H, Ar- $H^{b,b'}$), 4.74-4.67 (m, 1 H, CH^1), 2.62 (s, 3 H, CH_3^d), 1.97-1.88 (m, 4 H, $CH_2^{2,2'}$), 1.28-1.02 (m, 8 H, $CH_2^{3,3',4,4'}$), 0.75 (t, $^3J(H,H)$ = 7.0, 6 H, $CH_3^{5,5'}$). ^{13}C NMR (DMSO, 100 MHz) δ = 159.09 (C^c), 141.90 ($C^{a,a'}$), 128.48 ($C^{b,b'}$), 71.45 (C^1), 34.07, 26.88, 21.50, 21.31 ($C^{2,2'-4,4',d}$), 13.43 ($C^{5,5'}$).

N-(*l*'-Pentyl)-hexyl-4-methyl-pyridinium iodide **12d**:

1H NMR (DMSO, J /Hz, 400 MHz) δ = 9.01 (d, $^3J(H,H)$ = 6.84, 2 H, Ar- $H^{a,a'}$), 8.02 (d, $^3J(H,H)$ = 6.22, 2 H, Ar- $H^{b,b'}$), 4.62 (m, 1 H, CH^1), 2.61 (s, 3 H, CH_3^d), 1.93 (m, 4 H, $CH_2^{2,2'}$), 1.18 (m, 12 H, $CH_2^{3,3'-5,5'}$), 0.79 (t, $^3J(H,H)$ = 6.9, 6 H, $CH_3^{6,6'}$). ^{13}C NMR (100 MHz, DMSO) δ = 159.60 (C^c), 142.13 ($C^{a,a'}$), 128.72 ($C^{b,b'}$), 71.66 (C^1), 34.20, 30.41, 24.51, 21.65, 21.38 ($C^{2,2'-5,5',d}$), 13.69 ($C^{6,6'}$).

N-(*l*'-Hexyl)-heptyl-4-methyl-pyridinium iodide **12e**:

1H NMR (DMSO, J /Hz, 400 MHz) δ = 9.0 (d, $^3J(H,H)$ = 6.64, 2 H, Ar- $H^{a,a'}$), 8.02 (d, $^3J(H,H)$ = 6.43, 2 H, Ar- $H^{b,b'}$), 4.63-4.59 (m, 1 H, CH^1), 2.6 (s, 3 H, CH_3^d), 1.95-1.90 (m, 4 H, $CH_2^{2,2'}$), 1.23-0.84 (m, 16 H, $CH_2^{3,3'-6,6'}$), 0.81 (t, $J(H,H)$ = 6.8, 6 H, $CH_3^{7,7'}$). ^{13}C NMR (DMSO, 100 MHz) δ = 159.41 (C^c), 142.11 ($C^{a,a'}$), 128.71 ($C^{b,b'}$), 71.74 (C^1), 34.23, 30.78, 27.89, 24.83, 21.80, 21.32 ($C^{2,2'-6,6',d}$), 13.76 ($C^{7,7'}$), m. p. = 96 °C.

N-(1'-Heptyl)-octyl-4-methyl-pyridinium iodide **12f**:

^1H NMR (DMSO, J/Hz , 400 MHz) δ = 9.09 (d, $^3J(\text{H,H})$ = 6.84, 2 H, Ar- $\text{H}^{\text{a,a}'}$), 8.04 (d, $^3J(\text{H,H})$ = 6.22, 2 H, Ar- $\text{H}^{\text{b,b}'}$), 4.72-4.68 (m, 1 H, CH^{l}), 2.61 (s, 3 H, CH_3^{d}), 1.96-1.92 (m, 4 H, $\text{CH}_2^{2,2'}$), 1.21-0.83 (m, 20 H, $\text{CH}_2^{3,3'-7,7'}$), 0.78 (t, $^3J(\text{H,H})$ = 6.9, 6 H, $\text{CH}_3^{8,8'}$). ^{13}C NMR (DMSO, 100 MHz) δ = 159.24 (C^{c}), 142.08 ($\text{C}^{\text{a,a}'}$), 128.59 ($\text{C}^{\text{b,b}'}$), 71.54 (C^{l}), 34.16, 30.86, 28.12, 28.11, 24.76, 21.78, 21.32 ($\text{C}^{2,2'-7,7',\text{d}}$), 13.67 ($\text{C}^{8,8'}$).

MS (EI, 70 eV) m/z : 93, 128, 183, 275 ($\text{M}^+ - \text{HI}$).

N-(1'-Nonyl)-decyl-4-methyl-pyridinium iodide **12g**:

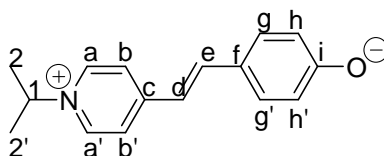
^1H NMR (DMSO, J/Hz , 400 MHz) δ = 8.99 (d, $^3J(\text{H,H})$ = 6.64, 2 H, Ar- $\text{H}^{\text{a,a}'}$), 8.01 (d, $^3J(\text{H,H})$ = 6.43, 2 H, Ar- $\text{H}^{\text{b,b}'}$), 4.62-4.59 (m, 1 H, CH^{l}), 2.61 (s, 3 H, CH_3^{d}), 1.95-1.89 (m, 4 H, $\text{CH}_2^{2,2'}$), 1.24-0.85 (m, 28 H, $\text{CH}_2^{3,3'-9,9'}$), 0.83 (t, $J(\text{H,H})$ = 6.8, 6 H, $\text{CH}_3^{10,10'}$). ^{13}C NMR (DMSO, 100 MHz) δ = 159.38 (C^{c}), 142.12 ($\text{C}^{\text{a,a}'}$), 128.69 ($\text{C}^{\text{b,b}'}$), 71.73 (C^{l}), 34.19, 31.11, 28.66, 28.53, 28.46, 28.18, 24.83, 21.94, 21.29 ($\text{C}^{2,2'-9,9',\text{d}}$), 13.82 ($\text{C}^{10,10'}$), m.p. = 59 °C.

MS (EI, 70 eV) m/z : 93, 128, 267, 359 ($\text{M}^+ - \text{HI}$). EA: $\text{C}_{25}\text{H}_{46}\text{IN}$ (Calc.) C: 61.59 %, H: 9.51 %, N: 2.87 %, (Found) C: 61.04 %, H: 9.49 %, N: 2.76 %.

m.p. = 59 °C

4.2.4. 4'-Hydroxy-stilbazolium dyes with secondary *N*-alkyl chain **13a – g**

1-Isopropyl-4'-oxy-stilbazolium dye **13a**:



Reagents: 4-Hydroxy-benzaldehyde (11 mmol, 1.34 g),
1-isopropyl-4-methyl-pyridinium iodide (11 mmol, 3 g),
piperidine (1.5 ml),
dry ethanol (18.33 ml).

Purification: Recrystallization from ethanol.

Yield: 68.3 % (7.52 mmol), red powder, m. p. = 129 °C

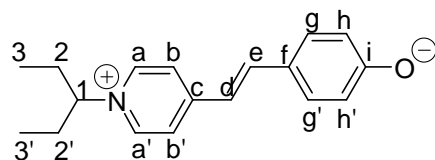
Analytical data: $\text{C}_{16}\text{H}_{17}\text{NO}$ M_w = 239.31

^1H NMR (DMSO, J/Hz , 400 MHz) δ = 8.93 (d, $^3J(\text{H,H})$ = 7.05, 2 H, Ar- $\text{H}^{\text{a,a}'}$), 8.13 (d, $^3J(\text{H,H})$ = 6.84, 2 H, Ar- $\text{H}^{\text{b,b}'}$), 7.95 (d, $^3J(\text{H,H})$ = 16.39, 1 H, CH^{e}), 7.59 (d, $^3J(\text{H,H})$ = 8.71, 2 H, Ar- $\text{H}^{\text{g,g}'}$), 7.26 (d, $^3J(\text{H,H})$ = 16.18, 1 H, CH^{d}), 6.82 (d, $^3J(\text{H,H})$ = 8.71, 2 H, Ar- $\text{H}^{\text{h,h}'}$), 4.87 (m, 1

H, CH^1), 1.57 (d, $^3J(\text{H,H}) = 6.64$, 6 H, $\text{CH}_3^{2,2'}$). ^{13}C NMR (DMSO, 100 MHz) $\delta = 160.68$ (C^i), 153.45 (C^c), 141.78 ($\text{C}^{a,a'}$), 141.28 (C^e), 130.13 ($\text{C}^{g,g'}$), 125.57 (C^f), 122.91 ($\text{C}^{b,b'}$), 118.90 (C^d), 116.04 ($\text{C}^{h,h'}$), 62.38 (C^1), 22.46 ($\text{C}^{2,2'}$).

MS (EI, 70 eV) m/z : 93, 197, 239 (M^+).

1-(1-Ethyl-propyl)-4'-oxy-stilbazolium dye 13b:



Reagents: 4-Hydroxy-benzaldehyde (5.8 mmol, 0.7 g),
1-(1-ethyl-propyl)-4-methyl-pyridinium iodide (5.8 mmol, 1.41 g),
piperidine (0.77 ml),
ethanol (9.7 ml),
deprotonation by heating for 30 min. with a mixture of ethanol/0.35 M KOH solution at 50 – 60 °C.

Purification: Column chromatography using diethyl ether and ethanol (see experimental part, page 82).

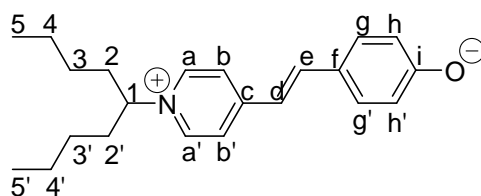
Yield: 24.13 % (1.4 mmol), red powder, m. p. = 123 °C

Analytical data: $\text{C}_{18}\text{H}_{21}\text{NO}$ $M_w = 267.37$

^1H NMR (DMSO, J/Hz , 400 MHz) $\delta = 8.94$ (d, $^3J(\text{H,H}) = 6.85$, 2 H, Ar- $\text{H}^{a,a'}$), 8.20 (d, $^3J(\text{H,H}) = 6.85$, 2 H, Ar- $\text{H}^{b,b'}$), 8.01 (d, $^3J(\text{H,H}) = 16.18$, 1 H, CH^e), 7.63 (d, $^3J(\text{H,H}) = 8.72$, 2 H, Ar- $\text{H}^{g,g'}$), 7.33 (d, $^3J(\text{H,H}) = 16.39$, 1 H, CH^d), 6.85 (d, $^3J(\text{H,H}) = 8.51$, 2 H, Ar- $\text{H}^{h,h'}$), 4.47 (m, 1 H, CH^1), 1.97-1.90 (m, 4 H, $\text{CH}_2^{2,2'}$), 0.72 (t, $^3J(\text{H,H}) = 7.26$, 6H, $\text{CH}_3^{3,3'}$). ^{13}C NMR (DMSO, 100 MHz) $\delta = 161.03$ (C^i), 153.54 (C^c), 142.27 ($\text{C}^{a,a'}$), 140.97 (C^e), 131.02 ($\text{C}^{g,g'}$), 126.27 (C^f), 121.60 ($\text{C}^{b,b'}$), 117.66 (C^d), 115.20 ($\text{C}^{h,h'}$), 61.51 (C^1), 22.41, 22.18 ($\text{C}^{2,2',3,3'}$).

MS (EI, 70 eV) m/z : 93, 148, 198, 266 (M^+).

1-(1-Butyl-pentyl)-4'-oxy-stilbazolium dye 13c:



Reagents: 4-Hydroxy-benzaldehyde (19.1 mmol, 2.34 g),
1-(1-butyl-pentyl)-4-methyl-pyridinium iodide (19.1 mmol, 6.6 g),
piperidine (2.54 ml),
dry ethanol (32 ml),
deprotonation by heating for 30 min. with a mixture of ethanol/0.35 M KOH
solution at 50 – 60 °C.

Purification: Column chromatography using diethyl ether and ethanol (see experimental part,
page 82).

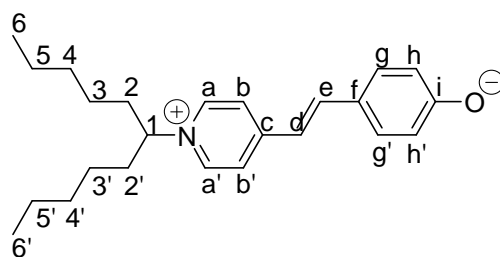
Yield: 23.3 % (4.45 mmol), red powder, m. p. = 125 °C

Analytical data: C₂₂H₂₉NO M_w = 323.47

¹H NMR (DMSO, J/Hz, 400 MHz) δ = 8.99 (d, ³J(H,H) = 6.85, 2 H, Ar-H^{a,a'}), 8.21 (d, ³J(H,H) = 6.85, 2 H, Ar-H^{b,b'}), 8.02 (d, ³J(H,H) = 16.18, 1 H, CH^c), 7.63 (d, ³J(H,H) = 8.71, 2 H, Ar-H^{g,g'}), 7.34 (d, ³J(H,H) = 16.18, 1 H, CH^d), 6.84 (d, ³J(H,H) = 8.51, 2 H, Ar-H^{h,h'}), 4.32 (m, 1 H, CH¹), 1.93-1.89 (m, 4 H, CH₂^{2,2'}), 1.24-1.12 (m, 8 H, CH₂^{3,3',4,4'}), 0.76 (t, ³J(H,H) = 7.26, 6H, CH₃^{5,5'}). ¹³C NMR (DMSO, 100 MHz) δ = 161.22 (Cⁱ), 154.03 (C^c), 142.27 (C^{a,a'}), 141.98 (C^e), 130.42 (C^{g,g'}), 125.68 (C^f), 123.30 (C^{b,b'}), 118.96 (C^d), 116.34 (C^{h,h'}), 71.26 (C¹), 34.04, 27.22, 21.55, (C^{2,2'-4,4'}), 13.62, (C^{5,5'}).

MS (ESI) *m/z*: 198, 324 (MH⁺).

1-(1-pentyl-hexyl)-4'-oxy-stilbazolium dye 13d:



Reagents: 4-Hydroxy-benzaldehyde (4 mmol, 0.5 g),
1-(1-pentyl-hexyl)-4-methyl-pyridinium iodide (4 mmol, 1.56 g),
piperidine (0.5 ml),
dry ethanol (7 ml),
deprotonation by heating for 30 min. with a mixture of ethanol/0.35 M KOH
solution at 50 – 60 °C.

Purification: Column chromatography using as a solvent diethyl ether and ethanol (see
experimental part, page 82).

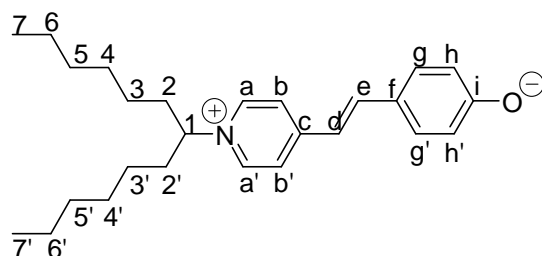
Yield: 10.5 % (0.42 mmol), red powder, m. p. = 85 °C

Analytical data: C₂₄H₃₄NO M_w = 352.52

¹H NMR (DMSO, *J*/Hz, 400 MHz) δ = 10.13 (bs, 1 H, OH), 8.97 (d, ³*J*(H,H) = 6.84, 2 H, Ar-H^{a,a'}), 8.19 (d, ³*J*(H,H) = 6.84, 2 H, Ar-H^{b,b'}), 8.00 (d, ³*J*(H,H) = 16.18, 1 H, CH^c), 7.62 (d, ³*J*(H,H) = 8.51, 2 H, Ar-H^{g,g'}), 7.32 (d, ³*J*(H,H) = 16.18, 1 H, CH^d), 6.87 (d, ³*J*(H,H) = 8.51, 2 H, Ar-H^{h,h'}), 4.57 (m, 1 H, CH¹), 1.97-1.87 (m, 4 H, CH₂^{2,2'}), 1.31-0.83 (m, 12 H, CH₂^{3,3',4,4',5,5'}), 0.79 (t, ³*J*(H,H) = 7.0, 6 H, CH₃^{6,6'}). ¹³C NMR (DMSO, 100 MHz) δ = 159.39 (Cⁱ), 153.31 (C^c), 141.77 (C^{a,a'}), 141.12 (C^e), 129.63 (C^{g,g'}), 125.66 (C^f), 122.87 (C^{b,b'}), 118.94 (C^d), 115.41 (C^{h,h'}), 70.67 (C¹), 33.71, 29.99, 24.13, 21.20 (C^{2,2'-5,5'}), 13.21 (C^{6,6'}).

MS (EI, 70 eV) *m/z*: 93, 128, 154, 197, 351 (M⁺).

1-(1-hexyl-heptyl)-4'-oxy-stilbazolium dye 13e:



Reagents: 4-Hydroxy-benzaldehyde (17.6 mmol, 2.14 g),
1-(1-hexyl-heptyl)-4-methyl-pyridinium iodide (17.6 mmol, 7.1 g),
piperidine (2.35 ml),
dry ethanol (19.5 ml),
deprotonation by heating for 30 min. with a mixture of ethanol/0.35 M KOH
solution at 50 – 60 °C.

Purification: 1.6 g dye was purified by column chromatography using silica gel and diethyl
ether and ethanol (see experimental part, page 82).

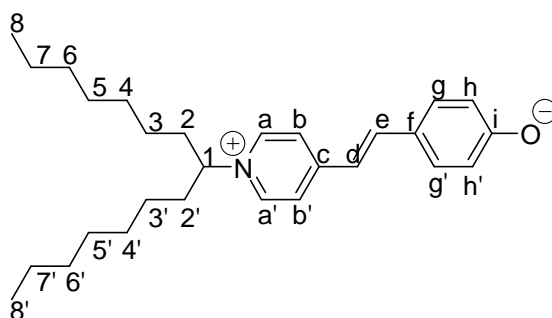
Yield: 7.44 % (1.31 mmol, 0.5 g), red powder, m. p. = 123 °C

Analytical data: C₂₆H₃₈NO M_w = 380.58

¹H NMR (DMSO, *J*/Hz, 400 MHz) δ = 8.95 (d, ³*J*(H,H) = 6.64, 2 H, Ar-H^{a,a'}), 8.18 (d, ³*J*(H,H) = 6.84, 2 H, Ar-H^{b,b'}), 8.00 (d, ³*J*(H,H) = 16.18, 1 H, CH^c), 7.60 (d, ³*J*(H,H) = 8.71, 2 H, Ar-H^{g,g'}), 7.30 (d, ³*J*(H,H) = 16.18, 1 H, CH^d), 6.81 (d, ³*J*(H,H) = 8.51, 2 H, Ar-H^{h,h'}), 4.60-4.52 (m, 1 H, CH¹), 1.94-1.79 (m, 4 H, CH₂^{2,2'}), 1.21-0.82 (m, 16 H, CH₂^{3,3',4,4',5,5',6,6'}), 0.75 (t, ³*J*(H,H) = 6.8, 6 H, CH₃^{7,7'}). ¹³C NMR (DMSO, 100 MHz) δ = 161.23 (Cⁱ), 154.46 (C^c), 142.80 (C^{a,a'}), 142.37 (C^e), 130.86 (C^{g,g'}), 126.40 (C^f), 123.84 (C^{b,b'}), 119.62 (C^d), 116.65 (C^{h,h'}), 71.63 (C¹), 34.87, 31.48, 28.60, 25.57, 22.48 (C^{2,2'-6,6'}), 14.44 (C^{7,7'}).

MS (EI, 70 eV) *m/z*: 128, 182, 197, 381 (MH⁺).

1-(1-heptyl-octyl)-4'-oxy-stilbazolium dye 13f:



Reagents: 4-Hydroxy-benzaldehyde (5.4 mmol, 0.66 g),
 1-(1-heptyl-octyl)-4-methyl-pyridinium iodide (5.4 mmol, 2.33 g),
 piperidine (0.72 ml),
 dry ethanol (9 ml),
 mixture of ethanol/0.35 M KOH solution for deprotonation.

Purification: column chromatography with silica gel and using as eluent diethyl ether and ethanol (see experimental part, page 82).

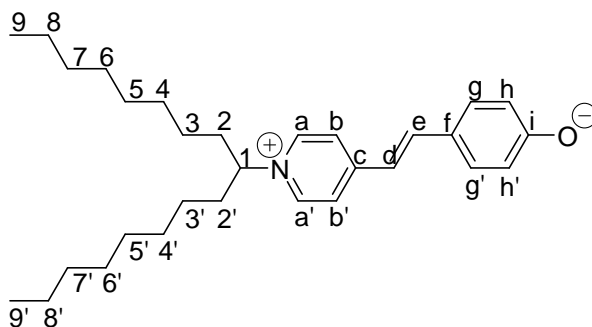
Yield: 18.14 % (0.98 mmol), red powder, m. p. = 119 °C

Analytical data: C₂₈H₄₂INO M_w = 535.54

¹H NMR (DMSO, *J*/Hz, 400 MHz) δ = 8.97 (d, ³*J*(H,H) = 6.84, 2 H, Ar-H^{a,a'}), 8.19 (d, ³*J*(H,H) = 6.84, 2 H, Ar-H^{b,b'}), 7.99 (d, ³*J*(H,H) = 16.18, 1 H, CH^e), 7.62 (d, ³*J*(H,H) = 8.71, 2 H, Ar-H^{g,g'}), 7.32 (d, ³*J*(H,H) = 16.18, 1 H, CH^d), 6.86 (d, ³*J*(H,H) = 8.71, 2 H, Ar-H^{h,h'}), 4.59-4.56 (m, 1 H, CH¹), 1.92-1.86 (m, 4 H, CH₂^{2,2'}), 1.22-0.84 (m, 20 H, CH₂^{3,3',4,4',5,5',6,6',7,7'}), 0.80 (t, ³*J*(H,H) = 6.8, 6 H, CH₃^{8,8'}). ¹³C NMR (DMSO, 100 MHz) δ = 159.87 (Cⁱ), 153.77 (C^c), 142.22 (C^{a,a'}), 141.57 (C^e), 130.10 (C^{g,g'}), 128.09 (C^f), 123.29 (C^{b,b'}), 119.32 (C^d), 115.83 (C^{h,h'}), 71.06 (C¹), 34.20, 30.99, 28.27, 28.25, 24.97, 21.93 (C^{2,2'-7,7'}), 13.83 (C^{8,8'}).

MS (EI, 70 eV) *m/z*: 128, 197, 210, 409 (MH⁺). EA: C₂₈H₄₂INO (Calc.) C: 62.80 %, H: 7.90 %, N: 2.62 %, (Found) C: 62.85 %, H: 7.83 %, N: 2.91 %.

1-(1-octyl-nonyl)-4'-oxy-stilbazolium dye 13g:



Reagents: 4-Hydroxy-benzaldehyde (7.2 mmol, 0.87 g),
1-(1-octyl-nonyl)-4-methyl-pyridinium iodide (7.2 mmol, 3.54 g),
piperidine (0.96 ml),
dry ethanol (8 ml),
Ethanol/KOH mixture.

Purification: the dye was purified by reverse phase chromatography using methanol as solvent (see experimental part, page 82).

Yield: 10.4 % (0.75 mmol), red powder, m. p. = 123 °C

Analytical data: C₃₂H₅₀NO M_w = 464.74

¹H NMR (DMSO, *J*/Hz, 400 MHz) δ = 10.31 (s, 1 H, OH), 9.07 (d, ³*J*(H,H) = 6.43, 2 H, Ar-H^{a,a'}), 8.24 (d, ³*J*(H,H) = 6.43, 2 H, Ar-H^{b,b'}), 8.06 (d, ³*J*(H,H) = 16.18, 1 H, CH^e), 7.63 (d, ³*J*(H,H) = 8.71, 2 H, Ar-H^{g,g'}), 7.36 (d, ³*J*(H,H) = 16.18, 1 H, CH^d), 6.88 (d, ³*J*(H,H) = 8.71, 2 H, Ar-H^{h,h'}), 4.65-4.64 (m, 1 H, CH^l), 1.96-1.84 (m, 4 H, CH₂^{2,2'}), 1.17-0.88 (m, 24 H, CH₂^{3,3'-8,8'}), 0.76 (t, ³*J*(H,H) = 6.8, 6 H, CH₃^{9,9'}). ¹³C NMR (DMSO, 100 MHz) δ = 159.95 (Cⁱ), 153.76 (C^c), 142.20 (C^{a,a'}), 141.61 (C^e), 130.00 (C^{g,g'}), 125.97 (C^f), 123.15 (C^{b,b'}), 119.11 (C^d), 115.76 (C^{h,h'}), 70.87 (C^l), 34.15, 31.07, 31.01, 30.91, 28.74, 28.63, 28.53, 28.50, 28.43, 28.34, 28.21, 24.88, 21.90 (C^{2,2'-8,8'}), 13.73 (C^{9,9'}).

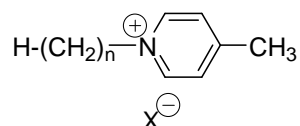
MS (EI, 70 eV) *m/z*: 94, 156, 198, 465 (MH⁺).

4.3. Synthesis of *N*-alkyl-4'-substituted-stilbazolium salts

4.3.1. *N*-alkyl-4-methyl-pyridinium salts 14a – n

General procedure:

To a cold solution of 4-picoline (0.2 mol) in isopropanol (20 ml) was added the appropriate alkyl halide (0.19 mol). The reaction mixture was heated at reflux for 2 h. After cooling to room temperature the solvent was removed under reduced pressure and the salt was washed with diethyl ether. The salts having alkyl chains longer than seven were heated for 5 h at 100 - 120 °C using dry toluene as a solvent (20 mmol of 4-picoline, 10 ml toluene). The salts were purified by recrystallization from ethanol.



<i>n</i>	X ⁻	R-X (mol)	4-picoline (mol)	Solvent (ml)	Yield (%/g)
1	I	0.200	0.190	20	62.50/29.40
3	I	0.100	0.095	10	55.90/14.70
4	Br	0.050	0.050	5	86.50/11.98
5	I	0.200	0.190	20	75.60/44.00
6	I	0.200	0.190	20	91.60/55.90
8	I	0.200	0.190	20	86.90/57.90
9	I	0.500	0.500	250	96.00/16.81
14	Br	0.100	0.100	50	83.00/30.90
16	Br	0.032	0.032	16	56.20/7.20
16	I	0.100	0.100	50	62.90/36.50
18	Br	0.006	0.006	3	89.60/2.29
18	I	0.026	0.026	13	89.50/11.09
20	Br	0.021	0.021	10.5	90.40/8.96
22	Br	0.018	0.018	9	94.40/8.20

N-methyl-4-methyl-pyridinium iodide **14a**:

¹H NMR (DMSO, *J*/Hz, 400 MHz) δ = 8.81 (d, ³*J*(H,H) = 6.64, 2 H, Ar-**H**^{a,a'}), 7.94 (d, ³*J*(H,H) = 6.22, 2 H, Ar-**H**^{b,b'}), 4.26 (s, 3 H, **CH**₃¹), 2.58 (s, 3 H, **CH**₃^d). ¹³C NMR (DMSO, 100 MHz) δ = 158.09 (**C**^c), 144.39 (**C**^{a,a'}), 127.86 (**C**^{b,b'}), 47.14 (**C**¹), 21.32 (**C**^d).

MS (EI, 70 eV) *m/z*: 93, 107, 127, 142. EA: C₇H₁₀IN (Calc.) C: 35.77 %, H: 4.29 %, N: 5.96 %, (Found) C: 35.72 %, H: 4.65 %, N: 5.92 %.

N-propyl-4-methyl-pyridinium iodide **14b**:

^1H NMR (DMSO, J/Hz , 200 MHz) δ = 8.92 (d, $^3J(\text{H,H})$ = 6.64, 2 H, Ar- $\text{H}^{\text{a,a}'}$), 7.99 (d, $^3J(\text{H,H})$ = 6.22, 2 H, Ar- $\text{H}^{\text{b,b}'}$), 4.49 (t, $^3J(\text{H,H})$ = 7.26, 2 H, CH_2^1), 2.60 (s, 3 H, CH_3^{d}), 1.99-1.81 (m, 2 H, CH_2^2), 0.85 (t, $^3J(\text{H,H})$ = 7.3, 3 H, CH_3^3). ^{13}C NMR (DMSO, 50 MHz) δ = 158.73 (C^{c}), 143.61 ($\text{C}^{\text{a,a}'}$), 128.28 ($\text{C}^{\text{b,b}'}$), 61.16 (C^1), 23.90 (C^2), 21.33 (C^{d}), 10.12 (C^3).

MS (EI, 70 eV) m/z : 93, 127, 135 ($\text{M}^+ - \text{I}$), 169. EA: $\text{C}_9\text{H}_{14}\text{IN}$ (Calc.) C: 41.08 %, H: 5.36 %, N: 5.32 %, (Found) C: 41.09 %, H: 5.55 %, N: 5.36 %.

N-butyl-4-methyl-pyridinium bromide **14c**:

^1H NMR (DMSO, J/Hz , 400 MHz) δ = 8.99 (d, $^3J(\text{H,H})$ = 6.84, 2 H, Ar- $\text{H}^{\text{a,a}'}$), 7.99 (d, $^3J(\text{H,H})$ = 6.22, 2 H, Ar- $\text{H}^{\text{b,b}'}$), 4.57 (t, $^3J(\text{H,H})$ = 7.3, 2 H, CH_2^1), 2.59 (s, 3 H, CH_3^{d}), 1.89-1.81 (m, 2 H, CH_2^2), 1.27-0.98 (m, 2 H, CH_3^3), 0.86 (t, $^3J(\text{H,H})$ = 7.3, 3 H, CH_3^4). ^{13}C NMR (DMSO, 100 MHz) δ = 158.43 (C^{c}), 143.50 ($\text{C}^{\text{a,a}'}$), 128.06 ($\text{C}^{\text{b,b}'}$), 59.20 (C^1), 32.41, 21.21, 18.46 ($\text{C}^{2,3,\text{d}}$), 13.18 (C^4).

MS (EI, 70 eV) m/z : 57, 93, 128, 149, 184. EA: $\text{C}_{10}\text{H}_{16}\text{IN}$ (Calc.) C: 43.34 %, H: 5.82 %, N: 5.05 %, (Found) C: 42.95 %, H: 6.12 %, N: 4.99 %.

N-pentyl-4-methyl-pyridinium iodide **14d**:

^1H NMR (DMSO, J/Hz , 400 MHz) δ = 8.94 (d, $^3J(\text{H,H})$ = 6.64, 2 H, Ar- $\text{H}^{\text{a,a}'}$), 7.98 (d, $^3J(\text{H,H})$ = 6.23, 2 H, Ar- $\text{H}^{\text{b,b}'}$), 4.53 (t, $^3J(\text{H,H})$ = 7.3, 2 H, CH_2^1), 2.60 (s, 3 H, CH_3^{d}), 1.92-1.84 (m, 2 H, CH_2^2), 1.33-1.19 (m, 4 H, $\text{CH}_2^{3,4}$), 0.84 (t, $^3J(\text{H,H})$ = 7.1, 3 H, CH_3^5). ^{13}C NMR (DMSO, 100 MHz) δ = 158.53 (C^{c}), 143.45 ($\text{C}^{\text{a,a}'}$), 128.15 ($\text{C}^{\text{b,b}'}$), 59.75 (C^1), 30.09, 27.36, 21.39 (C^{2-4}), 21.30 (C^{d}), 13.61 (C^5).

N-hexyl-4-methyl-pyridinium iodide **14e**:

^1H NMR (DMSO, J/Hz , 400 MHz) δ = 8.90 (d, $^3J(\text{H,H})$ = 6.64, 2 H, Ar- $\text{H}^{\text{a,a}'}$), 7.95 (d, $^3J(\text{H,H})$ = 6.22, 2 H, Ar- $\text{H}^{\text{b,b}'}$), 4.49 (t, $^3J(\text{H,H})$ = 7.47, 2 H, CH_2^1), 2.57 (s, 3 H, CH_3^{d}), 1.88-1.81 (m, 2 H, CH_2^2), 1.23-0.99 (m, 6 H, $\text{CH}_2^{3,4,5}$), 0.81 (t, $^3J(\text{H,H})$ = 6.84, 3 H, CH_3^6). ^{13}C NMR (DMSO, 100 MHz) δ = 158.45 (C^{c}), 143.38 ($\text{C}^{\text{a,a}'}$), 128.10 ($\text{C}^{\text{b,b}'}$), 59.78 (C^1), 30.42, 30.39, 24.92, 21.75 (C^{2-5}), 21.32 (C^{d}), 13.73 (C^6).

N-octyl-4-methyl-pyridinium iodide **14f**:

^1H NMR (DMSO, J/Hz , 400 MHz) δ = 8.95 (d, $^3J(\text{H,H})$ = 6.84, 2 H, Ar- $\text{H}^{\text{a,a}'}$), 7.99 (d, $^3J(\text{H,H})$ = 6.43, 2 H, Ar- $\text{H}^{\text{b,b}'}$), 4.53 (t, $^3J(\text{H,H})$ = 7.3, 2 H, CH_2^1), 2.60 (s, 3 H, CH_3^{d}), 1.91-1.85 (m, 2

H, CH_2^2), 1.25-1.00 (m, 10 H, $\text{CH}_2^{3,4,5,6,7}$), 0.82 (t, $^3J(\text{H,H}) = 6.8$, 3 H, CH_3^8). ^{13}C NMR (DMSO, 50 MHz) $\delta = 158.69$ (C^c), 143.61 ($\text{C}^{a,a'}$), 128.28 ($\text{C}^{b,b'}$), 59.85 (C^1), 31.03, 30.46, 28.35, 28.24, 25.28, 21.94 (C^{2-7}), 21.31 (C^d), 13.85 (C^8).

MS (EI, 70 eV) m/z : 93, 128, 206 (M^+-I). EA: $\text{C}_{14}\text{H}_{24}\text{IN}$ (Calc.) C: 50.46 %, H: 7.26 %, N: 4.20 %, (Found) C: 50.11 %, H: 7.22 %, N: 4.32 %.

N-nonyl-4-methyl-pyridinium iodide 14g:

^1H NMR (CDCl_3 , J/Hz , 400 MHz) $\delta = 9.14$ (d, $^3J(\text{H,H}) = 6.64$, 2 H, $\text{Ar-H}^{a,a'}$), 7.84 (d, $^3J(\text{H,H}) = 6.43$, 2 H, $\text{Ar-H}^{b,b'}$), 4.71 (t, $^3J(\text{H,H}) = 7.5$, 2 H, CH_2^1), 2.58 (s, 3 H, CH_3^d), 1.95-1.88 (m, 2 H, CH_2^2), 1.29-1.09 (m, 12 H, $\text{CH}_2^{3,4,5,6,7,8}$), 0.74 (t, $^3J(\text{H,H}) = 6.8$, 3 H, CH_3^9). ^{13}C NMR (CDCl_3 , 100 MHz) $\delta = 158.64$ (C^c), 143.72 ($\text{C}^{a,a'}$), 128.70 ($\text{C}^{b,b'}$), 60.97 (C^1), 31.47, 31.45, 30.19, 29.01, 28.84, 25.71, 22.31 (C^{2-8}), 21.16 (C^d), 13.80 (C^9).

MS (EI, 70 eV) m/z : 93, 128, 219 (M^+-HI), 254. EA: $\text{C}_{15}\text{H}_{26}\text{IN}$ (Calc.) C: 51.88 %, H: 7.55 %, N: 4.03 %, (Found) C: 51.61 %, H: 7.63 %, N: 4.20 %.

N-tetradecyl-4-methyl-pyridinium bromide 14h:

^1H NMR (DMSO, J/Hz , 400 MHz) $\delta = 8.97$ (d, $^3J(\text{H,H}) = 5.81$, 2 H, $\text{Ar-H}^{a,a'}$), 7.98 (d, $^3J(\text{H,H}) = 6.02$, 2 H, $\text{Ar-H}^{b,b'}$), 4.54 (t, $^3J(\text{H,H}) = 7.3$, 2 H, CH_2^1), 2.60 (s, 3 H, CH_3^d), 1.88-1.85 (m, 2 H, CH_2^2), 1.25-1.21 (m, 22 H, CH_2^{3-13}), 0.83 (t, $^3J(\text{H,H}) = 6.64$, 3 H, CH_3^{14}). ^{13}C NMR (DMSO, 100 MHz) $\delta = 159.18$ (C^c), 144.17 ($\text{C}^{a,a'}$), 128.80 ($\text{C}^{b,b'}$), 60.38 (C^1), 31.80, 31.11, 29.57, 29.55, 29.52, 29.43, 29.31, 28.90, 25.90, 22.60, (C^{2-13}), 21.89 (C^d), 14.45 (C^{14}).

MS (EI, 70 eV) m/z : 93, 289 (M^+-HBr). EA: $\text{C}_{20}\text{H}_{36}\text{BrN}$ (Calc.) C: 64.85 %, H: 9.80 %, Br: 21.57 %, N: 3.78 %, (Found) C: 64.43 %, H: 9.77 %, Br: 21.88 %, N: 3.79 %.

N-hexadecyl-4-methyl-pyridinium bromide 14i:

^1H NMR (DMSO, J/Hz , 400 MHz) $\delta = 8.91$ (d, $^3J(\text{H,H}) = 6.64$, 2 H, $\text{Ar-H}^{a,a'}$), 7.94 (d, $^3J(\text{H,H}) = 6.43$, 2 H, $\text{Ar-H}^{b,b'}$), 4.49 (t, $^3J(\text{H,H}) = 7.47$, 2 H, CH_2^1), 2.56 (s, 3 H, CH_3^d), 1.87-1.82 (m, 2 H, CH_2^2), 1.22 (bs, 26 H, CH_2^{3-15}), 0.81 (t, $^3J(\text{H,H}) = 6.8$, 3 H, CH_3^{16}). ^{13}C NMR (DMSO, 100 MHz) $\delta = 158.61$ (C^c), 143.56 ($\text{C}^{a,a'}$), 128.22 ($\text{C}^{b,b'}$), 59.82 (C^1), 31.21, 30.51, 28.96, 28.92, 28.92, 28.84, 28.72, 28.62, 28.31, 25.31, 22.01 (C^{2-15}), 21.30 (C^d), 13.86 (C^{16}).

MS (EI, 70 eV) m/z : 168, 197, 309 (M^+). EA: $\text{C}_{24}\text{H}_{44}\text{BrN}$ (Calc.) C: 67.58 %, H: 10.40 %, Br: 18.73 %, N: 3.28 %, (Found) C: 67.27 %, H: 10.48 %, Br: 18.24 %, N: 3.08 %.

N-hexadecyl-4-methyl-pyridinium iodide **14j**:

^1H NMR (DMSO, J/Hz , 200 MHz) δ = 8.91 (d, $^3J(\text{H,H})$ = 6.64, 2 H, Ar- $\text{H}^{\text{a,a}'}$), 7.97 (d, $^3J(\text{H,H})$ = 6.43, 2 H, Ar- $\text{H}^{\text{b,b}'}$), 4.50 (t, $^3J(\text{H,H})$ = 7.3, 2 H, CH_2^1), 2.59 (s, 3 H, CH_3^{d}), 1.90-1.86 (m, 2 H, CH_2^2), 1.22 (bs, 26 H, CH_2^{3-15}), 0.84 (t, $^3J(\text{H,H})$ = 6.3, 3 H, CH_3^{16}). ^{13}C NMR (DMSO, 100 MHz) δ = 158.45 (C^{c}), 143.40 ($\text{C}^{\text{a,a}'}$), 128.10 ($\text{C}^{\text{b,b}'}$), 59.81 (C^1), 31.20, 30.45, 29.74, 28.95, 28.91, 28.87, 28.82, 28.74, 28.69, 28.61, 25.30, 22.01 (C^{2-15}), 21.31 (C^{d}), 13.88 (C^{16}).

MS (EI, 70 eV) m/z : 93, 127, 225, 318 ($\text{M}^+ - \text{I}$). EA: $\text{C}_{22}\text{H}_{40}\text{IN}$ (Calc.) C: 59.32 %, H: 9.05 %, N: 3.14 %, (Found) C: 58.88 %, H: 9.59 %, N: 2.26 %.

N-octadecyl-4-methyl-pyridinium bromide **14k**:

^1H NMR (CDCl_3 , J/Hz , 400 MHz) δ = 9.25 (d, $^3J(\text{H,H})$ = 6.22, 2 H, Ar- $\text{H}^{\text{a,a}'}$), 7.85 (d, $^3J(\text{H,H})$ = 6.22, 2 H, Ar- $\text{H}^{\text{b,b}'}$), 4.87 (t, $^3J(\text{H,H})$ = 7.3, 2 H, CH_2^1), 2.64 (s, 3 H, CH_3^{d}), 1.99-1.93 (m, 2 H, CH_2^2), 1.29-1.19 (m, 30 H, CH_2^{3-17}), 0.84 (t, $^3J(\text{H,H})$ = 6.3, 3 H, CH_3^{18}). ^{13}C NMR (CDCl_3 , 125 MHz) δ = 158.77 (C^{c}), 144.15 ($\text{C}^{\text{a,a}'}$), 128.79 ($\text{C}^{\text{b,b}'}$), 61.33 (C^1), 31.87, 31.81, 29.65, 29.61, 29.55, 29.47, 29.32, 29.31, 29.04, 26.04, 26.04, 22.63 (C^{2-17}), 22.24 (C^{d}), 14.06 (C^{18}).

N-octadecyl-4-methyl-pyridinium iodide **14l**:

^1H NMR (DMSO, J/Hz , 400 MHz) δ = 8.90 (d, $^3J(\text{H,H})$ = 6.64, 2 H, Ar- $\text{H}^{\text{a,a}'}$), 7.97 (d, $^3J(\text{H,H})$ = 6.43, 2 H, Ar- $\text{H}^{\text{b,b}'}$), 4.49 (t, $^3J(\text{H,H})$ = 7.47, 2 H, CH_2^1), 2.59 (s, 3 H, CH_3^{d}), 1.88-1.85 (m, 2 H, CH_2^2), 1.22 (bs, 30 H, CH_2^{3-17}), 0.84 (t, $^3J(\text{H,H})$ = 6.8, 3 H, CH_3^{18}). ^{13}C NMR (DMSO, 100 MHz) δ = 158.45 (C^{c}), 143.40 ($\text{C}^{\text{a,a}'}$), 128.10 ($\text{C}^{\text{b,b}'}$), 59.81 (C^1), 31.19, 30.45, 28.93, 28.90, 28.82, 28.69, 28.60, 28.28, 25.30, 22.06 (C^{2-17}), 21.30 (C^{d}), 13.87 (C^{18}).

MS (EI, 70 eV) m/z : 127, 253, 345 ($\text{M}^+ - \text{I}$). EA: $\text{C}_{24}\text{H}_{44}\text{IN}$ (Calc.) C: 60.88 %, H: 9.37 %, N: 2.96 %, (Found) C: 60.50 %, H: 9.79 %, N: 2.56 %.

N-eicosyl-4-methyl-pyridinium bromide **14m**:

^1H NMR (CDCl_3 , J/Hz , 400 MHz) δ = 9.24 (d, $^3J(\text{H,H})$ = 6.22, 2 H, Ar- $\text{H}^{\text{a,a}'}$), 7.84 (d, $^3J(\text{H,H})$ = 6.22, 2 H, Ar- $\text{H}^{\text{b,b}'}$), 4.89 (t, $^3J(\text{H,H})$ = 7.3, 2 H, CH_2^1), 2.64 (s, 3 H, CH_3^{d}), 2.01-1.94 (m, 2 H, CH_2^2), 1.29-1.20 (m, 34 H, CH_2^{3-19}), 0.85 (t, $^3J(\text{H,H})$ = 6.8, 3 H, CH_3^{20}). ^{13}C NMR (CDCl_3 , 100 MHz) δ = 158.42 (C^{c}), 144.10 ($\text{C}^{\text{a,a}'}$), 128.70 ($\text{C}^{\text{b,b}'}$), 61.21 (C^1), 31.88, 31.83, 29.67, 29.62, 29.59, 29.51, 29.36, 29.32, 29.08, 26.08, 22.65 (C^{2-19}), 22.25 (C^{d}), 14.08 (C^{20}).

N-docosyl-4-methyl-pyridinium bromide **14n**:

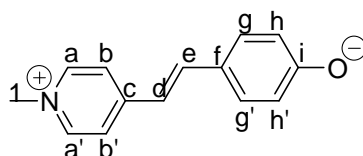
^1H NMR (CDCl_3 , J/Hz , 400 MHz) δ = 9.29 (d, $^3J(\text{H,H})$ = 6.64, 2 H, Ar- $\text{H}^{\text{a,a}'}$), 7.86 (d, $^3J(\text{H,H})$ = 6.43, 2 H, Ar- $\text{H}^{\text{b,b}'}$), 4.86 (t, $^3J(\text{H,H})$ = 7.47, 2 H, CH_2^1), 2.62 (s, 3 H, CH_3^{d}), 2.00-1.93 (m, 2 H, CH_2^2), 1.31-1.18 (m, 38 H, CH_2^{3-21}), 0.83 (t, $^3J(\text{H,H})$ = 6.8, 3 H, CH_3^{22}). ^{13}C NMR (CDCl_3 , 100 MHz) δ = 158.47 (C^{c}), 144.10 ($\text{C}^{\text{a,a}'}$), 128.68 ($\text{C}^{\text{b,b}'}$), 61.15 (C^1), 31.86, 31.82, 29.65, 29.61, 29.59, 29.57, 29.49, 29.34, 29.29, 29.06, 26.05, 22.63 (C^{2-21}), 22.22 (C^{d}), 14.06 (C^{22}).

4.3.2. *N*-alkyl-4'-oxy- and -hydroxy-stilbazolium compounds **15a – n**

General procedure:

The appropriate *N*-alkyl-4-methyl-picolinium salts **14a – n** (1 mmol), 4-substituted-benzaldehyde (1 mmol), piperidine (0.13 ml) and dry ethanol were heated under reflux for 8 h. By cooling the reaction to room temperature the products precipitate. The red solids were filtrate, washed with ether and purified for two or three times by recrystallization from ethanol.

N-methyl-4'-oxy-stilbazolium dye **15a**:



Reagents: 4-Hydroxy-benzaldehyde (0.1 mol, 12.3 g),
1-propyl-4-methyl-pyridinium iodide (0.1 mol, 24.1 g),
piperidine (8.5 ml),
dry ethanol (125 ml).

Purification: Recrystallization for three times from water and then from a mixture of ethanol/water = 2/1.

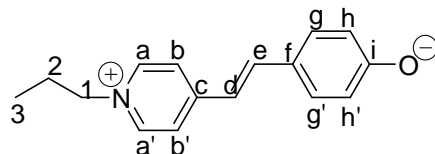
Yield: 62 % (0.062 mol), red crystals

Analytical data: $\text{C}_{14}\text{H}_{13}\text{NO}$ M_w = 211.26

^1H NMR (DMSO, J/Hz , 500 MHz) δ = 8.08 (d, $^3J(\text{H,H})$ = 7.06, 2 H, Ar- $\text{H}^{\text{a,a}'}$), 7.62 (d, $^3J(\text{H,H})$ = 14.94, 1 H, Ar- $\text{H}^{\text{e,e}'}$), 7.45 (d, $^3J(\text{H,H})$ = 6.85, 2 H, Ar- $\text{H}^{\text{b,b}'}$), 7.26 (d, $^3J(\text{H,H})$ = 8.33, 2 H, Ar- $\text{H}^{\text{g,g}'}$), 6.41 (d, $^3J(\text{H,H})$ = 15.15, 1 H, Ar- H^{d}), 6.04 (d, $^3J(\text{H,H})$ = 8.92, 2 H, Ar- $\text{H}^{\text{h,h}'}$), 3.88 (s, CH_3^1). ^{13}C NMR (DMSO, 125 MHz) δ = 179.48 (C^{i}), 152.70 (C^{c}), 143.82 (C^{e}), 141.59 ($\text{C}^{\text{a,a}'}$), 132.88 ($\text{C}^{\text{g,g}'}$), 121.47 ($\text{C}^{\text{h,h}'}$), 118.10 ($\text{C}^{\text{b,b}'}$), 115.54 (C^{f}), 107.02 (C^{d}), 44.53 (C^1).

MS (ESI): 212.3 (MH⁺). EA: C₁₄H₁₃NO (Calc.) C: 79.59 %, H: 6.20 %, N: 6.63 %, (Found) C: 78.04 %, H: 6.62 %, N: 6.52 %.

N-propyl-4'-oxy-stilbazolium dye **15b**:



Reagents: 4-Hydroxy-benzaldehyde (0.055 mol, 6.8 g),
1-propyl-4-methyl-pyridinium iodide (0.055 mol, 14.7 g),
piperidine (4.6 ml),
dry ethanol (70 ml),
0.35 M KOH.

Purification: Recrystallization for three times from water.

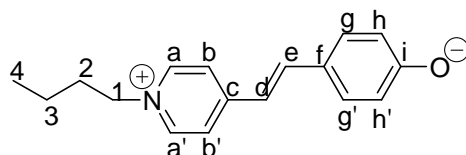
Yield: 60 % (0.033 mol), red powder

Analytical data: C₁₆H₁₇NO M_w = 239.31

¹H NMR (DMSO, J/Hz, 400 MHz) δ = 8.13 (d, ³J(H,H) = 7.26, 2 H, Ar-H^{a,a'}), 7.6 (d, ³J(H,H) = 14.94, 1 H, Ar-H^{e,e'}), 7.45 (d, ³J(H,H) = 6.85, 2 H, Ar-H^{b,b'}), 7.26 (d, ³J(H,H) = 7.88, 2 H, Ar-H^{g,g'}), 6.42 (d, ³J(H,H) = 14.95, 1 H, Ar-H^d), 6.04 (d, ³J(H,H) = 8.92, 2 H, Ar-H^{h,h'}), 4.08 (t, ³J(H,H) = 7.1, 2 H, CH₂¹), 1.83-1.74 (m, 2 H, CH₂²), 0.85, (t, ³J(H,H) = 7.3, 2 H, CH₃³).
¹³C NMR (DMSO, 100 MHz) δ = 179.56 (Cⁱ), 152.84 (C^c), 143.95 (C^e), 140.67 (C^{a,a'}), 132.95 (C^{g,g'}), 121.54 (C^{h,h'}), 118.10 (C^{b,b'}), 115.70 (C^f), 106.95 (C^d), 58.62 (C¹), 23.61 (C²), 10.28 (C³).

MS (EI, 70 eV): 93, 198, 240 (MH⁺). EA: C₁₆H₁₇NO·0.9H₂O (Calc.) C: 75.14 %, H: 7.36 %, N: 5.47 %, (Found) C: 75.22 %, H: 7.59 %, N: 5.10 %.

N-butyl-4'-oxy-stilbazolium dye **15c**:



Reagents: 4-Hydroxy-benzaldehyde (0.1 mol, 12.2 g),
1-butyl-4-methyl-pyridinium bromide (0.1 mol, 23 g),
piperidine (13.3 ml),

dry ethanol (111 ml),

0.35 M KOH.

Purification: Recrystallization from ethanol

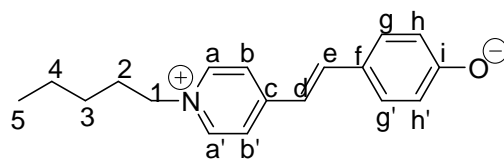
Yield: 40.15 % (0.04 mol), red powder

Analytical data: $C_{17}H_{19}NO$ $M_w = 253.37$

1H NMR (DMSO, J/Hz , 400 MHz) $\delta = 8.66$ (d, $^3J(H,H) = 6.84$, 2 H, Ar- $H^{a,a'}$), 7.93 (d, $^3J(H,H) = 6.85$, 2 H, Ar- $H^{b,b'}$), 7.85 (d, $^3J(H,H) = 15.98$, 1 H, CH^c), 7.46 (d, $^3J(H,H) = 8.72$, 2 H, Ar- $H^{g,g'}$), 6.97 (d, $^3J(H,H) = 15.77$, 1 H, CH^d), 6.60 (d, $^3J(H,H) = 8.71$, 2 H, Ar- $H^{h,h'}$), 4.36 (t, $^3J(H,H) = 7.26$, 2 H, CH_2^1), 1.86 - 1.78 (m, 2 H, CH_2^2), 1.30 - 1.22 (m, 2 H, CH_2^3), 0.89 (t, $^3J(H,H) = 7.3$, 3 H, CH_3^4). ^{13}C NMR (DMSO, 100 MHz) $\delta = 168.52$ (C^i), 153.55 (C^c), 142.82 ($C^{a,a'}$), 142.76 (C^e), 131.15 ($C^{g,g'}$), 121.57 (C^f), 121.46 ($C^{b,b'}$), 118.06 (C^d), 114.92 ($C^{h,h'}$), 58.45 (C^1), 32.38 , 18.75 ($C^{2,3}$), 13.30 (C^4).

MS (EI, 70 eV) m/z : 93, 106, 149, 197, 255 (MH^+).

N-pentyl-4'-oxy-stilbazolium dye **15d**:



Reagents: 4-Hydroxy-benzaldehyde (0.15 mol, 18.3 g),
1-pentyl-4-methyl-pyridinium iodide (0.15 mol, 44 g),
piperidine (20 ml),
dry ethanol (250 ml),
0.35 M KOH.

Purification: Recrystallization from ethanol

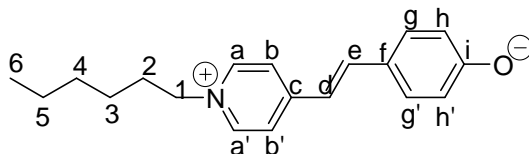
Yield: 63.4 % (0.095 mol), red powder

Analytical data: $C_{18}H_{21}NO$ $M_w = 267.37$

1H NMR (DMSO, J/Hz , 200 MHz) $\delta = 8.84$ (d, $^3J(H,H) = 6.64$, 2 H, Ar- $H^{a,a'}$), 8.12 (d, $^3J(H,H) = 6.64$, 2 H, Ar- $H^{b,b'}$), 7.93 (d, $^3J(H,H) = 16.18$, 1 H, CH^c), 7.58 (d, $^3J(H,H) = 8.5$, 2 H, Ar- $H^{g,g'}$), 7.23 (d, $^3J(H,H) = 16.18$, 1 H, CH^d), 6.82 (d, $^3J(H,H) = 8.51$, 2 H, Ar- $H^{h,h'}$), 4.44 (t, $^3J(H,H) = 7.26$, 2 H, CH_2^1), 1.95 - 1.81 (m, 2 H, CH_2^2), 1.36 - 1.05 (m, 4 H, $CH_2^{3,4}$), 0.86 (t, $^3J(H,H) = 6.7$, 3 H, CH_3^5). ^{13}C NMR (DMSO, 50 MHz) $\delta = 161.37$ (C^i), 153.45 (C^c), 143.70 ($C^{a,a'}$), 141.59 (C^e), 130.38 ($C^{g,g'}$), 125.51 (C^f), 122.87 ($C^{b,b'}$), 118.89 (C^d), 116.33 ($C^{h,h'}$), 59.28 (C^1), 30.12 , 27.51 , 21.50 , (C^{2-4}), 13.69 (C^5).

MS (EI, 70 eV) m/z : 71, 93, 197, 267 (M^+). EA: $C_{18}H_{22}NO$ (Calc.) C: 54.69 %, H: 5.61 %, N: 3.54 %, (Found) C: 55.96 %, H: 6.04 %, N: 3.53 %.

N-hexyl-4'-oxy-stilbazolium dye **15e**:



Reagents: 4-Hydroxy-benzaldehyde (0.175 mol, 21.44 g),
1-hexyl-4-methyl-pyridinium iodide (0.175 mol, 53.6 g),
piperidine (23.33 ml),
dry ethanol (290 ml),
0.35 M KOH.

Purification: Recrystallization from ethanol.

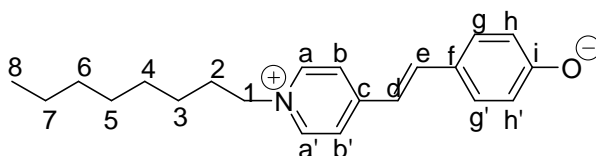
Yield: 59.6 % (0.13 mol), red powder

Analytical data: $C_{19}H_{23}NO$ $M_w = 281.39$

1H NMR (DMSO, J/Hz , 400 MHz) $\delta = 8.73$ (d, $^3J(H,H) = 6.64$, 2 H, Ar- $H^{a,a'}$), 8.02 (d, $^3J(H,H) = 6.64$, 2 H, Ar- $H^{b,b'}$), 7.87 (d, $^3J(H,H) = 16.18$, 1 H, CH^e), 7.50 (d, $^3J(H,H) = 8.51$, 2 H, Ar- $H^{g,g'}$), 7.10 (d, $^3J(H,H) = 16.18$, 1 H, CH^d), 6.70 (d, $^3J(H,H) = 8.51$, 2 H, Ar- $H^{h,h'}$), 4.37 (t, $^3J(H,H) = 7.3$, 2 H, CH_2^1), 1.85 - 1.81 (m, 2 H, CH_2^2), 1.24 - 1.21 (m, 6 H, $CH_2^{3,4,5}$), 0.81 (t, $^3J(H,H) = 6.0$, 3 H, CH_3^6). ^{13}C NMR (DMSO, 100 MHz) $\delta = 164.02$ (C^i), 153.32 (C^c), 143.17 ($C^{a,a'}$), 141.91 (C^e), 130.50 ($C^{g,g'}$), 123.78 (C^f), 122.19 ($C^{b,b'}$), 117.21 (C^d), 116.84 ($C^{h,h'}$), 59.02 (C^1), 30.49 , 30.35 , 25.02 , 21.80 , (C^{2-5}), 13.77 (C^6).

MS (EI, 70 eV) m/z : 85, 93, 197, 281 (M^+). EA: $C_{19}H_{24}NO$ (Calc.) C: 55.75 %, H: 5.91 %, N: 3.42 %, (Found) C: 58.29 %, H: 6.47 %, N: 3.32 %.

N-octyl-4'-oxy-stilbazolium dye **15f**:



Reagents: 4-Hydroxy-benzaldehyde (0.17 mol, 21.2 g),
1-octyl-4-methyl-pyridinium iodide (0.17 mol, 57.9 g),
piperidine (23 ml),

dry ethanol (315 ml),

0.35 M KOH.

Purification: Recrystallization from ethanol for two times.

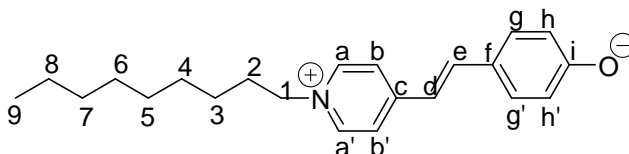
Yield: 70.6 % (0.12 mol), red powder

Analytical data: C₂₁H₂₇NO M_w = 309.45

¹H NMR (DMSO, *J*/Hz, 200 MHz) δ = 8.75 (d, ³*J*(H,H) = 6.64, 2 H, Ar-**H**^{a,a'}), 8.03 (d, ³*J*(H,H) = 6.64, 2 H, Ar-**H**^{b,b'}), 7.89 (d, ³*J*(H,H) = 15.98, 1 H, **CH**^e), 7.52 (d, ³*J*(H,H) = 8.72, 2 H, Ar-**H**^{g,g'}), 7.09 (d, ³*J*(H,H) = 15.98, 1 H, **CH**^d), 6.71 (d, ³*J*(H,H) = 8.72, 2 H, Ar-**H**^{h,h'}), 4.39 (t, ³*J*(H,H) = 7.1, 2 H, **CH**₂¹), 1.84 (m, 2 H, **CH**₂²), 1.21 (bs, 10 H, **CH**₂³⁻⁷), 0.82 (t, ³*J*(H,H) = 6.3, 3 H, **CH**₃⁸). ¹³C NMR (DMSO, 50 MHz) δ = 165.49 (**C**ⁱ), 153.55 (**C**^c), 143.19 (**C**^{a,a'}), 142.29 (**C**^e), 130.74 (**C**^{g,g'}), 123.20 (**C**^f), 122.14 (**C**^{b,b'}), 117.21 (**C**^d), 116.73 (**C**^{h,h'}), 58.96 (**C**¹), 31.05, 30.42, 28.39, 28.29, 25.37, 21.97 (**C**²⁻⁷), 13.86 (**C**⁸).

MS (EI, 70 eV) *m/z*: 93, 197, 309 (M⁺-HI). EA: C₂₁H₂₈INO (Calc.) C: 57.67 %, H: 6.45 %, N: 3.20 %, (Found) C: 62.26 %, H: 7.07 %, N: 3.22 %.

N-nonyl-4'-oxy-stilbazolium dye **15g**:



Reagents: 4-Hydroxy-benzaldehyde (0.024 mol, 3.02 g),
1-nonyl-4-methyl-pyridinium iodide (0.024 mol, 8.6 g),
piperidine (3.2 ml),
dry ethanol (40 ml),
0.35 M KOH solution for deprotonation.

Purification: Recrystallization from ethanol.

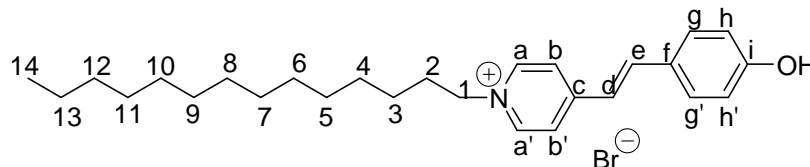
Yield: 66.6 % (0.016 mol), red powder

Analytical data: C₂₂H₂₉NO M_w = 323.47

¹H NMR (DMSO, *J*/Hz, 400 MHz) δ = 8.72 (d, ³*J*(H,H) = 6.84, 2 H, Ar-**H**^{a,a'}), 8.00 (d, ³*J*(H,H) = 6.84, 2 H, Ar-**H**^{b,b'}), 7.86 (d, ³*J*(H,H) = 15.98, 1 H, **CH**^e), 7.49 (d, ³*J*(H,H) = 8.71, 2 H, Ar-**H**^{g,g'}), 7.08 (d, ³*J*(H,H) = 15.98, 1 H, **CH**^d), 6.69 (d, ³*J*(H,H) = 8.71, 2 H, Ar-**H**^{h,h'}), 4.36 (t, ³*J*(H,H) = 7.26, 2 H, **CH**₂¹), 1.84-1.80 (m, 2 H, **CH**₂²), 1.22-1.07 (m, 12 H, **CH**₂³⁻⁸), 0.82 (t, ³*J*(H,H) = 6.8, 3 H, **CH**₃⁹). ¹³C NMR (DMSO, 100 MHz) δ = 165.73 (**C**ⁱ), 153.46 (**C**^c), 143.08 (**C**^{a,a'}), 142.27 (**C**^e), 130.74 (**C**^{g,g'}), 122.98 (**C**^f), 121.97 (**C**^{b,b'}), 117.28 (**C**^d), 116.43 (**C**^{h,h'}), 58.96 (**C**¹), 31.05, 30.42, 28.39, 28.29, 25.37, 21.97 (**C**²⁻⁷), 13.86 (**C**⁹).

MS (EI, 70 eV) m/z : 93, 197, 323 (M^+ -HI). EA: $C_{22}H_{30}INO$ (Calc.) C: 58.54 %, H: 6.70 %, N: 3.10 %, (Found) C: 62.76 %, H: 7.43 %, N: 3.06 %.

N-tetradecyl-4'-hydroxy-stilbazolium bromide **15h**:



Reagents: 4-Hydroxy-benzaldehyde (5.40 mmol, 0.66 g),
1-tetradecyl-4-methyl-pyridinium bromide (5.40 mmol, 2 g),
piperidine (0.72 ml),
dry ethanol (9 ml).

Purification: Recrystallization from ethanol

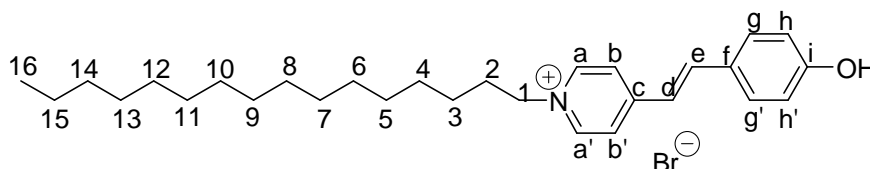
Yield: 50.7 % (2.74 mmol), red powder

Analytical data: $C_{27}H_{40}BrNO$ $M_w = 474.52$

1H NMR (DMSO, J /Hz, 400 MHz) $\delta = 8.70$ (d, $^3J(H,H) = 6.84$, 2 H, Ar- $H^{a,a'}$), 7.98 (d, $^3J(H,H) = 6.84$, 2 H, Ar- $H^{b,b'}$), 7.85 (d, $^3J(H,H) = 15.97$, 1 H, CH^e), 7.49 (d, $^3J(H,H) = 8.71$, 2 H, Ar- $H^{g,g'}$), 7.05 (d, $^3J(H,H) = 15.97$, 1 H, CH^d), 6.67 (d, $^3J(H,H) = 8.51$, 2 H, Ar- $H^{h,h'}$), 4.35 (t, $^3J(H,H) = 7.26$, 2 H, CH_2^1), 1.84 - 1.80 (m, 2 H, CH_2^2), 1.22 - 1.18 (m, 22 H, CH_2^{3-13}), 0.81 (t, $^3J(H,H) = 6.8$, 3 H, CH_3^{14}). ^{13}C NMR (DMSO, 100 MHz) $\delta = 164.91$ (C^i), 153.48 (C^c), 143.20 ($C^{a,a'}$), 142.17 (C^e), 130.65 ($C^{g,g'}$), 123.47 (C^f), 122.11 ($C^{b,b'}$), 117.10 (C^d), 116.86 ($C^{h,h'}$), 58.95 (C^1), 31.19 , 30.37 , 28.95 , 28.91 , 28.88 , 28.79 , 28.68 , 28.60 , 28.29 , 25.33 , 21.98 (C^{2-13}), 13.84 (C^{14}).

MS (EI, 70 eV) m/z : 93, 197, 393 (M^+ -HBr). EA: $C_{27}H_{40}BrNO$ (Calc.) C: 68.34 %, H: 8.50 %, Br: 16.84 %, N: 2.95 %, (Found) C: 69.34 %, H: 8.82 %, Br: 13.39 %, N: 2.98 %.

N-hexadecyl-4'-hydroxy-stilbazolium bromide **15i**:



Reagents: 4-Hydroxy-benzaldehyde (2.51 mmol, 0.31 g),
1-hexadecyl-4-methyl-pyridinium bromide (2.51 mmol, 1 g),
piperidine (0.3 ml),

dry ethanol (5 ml).

Purification: Recrystallization from ethanol.

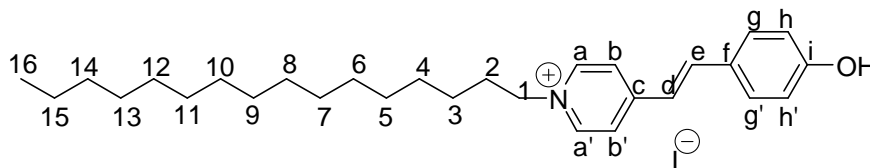
Yield: 59.36 % (1.49 mmol), red powder

Analytical data: C₂₉H₄₄BrNO M_w = 502.57

¹H NMR (DMSO, J/Hz, 400 MHz) δ = 8.72 (d, ³J(H,H) = 6.84, 2 H, Ar-H^{a,a'}), 8.02 (d, ³J(H,H) = 6.84, 2 H, Ar-H^{b,b'}), 7.86 (d, ³J(H,H) = 15.97, 1 H, CH^e), 7.51 (d, ³J(H,H) = 8.71, 2 H, Ar-H^{g,g'}), 7.10 (d, ³J(H,H) = 15.97, 1 H, CH^d), 6.70 (d, ³J(H,H) = 8.71, 2 H, Ar-H^{h,h'}), 4.36 (t, ³J(H,H) = 7.26, 2 H, CH₂¹), 1.84-1.80 (m, 2 H, CH₂²), 1.22-1.17 (m, 26 H, CH₂³⁻¹⁵), 0.80 (t, ³J(H,H) = 6.8, 3 H, CH₃¹⁶). ¹³C NMR (DMSO, 100 MHz) δ = 160.77 (Cⁱ), 154.02 (C^c), 143.91 (C^{a,a'}), 142.56 (C^e), 131.17 (C^{g,g'}), 124.69 (C^f), 122.88 (C^{b,b'}), 118.01 (C^d), 117.49 (C^{h,h'}), 59.66 (C¹), 31.80, 30.97, 29.55, 29.51, 29.49, 29.40, 29.29, 29.20, 28.89, 25.95, 22.60 (C²⁻¹⁵), 14.46 (C¹⁶).

MS (EI, 70 eV) m/z: 93, 197, 225, 421 (M⁺-HBr). EA: C₂₉H₄₄BrNO (Calc.) C: 69.31 %, H: 8.82 %, Br: 15.90 %, N: 2.79 %, (Found) C: 70.01 %, H: 9.11 %, Br: 13.18 %, N: 2.78 %.

N-hexadecyl-4'-hydroxy-stilbazolium iodide **15j**:



Reagents: 4-Hydroxy-benzaldehyde (0.06 mol, 26.7 g).

1-hexadecyl-4-methyl-pyridinium iodide (0.06 mol, 7.32 g),

piperidine (8 ml),

dry ethanol (100 ml).

Purification: Recrystallization from ethanol.

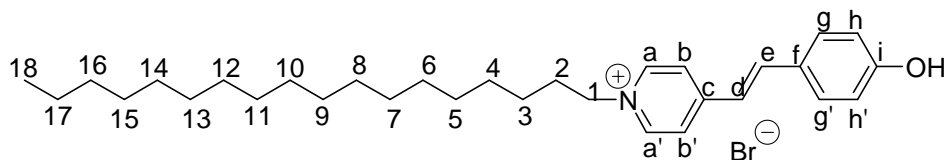
Yield: 50 % (0.03 mol), red powder

Analytical data: C₂₉H₄₄INO M_w = 549.57

¹H NMR (DMSO, J/Hz, 400 MHz) δ = 8.72 (d, ³J(H,H) = 6.84, 2 H, Ar-H^{a,a'}), 8.00 (d, ³J(H,H) = 6.84, 2 H, Ar-H^{b,b'}), 7.86 (d, ³J(H,H) = 15.97, 1 H, CH^e), 7.49 (d, ³J(H,H) = 8.71, 2 H, Ar-H^{g,g'}), 7.08 (d, ³J(H,H) = 16.18, 1 H, CH^d), 6.69 (d, ³J(H,H) = 8.71, 2 H, Ar-H^{h,h'}), 4.36 (t, ³J(H,H) = 7.26, 2 H, CH₂¹), 1.84-1.82 (m, 2 H, CH₂²), 1.21-1.02 (m, 26 H, CH₂³⁻¹⁵), 0.80 (t, ³J(H,H) = 6.8, 3 H, CH₃¹⁶). ¹³C NMR (DMSO, 50 MHz) δ = 164.84 (Cⁱ), 153.51 (C^c), 143.25 (C^{a,a'}), 142.18 (C^e), 130.70 (C^{g,g'}), 123.55 (C^f), 122.18 (C^{b,b'}), 117.10 (C^d), 116.97 (C^{h,h'}), 59.01 (C¹), 31.23, 30.40, 28.99, 28.83, 28.72, 28.64, 28.33, 25.36, 22.03, (C²⁻¹⁵), 13.88 (C¹⁶).

MS (EI, 70, eV) m/z : 93, 197, 225, 421 (M^+ -HI). EA: $C_{29}H_{44}INO$ (Calc.) C: 63.38 %, H: 8.07 %, N: 2.55 %, (Found) C: 67.01 %, H: 8.03 %, N: 2.45 %.

N-octadecyl-4'-hydroxy-stilbazolium bromide **15k**:



Reagents: 4-Hydroxy-benzaldehyde (0.94 mmol, 0.11 g),
1-octadecyl-4-methyl-pyridinium bromide (0.94 mmol, 0.4 g),
piperidine (0.12 ml),
dry ethanol (5 ml).

Purification: Recrystallization from ethanol.

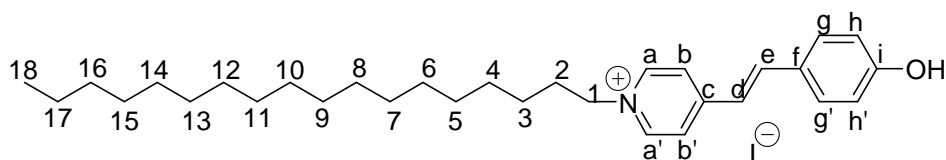
Yield: 60 % (0.56 mmol), red powder

Analytical data: $C_{31}H_{48}BrNO$ $M_w = 530.62$

1H NMR (DMSO, J /Hz, 400 MHz) $\delta = 8.77$ (d, $^3J(H,H) = 6.64$, 2 H, Ar- $H^{a,a'}$), 8.06 (d, $^3J(H,H) = 6.84$, 2 H, Ar- $H^{b,b'}$), 7.89 (d, $^3J(H,H) = 16.18$, 1 H, CH^c), 7.56 (d, $^3J(H,H) = 8.71$, 2 H, Ar- $H^{g,g'}$), 7.18 (d, $^3J(H,H) = 16.18$, 1 H, CH^d), 6.78 (d, $^3J(H,H) = 8.71$, 2 H, Ar- $H^{h,h'}$), 4.40 (t, $^3J(H,H) = 7.3$, 2 H, CH_2^1), 1.87 - 1.83 (m, 2 H, CH_2^2), 1.24 - 1.20 (m, 30 H, CH_2^{3-17}), 0.83 (t, $^3J(H,H) = 6.8$, 3 H, CH_3^{18}). ^{13}C NMR (DMSO, 100 MHz) $\delta = 160.52$ (C^i), 153.32 (C^c), 143.60 ($C^{a,a'}$), 141.36 (C^e), 130.21 ($C^{g,g'}$), 125.78 (C^f), 122.86 ($C^{b,b'}$), 119.12 (C^d), 116.08 ($C^{h,h'}$), 59.35 (C^1), 31.16 , 30.35 , 28.88 , 28.75 , 28.63 , 28.55 , 28.24 , 25.29 , 21.96 (C^{2-17}), 13.82 (C^{18}).

MS (EI, 70 eV) m/z : 197, 253, 449 (M-HBr). EA: $C_{31}H_{48}BrNO$ (Calc.) C: 70.17 %, H: 9.12 %, Br: 15.06 %, N: 2.64 %, (Found) C: 70.73 %, H: 9.45 %, Br: 12.22 %, N: 2.64 %.

N-octadecyl-4'-hydroxy-stilbazolium iodide **15l**:



Reagents: 4-Hydroxy-benzaldehyde (0.036 mol, 17.1 g),
1-octadecyl-4-methyl-pyridinium iodide (0.036 mol, 4.41 g),
piperidine (4.8 ml),

dry ethanol (60 ml).

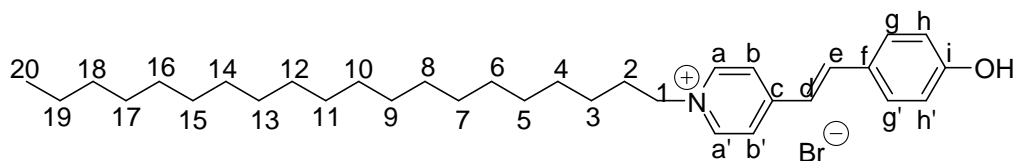
Purification: Recrystallization from ethanol

Yield: 47.2 % (0.017 mol), red powder

Analytical data: C₃₁H₄₈INO M_w = 577.62

¹H NMR (DMSO, *J*/Hz, 400 MHz) δ = 8.75 (d, ³*J*(H,H) = 6.84, 2 H, Ar-H^{a,a'}), 8.03 (d, ³*J*(H,H) = 6.84, 2 H, Ar-H^{b,b'}), 7.87 (d, ³*J*(H,H) = 15.97, 1 H, CH^e), 7.52 (d, ³*J*(H,H) = 8.71, 2 H, Ar-H^{g,g'}), 7.13 (d, ³*J*(H,H) = 15.97, 1 H, CH^d), 6.73 (d, ³*J*(H,H) = 8.51, 2 H, Ar-H^{h,h'}), 4.38 (t, ³*J*(H,H) = 7.26, 2 H, CH₂¹), 1.85-1.83 (m, 2 H, CH₂²), 1.23-1.18 (m, 30 H, CH₂³⁻¹⁷), 0.83 (t, ³*J*(H,H) = 6.7, 3 H, CH₃¹⁸). ¹³C NMR (DMSO, 50 MHz) δ = 161.66 (Cⁱ), 153.40 (C^c), 143.61 (C^{a,a'}), 141.61 (C^e), 130.37 (C^{g,g'}), 125.28 (C^f), 122.74 (C^{b,b'}), 118.63 (C^d), 116.38 (C^{h,h'}), 59.27 (C¹), 31.24, 30.41, 28.98, 28.83, 28.72, 28.64, 28.32, 25.36, 22.04 (C²⁻¹⁷), 13.89 (C¹⁸). MS (EI, 70 eV) *m/z*: 197, 253, 449 (M-HI). EA: C₃₁H₄₈INO (Calc.) C: 64.46 %, H: 8.38 %, N: 2.42 %, (Found) C: 67.30 %, H: 9.18 %, N: 2.23 %.

N-eicosyl-4'-hydroxy-stilbazolium bromide **15m**:



Reagents: 4-Hydroxy-benzaldehyde (2.20 mmol, 0.26 g),
1-eicosyl-4-methyl-pyridinium bromide (2.20 mmol, 1 g),
piperidine (0.29 ml),
dry ethanol (4 ml).

Purification: Recrystallization from ethanol

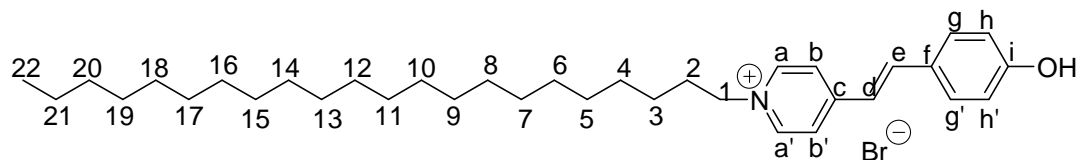
Yield: 66 % (1.46 mmol), red powder

Analytical data: C₃₃H₅₂BrNO M_w = 558.68

¹H NMR (CDCl₃, *J*/Hz, 400 MHz) δ = 8.51 (d, ³*J*(H,H) = 6.22, 2 H, Ar-H^{a,a'}), 7.68 (d, ³*J*(H,H) = 6.02, 2 H, Ar-H^{b,b'}), 7.36 (d, ³*J*(H,H) = 15.77, 1 H, CH^e), 7.25 (d, ³*J*(H,H) = 8.47, 2 H, Ar-H^{g,g'}), 6.76 (d, ³*J*(H,H) = 7.88, 2 H, Ar-H^{h,h'}), 6.65 (d, ³*J*(H,H) = 15.77, 1 H, CH^d), 4.43 (bs, CH₂¹), 1.84 (bs, 2 H, CH₂²), 1.22-1.16 (m, 34 H, CH₂³⁻¹⁹), 0.83 (t, ³*J*(H,H) = 6.8, 3 H, CH₃²⁰). ¹³C NMR (CDCl₃, 100 MHz) δ = 162.65 (Cⁱ), 153.78 (C^c), 142.74 (C^{a,a'}), 142.24 (C^e), 130.78 (C^{g,g'}), 125.07 (C^f), 123.17 (C^{b,b'}), 117.98 (C^d), 117.14 (C^{h,h'}), 60.66 (C¹), 31.96, 31.44, 29.80, 29.78, 29.77, 29.71, 29.66, 29.53, 29.40, 29.18, 26.31, 25.86, 24.84, 22.73 (C²⁻¹⁹), 14.16 (C²⁰).

MS (EI, 70 eV) m/z : 197, 281, 477 (M-HBr). EA: C₃₃H₅₂BrNO (Calc.) C: 70.95 %, H: 9.38 %, Br: 14.30 %, N: 2.51 %, (Found) C: 72.55 %, H: 9.72 %, Br: 11.31 %, N: 2.54 %.

N-docosyl-4'-hydroxy-stilbazolium bromide **15n**:



Reagents: 4-Hydroxy-benzaldehyde (2.07 mmol, 0.25 g),
1-docosyl-4-methyl-pyridinium bromide (2.07 mmol, 1 g),
piperidine (0.28 ml),
dry ethanol (3.5 ml).

Purification: Recrystallization from ethanol.

Yield: 83.1 % (1.72 mmol), red powder

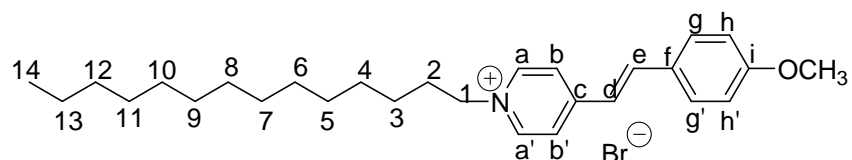
Analytical data: C₃₅H₅₆BrNO M_w = 586.73

¹H NMR (DMSO, J /Hz, 400 MHz) δ = 8.81 (d, ³ J (H,H) = 6.84, 2 H, Ar-H^{a,a'}), 8.10 (d, ³ J (H,H) = 6.64, 2 H, Ar-H^{b,b'}), 7.89 (d, ³ J (H,H) = 15.97, 1 H, CH^e), 7.57 (d, ³ J (H,H) = 8.71, 2 H, Ar-H^{g,g'}), 7.23 (d, ³ J (H,H) = 16.39, 1 H, CH^d), 6.83 (d, ³ J (H,H) = 8.51, 2 H, Ar-H^{h,h'}), 4.41 (t, ³ J (H,H) = 7.4, 2 H, CH₂¹), 1.84 (m, 2 H, CH₂²), 1.23-1.18 (m, 38 H, CH₂³⁻²¹), 0.81 (t, ³ J (H,H) = 6.6, 3 H, CH₃²²). ¹³C NMR (DMSO, 100 MHz) δ = 162.13 (Cⁱ), 152.61 (C^e), 141.48 (C^{a,a'}), 141.16 (C^e), 129.69 (C^{g,g'}), 123.55 (C^f), 121.93 (C^{b,b'}), 116.51 (C^d), 116.11 (C^{h,h'}), 59.38 (C¹), 30.77, 30.22, 28.37, 28.20, 28.00, 25.13, 21.53 (C²⁻²¹), 12.94 (C²²).

MS (EI, 70 eV) m/z : 197, 309, 505 (M-HBr). EA: C₃₅H₅₆BrNO (Calc.) C: 71.65 %, H: 9.62 %, Br: 13.62 %, N: 2.39 %, (Found) C: 73.11 %, H: 10.00 %, Br: 10.90 %, N: 2.35 %.

4.3.3. *N*-alkyl-4'-methoxy-stilbazolium salts **16a – f**

N-tetradecyl-4'-methoxy-stilbazolium bromide **16a**:



Reagents: 4-Methoxy-benzaldehyde (5.4 mmol, 0.73 g),
1-tetradecyl-4-methyl-pyridinium bromide (5.4 mmol, 2 g),
piperidine (0.72 ml),

dry ethanol (9 ml).

Purification: Recrystallization from ethanol.

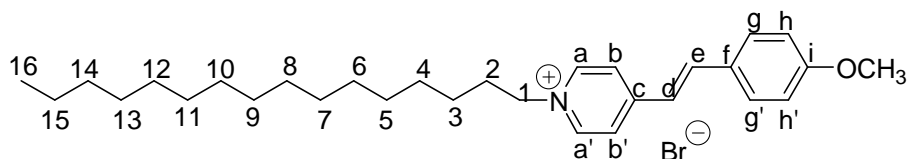
Yield: 47.4 % (2.56 mmol), red powder

Analytical data: C₂₈H₄₂BrNO M_w = 488.54

¹H NMR (DMSO, *J*/Hz, 400 MHz) δ = 8.90 (d, ³*J*(H,H) = 6.84, 2 H, Ar-**H**^{a,a'}), 8.16 (d, ³*J*(H,H) = 6.84, 2 H, Ar-**H**^{b,b'}), 7.98 (d, ³*J*(H,H) = 16.18, 1 H, **CH**^e), 7.68 (d, ³*J*(H,H) = 8.71, 2 H, Ar-**H**^{g,g'}), 7.35 (d, ³*J*(H,H) = 16.18, 1 H, **CH**^d), 7.01 (d, ³*J*(H,H) = 8.71, 2 H, Ar-**H**^{h,h'}), 4.45 (t, ³*J*(H,H) = 7.3, 2 H, **CH**₂¹), 3.79 (s, 3 H, **OCH**₃), 1.87-1.83 (m, 2 H, **CH**₂²), 1.23-1.18 (m, 22 H, **CH**₂³⁻¹³), 0.80 (t, ³*J*(H,H) = 6.8, 3 H, **CH**₃¹⁴). ¹³C NMR (DMSO, 100 MHz) δ = 161.66 (**C**ⁱ), 153.72 (**C**^c), 144.45 (**C**^{a,a'}), 141.32 (**C**^e), 130.46 (**C**^{g,g'}), 128.30 (**C**^f), 123.81 (**C**^{b,b'}), 121.19 (**C**^d), 115.14 (**C**^{h,h'}), 60.09 (**C**¹), 56.03 (**OCH**₃), 31.89, 31.11, 29.66, 29.64, 29.61, 29.59, 29.50, 29.38, 29.30, 28.98, 28.99, 26.03, 22.69 (**C**²⁻¹³), 14.56 (**C**¹⁴).

EA: C₂₈H₄₂BrNO (Calc.) C: 68.84 %, H: 8.67 %, Br: 16.36 %, N: 2.87 %, (Found) C: 68.51 %, H: 8.85 %, Br: 16.30 %, N: 3.15 %.

N-hexadecyl-4'-methoxy-stilbazolium bromide **16b**:



Reagents: 4-Methoxy-benzaldehyde (2.51 mmol, 0.34 g),
1-hexadecyl-4-methyl-pyridinium bromide (2.51 mmol, 1 g),
piperidine (0.33 ml),
dry ethanol (3 ml).

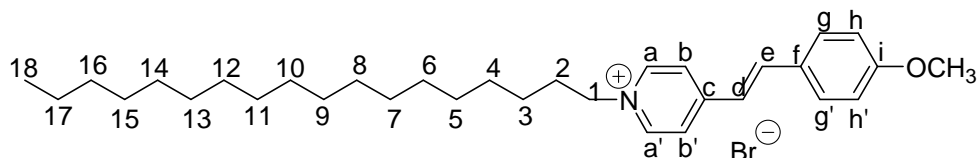
Yield: 46.2 % (1.16 mmol), red powder

Analytical data: C₃₀H₄₆BrNO M_w = 516.60

¹H NMR (DMSO, *J*/Hz, 400 MHz) δ = 8.91 (d, ³*J*(H,H) = 6.84, 2 H, Ar-**H**^{a,a'}), 8.17 (d, ³*J*(H,H) = 6.84, 2 H, Ar-**H**^{b,b'}), 7.99 (d, ³*J*(H,H) = 16.18, 1 H, **CH**^e), 7.71 (d, ³*J*(H,H) = 8.92, 2 H, Ar-**H**^{g,g'}), 7.36 (d, ³*J*(H,H) = 16.39, 1 H, **CH**^d), 7.05 (d, ³*J*(H,H) = 8.71, 2 H, Ar-**H**^{h,h'}), 4.46 (t, ³*J*(H,H) = 7.26, 2 H, **CH**₂¹), 3.82 (s, 3 H, **OCH**₃), 1.90-1.86 (m, 2 H, **CH**₂²), 1.26-1.21 (m, 26 H, **CH**₂³⁻¹⁵), 0.83 (t, ³*J*(H,H) = 6.8, 3 H, **CH**₃¹⁶). ¹³C NMR (DMSO, 100 MHz) δ = 161.09 (**C**ⁱ), 153.15 (**C**^c), 143.87 (**C**^{a,a'}), 140.74 (**C**^e), 129.87 (**C**^{g,g'}), 127.71 (**C**^f), 123.21 (**C**^{b,b'}), 120.58 (**C**^d), 114.51 (**C**^{h,h'}), 59.39 (**C**¹), 55.35 (**OCH**₃), 31.18, 30.42, 28.94, 28.90, 28.80, 28.68, 28.59, 28.29, 25.32, 21.98 (**C**²⁻¹⁵), 13.83 (**C**¹⁶).

EA: C₃₀H₄₆BrNO·0.5H₂O (Calc.) C: 68.49 %, H: 8.94 %, Br: 15.22 %, N: 2.66 %, (Found) C: 68.47 %, H: 9.14 %, Br: 15.92 %, N: 2.53 %.

N-octadecyl-4'-methoxy-stilbazolium bromide **16c**:



Reagents: 4-Methoxy-benzaldehyde (1.17 mmol, 0.15 g),
1-octadecyl-4-methyl-pyridinium bromide (1.17 mmol, 0.5 g),
piperidine (0.16 ml),
dry ethanol (4 ml).

Purification: Recrystallization from ethanol.

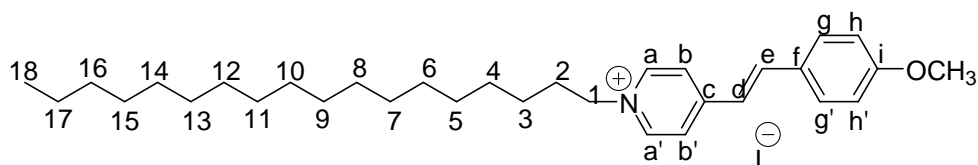
Yield: 45.55 % (0.53 mmol), red powder

Analytical data: C₃₂H₅₀BrNO M_w = 544.65

¹H NMR (CDCl₃, *J*/Hz, 400 MHz) δ = 9.05 (d, ³*J*(H,H) = 6.84, 2 H, Ar-H^{a,a'}), 8.01 (d, ³*J*(H,H) = 6.84, 2 H, Ar-H^{b,b'}), 7.67 (d, ³*J*(H,H) = 16.18, 1 H, CH^e), 7.56 (d, ³*J*(H,H) = 8.71, 2 H, Ar-H^{g,g'}), 6.99 (d, ³*J*(H,H) = 16.18, 1 H, CH^d), 6.87 (d, ³*J*(H,H) = 8.71, 2 H, Ar-H^{h,h'}), 4.68 (t, ³*J*(H,H) = 7.3, 2 H, CH₂¹), 3.79 (s, 3 H, OCH₃), 1.95-1.88 (m, 2 H, CH₂²), 1.26-1.16 (m, 30 H, CH₂³⁻¹⁷), 0.82 (t, ³*J*(H,H) = 6.8, 3 H, CH₃¹⁸). ¹³C NMR (CDCl₃, 100 MHz) δ = 161.97 (Cⁱ), 153.70 (C^c), 143.93 (C^{a,a'}), 141.87 (C^e), 130.27 (C^{g,g'}), 127.30 (C^f), 123.68 (C^{b,b'}), 119.70 (C^d), 114.61 (C^{h,h'}), 60.68 (C¹), 55.43 (OCH₃), 31.87, 31.65, 29.56, 29.48, 29.34, 29.30, 29.06, 26.09, 22.63 (C²⁻¹⁷), 14.05 (C¹⁸).

EA: C₃₂H₅₀BrNO·H₂O (Calc.) C: 69.44 %, H: 9.22 %, Br: 14.46 %, N: 2.53 %, (Found) C: 69.38 %, H: 9.63 %, Br: 14.98 %, N: 2.32 %.

N-octadecyl-4'-methoxy-stilbazolium iodide **16d**:



Reagents: 4-Methoxy-benzaldehyde (2.11 mmol, 0.29 g),
1-octadecyl-4-methyl-pyridinium iodide (2.11 mmol, 1 g),
piperidine (0.28 ml),

dry ethanol (4 ml).

Purification: Recrystallization from ethanol.

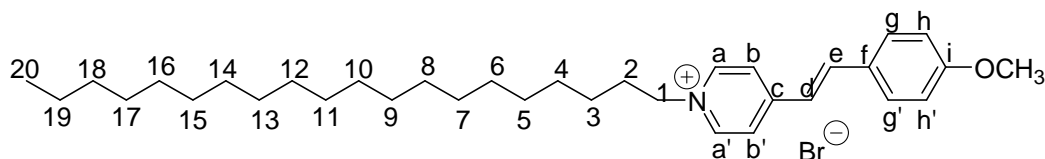
Yield: 40.1 % (0.84 mmol), red powder

Analytical data: C₃₂H₅₀INO M_w = 591.65

¹H NMR (CDCl₃, J/Hz, 400 MHz) δ = 8.92 (d, ³J(H,H) = 6.84, 2 H, Ar-H^{a,a'}), 8.01 (d, ³J(H,H) = 6.64, 2 H, Ar-H^{b,b'}), 7.68 (d, ³J(H,H) = 16.18, 1 H, CH^e), 7.59 (d, ³J(H,H) = 8.92, 2 H, Ar-H^{g,g'}), 7.01 (d, ³J(H,H) = 16.18, 1 H, CH^d), 6.90 (d, ³J(H,H) = 8.92, 2 H, Ar-H^{h,h'}), 4.64 (t, ³J(H,H) = 7.3, 2 H, CH₂¹), 3.81 (s, 3 H, OCH₃), 1.97-1.89 (m, 2 H, CH₂²), 1.35-1.19 (m, 30 H, CH₂³⁻¹⁷), 0.84 (t, ³J(H,H) = 6.7, 3 H, CH₃¹⁸). ¹³C NMR (CDCl₃, 100 MHz) δ = 161.96 (Cⁱ), 153.77 (C^c), 143.62 (C^{a,a'}), 141.96 (C^e), 130.38 (C^{g,g'}), 127.27 (C^f), 123.77 (C^{b,b'}), 119.61 (C^d), 114.59 (C^{h,h'}), 60.74 (C¹), 55.44 (OCH₃), 31.83, 31.49, 29.62, 29.57, 29.54, 29.45, 29.31, 29.26, 29.01, 26.02, 22.59 (C²⁻¹⁷), 14.02 (C¹⁸).

EA: C₃₂H₅₀INO·0.2H₂O (Calc.) C: 64.51 %, H: 8.47 %, N: 2.35 %, (Found) C: 64.56 %, H: 8.93 %, N: 2.09 %.

N-eicosyl-4'-methoxy-stilbazolium bromide **16e**:



Reagents: 4-Methoxy-benzaldehyde (2.20 mmol, 0.3 g),
1-eicosyl-4-methyl-pyridinium bromide (2.20 mmol, 1 g),
piperidine (0.29 ml),
dry ethanol (4 ml).

Purification: Recrystallization from ethanol.

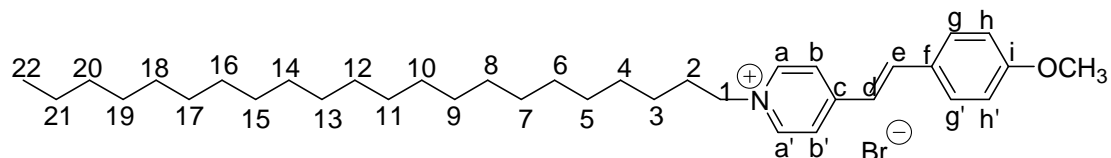
Yield: 59.5 % (1.31 mmol), red powder

Analytical data: C₃₄H₅₄BrNO M_w = 572.70

¹H NMR (CDCl₃, J/Hz, 400 MHz) δ = 9.04 (d, ³J(H,H) = 6.02, 2 H, Ar-H^{a,a'}), 8.00 (d, ³J(H,H) = 6.02, 2 H, Ar-H^{b,b'}), 7.67 (d, ³J(H,H) = 15.97, 1 H, CH^e), 7.57 (d, ³J(H,H) = 8.71, 2 H, Ar-H^{g,g'}), 7.00 (d, ³J(H,H) = 15.82, 1 H, CH^d), 6.90 (d, ³J(H,H) = 8.71, 2 H, Ar-H^{h,h'}), 4.71 (t, ³J(H,H) = 7.01, 2 H, CH₂¹), 3.82 (s, 3 H, OCH₃), 1.95-1.91 (m, 2 H, CH₂²), 1.28-1.18 (m, 34 H, CH₂³⁻¹⁹), 0.84 (t, ³J(H,H) = 6.8, 3 H, CH₃²⁰). ¹³C NMR (CDCl₃, 125 MHz) δ = 162.07 (Cⁱ), 153.77 (C^c), 144.07 (C^{a,a'}), 141.99 (C^e), 130.44 (C^{g,g'}), 127.28 (C^f), 123.69 (C^{b,b'}), 119.69 (C^d), 114.66 (C^{h,h'}), 60.77 (C¹), 55.45 (OCH₃), 31.86, 31.79, 31.67, 29.65, 29.60, 29.56, 29.47, 29.33, 29.30, 29.05, 26.08, 22.63 (C²⁻¹⁹), 14.06 (C²⁰).

EA: C₃₄H₅₄BrNO·0.2H₂O (Calc.) C: 70.79 %, H: 9.44 %, Br: 13.88 %, N: 2.43 %, (Found) C: 70.51 %, H: 9.63 %, Br: 13.95 %, N: 2.39 %.

N-docosyl-4'-methoxy-stilbazolium bromide **16f**:



Reagents: 4-Methoxy-benzaldehyde (2.07 mmol, 0.282 g),
1-docosyl-4-methyl-pyridinium bromide (2.07 mmol, 1 g),
piperidine (0.28 ml),
dry ethanol (4 ml).

Purification: Recrystallization from ethanol.

Yield: 68.1 % (1.41 mmol), red powder

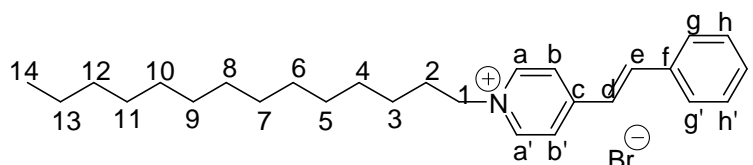
Analytical data: C₃₆H₅₈BrNO M_w = 600.76

¹H NMR (CDCl₃, J/Hz, 400 MHz) δ = 9.06 (d, ³J(H,H) = 6.64, 2 H, Ar-H^{a,a'}), 8.01 (d, ³J(H,H) = 6.64, 2 H, Ar-H^{b,b'}), 7.67 (d, ³J(H,H) = 16.18, 1 H, CH^c), 7.57 (d, ³J(H,H) = 8.71, 2 H, Ar-H^{g,g'}), 6.99 (d, ³J(H,H) = 16.18, 1 H, CH^d), 6.88 (d, ³J(H,H) = 8.92, 2 H, Ar-H^{h,h'}), 4.70 (t, ³J(H,H) = 7.26, 2 H, CH₂¹), 3.80 (s, 3 H, OCH₃), 1.92 (m, 2 H, CH₂²), 1.27-1.17 (m, 38 H, CH₂³⁻²¹), 0.83 (t, ³J(H,H) = 6.8, 3 H, CH₃²²). ¹³C NMR (CDCl₃, 125 MHz) δ = 161.94 (Cⁱ), 153.69 (C^c), 143.93 (C^{a,a'}), 141.85 (C^e), 130.28 (C^{g,g'}), 127.29 (C^f), 123.69 (C^{b,b'}), 119.70 (C^d), 114.62 (C^{h,h'}), 60.61 (C¹), 55.38 (OCH₃), 31.80, 31.60, 29.58, 29.56, 29.54, 29.52, 29.29, 29.24, 29.01, 26.02, 22.57 (C²⁻²¹), 13.99 (C²²).

EA: C₃₆H₅₈BrNO·0.2H₂O (Calc.) C: 71.48 %, H: 9.66 %, Br: 13.23 %, N: 2.31 %, (Found) C: 71.44 %, H: 9.75 %, Br: 12.82 %, N: 2.24 %.

4.3.4. *N*-alkyl-stilbazolium salts **17a - f**

N-tetradecyl-stilbazolium bromide **17a**:



Reagents: Benzaldehyde (1.08 mmol, 0.11 g),

1-tetradecyl-4-methyl-pyridinium bromide (1.08 mmol, 0.4 g),
 piperidine (0.15 ml),
 dry ethanol (2 ml).

Purification: Recrystallization from ethanol.

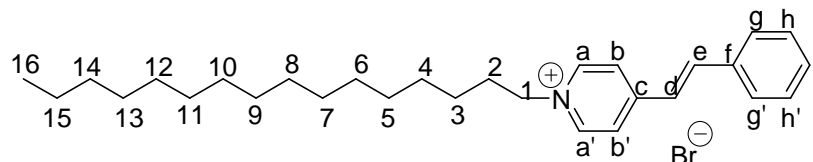
Yield: 46.3 % (0.5 mmol), yellowish powder

Analytical data: C₂₇H₄₀BrN M_w = 458.52

¹H NMR (DMSO, *J*/Hz, 400 MHz) δ = 8.68 (d, ³*J*(H,H) = 6.64, 2 H, Ar-**H**^{a,a'}), 8.27 (d, ³*J*(H,H) = 6.64, 2 H, Ar-**H**^{b,b'}), 8.04 (d, ³*J*(H,H) = 16.93, 1 H, **CH**^e), 7.75 (d, ³*J*(H,H) = 6.84, 2 H, Ar-**H**^{g,g'}), 7.54 (d, ³*J*(H,H) = 16.39, 1 H, **CH**^d), 7.50-7.44 (m, 3 H, Ar-**H**^{h,h',i}), 4.50 (t, ³*J*(H,H) = 7.26, 2 H, **CH**₂¹), 1.91-1.89 (m, 2 H, **CH**₂²), 1.26-1.21 (m, 22 H, **CH**₂³⁻¹³), 0.83 (t, ³*J*(H,H) = 6.6, 3 H, **CH**₃¹⁴). ¹³C NMR (DMSO, 100 MHz) δ = 152.70 (C^c), 144.13 (C^{a,a'}), 140.70 (C^e), 135.02 (C^f), 130.24 (Cⁱ), 128.95 (C^{h,h'}), 127.96 (C^{g,g'}), 123.78 (C^{b,b'}), 123.17 (C^d), 59.63 (C¹), 31.18, 30.42, 28.93, 28.89, 28.79, 28.66, 28.58, 28.28, 25.31, 21.98 (C²⁻¹³), 13.84 (C¹⁴).

EA: C₂₇H₄₀BrN (Calc.) C: 70.73 %, H: 8.59 %, Br: 17.43 %, N: 3.05 %, (Found) C: 71.36 %, H: 9.58 %, Br: 16.55 %, N: 3.04 %.

N-hexadecyl-stilbazolium bromide **17b**:



Reagents: Benzaldehyde (2.51 mmol, 0.27 g),
 1-hexadecyl-4-methyl-pyridinium bromide (2.51 mmol, 1 g),
 piperidine (0.33 ml),
 dry ethanol (5 ml).

Purification: Recrystallization from ethanol.

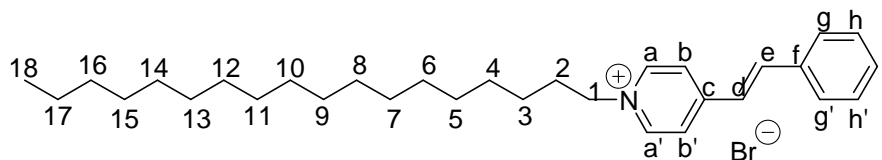
Yield: 46 % (1.15 mmol), yellowish powder

Analytical data: C₂₉H₄₄BrN M_w = 486.57

¹H NMR (CDCl₃, *J*/Hz, 400 MHz) δ = 9.11 (d, ³*J*(H,H) = 6.43, 2 H, Ar-**H**^{a,a'}), 8.09 (d, ³*J*(H,H) = 6.43, 2 H, Ar-**H**^{b,b'}), 7.73 (d, ³*J*(H,H) = 16.18, 1 H, **CH**^e), 7.63-7.61 (m, 2 H, Ar-**H**^{g,g'}), 7.39-7.37 (m, 3 H, Ar-**H**^{h,h',i}), 7.17 (d, ³*J*(H,H) = 16.18, 1 H, **CH**^d), 4.75 (t, ³*J*(H,H) = 7.26, 2 H, **CH**₂¹), 1.96-1.93 (m, 2 H, **CH**₂²), 1.28-1.18 (m, 26 H, **CH**₂³⁻¹⁵), 0.84 (t, ³*J*(H,H) = 6.84, 3 H, **CH**₃¹⁶). ¹³C NMR (CDCl₃, 100 MHz) δ = 153.37 (C^c), 144.29 (C^{a,a'}), 142.07 (C^e), 134.55 (C^f), 130.86 (Cⁱ), 129.12 (C^{h,h'}), 128.43 (C^{g,g'}), 124.34 (C^{b,b'}), 122.28 (C^d), 61.01 (C¹), 32.02, 31.92, 31.84, 29.80, 29.76, 29.72, 29.64, 29.50, 29.46, 29.22, 26.26, 22.80 (C²⁻¹⁵), 14.23 (C¹⁶).

EA: C₂₉H₄₄BrN·H₂O (Calc.) C: 69.03 %, H: 9.19 %, Br: 15.84 %, N: 2.78 %, (Found) C: 69.07 %, H: 9.20 %, Br: 16.71 %, N: 2.74 %.

N-octadecyl-stilbazolium bromide **17c**:



Reagents: Benzaldehyde (2.34 mmol, 0.25 g),
1-octadecyl-4-methyl-pyridinium bromide (2.34 mmol, 1 g),
piperidine (0.32 ml),
dry ethanol (5 ml).

Purification: Recrystallization two times from ethanol.

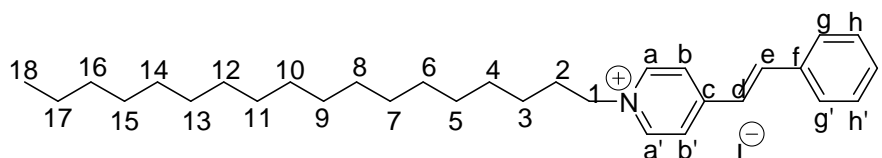
Yield: 33.2 % (0.78 mmol), yellowish powder

Analytical data: C₃₁H₄₈BrN M_w = 514.62

¹H NMR (CDCl₃, J/Hz, 400 MHz) δ = 9.15 (d, ³J(H,H) = 6.64, 2 H, Ar-H^{a,a'}), 8.07 (d, ³J(H,H) = 6.84, 2 H, Ar-H^{b,b'}), 7.71 (d, ³J(H,H) = 16.39, 1 H, CH^c), 7.68-7.60 (m, 2 H, Ar-H^{g,g'}), 7.42-7.38 (m, 3 H, Ar-H^{h,h',i}), 7.16 (d, ³J(H,H) = 16.86, 1 H, CH^d), 4.77 (t, ³J(H,H) = 7.3, 2 H, CH₂¹), 1.98-1.88 (m, 2 H, CH₂²), 1.28-1.19 (m, 30 H, CH₂³⁻¹⁷), 0.84 (t, ³J(H,H) = 6.8, 3 H, CH₃¹⁸). ¹³C NMR (CDCl₃, 100 MHz) δ = 153.41 (C^c), 144.35 (C^{a,a'}), 142.16 (C^e), 134.48 (C^f), 130.98 (Cⁱ), 129.18 (C^{h,h'}), 128.43 (C^{g,g'}), 124.25 (C^{b,b'}), 122.21 (C^d), 61.08 (C¹), 31.96, 31.78, 29.74, 29.70, 29.64, 29.55, 29.41, 29.39, 29.13, 26.18, 22.72 (C²⁻¹⁷), 14.14 (C¹⁸).

EA: C₃₁H₄₈BrN·0.5H₂O (Calc.) C: 71.12 %, H: 9.36 %, N: 2.67 %, (Found) C: 71.02 %, H: 9.62 %, N: 2.52 %.

N-octadecyl-stilbazolium iodide **17d**:



Reagents: Benzaldehyde (2.11 mmol, 0.22 g),
1-octadecyl-4-methyl-pyridinium iodide (2.11 mmol, 1 g),
piperidine (0.28 ml),
dry ethanol (4 ml).

Purification: Recrystallization two times from ethanol.

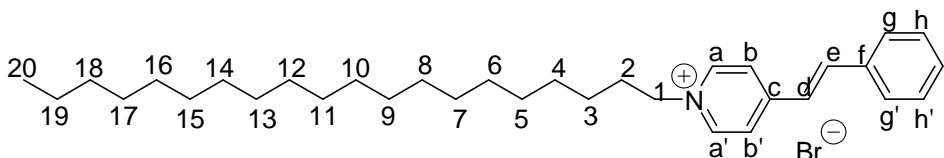
Yield: 42.18 % (0.89 mmol), orange powder

Analytical data: C₃₁H₄₈IN M_w = 561.62

¹H NMR (CDCl₃, J/Hz, 400 MHz) δ = 9.02 (d, ³J(H,H) = 6.84, 2 H, Ar-H^{a,a'}), 8.10 (d, ³J(H,H) = 6.84, 2 H, Ar-H^{b,b'}), 7.73 (d, ³J(H,H) = 16.39, 1 H, CH^c), 7.64-7.62 (m, 2 H, Ar-H^{g,g'}), 7.40-7.36 (m, 3 H, Ar-H^{h,h',i}), 7.18 (d, ³J(H,H) = 16.18, 1 H, CH^d), 4.68 (t, ³J(H,H) = 7.47, 2 H, CH₂¹), 1.98-1.91 (m, 2 H, CH₂²), 1.28-1.18 (m, 30 H, CH₂³⁻¹⁷), 0.84 (t, ³J(H,H) = 6.8, 3 H, CH₃¹⁸). ¹³C NMR (CDCl₃, 100 MHz) δ = 153.52 (C^c), 144.10 (C^{a,a'}), 142.26 (C^e), 134.49 (C^f), 130.99 (Cⁱ), 129.18 (C^{h,h'}), 128.54 (C^{g,g'}), 124.43 (C^{b,b'}), 122.17 (C^d), 61.19 (C¹), 31.95, 31.66, 29.74, 29.69, 29.65, 29.56, 29.41, 29.38, 29.11, 26.15, 22.72 (C²⁻¹⁷), 14.14 (C¹⁸).

EA: C₃₁H₄₈IN·0.2H₂O (Calc.) C: 65.81 %, H: 8.56 %, N: 2.47 %, (Found) C: 65.86 %, H: 8.99 %, N: 2.28 %.

N-eicosyl-stilbazolium bromide **17e**:



Reagents: Benzaldehyde (2.20 mmol, 0.23 g),
1-eicosyl-4-methyl-pyridinium bromide (2.20 mmol, 1 g),
piperidine (0.29 ml),
dry ethanol (4 ml).

Purification: Recrystallization from ethanol.

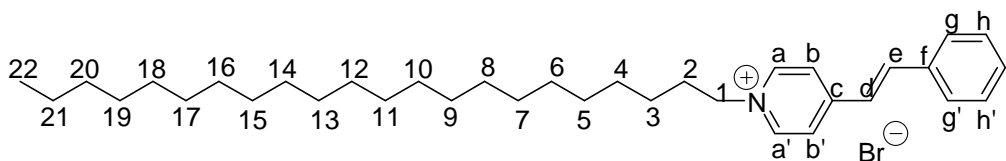
Yield: 69.5 % (1.53 mmol), reddish powder

Analytical data: C₃₃H₅₂BrN M_w = 542.68

¹H NMR (CDCl₃, J/Hz, 400 MHz) δ = 9.18 (d, ³J(H,H) = 6.64, 2 H, Ar-H^{a,a'}), 8.10 (d, ³J(H,H) = 6.64, 2 H, Ar-H^{b,b'}), 7.73 (d, ³J(H,H) = 16.18, 1 H, CH^c), 7.62-7.60 (m, 2 H, Ar-H^{g,g'}), 7.37-7.34 (m, 3 H, Ar-H^{h,h',i}), 7.17 (d, ³J(H,H) = 16.18, 1 H, CH^d), 4.76 (t, ³J(H,H) = 7.3, 2 H, CH₂¹), 1.97-1.92 (m, 2 H, CH₂²), 1.30-1.17 (m, 34 H, CH₂³⁻¹⁹), 0.83 (t, ³J(H,H) = 6.8, 3 H, CH₃²⁰). ¹³C NMR (CDCl₃, 100 MHz) δ = 153.28 (C^c), 144.24 (C^{a,a'}), 142.00 (C^e), 134.43 (C^f), 130.78 (Cⁱ), 129.02 (C^{h,h'}), 128.31 (C^{g,g'}), 124.18 (C^{b,b'}), 122.16 (C^d), 60.97 (C¹), 31.93, 31.76, 29.72, 29.66, 29.63, 29.54, 29.40, 29.36, 29.13, 26.16, 22.70 (C²⁻¹⁹), 14.12 (C²⁰).

EA: C₃₃H₅₂BrN·H₂O (Calc.) C: 72.49 %, H: 9.59 %, Br: 14.64 %, N: 2.56 %, (Found) C: 72.50 %, H: 10.06 %, Br: 14.16 %, N: 2.54 %.

N-docosyl-stilbazolium bromide **17f**:



Reagents: Benzaldehyde (8.29 mmol, 0.88 g),
1-docosyl-4-methyl-pyridinium bromide (8.29 mmol, 4 g),
piperidine (1.1 ml),
dry ethanol (14 ml).

Purification: Recrystallization from ethanol.

Yield: 76.9 % (6.39 mmol), reddish powder

Analytical data: C₃₅H₅₆BrN M_w = 570.73

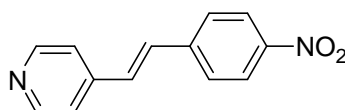
¹H NMR (CDCl₃, J/Hz, 400 MHz) δ = 9.17 (d, ³J(H,H) = 6.22, 2 H, Ar-H^{a,a'}), 8.10 (d, ³J(H,H) = 6.22, 2 H, Ar-H^{b,b'}), 7.72 (d, ³J(H,H) = 16.18, 1 H, CH^c), 7.61-7.59 (m, 2 H, Ar-H^{g,g'}), 7.39-7.35 (m, 3 H, Ar-H^{h,h',i}), 7.16 (d, ³J(H,H) = 16.18, 1 H, CH^d), 4.74 (t, ³J(H,H) = 7.26, 2 H, CH₂¹), 1.95-1.90 (m, 2 H, CH₂²), 1.26-1.16 (m, 38 H, CH₂³⁻²¹), 0.82 (t, ³J(H,H) = 6.7, 3 H, CH₃²²). ¹³C NMR (CDCl₃, 100 MHz) δ = 153.22 (C^c), 144.26 (C^{a,a'}), 141.94 (C^e), 134.41 (C^f), 130.74 (Cⁱ), 128.99 (C^{h,h'}), 128.29 (C^{g,g'}), 124.21 (C^{b,b'}), 122.16 (C^d), 60.92 (C¹), 31.89, 31.76, 29.69, 29.65, 29.63, 29.61, 29.52, 29.38, 29.33, 29.11, 26.15, 22.67 (C²⁻²¹), 14.01 (C²²).

EA: C₃₅H₅₆BrN·0.2H₂O (Calc.) C: 73.13 %, H: 9.82 %, Br: 13.92 %, N: 2.44 %, (Found) C: 72.91 %, H: 10.04 %, Br: 14.33 %, N: 2.30 %.

4.3.5. *N*-docosyl-4'-nitro-stilbazolium bromide **19**

Synthesis of 4-(4-nitro-styryl)-pyridine:

In a three-necked flask equipped with a reflux condenser, thermometer and a magnetic stirring bar were mixed 4-nitrobenzaldehyde (0.033 mol, 4.98 g), 4-picoline (0.039 mol, 3.68 g) and acetic anhydride (6.6 ml). The solution was heated under argon atmosphere for 48 h at 70 °C. After cooling to room temperature, the reaction mixture was poured into cooled water and the resulting precipitate was collected by filtration. The crude product was purified by column chromatography with silica gel and CHCl₃/CH₃OH = 20/1 as eluent, followed by recrystallization from methanol to give a reddish powder, 0.018 mol, yield 54.4 %.



18

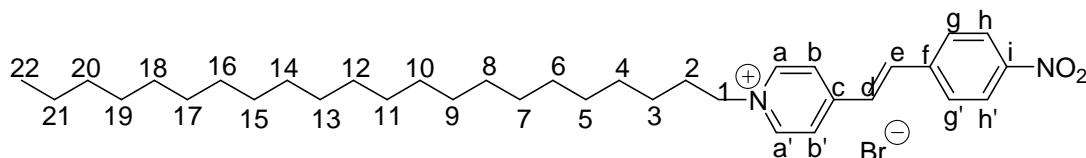
Analytical data: C₁₃H₁₀N₂O₂ M_w = 226.23

¹H NMR (CDCl₃, *J*/Hz, 400 MHz) δ = 8.62 (d, ³*J*(H,H) = 5.60, 2 H, Ar-**H**), 8.23 (m, 2 H, Ar-**H**), 7.67 (m, 2 H, Ar-**H**), 7.43 (d, ³*J*(H,H) = 6.22, 2 H, Ar-**H**), 7.34 (d, ³*J*(H,H) = 16.39, 1 H, **CH**), 7.16 (d, ³*J*(H,H) = 16.39, 1 H, **CH**).

Synthesis of *N*-docosyl-4'-nitro-stilbazolium bromide **19**:

In a two-necked flask equipped with thermometer, reflux condenser and magnetic stirring was added 2.21 mmol (0.5 g) 4-(4-nitro-styryl)-pyridine and 11 mmol 1-bromodocosane (4.3 g) in 6 ml dimethylformamide. After heating for 72 h at 70 °C the reaction mixture was cooled to room temperature and poured into ethyl acetate. The precipitate was collected by filtration and washed with ethyl acetate (50 ml). The product was purified by precipitation from chloroform using ethyl acetate to give a yellow powder, 1.7 mmol, yield: 76.9 %.

N-docosyl-4'-nitro-stilbazolium bromide **19**:



Analytical data: C₃₅H₅₅BrN₂O₂ M_w = 615.73

¹H NMR (CDCl₃, *J*/Hz, 500 MHz, 50°C) δ = 9.16 (d, ³*J*(H,H) = 3.81, 2 H, Ar-**H**^{a,a'}), 8.33 (d, ³*J*(H,H) = 3.81, 2 H, Ar-**H**^{b,b'}), 8.16 (d, ³*J*(H,H) = 8.39, 2 H, Ar-**H**^{h,h'}), 7.98 (d, ³*J*(H,H) = 16.17, 1 H, **CH**^e), 7.88 (d, ³*J*(H,H) = 8.39, 2 H, Ar-**H**^{g,g'}), 7.53 (d, ³*J*(H,H) = 16.02, 1 H, **CH**^d), 4.65 (t, ³*J*(H,H) = 6.71, 2 H, **CH**₂¹), 1.99 (bs, 2 H, **CH**₂²), 1.35-1.19 (m, 38 H, **CH**₂³⁻²¹), 0.85 (t, ³*J*(H,H) = 6.9, 3 H, **CH**₃²²). ¹³C NMR (CDCl₃, 125 MHz, 50°C) δ = 152.84 (**C**^c), 148.66 (**C**ⁱ), 144.60 (**C**^{a,a'}), 140.82 (**C**^f), 139.37 (**C**^e), 129.22 (**C**^{g,g'}), 126.53 (**C**^d), 125.30 (**C**^{b,b'}), 124.20 (**C**^{h,h'}), 61.46 (**C**¹), 31.88, 31.74, 29.66, 29.63, 29.61, 29.58, 29.50, 29.36, 29.29, 29.08, 26.17, 22.61 (**C**²⁻²¹), 13.98 (**C**²²).

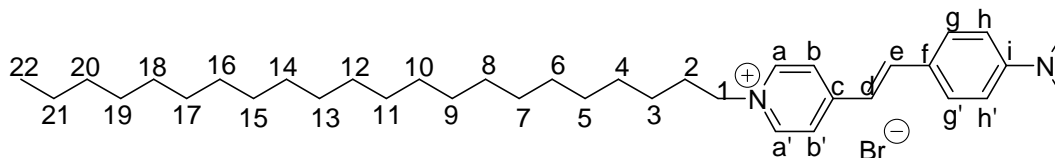
EA: C₃₅H₅₅BrN₂O₂ (Calc.) C: 68.27 %, H: 9.00 %, Br: 12.98 %, N: 4.55 %, (Found) C: 68.13 %, H: 8.92 %, Br: 13.78 %, N: 4.58 %.

4.3.6. *N*-docosyl-4'-dimethylamino-stilbazolium bromide **20**

A mixture of 4-dimethylamino-benzaldehyde (1.037 mmol, 0.154 g), 1-docosyl-4-methylpyridinium bromide (1.037 mmol, 0.5 g), piperidine (0.15 ml) and dry ethanol (4 ml) was

heated under reflux for 10 h. The product precipitate by cooling to room temperature and after filtration was purified by recrystallization from ethanol to give a red powder, 0.73 mmol, yield 70.4 %.

N-docosyl-4'-dimethylamino-stilbazolium bromide **20**:



Analytical data: $C_{37}H_{61}BrN_2$ $M_w = 613.80$

1H NMR ($CDCl_3$, J/Hz , 500 MHz) $\delta = 8.93$ (d, $^3J(H,H) = 6.84$, 2 H, Ar- $H^{a,a'}$), 7.91 (d, $^3J(H,H) = 6.43$, 2 H, Ar- $H^{b,b'}$), 7.63 (d, $^3J(H,H) = 15.97$, 1 H, CH^c), 7.57 (d, $^3J(H,H) = 8.92$, 2 H, Ar- $H^{g,g'}$), 6.91 (d, $^3J(H,H) = 15.77$, 1 H, CH^d), 6.8 (bs, 2 H, Ar- $H^{h,h'}$), 4.65 (t, $^3J(H,H) = 7.3$, 2 H, CH_2^1), 3.06 (s, 6 H, $N(CH_3)_2$), 1.95-1.89 (m, 2 H, CH_2^2), 1.35-1.19 (m, 38 H, CH_2^{3-21}), 0.84 (t, $^3J(H,H) = 6.8$, 3 H, CH_3^{22}). ^{13}C NMR ($CDCl_3$, 125 MHz) $\delta = 153.97$ (C^c), 152.07 (C^i), 143.27 ($C^{a,a'}$), 142.98 (C^e), 133.52 ($C^{g,g'}$), 130.53 ($C^{b,b'}$), 122.68 (C^f), 116.46 (C^d), 112.00 ($C^{h,h'}$), 60.32 (C^1), 40.18 ($N(CH_3)_2$), 31.93, 31.64, 29.72, 29.68, 29.66, 29.64, 29.55, 29.42, 29.36, 29.13, 26.17, 22.70 (C^{2-21}), 14.14 (C^{22}).

EA: $C_{37}H_{61}BrN_2 \cdot 0.2 H_2O$ (Calc.) C: 71.91 %, H: 9.94 %, Br: 12.96 %, N: 4.54 % (Found) C: 71.95 %, H: 9.51 %, Br: 13.48 %, N: 4.50 %.

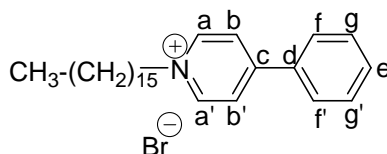
4.4. Synthesis of *N*-alkyl-4- and -3-phenyl-pyridinium salts

4.4.1. Synthesis of *N*-alkyl-4-phenyl-pyridinium salts 21a – j

General procedure:

The appropriate alkyl halide (3.22 mmol), 4-phenyl-pyridine or 3-phenyl-pyridine (3.22 mmol) and dry toluene (10 ml) were heated for 10 h at 100 – 110 °C. After cooling to room temperature, the crude product was purified by washing with diethyl ether and recrystallization from ethanol.

N-hexadecyl-4-phenyl-pyridinium bromide 21a:



Reagents: 4-Phenyl-pyridine (3.22 mmol, 0.5 g),
1-bromohexadecane (3.22 mmol, 0.98 g),
dry toluene (10 ml).

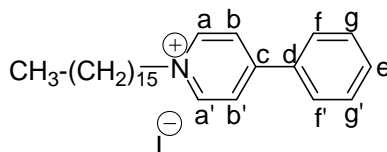
Purification: Washing with diethyl ether (2 x 50 ml) and recrystallization for two times from ethanol.

Yield: 41.92 % (1.35 mmol), colourless solid

Analytical data: C₂₇H₄₂BrN M_w = 460.53

¹H NMR (CDCl₃, J/Hz, 400 MHz) δ = 9.39 (d, ³J(H,H) = 6.64, 2 H, Ar-H^{a,a'}), 8.22 (d, ³J(H,H) = 6.22, 2 H, Ar-H^{b,b'}), 7.77 (m, 2 H, Ar-H^{e,e'}), 7.59-7.52 (m, 3 H, Ar-H^{f,f',g}), 4.90 (t, ³J(H, H) = 7.3, 2 H, CH₂¹), 2.05-1.98 (m, 2 H, CH₂²), 1.38-1.19 (m, 26 H, CH₂³⁻¹⁵), 0.85 (t, ³J(H,H) = 6.8, 3 H, CH₃¹⁶). ¹³C NMR (CDCl₃, 100 MHz) δ = 156.36 (C^c), 144.97 (C^{a,a'}), 133.55 (C^d), 132.40 (C^g), 129.94 (C^{f,f'}), 127.82 (C^{e,e'}), 124.97 (C^{b,b'}), 61.37 (C¹), 31.92, 31.86, 29.69, 29.65, 29.60, 29.51, 29.37, 29.35, 29.10, 26.17, 22.68 (C²⁻¹⁵), 14.09 (C¹⁶).

N-hexadecyl-4-phenyl-pyridinium iodide 21b:



Reagents: 4-Phenyl-pyridine (3.22 mmol, 0.5 g),
1-iodohexadecane (3.22 mmol, 1.135 g),

dry toluene (10 ml).

Purification: Washing with diethyl ether (50 ml) and recrystallization from ethanol.

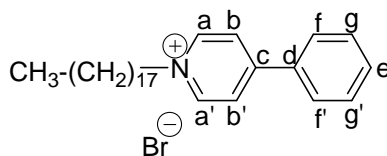
Yield: 73.60 % (2.36 mmol, 1.2 g), yellow powder

Analytical data: C₂₇H₄₂IN M_w = 507.53

¹H-NMR (CDCl₃, J/Hz, 400 MHz) δ = 9.34 (d, ³J(H,H) = 6.84, 2 H, Ar-H^{a,a'}), 8.24 (d, ³J(H,H) = 6.84, 2 H, Ar-H^{b,b'}), 7.78 (m, 2 H, Ar-H^{e,e'}), 7.57-7.53 (m, 3 H, Ar-H^{f,f',g}), 4.85 (t, ³J(H,H) = 7.47, 2 H, CH₂¹), 2.06-2.01 (m, 2 H, CH₂²), 1.40-1.19 (m, 26 H, CH₂³⁻¹⁵), 0.84 (t, ³J(H,H) = 6.8, 3 H, CH₃¹⁶). ¹³C NMR (CDCl₃, 125 MHz) δ = 156.41 (C^c), 144.78 (C^{a,a'}), 133.46 (C^d), 132.48 (C^g), 129.97 (C^{f,f'}), 127.88 (C^{e,e'}), 125.08 (C^{b,b'}), 61.35 (C¹), 31.87, 31.73, 29.65, 29.61, 29.56, 29.48, 29.33, 29.31, 29.04, 26.06, 22.64 (C²⁻¹⁵), 14.07 (C¹⁶).

MS (EI, 70 eV) *m/z*: 155, 225, 380 (M⁺-I). EA: C₂₇H₄₂IN·0.8H₂O (Calc.) C: 62.08 %, H: 8.36 %, N: 2.68 %, (Found) C: 62.19 %, H: 8.79 %, N: 2.32 %.

N-octadecyl-4-phenyl-pyridinium bromide **21c**:



Reagents: 4-Phenyl-pyridine (3.22 mmol, 0.5 g),
1-bromooctadecane (3.22 mmol, 1.07 g),
dry toluene (10 ml).

Purification: Washing with diethyl ether (3 x 50 ml) and recrystallization from ethanol.

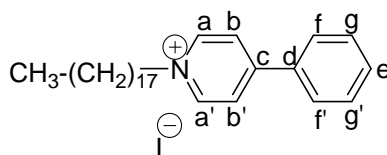
Yield: 55.90 % (1.8 mmol), white powder

Analytical data: C₂₉H₄₆BrN M_w = 488.59

¹H NMR (CDCl₃, J/Hz, 400 MHz) δ = 9.43 (d, ³J(H,H) = 6.22, 2 H, Ar-H^{a,a'}), 8.22 (d, ³J(H,H) = 6.02, 2 H, Ar-H^{b,b'}), 7.76 (m, 2 H, Ar-H^{e,e'}), 7.58-7.51 (m, 3 H, Ar-H^{f,f',g}), 4.92 (t, ³J(H,H) = 7.26, 2 H, CH₂¹), 2.04-2.00 (m, 2 H, CH₂²), 1.36-1.07 (m, 30 H, CH₂³⁻¹⁷), 0.84 (t, ³J(H,H) = 6.7, 3 H, CH₃). ¹³C NMR (CDCl₃, 100 MHz) δ = 156.26 (C^c), 145.03 (C^{a,a'}), 133.56 (C^d), 132.33 (C^g), 129.89 (C^{f,f'}), 127.83 (C^{e,e'}), 125.00 (C^{b,b'}), 61.34 (C¹), 31.90, 31.85, 29.67, 29.63, 29.59, 29.50, 29.36, 29.32, 29.10, 26.16, 22.65 (C²⁻¹⁷), 14.06 (C¹⁸).

MS (EI, 70 eV) *m/z*: 155, 253, 408 (M⁺-Br). EA: C₂₉H₄₆BrN·0.5H₂O (Calc.) C: 69.93 %, H: 9.44 %, Br: 16.07 %, N: 2.81 %, (Found) C: 69.77 %, H: 9.62 %, Br: 15.95 %, N: 2.83 %.

N-octadecyl-4-phenyl-pyridinium iodide **21d**:



Reagents: 4-Phenyl-pyridine (3.22 mmol, 0.5 g),
1-iodooctadecane (3.22 mmol, 1.22 g),
dry toluene (10 ml).

Purification: Washing with diethyl ether (2 x 50 ml) and recrystallization for two times from ethanol.

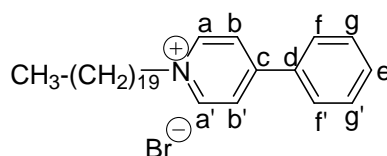
Yield: 71.4 % (2.3 mmol, 1.23 g), yellow powder

Analytical data: C₂₉H₄₆IN M_w = 535.59

¹H NMR (CDCl₃, J/Hz, 500 MHz) δ = 9.27 (d, ³J(H,H) = 6.71, 2 H, Ar-H^{a,a'}), 8.20 (d, ³J(H,H) = 6.71, 2 H, Ar-H^{b,b'}), 7.75 (m, 2 H, Ar-H^{e,e'}), 7.55-7.49 (m, 3 H, Ar-H^{f,f',g}), 4.82 (t, ³J(H, H) = 7.40, 2 H, CH₂¹), 2.02-1.96 (m, 2 H, CH₂²), 1.36-1.16 (m, 30 H, CH₂³⁻¹⁷), 0.80 (t, ³J(H,H) = 7.00, 3 H, CH₃¹⁸). ¹³C NMR (CDCl₃, 125 MHz) δ = 156.49 (C^c), 144.85 (C^{a,a'}), 133.46 (C^d), 132.50 (C^g), 129.99 (C^{f,f'}), 127.92 (C^{e,e'}), 125.14 (C^{b,b'}), 61.49 (C¹), 31.88, 31.76, 29.66, 29.61, 29.56, 29.48, 29.33, 29.31, 29.05, 26.12, 22.64 (C²⁻¹⁷), 14.07 (C¹⁸).

MS (EI, 70 eV) *m/z*: 155, 253, 408 (M⁺-I). EA: C₂₉H₄₆IN·0.5H₂O (Calc.) C: 63.90 %, H: 8.63 %, N: 2.57 %, (Found) C: 64.14 %, H: 8.90 %, N: 2.14 %.

N-eicosyl-4-phenyl-pyridinium bromide **21e**:



Reagents: 4-Phenyl-pyridine (3.22 mmol, 0.5 g),
1-bromoeicosane (3.22 mmol, 1.165 g),
dry toluene (10 ml).

Purification: Washing with diethyl ether (50 ml) and recrystallization from ethanol.

Yield: 61.80 % (1.99 mmol), white powder

Analytical data: C₃₁H₅₀BrN M_w = 516.64

¹H NMR (CDCl₃, J/Hz, 400 MHz) δ = 9.44 (d, ³J(H,H) = 6.64, 2 H, Ar-H^{a,a'}), 8.23 (d, ³J(H,H) = 6.64, 2 H, Ar-H^{b,b'}), 7.77 (m, 2 H, Ar-H^{e,e'}), 7.56-7.51 (m, 3 H, Ar-H^{f,f',g}), 4.90 (t, ³J(H,H) = 7.3, 2 H, CH₂¹), 2.02-1.99 (m, 2 H, CH₂²), 1.37-1.18 (m, 34 H, CH₂³⁻¹⁹), 0.84 (t, ³J(H,H) =

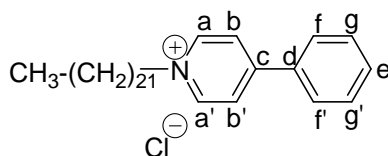
7.8, 3 H, CH_3^{20}). ^{13}C NMR (CDCl_3 , 100 MHz) δ = 156.24 (C^c), 145.02 ($\text{C}^{\text{a,a}'}$), 133.53 (C^d), 132.34 (C^g), 129.89 ($\text{C}^{\text{f,f}'}$), 127.79 ($\text{C}^{\text{e,e}'}$), 124.95 ($\text{C}^{\text{b,b}'}$), 61.25 (C^1), 31.9, 31.86, 29.68, 29.63, 29.59, 29.50, 29.36, 29.33, 29.09, 26.14, 22.66 (C^{2-19}), 14.07 (C^{20}).

MS (EI, 70 eV) m/z : 155, 281, 436 ($\text{M}^+ \text{-Br}$). EA: $\text{C}_{31}\text{H}_{50}\text{BrN}\cdot\text{H}_2\text{O}$ (Calc.) C: 69.64 %, H: 9.80 %, Br: 14.94 %, N: 2.62 %, (Found) C: 69.57 %, H: 9.79 %, Br: 15.01 %, N: 2.62 %.

General procedure for preparation of the salts **21f – j** by ion exchange method:

Compound **21h** was prepared using Dowex 1 x 8-400, ion exchange resin (Acros), N-docosyl-4-phenyl-pyridinium bromide **21g**, NaI and methanol: 10 g of Dowex resin was suspended in 100 ml water for 2 h. After removing the water, the resin was washed with NaI (or NaCl, $\text{NaB}(\text{C}_6\text{H}_5)_4$, $\text{CH}_3\text{-C}_6\text{H}_5\text{-SO}_3\text{H}$) solution for three times. The resin was kept in contact for 2 days with the third part of NaI solution and then filtered. The ration of **21g**/NaI was 1/10. 100 mg of salt **21g** (0.18 mmol) was dissolved in 10 ml of methanol and mixed with resin. After keeping the resin in contact with the salt **21g** for 2 days, the product was extracted with methanol and washed with water to remove the excess of NaI. The solvent was evaporated by distillation and pure **21h** was obtained. Compounds **21f – j** were investigated by ESI-MS and no bromide ion was identified in spectrum, which indicates that the exchange procedure was complete.

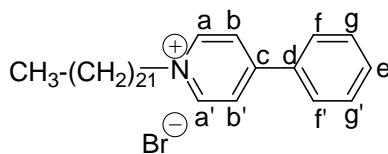
*1-docosyl-4-phenyl-pyridinium chloride **21f**:*



Analytical data: $\text{C}_{33}\text{H}_{54}\text{ClN}$ $M_w = 500.24$

MS (ESI, 4.1 kV) m/z : 464.6 (M^+).

*1-docosyl-4-phenyl-pyridinium bromide **21g**:*



Reagents: 4-Phenyl-pyridine (3.22 mmol, 0.5g),
1-bromodocosane (3.22 mmol, 1.254g),

dry toluene (10 ml).

Purification: Washing with diethyl ether (50 ml) and recrystallization for two times from ethanol

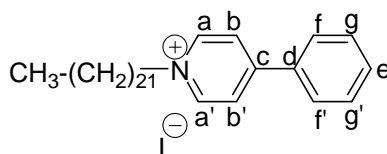
Yield: 79.19 % (2.55 mmol), white powder

Analytical data: $C_{33}H_{54}NBr$ $M_w = 544.69$

1H NMR ($CDCl_3$, J/Hz , 400 MHz) $\delta = 9.41$ (d, $^3J(H,H) = 6.64$, 2 H, Ar- $H^{a,a'}$), 8.22 (d, $^3J(H,H) = 6.64$, 2 H, Ar- $H^{b,b'}$), 7.77 (m, 2 H, Ar- $H^{e,e'}$), $7.59-7.51$ (m, 3 H, Ar- $H^{f,f',g}$), 4.91 (t, $^3J(H,H) = 7.3$, 2 H, CH_2^1), $2.05-2.01$ (m, 2 H, CH_2^2), $1.37-1.19$ (m, 38 H, CH_2^{3-21}), 0.85 (t, $^3J(H,H) = 7.8$, 3 H, CH_3). ^{13}C NMR ($CDCl_3$, 100 MHz) $\delta = 156.32$ (C^c), 144.97 ($C^{a,a'}$), 133.53 (C^d), 132.40 (C^g), 129.93 ($C^{f,f'}$), 127.80 ($C^{e,e'}$), 124.95 ($C^{b,b'}$), 61.33 (C^1), 31.92 , 31.88 , 29.71 , 29.65 , 29.61 , 29.52 , 29.37 , 29.35 , 29.11 , 29.16 , 22.68 (C^{2-21}), 14.01 (C^{22}).

MS (EI, 70 eV): m/z 155, 309, 464 (M^+-Br). EA: $C_{33}H_{54}NBr \cdot H_2O$ (Calc.) C: 70.44 %, H: 10.03 %, Br: 14.20 %, N: 2.49 %, (Found) C: 70.14 %, H: 9.96 %, Br: 14.39 %, N: 2.23 %.

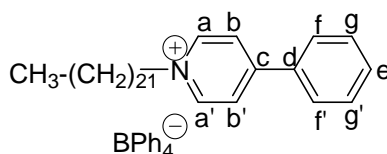
1-docosyl-4-phenyl-pyridinium iodide 21h:



Analytical data: $C_{33}H_{54}IN$ $M_w = 591.69$

MS (ESI, 4.1 kV) m/z : 127,3 (I^-), 464.6 (M^+)

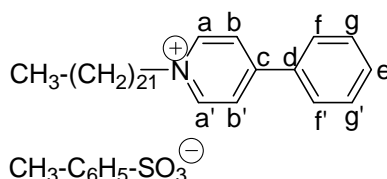
1-docosyl-4-phenyl-pyridinium tetraphenylborate 21i:



Analytical data: $C_{57}H_{74}BN$ $M_w = 784.02$

MS (ESI, 4.1 kV) m/z : 319.5 (BPh_4^-), 464.5 (M^+).

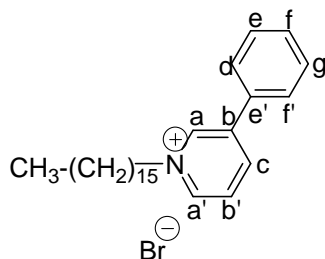
1-docosyl-4-phenyl-pyridinium p-toluenesulfonate 21j:



Analytical data: $C_{40}H_{61}NO_3S$ $M_w = 635.98$
 MS (ESI, 4.1 kV) m/z : 171.3 ($CH_3-C_6H_5-SO_3^-$), 464.6 (M^+).

4.4.2. Synthesis of *N*-alkyl-3-phenyl-pyridinium salts 22a – f

N-dexadecyl-3-phenyl-pyridinium bromide **22a**:



Reagents: 3-Phenyl-pyridine (3.22 mmol, 0.5 g),
 1-bromoeicosane (3.22 mmol, 0.98 g),
 dry toluene (10 ml).

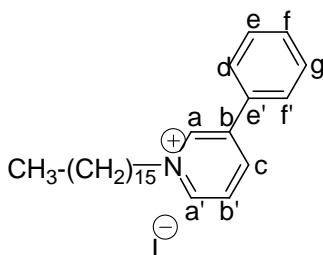
Purification: Washing with diethyl ether (2 x 50 ml) and recrystallization from ethanol.

Yield: 34.16 % (1.10 mmol), colourless solid

Analytical data: $C_{27}H_{42}BrN$ $M_w = 460.53$

1H NMR ($CDCl_3$, J/Hz , 400 MHz) $\delta = 9.56$ (s, 1 H, Ar- H^a), 9.35 (bs, 1 H, Ar- $H^{a'}$), 8.55 (d, $^3J(H,H) = 7.68$, 1 H, Ar- H^b), 8.12 (m, 1 H, Ar- $H^{b'}$), 7.85 (d, $^3J(H,H) = 6.85$, 2 H, Ar- $H^{d,f}$), 7.51-7.44 (m, 3 H, Ar- $H^{e,f,g}$), 5.11 (t, $^3J(H,H) = 6.64$, 2 H, CH_2^1), 2.08-1.99 (m, 2 H, CH_2^2), 1.33-1.15 (m, 26 H, CH_2^{3-15}), 0.84 (t, $^3J(H,H) = 6.8$, 3 H, CH_3^{16}). ^{13}C NMR ($CDCl_3$, 100 MHz) $\delta = 143.00$ ($C^{a'}$), 142.64 (C^c), 142.24 (C^a), 141.28 (C^b), 132.62 (C^e), 130.59 (C^f), 129.82 ($C^{e,g}$), 128.32 ($C^{b'}$), 127.68 ($C^{d,f}$), 62.43 (C^1), 32.28, 32.02, 29.78, 29.76, 29.74, 29.70, 29.62, 29.45, 29.23, 26.25, 22.79 (C^{2-15}), 14.21 (C^{16}).

N-hexadecyl-3-phenyl-pyridinium iodide **22b**:



Reagents: 3-Phenyl-pyridine (3.22 mmol, 0.5 g),
 1-bromoeicosane (3.22 mmol, 1.135 g),

dry toluene (10 ml).

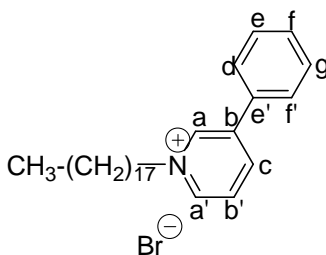
Purification: Washing with diethyl ether (2x50 ml) and recrystallization from ethanol.

Yield: 50.62 % (1.63 mmol), yellow solid

Analytical data: C₂₇H₄₂IN M_w = 507.53

¹H NMR (CDCl₃, J/Hz, 400 MHz) δ = 9.48 (s, 1 H, Ar-**H**^a), 9.23 (d, ³J(H,H) = 6.02, 1 H, Ar-**H**^{a'}), 8.60 (d, ³J(H,H) = 8.3, 1 H, Ar-**H**^b), 8.17-8.14 (m, 1 H, Ar-**H**^{b'}), 7.86-7.83 (m, 2 H, Ar-**H**^{d,f}), 7.65-7.41 (m, 3 H, Ar-**H**^{e,f,g}), 5.02 (t, ³J(H, H) = 7.47, 2 H, CH₂¹), 2.02-1.95 (m, 2 H, CH₂²), 1.37-1.15 (m, 26 H, CH₂³⁻¹⁵), 0.81 (t, ³J(H,H) = 6.8, 3 H, CH₃¹⁶). ¹³C NMR (CDCl₃, 100 MHz) δ = 142.60 (C^{a'}), 142.51 (C^c), 142.02 (C^a), 141.05 (C^b), 132.34 (C^{e'}), 130.46 (C^f), 129.61 (C^{e,g}), 128.49 (C^{b'}), 127.64 (C^{d,f}), 62.19 (C¹), 31.89, 31.76, 29.53, 29.49, 29.46, 29.39, 29.22, 29.19, 28.97, 25.89, 22.52 (C²⁻¹⁵), 13.94 (C¹⁶).

N-octadecyl-3-phenyl-pyridinium bromide **22c**:



Reagents: 3-Phenyl-pyridine (1.5 mmol, 0.233 g),
1-bromooctadecane (1.5 mmol, 0.5 g),
dry toluene (5 ml).

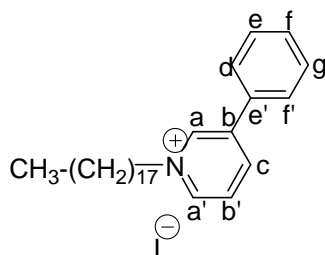
Purification: Washing with diethyl ether (30 ml) and recrystallization from ethanol

Yield: 40.93 % (0.614 mmol), colourless solid

Analytical data: C₂₉H₄₆BrN M_w = 488.59

¹H NMR (CDCl₃, J/Hz, 400 MHz) δ = 9.60 (s, 1 H, Ar-**H**^a), 9.36 (d, ³J(H,H) = 6.02, 1 H, Ar-**H**^{a'}), 8.56 (d, ³J(H,H) = 8.30, 1 H, Ar-**H**^b), 8.15-8.11 (m, 1 H, Ar-**H**^{b'}), 7.84 (dd, ³J₁(H, H) = 8.3, ³J₂(H, H) = 7.68, 2 H, Ar-**H**^{d,f}), 7.58-7.43 (m, 3 H, Ar-**H**^{e,f,g}), 5.10 (t, ³J(H, H) = 7.3, 2 H, CH₂¹), 2.12-1.97 (m, 2 H, CH₂²), 1.37-1.06 (m, 30 H, CH₂³⁻¹⁷), 0.83 (t, ³J(H,H) = 6.8, 3 H, CH₃¹⁸). ¹³C NMR (CDCl₃, 100 MHz) δ = 142.98 (C^{a'}), 142.60 (C^c), 142.20 (C^a), 141.18 (C^b), 132.60 (C^{e'}), 130.51 (C^f), 129.75 (C^{e,g}), 128.31 (C^{b'}), 127.62 (C^{d,f}), 62.23 (C¹), 32.83, 32.13, 31.87, 29.65, 29.61, 29.56, 29.48, 29.31, 29.30, 29.08, 28.73, 26.08, 22.63 (C²⁻¹⁷), 14.04 (C¹⁸).
EA: C₂₉H₄₆BrN (Calc.) C: 71.29 %, H: 9.49 %, Br: 16.35 %, N: 2.87 %, (Found) C: 70.85 %, H: 9.61 %, Br: 17.53 %, N: 2.51 %.

N-octadecyl-3-phenyl-pyridinium iodide **22d**:



Reagents: 3-Phenyl-pyridine (0.53 mmol, 0.081 g),
1-iodooctadecane (0.53 mmol, 0.2 g),
dry toluene (2 ml).

Purification: Washing with diethyl ether (20 ml) and recrystallization from ethanol.

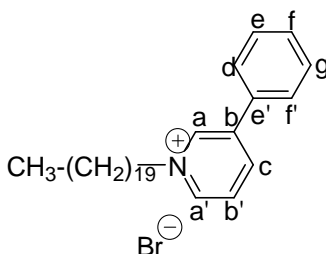
Yield: 53.23 % (0.28 mmol), yellow powder

Analytical data: C₂₉H₄₆IN M_w = 535.59

¹H NMR (CDCl₃, *J*/Hz, 500 MHz) δ = 9.37 (s, 1 H, Ar-**H^a**), 9.21 (d, ³*J*(H,H) = 5.00, 1 H, Ar-**H^{a'}**), 8.52 (d, ³*J*(H,H) = 7.69, 1 H, Ar-**H^b**), 8.08 (m, 1 H, Ar-**H^{b'}**), 7.77 (d, ³*J*_I(H, H) = 6.95, 2 H, Ar-**H^{d,f}**), 7.53-7.40 (m, 3 H, Ar-**H^{e,f,g}**), 4.99 (t, ³*J*(H, H) = 6.8, 2 H, **CH₂¹**), 2.02-1.99 (m, 2 H, **CH₂²**), 1.38-1.16 (m, 30 H, **CH₂³⁻¹⁷**), 0.81 (t, ³*J*(H,H) = 7.0, 3 H, **CH₃¹⁸**). ¹³C NMR (CDCl₃, 125 MHz) δ = 142.96 (**C^{a'}**), 142.53 (**C^c**), 142.49 (**C^a**), 141.85 (**C^b**), 132.57 (**C^{e'}**), 130.77 (**C^f**), 129.96 (**C^{e,g}**), 128.53 (**C^{b'}**), 127.71 (**C^{d,f}**), 62.82 (**C¹**), 32.09, 31.88, 29.66, 29.62, 29.60, 29.56, 29.47, 29.32, 29.05, 26.19, 22.65 (**C²⁻¹⁷**), 14.07 (**C¹⁸**).

EA: C₂₉H₄₆IN·0.5H₂O (Calc.) C: 63.90 %, H: 8.63 %, N: 2.57 %, (Found) C: 63.95 %, H: 8.70 %, N: 2.38 %.

N-eicosyl-3-phenyl-pyridinium bromide **22e**:



Reagents: 3-Phenyl-pyridine (3.22 mmol, 0.5 g),
1-bromoeicosane (3.22 mmol, 1.165 g),
dry toluene (10 ml).

Purification: Washing with diethyl ether (50 ml) and recrystallization from ethanol.

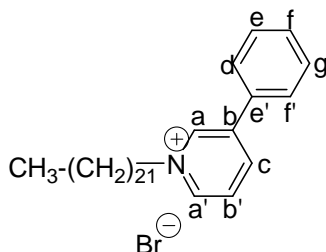
Yield: 42.23 % (1.36 mmol), colourless solid

Analytical data: C₃₁H₅₀BrN M_w = 516.64

¹H NMR (CDCl₃, J/Hz, 400 MHz) δ = 9.54 (s, 1 H, Ar-**H^a**), 9.34 (d, ³J(H,H) = 6.02, 1 H, Ar-**H^{a'}**), 8.55 (d, ³J(H,H) = 8.09, 1 H, Ar-**H^c**), 8.14-8.11 (m, 1 H, Ar-**H^{b'}**), 7.84 (d, ³J(H,H) = 6.84, 2 H, Ar-**H^{d,f}**), 7.53-7.44 (m, 3 H, Ar-**H^{e,f,g}**), 5.09 (t, ³J = 7.3, 2 H, **CH₂¹**), 2.03-1.97 (m, 2 H, **CH₂²**), 1.36-1.17 (m, 34 H, **CH₂³⁻¹⁹**), 0.84 (t, ³J(H,H) = 6.7, 3 H, **CH₃²⁰**). ¹³C NMR (CDCl₃, 100 MHz) δ = 143.06 (**C^{a'}**), 142.62 (**C^c**), 142.31 (**C^a**), 141.20 (**C^b**), 132.65 (**C^{e'}**), 130.56 (**C^f**), 129.80 (**C^{e,g}**), 128.45 (**C^{b'}**), 127.69 (**C^{d,f}**), 62.30 (**C¹**), 32.89, 32.19, 31.94, 29.73, 29.68, 29.63, 29.56, 29.46, 29.39, 29.37, 29.16, 28.79, 28.22, 26.15, 22.71 (**C²⁻¹⁹**), 14.12 (**C²⁰**).

MS (EI, 70 eV): *m/z* 155, 281, 436 (M⁺-Br). EA: C₃₁H₅₀BrN·0.5H₂O (Calc.) C: 70.77 %, H: 9.70 %, N: 2.66 %, (Found) C: 70.78 %, H: 10.12 %, N: 2.02 %.

N-docosyl-3-phenyl-pyridinium bromide **22f**:



Reagents: 3-Phenyl-pyridine (1.22 mmol, 0.19 g),
1-bromodocosane (1.28 mmol, 0.5 g),
dry toluene (4 ml).

Purification: Washing with diethyl ether (20 ml) and recrystallization from ethanol.

Yield: 57.42 % (0.73 mmol), white powder

Analytical data: C₃₃H₅₄BrN M_w = 544.69

¹H NMR (CDCl₃, J/Hz, 400 MHz) δ = 9.52 (s, 1 H, Ar-**H^a**), 9.35 (d, ³J(H,H) = 6.02, 1 H, Ar-**H^{a'}**), 8.55 (d, ³J(H, H) = 8.09, 1 H, Ar-**H^c**), 8.12-8.09 (m, 1 H, Ar-**H^{b'}**), 7.84 (dd, ³J_I(H, H) = 8.3, ³J₂(H, H) = 7.88, 2 H, Ar-**H^{d,f}**), 7.55-7.49 (m, 3 H, Ar-**H^{f,f,g}**), 5.12 (t, ³J(H, H) = 7.3, 2 H, **CH₂¹**), 1.99 (m, 2 H, **CH₂²**), 1.38-1.19 (m, 38 H, **CH₂³⁻²¹**), 0.85 (t, ³J(H, H) = 6.8, 3 H, **CH₃²²**). ¹³C NMR (CDCl₃, 100 MHz) δ = 142.95 (**C^{a'}**), 142.63 (**C^c**), 142.23 (**C^a**), 141.45 (**C^b**), 132.61 (**C^{e'}**), 130.65 (**C^f**), 129.87 (**C^{e,g}**), 128.22 (**C^{b'}**), 127.65 (**C^{d,f}**), 62.46 (**C¹**), 32.16, 31.93, 29.71, 29.66, 29.60, 29.52, 29.36, 29.11, 26.15, 22.69 (**C²⁻²¹**), 14.11 (**C²²**).

MS (EI, 70 eV): *m/z* 155, 309, 464 (M⁺-Br). EA: C₃₃H₅₄BrN·0.3H₂O (Calc.) C: 71.99 %, H: 9.93 %, N: 2.54 %, (Found) C: 71.91 %, H: 10.03 %, N: 2.36 %.

5. References

- [1] K. Binnemans, *Chem. Rev.*, **2005**, *105*, 4148.
- [2] P. Wasserscheid, T. Welton, *Ionic liquids in synthesis*, Wiley-VCH, Weinheim, **2002**.
- [3] I. Dierking, *Textures of liquid crystals*, Wiley-VCH, Weinheim, **2003**.
- [4] C. Tschierske, *Progr. Polym. Sci.*, **1996**, *21*, 775.
- [5] C. Tanford, *The Hydrophobic Effect*, Wiley, New York, **1973**.
- [6] D. Vorländer, *Ber. Dtsch. Chem. Ges.*, **1910**, *43*, 3120.
- [7] K. Bijma, J. B. F. N. Engberts, *Langmuir*, **1997**, *13*, 4843.
- [8] J. W. Steed, J. Atwood, *Supramolecular Chemistry*, John Wiley & Sons, Ltd., **2000**, p. 19.
- [9] G. A. Knight, B. D. Shaw, *J. Chem. Soc.*, **1938**, 682.
- [10] R. Somashekar, *Mol. Cryst. Liq. Cryst.*, **1987**, *146*, 225.
- [11] C. M. Gordon, J. D. Holbrey, A. R. Kennedy, K. R. Seddon, *J. Mat. Chem.*, **1998**, *8*, 2627.
- [12] D. P. Jackson, B. M. Fung, *Mol. Cryst. Liq. Cryst.*, **1997**, *303*, 73.
- [13] G. W. Gray, *Thermotropic liquid crystals*, John Wiley & Sons, Inc., 1987, p. 28.
- [14] C. G. Bazuin, D. Guillon, A. Skoulios, R. Zana, *J. Phys. (France)*, **1986**, *47*, 927.
- [15] M. Tabrizian, A. Soldera, M. Couturier, C. G. Bazuin, *Liquid Crystals*, **1995**, *18(3)*, 475.
- [16] C. J. Bowlas, D. W. Bruce, K. R. Seddon, *Chem. Commun.*, **1996**, 1625.
- [17] J.-J. H. Nusselder, J. B. F. N. Engberts, H. E. Van Doren, *Liquid Crystals*, **1993**, *13(2)*, 213.
- [18] C. G. Bazuin, D. Guillon, A. Skoulios, *Liquid Crystals*, **1986**, *1(2)*, 181.
- [19] D. Demus, in *Handbook of Liquid Crystals*, ed. D. Demus, J. Goodby, G. W. Gray, H.-W. Spiess, V. Vill, Wiley-VCH, Weinheim, **1998**, vol. 1, p. 170.
- [20] T. A. Bleasdale, G. J. Tiddy, E. Wyn-Jones, *J. Phys. Chem.*, **1991**, *95*, 5385.
- [21] J.-J. H. Nusselder, T.-J. de Groot, M. Trimbos, J. B. F. N. Engberts, *J. Org. Chem.*, **1988**, *53*, 2423.
- [22] J.-J. H. Nusselder, J. B. F. N. Engberts, *J. Am. Chem. Soc.*, **1989**, *111*, 5000.
- [23] J.-J. H. Nusselder, J. B. F. N. Engberts, *J. Org. Chem.*, **1991**, *56*, 5522.
- [24] J.-J. H. Nusselder, J. B. F. N. Engberts, *Langmuir*, **1991**, *7*, 2089.
- [25] J. M. de Gooijer, J. B. F. N. Engberts, M. J. Blandamer, *J. Colloid Interface Sci.*, **2000**, *224*, 4.

- [26] J. B. F. N. Engberts, J.-J. H. Nusselder, *Pure & Appl. Chem.*, **1990**, 62(1), 47.
- [27] A. L. Underwood, E. W. Anacker, *J. Colloid Interface Sci.*, **1973**, 44, 505.
- [28] Y. Kosaka, T. Kato, T. Uryu, *Liquid Crystals*, **1995**, 18(5), 693.
- [29] K. Binnemans, C. Bex, R. Van Deun, *J. Inclusion Phenom. Macrocycl. Chem.*, **1999**, 35, 63.
- [30] K. Z. Wang, C. H. Huang, G. X. Xu, Q. F. Zhou, *Solid State Comm.*, **1995**, 95, 223.
- [31] F. Würthner, S. Yao, U. Beginn, *Angew. Chem. Int. Ed.*, **2003**, 42, 3247.
- [32] F. Würthner, *Supramolecular Dye Chemistry*, Springer-Verlag, Berlin Heidelberg, **2005**.
- [33] A. Sautter, C. Thalacker, F. Würthner, *Angew. Chem. Int. Ed.*, **2001**, 40, 4425.
- [34] F. Würthner, C. Thalacker, S. Diele, C. Tschierske, *Chem. Eur. J.*, **2001**, 40, 4425.
- [35] C. Zhijian, U. Baumeister, C. Tschierske, F. Würthner, *Chem. Eur. J.*, **2007**, 13, 450.
- [36] C. F. Van Nostrum, *Adv. Mater.*, **1996**, 8, 1027.
- [37] J. Vacus, J. Simon, *Adv. Mater.*, **1995**, 7, 797.
- [38] F. S. Schoonbeek, J. H. van Esch, B. Wegewijs, B. A. Rep, M. P. de Haas, T. M. Klapwijk, R. M. Kellogg, B. L. Feringa, *Angew. Chem. Int. Ed.*, **1999**, 38, 1393.
- [39] A. Ajayaghosh, S. J. George, V. K. Praveen, *Angew. Chem. Int. Ed.*, **2003**, 42, 332.
- [40] S. Yao, U. Beginn, T. Gress, M. Lysetska, F. Würthner, *J. Am. Chem. Soc.*, **2004**, 126, 8336.
- [41] L. G. S. Brooker, G. H. Keyes, R. H. Sprague, R. H. van Dyke, E. van Lare, G. van Zandt, F. L. White, *J. Am. Chem. Soc.*, **1951**, 73, 5326.
- [42] I. D. L. Albert, T. J. Marks, M. A. Ratner, *J. Phys. Chem.*, **1996**, 100, 9714.
- [43] D. J. Williams, *Angew. Chem.*, **1984**, 96, 637.
- [44] C. Bosshard, F. Pan, M. S. Wong, S. Manetta, R. Spreiter, C. Cai, P. Gunter, V. Gramlich, *Chem. Phys.*, **1999**, 245, 377.
- [45] G. Yang, Y. Li, Z. A. Dreger, J. O. White, H. G. Drickamer, *Chem. Phys. Lett.*, **1997**, 280, 375.
- [46] X.-M. Duan, S. Okada, H. Oikawa, H. Matsuda, H. Nakanishi, *Mol. Cryst. Liq. Cryst. Sci. Technol., Sect. A*, **1995**, 267, 89.
- [47] G. L. Gaines, *Angew. Chem.*, **1987**, 99, 346.
- [48] Y. Mineo, K. Itoh, *J. Phys. Chem.*, **1991**, 95, 2451.
- [49] W. Konig, *Ber. dtsc. Chem. Ges.*, **1922**, 55, 330.
- [50] N. Tyutyulkov, J. Fabian, A. Mehlhorn, F. Dietz, A. Tadjer, *Polymethine dyes structure and properties*, St. Kliment Ohridski Univ. Press., Sofia, **1991**.

- [51] J. Fabian, H. Hartmann, *Dye Chemistry*, Springer-Verlag, Berlin Heidelberg New York, **1980**, p. 162.
- [52] H. von Belepsch, C. Böttcher, A. Quart, C. Burger, S. Dähne, S. Kirstein, *J. Phys. Chem. B*, **2000**, *104*, 5255.
- [53] a) G. Scheibe, *Angew. Chem.*, **1936**, *49*, 563. b) G. Scheibe, *Angew. Chem.*, **1937**, *50*, 212. c) G. Scheibe, *Kolloid-Z.*, **1938**, *82*, 1. d) G. Scheibe, H. E. Kandler, *Naturwiss.*, **1937**, *25*, 75. e) G. Scheibe, A. Mareis, H. Ecker., *Naturwiss.*, **1937**, *25*, 474.
- [54] a) E. Jelley, *Nature*, **1936**, *138*, 1009; b) E. Jelley, *Nature*, **1937**, *139*, 631.
- [55] W. J. Harrison, D. L. Mateer, G. J. T. Tiddy, *J. Phys. Chem.*, **1996**, *100*, 2310.
- [56] J. O. Morley, R. M. Morley, R. Docherty, M. H. Charlton, *J. Am. Chem. Soc.*, **1997**, *119*, 10192.
- [57] A. Botrel, A. Beuze, P. Jacques, H. Strub, *J. Chem. Soc., Faraday Trans.*, **1984**, *80*, 1235.
- [58] S. T. Abdel-Halim, *J. Chem. Soc. Faraday Trans.*, **1993**, *89*, 55.
- [59] P. Jacques, *J. Phys. Chem.*, **1986**, *90*, 5535.
- [60] U. E. Steiner, M. H. Abdel-Kader, P. Fischer, H. E. A. Kramer, *J. Am. Chem. Soc.*, **1978**, *100(10)*, 3190.
- [61] D. H. Waldeck, *Chem. Rev.*, **1991**, *91*, 415.
- [62] S. T. Abdel-Halim, M. H. Abdel-Kader, U. E. Steiner, *J. Phys. Chem.*, **1988**, *92*, 4324.
- [63] L. G. S. Brooker, G. H. Keyes, D. W. Heseltine, *J. Am. Chem. Soc.*, **1951**, *73*, 5332.
- [64] C. Reichardt, *Solvents and Solvent Effects in Organic Chemistry*, Wiley-VCH, Weinheim, **2003**.
- [65] C. Reichardt, *Solvatochromic Dyes as Solvent Polarity Indicators*, *Chem. Rev.*, **1994**, *94*, 2319.
- [66] E. M. Kosower, P. E. Jr. Klinedinst, *J. Am. Chem. Soc.*, **1956**, *78*, 3493.
- [67] E. M. Kosower, *J. Amer. Chem. Soc.*, **1958**, *80*, 3253.
- [68] F. Würthner, S. Yao, B. Heise, C. Tschierske, *Chem. Commun.*, **2001**, 2260.
- [69] Autorenkollektive, *Organikum*, VEB Deutsche Verlag der Wissenschaften Berlin, **2000**.
- [70] A. R. Battersby, W. Westwood, *J. Chem. Soc. Perkin Trans. I*, **1987**, 1679.
- [71] C. J. Drummond, T. Grieser, T. W. Healy, *J. Phys. Chem.*, **1988**, *92*, 2604.
- [72] I. A. Pearl, D. L. Beyer, *J. Am. Chem. Soc.*, **1953**, *75*, 2630.
- [73] H. Stone, H. Schechter, *Organic Syntheses*, **1963**, *4*, 543.

- [74] R. Matissek, *Lebensmittelanalytik: Grundzüge, Methoden, Anwendungen*, Springer, Berlin **2006**, 187.
- [75] Y. Marcus, *J. Chem. Soc. Faraday Trans.*, **1991**, 87 (18), 2995.
- [76] The average lateral distance a of the molecules is calculated according to $a = 1.12 \times d$ from the relation for randomly packed long cylinders as usually applied for calamitic liquid crystals, see e.g. M. J. Seddon, in *Handbook of Liquid Crystals*, ed. D. Demus, J. Goodby, G. W. Gray, H.-W. Spiess, V. Vill, WILEY-VCH Verlag GmbH, Weinheim, **1998**, vol. 1, p. 648.
- [77] T. Nhujak, D. M. Goodall, *Electrophoresis*, **2001**, 22, 117.
- [78] R. A. Mackay, J. R. Landolph, E. J. Poziomek, *J. Amer. Chem. Soc.*, **1971**, 93, 5026.
- [79] P. Krafft, H. Wiglow, *Berichte*, **1895**, 28, 2566.
- [80] P. Garidel, A. Hildebrand, R. Neubert, A. Blume, *Langmuir*, **2000**, 16, 5267.
- [81] B. Lindmann, H. Wennerström, *Micelles*, Springer-Verlag, Berlin, **1980**, p.30.
- [82] G. Harald, *NMR Spectroscopy*, John Wiley & Sons, Inc., **1995**, p.116.
- [83] C. N. R. Rao, *Ultra-Violet and Visible Spectroscopy*, Butterworths, London, **1961**, p. 3.
- [84] D. J. A. De Ridder, D. Heijdenrijk, H. Schenk, *Acta Cryst.*, **1990**, 46, 2197.
- [85] G. Israel, F. W. Muller, C. Damm, J. Harenburg, *J. Inf. Recording*, **1997**, 23, 559.
- [86] H. Dember, *Physik, Zeitschr.*, **1932**, 32, 207, 554, 856.
- [87] G. M. Sheldrick, SHELX-86, Program for Crystal Structure Solution, University of Göttingen, Göttingen, Germany, **1997**.
- [88] G. M. Sheldrick, SHELX-97, Program for the Refinement of Crystal Structures, University of Göttingen, Göttingen, Germany, **1997**.
- [89] prepared by students in our working group.

6. Appendix

X-ray crystal structure determination

Crystal data and structure refinement for 15a

Empirical formula	C ₁₄ H ₁₉ NO ₄	
Formula weight	265.3	
Temperature T (K)	220 (2)	
Wavelength (Å)	0.71073	
Crystal system	monoclinic	
Space group	P2 ₁ /a	
Unit cell dimensions	a = 11.780 (2)	α = 90°
	b = 7.2399 (12)	β = 109.43(2)°
	c = 17.178 (4)	γ = 90°
Volume V (Å ³)	1381.5 (4)	
Z	4	
Calculated density ρ (Mg/m ³)	1.276	
Absorption coefficient (mm ⁻¹)	0.093	
F (000)	568	
θ range (°)	3.08 – 25.98	
Limiting indices	-14 ≤ h ≤ 13, -8 ≤ k ≤ 8, -21 ≤ l ≤ 21	
Reflections collected	9557	
Reflections independent	2651 (R _{int} = 0.0879)	
Completeness to θ = 25.98	98.1 %	
Absorption correction	Numerical	
Max. and min. transmission	0.9948 and 0.9496	
Data/restraints/parameters	2651/0/248	
Goodness-of-fit on F ²	1.039	
R ₁ , wR ₂ [I > 2σ(I)]	0.0415, 0.1085	
R ₁ , wR ₂ (all data)	0.0510, 0.1144	
Largest diff. peak and hole (e/Å ³)	0.197 and -0.164	

Additional informations

Operator	C. W.
Identification code:	IPDS 2703
Recrystallization:	water/ethanol
Crystal size (mm)	0.75 x 0.57 x 0.45
Red neddles	

Influence of the counter ions on the UV/Vis absorption spectra of *N*-alkyl-4-phenyl-pyridinium salts **21**

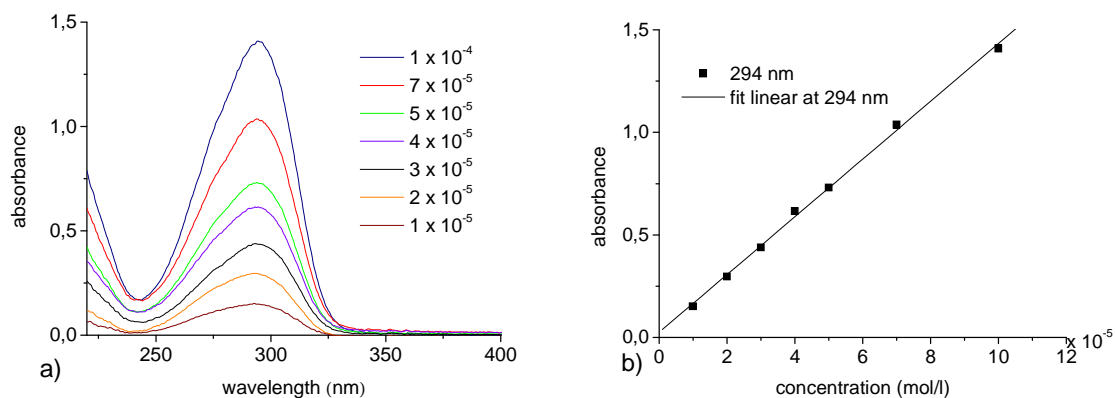
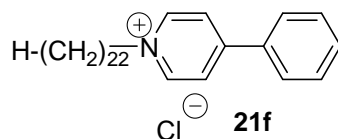


Figure A1. a) Concentration dependence of *N*-docosyl-4-phenyl-pyridinium chloride **21f** in acetonitrile, $l = 1$ cm, l – path length of the quartz cell b) Lambert-Beer plot $A = f(\text{conc.})$ at $\lambda = 294$ nm, $R = 0.998$.

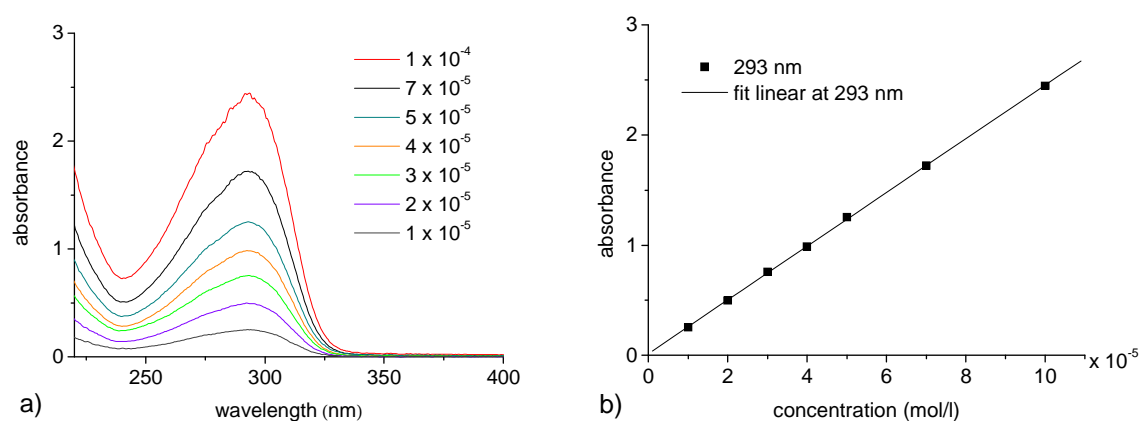
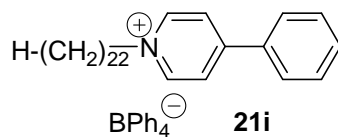
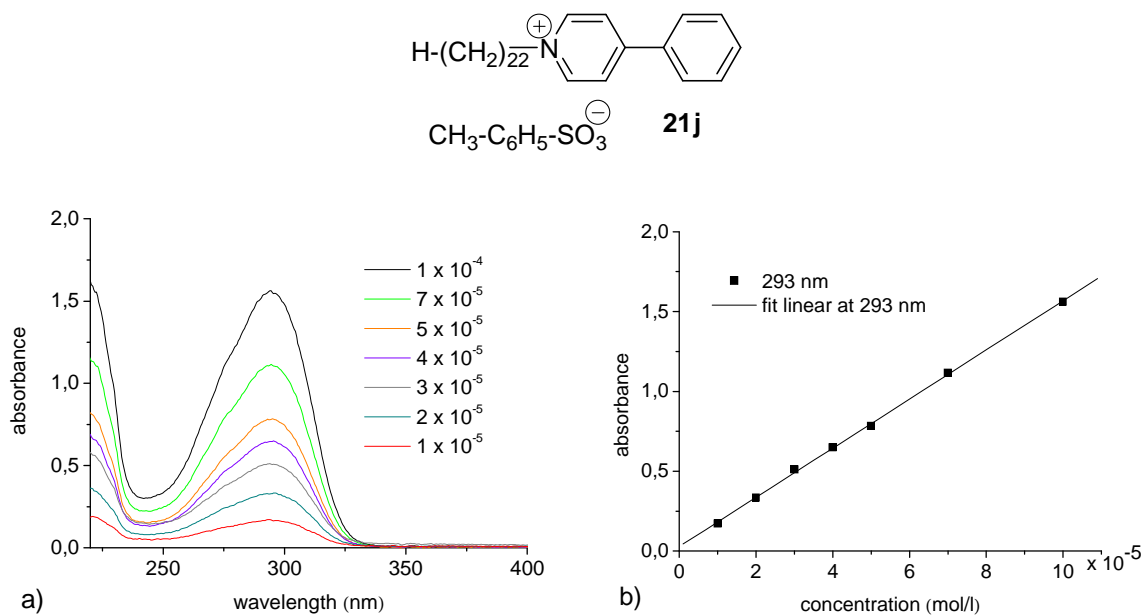


Figure A2. a) Concentration dependence of *N*-docosyl-4-phenyl-pyridinium tetraphenylborate **21i** in acetonitrile, $l = 1$ cm, l – path length of the quartz cell b) Lambert-Beer plot $A = f(\text{conc.})$ at $\lambda = 293$ nm, $R = 0.999$.



Concentration dependence measurements of *N*-alkyl-4'-substituted-stilbazolium salts

a) Concentration dependence in acetonitrile

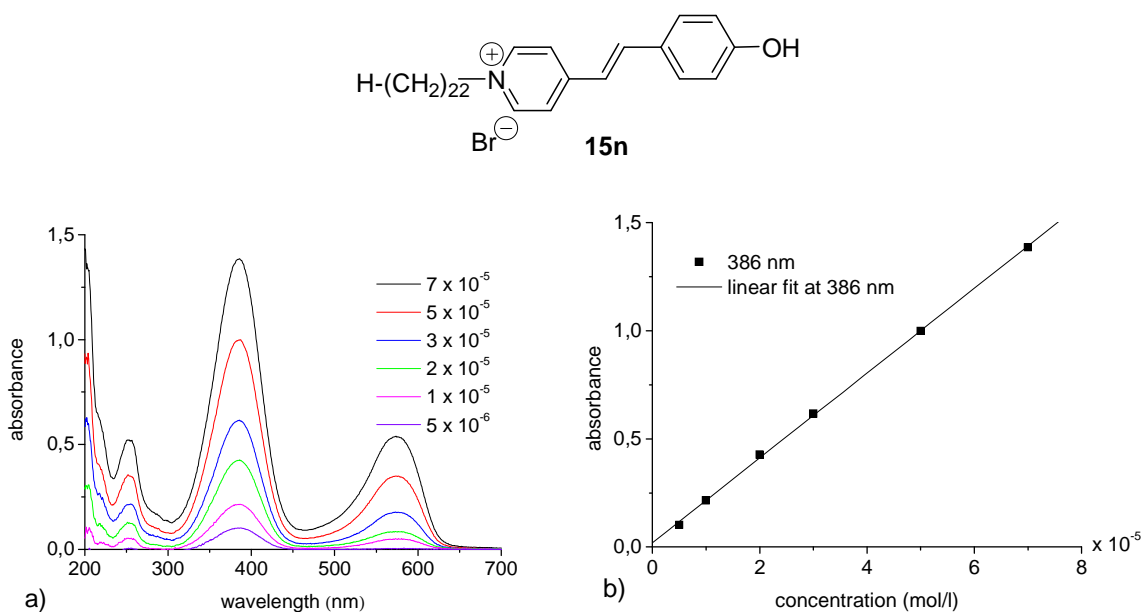


Figure A4. a) Concentration dependence measurements of *N*-docosyl-4'-hydroxy-stilbazolium bromide **15n** in acetonitrile, $l = 1$ cm, b) Lambert-Beer plot $A = f(\text{conc.})$ at $\lambda = 386$ nm, $R = 0.999$.

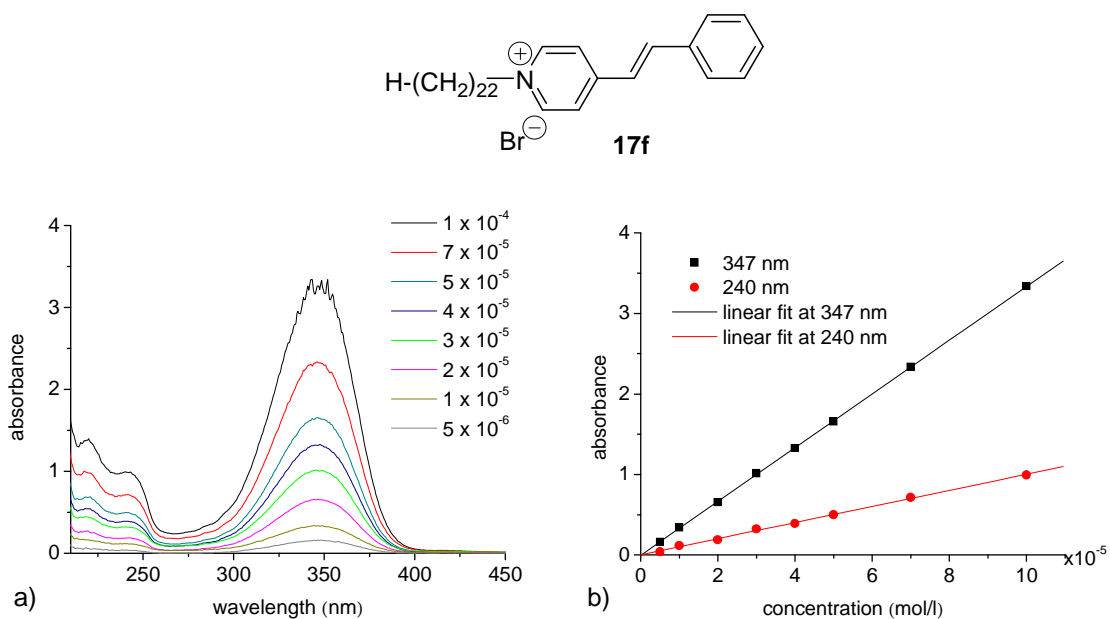


Figure A5. a) Concentration dependence measurements of *N*-docosyl-stilbazolium bromide **17f** in acetonitrile, $l = 1$ cm, b) Lambert-Beer plot $A = f(\text{conc.})$, $R_1 = 0.999$ (at $\lambda = 347$ nm), $R_2 = 0.999$ (at $\lambda = 240$ nm).

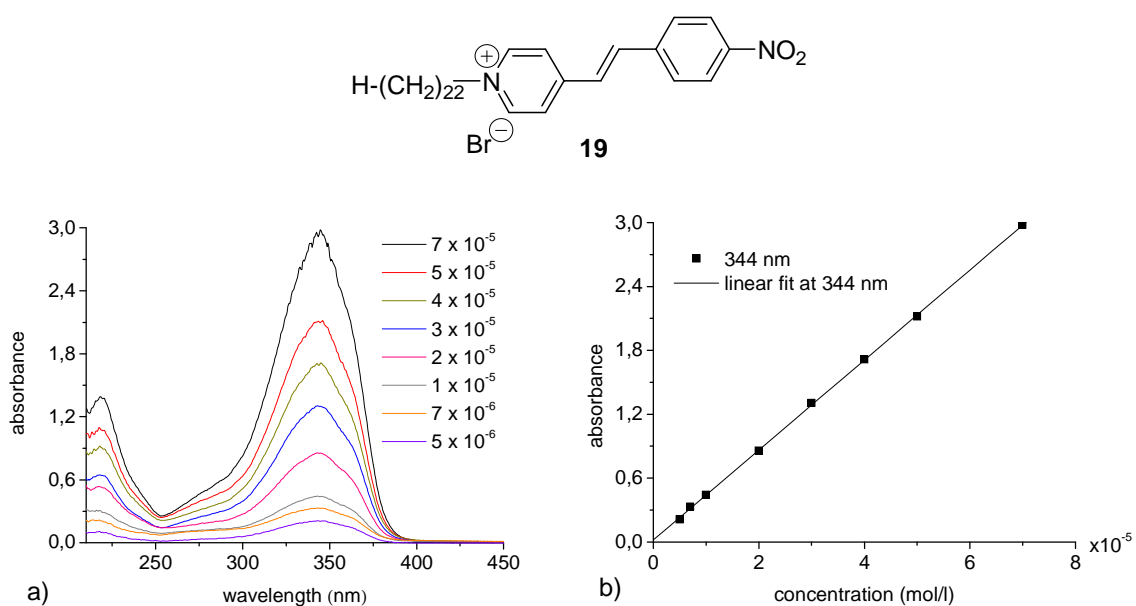


Figure A6. a) Concentration dependence measurements of *N*-docosyl-4'-nitro-stilbazolium bromide **19** in acetonitrile, $l = 1$ cm, b) Lambert-Beer plot $A = f(\text{conc.})$ at $\lambda = 344$ nm, $R = 0.999$.

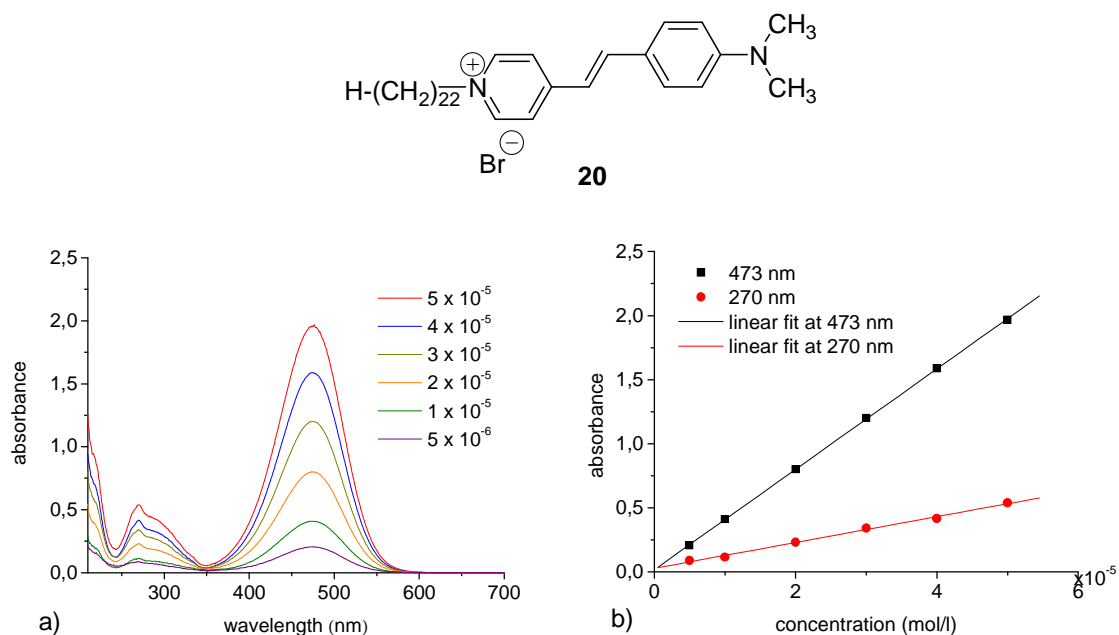


Figure A7. a) Concentration dependence measurements of *N*-docosyl-4'-dimethylamino-stilbazolium bromide **20** in acetonitrile, $l = 1$ cm, b) Lambert-Beer plot $A = f(\text{conc.})$, $R_1 = 0.999$ (at $\lambda = 473$ nm), $R_2 = 0.999$ (at $\lambda = 270$ nm).

b) Concentration dependence in chloroform

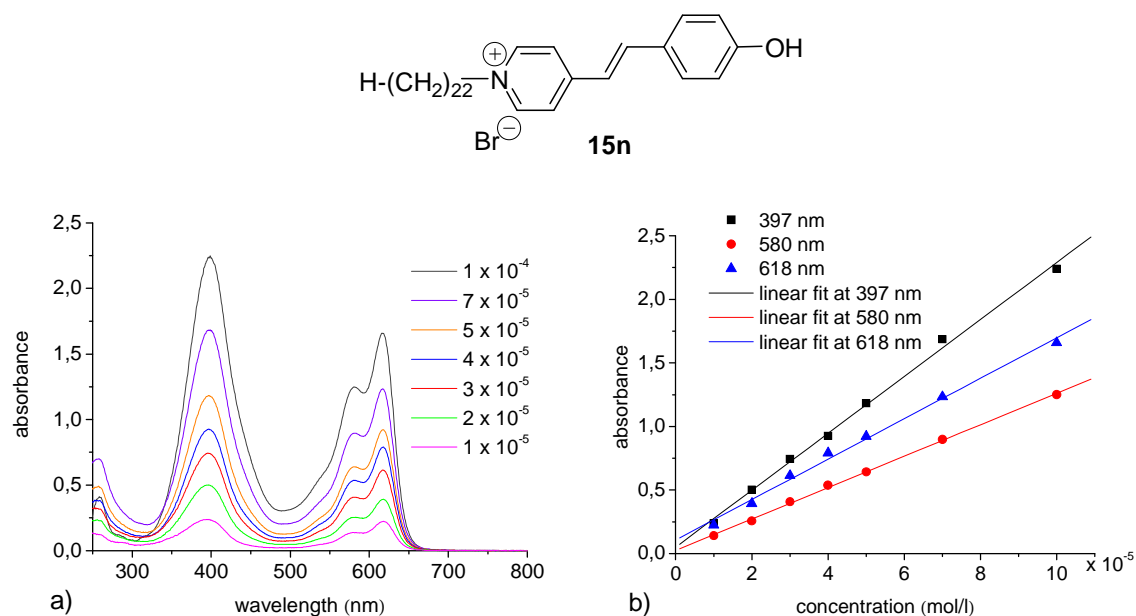


Figure A8. a) Concentration dependence measurements of *N*-docosyl-4'-hydroxy-stilbazolium bromide **15n** in chloroform, $l = 1$ cm, b) Lambert-Beer plot $A = f(\text{conc.})$, $R_1 = 0.998$ (at $\lambda = 397$ nm), $R_2 = 0.999$ (at 580 nm), $R_3 = 0.997$ (at $\lambda = 618$ nm).

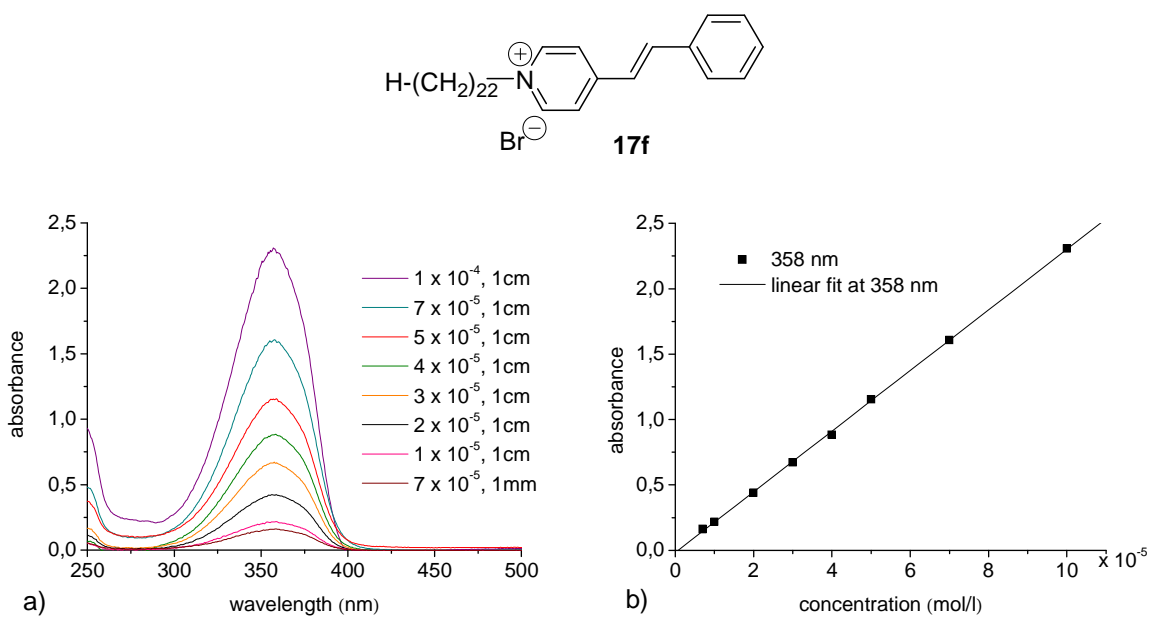


Figure A9. a) Concentration dependence measurements of *N*-docosyl-stilbazolium bromide **17f** in chloroform, $l = 1$ cm, b) Lambert-Beer plot $A = f(\text{conc.})$ at $\lambda = 358$ nm, $R = 0.999$.

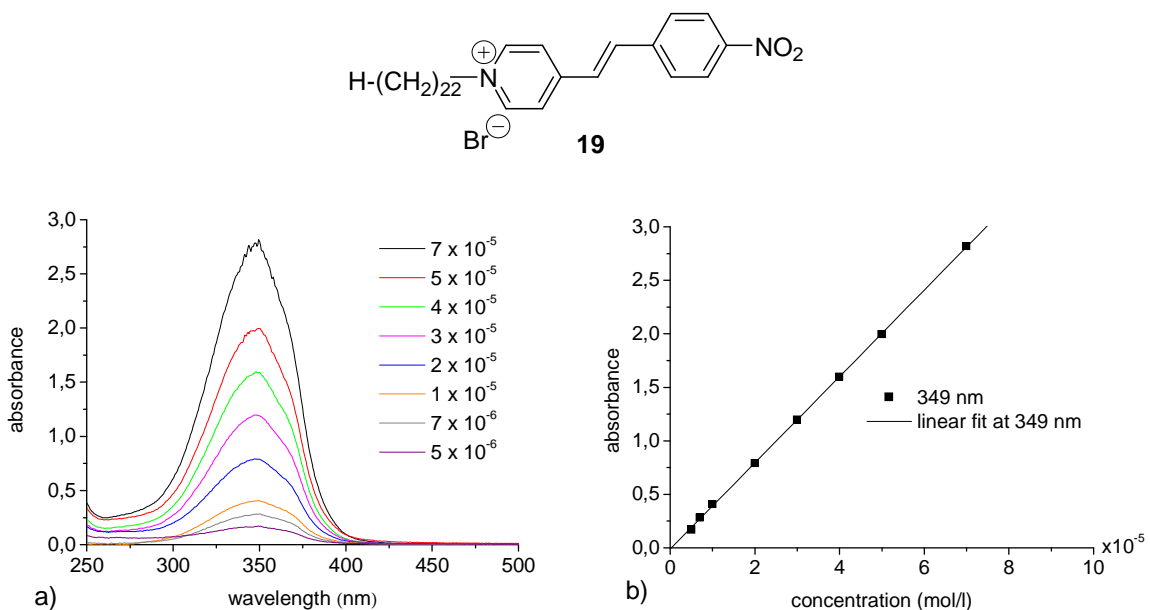


Figure A10. a) Concentration dependence measurements of *N*-docosyl-4'-nitro-stilbazolium bromide **19** in chloroform, $l = 1$ cm, b) Lambert-Beer plot $A = f(\text{conc.})$ at $\lambda = 349$ nm, $R = 0.999$.

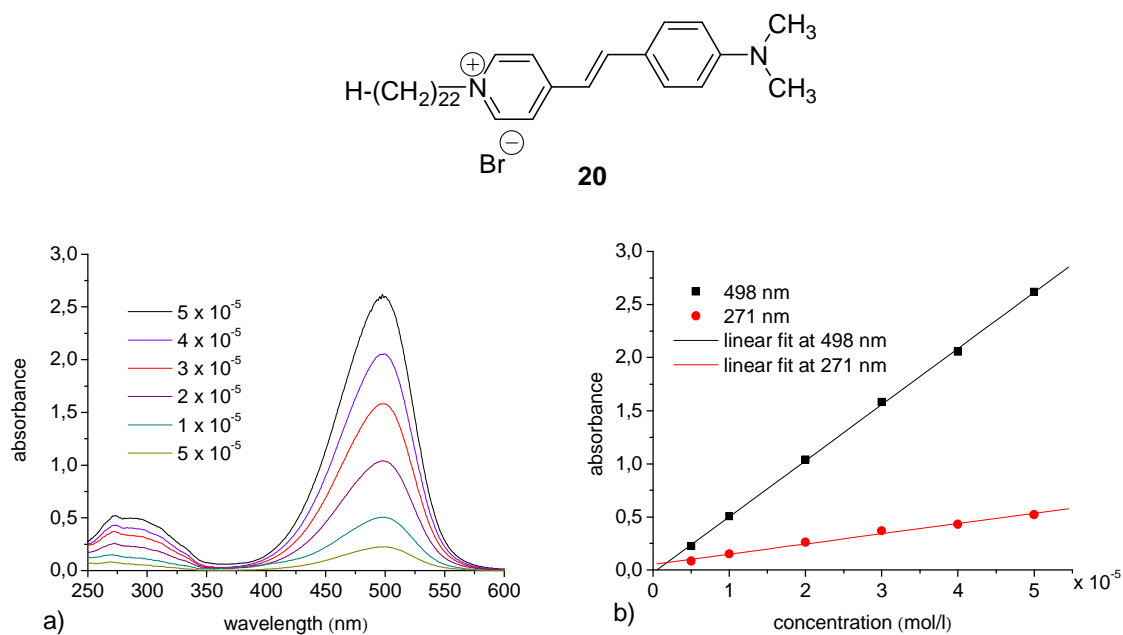


Figure A11. a) Concentration dependence measurements of *N*-docosyl-4'-dimethylamino-stilbazolium bromide **20** in chloroform, $l = 1$ cm, b) Lambert-Beer plot $A = f(\text{conc.})$, $R_1 = 0.999$ (at $\lambda = 498$ nm) and $R_2 = 0.994$ (at $\lambda = 271$ nm).

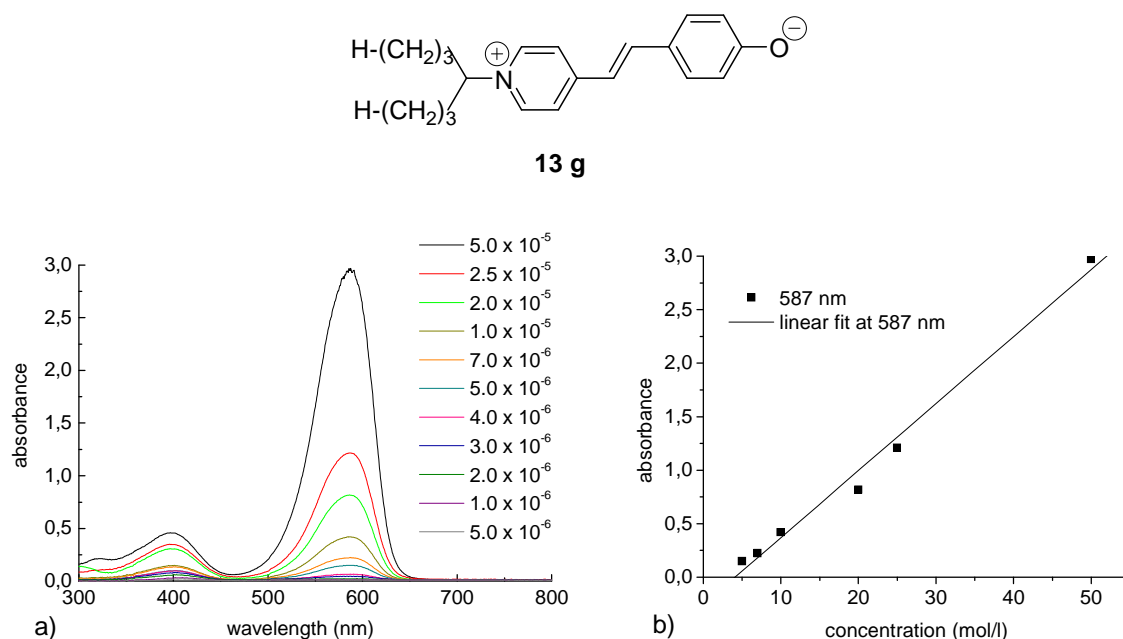


Figure A12. a) Concentration dependence in mol l⁻¹ of 1-(1-octyl-nonyl)-4'-oxy-stilbazolium dye **13g** in DMF, $T = 22$ °C, $l = 1$ cm, l – path length of the quartz cell b) Lambert-Beer plot $A = f(\text{conc.})$ at $\lambda = 587$ nm in the concentration range between 5×10^{-6} mol l⁻¹ and 5×10^{-5} mol l⁻¹, $R = 0.994$.

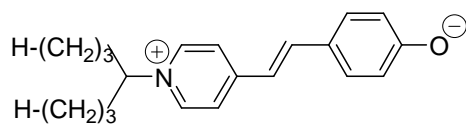
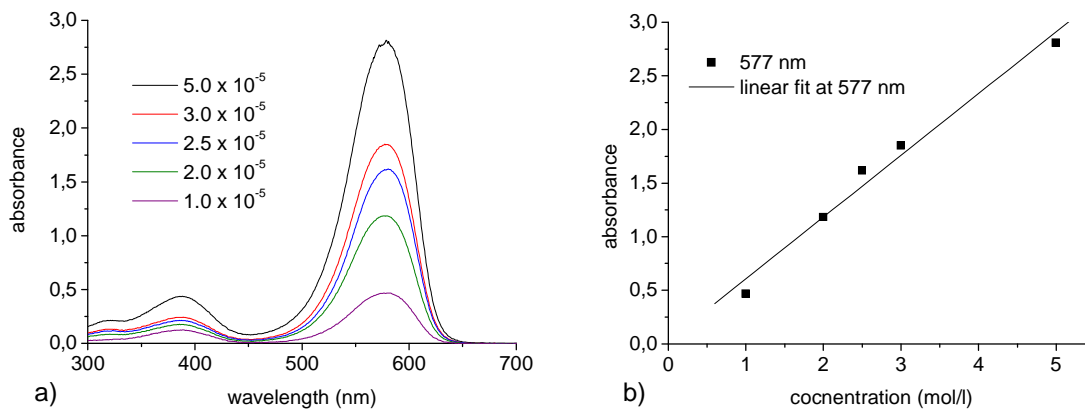
**13 g**

Figure A13. a) Concentration dependence in mol l⁻¹ of 1-(1-octyl-nonyl)-4'-oxy-stilbazolium dye **13g** in acetonitrile, T = 22 °C, l = 1 cm, l – path length of the quartz cell b) Lambert-Beer plot A = f (conc.) at $\lambda = 577$ nm, R = 0.989.

Acknowledgment

I want to thank my supervisor and tutor Prof. Dr. G. Israel for giving me the opportunity to make my Ph.D. in his group and for the interesting and nice topic which I got. I am deeply grateful for his strong support and encouragement and for fruitful discussions which we had during my Ph.D. studies.

Many thanks go to Prof. Dr. C. Tschierske for his advice and for permission of using different equipments in his working group.

I am thankful to Dr. U. Baumeister and J. Lorenzo Chao for 2D X-ray measurements and for helping me with interpretation of the data.

I want to thank Prof. Dr. K. Merzweiler and Dr. C. Wagner for 3D X-Ray investigations.

I am thankful to Prof. Dr. A. Blume, Dr. A. Hauser, Dag Leine and Anja Huster for lyotropic investigations.

ESI-MS measurements were made by Dr. R. Kluge and thermogravimetric analysis by Dr. T. Müller. I thank for it.

I would like to thank Prof. Dr. H. Kresse and Z. Vakhovskaya for conductivity measurements and for helping me with data interpretation.

My thanks also go to Dr. C. Damm for helping me with Photo-E.M.F. measurements.

I am thankful to my colleagues from Prof. Tschierske group for help. My special thanks go to Ms. Neubauer for performing DSC measurements.

Many thanks also to the co-workers of the Institute of Chemistry for performing the NMR, elemental analysis and mass spectroscopy.

I want to express my gratitude to my family and friends for their encouragement and support. Without them I wouldn't be able to finish my thesis.

Publications

1. D. Ster, U. Baumeister, J. Lorenzo Chao, C. Tschierske, G. Israel, "Synthesis and mesophase behaviour of ionic liquid crystals", *J. Mater. Chem.*, **2007**, DOI: 10.1039/b705519f.
2. "Mesophase behaviour of ionic liquid crystals", D. Ster, U. Baumeister, J. Lorenzo Chao, C. Tschierske, G. Israel, *Poster P-7, 35. Arbeitstagung Flüssigkristalle*, Bayreuth, **2007**, 21–23 March.
3. "Synthesis and properties of merocyanine dyes", D. Ster, K. Merzweiler, C. Wagner, C. Tschierske, G. Israel, *Poster D-PO-122, 1st European Chemistry Congress*, Budapest, **2006**, 27–31 August.
4. "Supramolecular behaviour of merocyanine dyes", D. Ster, K. Merzweiler, C. Wagner, C. Tschierske, G. Israel, *Poster P-5, 34. Arbeitstagung Flüssigkristalle*, Freiburg, **2006**, 29–31 March.

Lebenslauf

Name: Ster
Vorname: Diana
Geburtsdatum: 01.02.1979
Geburtsort: Baia Mare, Rumänien
Staatsangehörigkeit: rumänisch
Familienstand: ledig

Ausbildung

1985-1993 Grundschule, Baia Mare.

1993-1997 Theoretisches Lyzeum “Vasile Lucaciu”, Baia Mare, Schwerpunkt:
Mathematik-Physik-Englisch, Abschluss: Abitur

1998-2003 Studium der Chemie an der Polytechnischen Universität Timisoara,
Fakultät für Industrielle Chemie und Umweltingenieurwesen,
Rumänien, Abschluss Diplom: 1.0

04.2003-09.2003 Socrates/Erasmus Stipendium an der Technische Universität
Braunschweig, Institut für Organische Chemie, Forschungsgruppe Prof.
Dr. H. Hopf, Thema: “Synthese von Biarylen”

ab 10.2003- Promotionstudium an der Martin-Luther-Universität Halle-Wittenberg,
Institut für Organische Chemie/Graduiertenkolleg (GRK) 894/1
“Selbstorganisation durch koordinative und nichtkovalente
Wechselwirkungen”, Forschungsgruppe Prof. Dr. G. Israel.

Halle (Saale), den 12.06.2007

Diana Ster

Erklärung

Hiermit erkläre ich, dass ich die vorliegende Arbeit selbständig und ohne fremde Hilfe verfasst, andere als die von mir angegebenen Quellen und Hilfsmittel nicht benutzt und die den benutzten Werken wörtlich oder inhaltlich entnommenen Stellen als solche kenntlich gemacht habe.

Halle (Saale), 12.06.2007

Diana Ster

Erklärung

Die vorliegende Arbeit wurde erstmalig eingereicht. Ich habe auch an keiner anderen Universität die vorliegende oder eine andere Arbeit eingereicht.

Halle (Saale), 12.06.2007

Diana Ster